Universita' degli studi di Lecce

The CBF theory for medium-heavy nuclei

Advisor: *Prof. Giampaolo Co'*
Co-advisor: *Prof. Fernando Arias de Saavedra*

Candidate: *Cristian Bisconti*

Abstract

The correlated basis function theory is applied to the study of medium-heavy doubly closed shell nuclei with different wave functions for protons and neutrons and in the jj coupling scheme. State dependent correlations including tensor correlations are used. Realistic two-body interactions of Argonne and Urbana type, together with three-body interactions have been used to calculate ground state energies and density distributions of the ^{12}C , ^{16}O , ^{40}Ca , ^{48}Ca and ^{208}Pb nuclei.

La teoria delle funzioni a base correlata e' stata applicata allo studio dei nuclei doppio magici con differenti funziona d'onda per protoni e neutroni e usando una raprresentazione in accoppiamento jj. Le correlazioni dipendenti dallo stato includono anche la parte tensoriale. Interazioni a due corpi realistiche of tipo Argonne e Urbana, insieme con interazioni a tre corpi sono state usate per calcolare le energie dello stato fondamentale e le distribuzioni a uno e a due corpi del ^{12}C , ^{16}O , ^{40}Ca , ^{48}Ca and ^{208}Pb .

Contents

Chapter 1

Introduction

Aim of the many-body theories is the description of composite systems in terms of their elementary components and of their mutual interactions. The first problem to solve is the identification of the elementary components of the systems. We know that matter is composed by leptons and quarks, but we cannot think to describe all the physical systems of our interest in terms of these entities. For this reason in any many-body theory it is necessary to define the basic components to be used for the description, and these components are assumed to be pointlike, i.e. without internal structure. For example, the study of liquid helium properties is done by assuming helium atoms as the basic degrees of freedom. In the case of our interest, atomic nuclei, we shall use the nucleons as elementary components.

The interaction between the elementary components of the system is, the second necessary ingredient to make a many-body description of it. Also in this case there is a difference between the fundamental interactions, gravity, electromagnetic, weak and strong nuclear forces, and that used in the many-body calculation. For example, in the liquid helium case the interaction between two helium atoms is obviously related to the Coulomb interaction. A description of the full many-body system starting from this interaction would not be feasible. For this reason an effective interaction between helium atoms is used, for example a Lennard-Jones type of interaction.

For the atomic nuclei the situation is somehow a similar one. We have good reasons to believe that the Quantum Chromodynamics is the basic theory of strong interactions. However, despite the progresses done in the last two decades, a description of the interaction between two nucleons in terms of quarks and gluons is not yet feasible, and in any case, it would not be very useful in the

	$AV8'$	$AV18$	UIX	$Expt$
$^3H(\frac{1}{2}^+)$	-7.76(1)	-7.61(1)	-8.46(1)	-8.48
$^3He(\frac{1}{2}^+)$	-7.02(1)	-6.87(1)	-7.71(1)	-7.72
$^4He(0^+)$	-25.14(2)	-24.07(4)	-28.33(2)	-28.30
$^6He(0^+)$	-25.20(6)	-23.9(1)	-28.1(1)	-29.27
$^6He(2^+)$	-23.18(6)	-21.8(1)	-26.3(1)	-27.47
$^6Li(0^+)$	-28.19(5)	-26.9(1)	-31.1(1)	-31.99

Table 1.1: Experimental and Green function Montecarlo energies (in MeV). Montecarlo statistical errors in the last digits are shown in parentheses [Pie01]. AV8' and AV18 are two different parametrizations of the two–body potential. UIX includes a three-nucleon potential.

description nuclear systems. For these reasons the nucleon-nucleon interaction is fixed in order to reproduce the properties of two-nucleon systems, i.e. those of the deuteron, and the nucleon-nucleon elastic scattering phase shifts.

Modern two-nucleon potentials [Mac96], [Sto94], [Wir95] are able to describe with great accuracy, with a χ^2 of about 1 per degree of freedom, the about 3000 phase shift data [Sto93]. In the past, because of the relatively limited number of data to be fitted, there were noticeable differences between the nucleon-nucleon potentials obtained with various approaches. Nowadays these differences have been strongly reduced.

After defining the basic degrees of freedom and their interaction, it is necessary to define the theoretical framework to describe the many-body system. If one assume that relativistic effects are negligible, the problem consists in solving the many-body Schrödinger equation. A this point the problem to be solved is well defined, and in principle, it remains only to clarify the technical approach to be used to solve a complicated equation. The Schrödinger equation is solved without approximations for the two-body systems. As we have seen, this is used to define the potential. The next step is the solution for the three-body systems. In this case the equations to be solved are much more complicated. In any case, various approaches have been developed to solve the three-nucleon Schrödinger exactly, i.e. without approximations, in the jargon of the many-body physicists. For a fixed nucleon-nucleon interaction, the values of binding energies obtained with these different techniques are within a 1% uncertainty [Kam01]. All the calculations agree with the fact that the use of two-body potential only underbinds the three-body systems. We show in Table 1.1 an example of these results obtained with Green function Montecarlo GFMC technique [Pie01].

One of the basic hypotheses of the many-body calculation is that the basic degrees of freedom, the nucleons in our case, are pointlike entities, i.e. their internal structure is neglected. It may look a paradox but this approximation is better fulfilled by the helium atoms in the study of their quantum liquid systems than by the nucleons in the nucleus. The binding energy of the fermionic liquid helium system is of the order of 10^{-4} eV, to be compared with the 21 eV of the first excited state of the atom. One has to compare the ratio of these two energies with that between the about 10 MeV of nuclear binding energy (16 MeV for nuclear matter) and the 300 MeV necessary to excite the nucleonic degrees of freedom. This means that, in nuclear systems, the presence of effects related to the internal structure of the nucleons are more important than in liquid helium. In order to reproduce the ^{3}H binding energy it is necessary to include a three-body interaction in the nuclear hamiltonian which consider the excitation of sub-nucleonic degrees of freedom.

The nuclear structure calculations with the hamiltonian containing two- and three-body interactions are able to reproduce the binding energies of the ^{3}He and ^{4}He nuclei. In these last decade the Green function Montecarlo technique has been applied with success to the study of various light nuclei, see Table 1.1 [Pie05]. Recently, results for $A = 12$ systems have been presented [Pie05]. These results show the validity of the non-relativistic many-body approach in the description of finite nuclei.

There are no principle reasons forbidding the application of the Green function Montecarlo technique to any nuclear systems. The limitations are related to the large computational effort. We show in Table 1.2 the number of spin and isospin configurations to be calculated for a set of nuclei. It is evident that, even the more optimistic predictions of the improvement of the computer performances do not give much hope to possibility of applying the Montecarlo technique to medium and heavy nuclei. The goal of the many-body theories is to solve the many-body Schrödinger equations by doing some approximations that simplifies the problem to allow its solution. The control on the effects of these approximations on the observables is one of main problems of the many-body theories.

In nuclear physics sophisticated many-body theories have been mainly applied to the study of nuclear matter. Nuclear matter is an ideal system composed by an equal, and infinite, number of protons and neutrons where the Coulomb

$Nucleus$	Z	$N = A - Z$	N_{conf}
^3H	1	2	24
^3He	2	1	24
^4He	2	2	96
^6He	2	4	960
^6Li	3	3	1280
^8He	2	6	7168
^{12}C	6	6	3784704
^{16}O	8	8	$8.4 \cdot 10^8$
^{40}Ca	20	20	$1.5 \cdot 10^{23}$
^{48}Ca	20	28	$4.7 \cdot 10^{27}$

Table 1.2: Numbers of spin and isospin for some nuclei.

interaction has been switched off. The extrapolation of the properties of the interior of medium and heavy nuclei allows us to identify the empirical values of the binding energy per nucleon, -16 ± 1 MeV, and density, 0.17 ± 0.01 nucleons fm $^{-3}$, at the nuclear matter saturation point. The description of the saturation properties of nuclear matter has been, and still it is, one of the problems more investigated in nuclear physics. In reality, the description of the nuclear matter properties can be considered a kind of homework problem to test the validity of the various many-body theories [Bet71].

The main problem one encounters in the development of theories searching for approximated solution of the Schrödinger equation is the presence of a hard repulsive core in the nucleon-nucleon interaction which makes impossible the straightforward application of the naive perturbation theory. In order to solve this problem, the nuclear many-body theories for nuclear matter have been developed following two different lines.

The first one, and most widely used, is based on the idea of constructing an effective interaction. Resummation techniques based on field theory are used to renormalize the nucleon-nucleon interaction in the hard core region. The resulting interaction behaving well at short internucleon distances can be used in a perturbation theory. These are the basic ideas of the Brueckner theory which construct the effective interaction called G-matrix [Bru54], [Day67], [Jen76], [Dic82], [Son98], [Bal05].

An opposite point of view is that of the Correlated Basis Function (CBF) theory [Pan79], [Akm97]. This theory is based on the variational principle. The search of the minimum of the energy functional is done within a sub-space of the Hilbert space spanned by wave functions describing a system of non-interacting particles multiplied by a correlation function. Contrary to what happens in Brueckner theory the nucleon-nucleon interaction is not modified and the presence of the hard core is taken care by the correlation function.

After a long struggle [Cla79], which is part of the nuclear physics history, it has been shown that the two approaches provide analogous results [Mut00]. Modern two-body interactions, implemented with three-body interactions, underbind nuclear matter at the saturation density by about 1 MeV [Akm97] [Son98].

The application of these many-body theories to finite systems had two different histories. The Brueckner G-matrix has been used in Hartree-Fock calculations [Sch91] [Mut00]. This approach is the microscopic basis for the construction of various phenomenological interactions used in effective theories, such as Hartree-Fock or Random Phase Approximation. Only recently, effective interactions have been constructed by using the CBF idea of a correlation function. This method called Unitary Correlation Operator has produced effective interactions which have been used in Hartee-Fock and shell model calculations [Nef03].

The history of the application of the CBF theory to finite systems is a more recent one. The extension of the original CBF theory to finite Fermi systems has been formulated in the late seventies [Fan74] [Fan79]. In these works it was shown the possibility of making formal cluster expansions with infinite numbers of terms, even in finite systems. Furthermore the idea of the so-called vertex corrections, see section 2.1.1 , which modify the Fermi Hypernetted Chain (FHNC) resummation techniques, have been introduced.

The first specific application to model nuclei has been done in [Co92]. In this article finite nuclear systems were described by using a unique mean field potential for both protons and neutrons and by using a ls coupling scheme. Also the interactions were very simple, they did not contain tensor terms, and the correlations were purely scalar functions. This simplified situation has been used to show the theoretical and numerical feasibility of the project. The momentum distribution of these systems have been calculated in another paper [Co94].

In a following article [Ari96] the same interactions and correlations have been been used to investigate nuclei with different number of neutrons and protons whose single particle wave functions were generated with different mean field potentials containing spin-orbit terms. In this article the technique to treat systems not saturated in spin and isospin has been developed and tested.

Another step forward was done in [Fab98] where realistic nucleon-nucleon interactions, with terms up to the tensor ones have been used together with state dependent correlations. In this article the FHNC resummation technique was extended to treat correlations containing parts that do not commute any more with the hamiltonian, ad among themselves. In analogy to what has been done in nuclear matter, also in this case the Single Operator Chain approximation has been used (see sect. 2.3). The novelty here consisted in defining the full FHNC/SOC computational scheme for finite Fermi systems. Because of the relevant technical difficulties pushed us to work again a single particle basis saturated in spin and isospin was used in order to use some of the techniques developed for the nuclear matter. The calculations of [Fab98] have been extended in [Fab00] where spin-orbit terms of the two-body interaction have been inserted, and, more important, the three-body interaction.

The next step, and the final one, is to extend the formalism above described to deal with realistic nuclear systems. They are systems where the neutrons and protons are separately treated and are described in a jj coupling scheme. This was the aim of this thesis.

From the first principles point of view, the work done in this thesis, is the final part of a project started long time ago. From the technical point of view, the problem is extremely complicated. The distinction between protons and neutrons leads to a quadruplication of the number of equations to be solved, and this is the easy part of the story. What makes the problem extremely difficult is the presence of the various non commuting operators. The traditional techniques to calculate traces of these operators cannot be applied any more since they have been developed for spin and isospin saturated systems. It has been necessary to develop different manners of calculating traces. Fortunately, despite of the increase of linked integral equations to be solved, no particular numerical problems have been encountered.

In any case, the final results are quite rewarding, since, to the best of our knowledge, it is the first time that the structure of nuclei as heavy as the Calcium isotopes and especially ^{208}Pb have been investigated with a fully microscopic model with theory containing realistic interactions. Furthermore the formalism developed here opens the possibility to a large number of applications in the evaluation of variuos observables.

This document has been written having in mind a slightly pedagogical presentation of the CBF theory. For this reason in the first part of the thesis we summarize the basic ideas of the CBF and FHNC/SOC approach developed for infinite systems. The reader familiar with these results can directly jump to the second part of the thesis, where finite nuclear systems are treated. Also in this case there is first a short review of the previous results, but the main part is dedicated to the presentation of the original results concerning the FHNC/SOC equations applied to realistic finite nuclear systems. Finally the specific application of the theory to the study of the binding energies and of the density distributions of ^{12}C, ^{16}O, ^{40}Ca, ^{48}Ca and ^{208}Pb nuclei is presented in Chapter 4.

Chapter 2

Infinite systems

2.1 The correlated basis function (CBF) theory

As it has been said in the introduction, aim of the CBF theory is the solution of the many-body Schrödinger equation

$$H\Psi(1,....,A) = E\Psi(1,...,A) \tag{2.1}$$

where $\Psi(1,...,A)$ is the wave function describing the system of A particles and H the many-body hamiltonian.

The basic idea of the CBF theory is to search solutions of the eq. (2.1) of the type

$$\Psi(1,...,A) = F(1,...,A)\Phi(1,....,A). \tag{2.2}$$

where F is called *correlation function* and $\Phi(1,..,A)$ is the wave function of system corresponding to the independent particle model (IPM). In the CBF theory the Schrödinger equation (2.1) is solved by using the variational principle

$$\delta E[\Psi] = \delta \frac{<\Psi|H|\Psi>}{<\Psi|\Psi>} = 0. \tag{2.3}$$

The minimum obtained in this manner is an upper bound of the true eigenstate of the eq. (2.1).

2.2 Bosons

In this section we shall describe the cluster expansion for infinite bosonic systems. We get the infinite system by making the thermodynamic limit of a finite system. We consider A particles contained in a volume, V. After making the cluster expansion we take the limit for A and V going to infinity but we keep their ratio, $\rho = A/V$, constant. We write the wave function of a system of A non interacting bosons without degeneracy as:

$$\Phi(x_1, x_2, \ldots, x_A) = \mathcal{S}\Big(\phi_1(x_1)\cdots\phi_A(x_A)\Big) \tag{2.4}$$

In the above equation we have indicated with $\mathcal{S}$ the symmetrization operator, and with $\phi_i(x_i)$ the single particle wave functions. The label i indicates the set of quantum numbers of the i-th particle, and x_i is the generalized coordinate of the i-th particle. We consider the ground state of the system, therefore, in the uncorrelated description, all the bosons occupy the lowest single particles state:

$$\phi_i(x) = \phi(x) = \frac{1}{\sqrt{V}} e^{i\boldsymbol{k}\cdot\boldsymbol{r}} \tag{2.5}$$

where the last expression is due to the fact that the system is infinite, i.e. translationally invariant, and composed by bosons with spin zero. In this case the generalized coordinate x corresponds to r and the density of this system given by

$$\rho_0(x) = A\phi^*(x)\phi(x) = \rho \tag{2.6}$$

is constant. As already stated, in the framework of the Correlated Basis Function (CBF) theory the trial wave function describing the interacting system is written as:

$$\Psi(x_1, ..., x_A) = F(x_1, ..., x_A)\Phi(x_1, ..., x_A) \tag{2.7}$$

The function $F(x_1, ...x_A)$ which modifies Φ is called many-body correlation function (MBCF). The usual ansatz for the explicit functional expression of F is [Jas55]

$$F(x_1, ..., x_A) = \prod_{j>i=1}^{A} f(r_{ij}) \tag{2.8}$$

The two body correlation function (TBCF) $f(r_{ij})$ is a scalar function of r_{ij}, the distance between the i-th and j-th particles. The TBCF goes to unity at large interparticle distances. In the description of the interacting system, a useful quantity is the two-body distribution function (TBDF) defined as:

$$g(x_1, x_2) = \frac{A(A-1)\int dx_3 \ldots dx_A \Psi^*(x_1, \ldots, x_A)\Psi(x_1, \ldots, x_A)}{\rho^2 \int dx_1 dx_2 \ldots dx_A \Psi^*(x_1, \ldots, x_A)\Psi(x_1, \ldots, x_A)} \tag{2.9}$$

The TBDF can be used to evaluate the expectation value of a two-body operator $O(1, 2, \ldots, A) = \sum_{j>i=1}^{A} O_{ij}$ as:

$$< O >= \frac{1}{2}\rho^2 \int dx_1 dx_2 g(x_1, x_2) O_{12} \tag{2.10}$$

By using the eqs. (2.5),(2.6), (2.7),(2.8) the numerator and the denominator of the eq. (2.9) can be written as:

$$\mathcal{N} = A(A-1) \int dx_3 dx_4 \ldots dx_A \frac{\rho^{A-2}}{A^A} \prod_{i<j} f^2(r_{ij}) \tag{2.11}$$

$$\mathcal{D} = \int dx_1 dx_2 \ldots dx_A \frac{\rho^A}{A^A} \prod_{i<j} f^2(r_{ij}) \tag{2.12}$$

In the previous expression we have used the fact that f is a scalar function, therefore it commutes with the single particle w.f. $\phi(x)$. We define a new function $h(r_{ij})$ as:

$$f^2(r_{ij}) = 1 + h(r_{ij}) \ , \tag{2.13}$$

and this allows us to rewrite the denominator as:

$$\mathcal{D} = \int dx_1 dx_2 \ldots dx_A \frac{\rho^A}{A^A} \left[1 + \sum_{i<j} h(r_{ij}) + \sum_{i<j<k} h(r_{ij}) h(r_{jk}) + \ldots \right] \tag{2.14}$$

where we have separated the various terms containing an increasing number of correlation functions h. A useful way of handling with these integrals is to use a graphical representation introduced by Yvon and Mayer [May40]. A solid circle indicates an integration point and has a density ρ associated to it, and a dashed line the correlation h. The second term of the eq. (2.14) is represented in figure 2.1. We show in fig. 2.2 the terms containing two correlation functions h. In the term represented by the diagram A the two correlation functions h have a

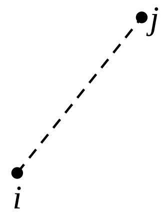

Figure 2.1: Graphical representation of the second term of eq.(2.14). The dashed line represents the correlation function h. The black dots represents the integration points i and j.

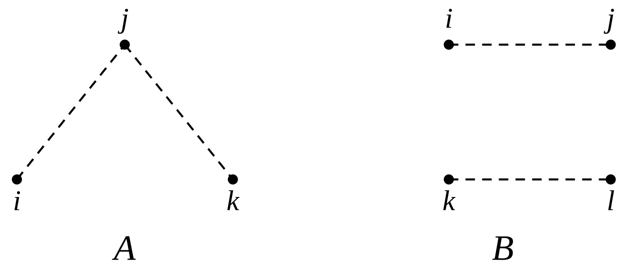

Figure 2.2: Graphical representation of the terms given by the eqs. (2.15) and (2.16) respectively.

common point. Its contribution is

$$\frac{1}{3!}\frac{A^2-3A+2}{A^2}\rho^3\int dx_i dx_j dx_k h(r_{ij})h(r_{jk}) \tag{2.15}$$

In the term represented by the diagram B there are not common points

$$\frac{1}{4!}(1-\frac{6}{A}+\frac{11}{A^2}-\frac{6}{A^3})\rho^4\int dx_i dx_j dx_k dx_l h(r_{ij})h(r_{kl}) \tag{2.16}$$

The *order* of the diagram is given by the number of points involved. The technique presented above can also be applied to the numerator. By using the same techniques applied to write the denominator, we obtain for the numerator the following expression:

$$\begin{aligned}\mathcal{N} &= f^2(r_{12})\frac{(A-1)}{A}\Bigg[1+2\frac{\rho}{A}(A-2)\int dx_j h(r_{1j}) \\ &\quad +\frac{(A-2)(A-3)}{2}\frac{\rho^2}{A^2}\int dx_i dx_j h(r_{ij})+\ldots\Bigg] \end{aligned}\tag{2.17}$$

In this case, the many-body integral does not imply the integration on two coordinates that we have labeled 1 and 2, for simplicity. These two points are called external points, and are indicated by white dots in the graphical representation.

The integrated points, the black dots, are obviously called, internal points. The graphical representation is applied to the term in square brackets of the numerator. The first term is the uncorrelated part, the second term contains a single correlation function h which connects the external point 1 with the internal point j. Also the third term is linear in h but in this case the correlation connects two internal points i and j. The graphical representation of these three terms of is given in fig. 2.3.

At this point the numerator and denominator in eq.(2.9) have been written as

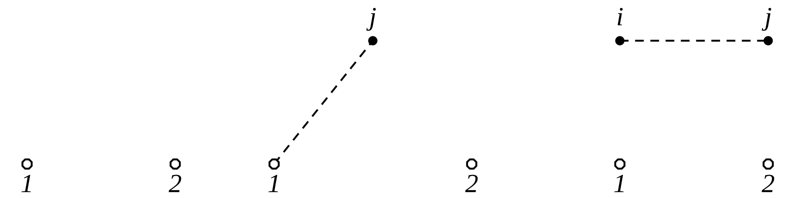

Figure 2.3: Graphical representation of three terms of the numerator, eq. (2.17). The white dots indicate the external points.

sum of integrals called *clusters* and each integral can be represented by a diagram. We analyze the topological structure of the diagrams to simplify the calculation. A first classification identifies linked and unlinked diagrams. An example of these two different types of diagrams is given in fig. 2.2. The diagram B can be factorized in two independent pieces

$$\frac{1}{4!}(1-\frac{6}{A}+\frac{11}{A^2}-\frac{6}{A^3})\rho^4\int dr_i dr_j dr_k dr_l h(r_{ij})h(r_{kl}) =$$
$$\frac{1}{4!}(1-\frac{6}{A}+\frac{11}{A^2}-\frac{6}{A^3})\rho^2\int dr_i dr_j h(r_{ij})\cdot\rho^2\int dr_k dr_l h(r_{kl})$$

Any diagram that can be factorized in two or more pieces is called *unlinked diagram*. Diagrams that cannot be factorized, such as the diagram A of fig. 2.2, are called *linked diagrams*. On the other hand the diagram A of fig. 2.2 is reducible. In effect because of the translational invariance of the system, only relative distances are important, therefore by doing a change of variables $\boldsymbol{R}_{ij} = \frac{1}{2}(\boldsymbol{r}_i + \boldsymbol{r}_j)$, $\boldsymbol{r}_{ij} = \boldsymbol{r}_i - \boldsymbol{r}_j$ we can write:

$$\frac{1}{3}\frac{A^2-3A+2}{A^2}\rho^3\int dr_i dr_j dr_k h(r_{ij})h(r_{jk}) =$$
$$\frac{1}{3}\frac{A^2-3A+2}{A}\rho^2\int dr_{ij} h(r_{ij})\int dr_{jk} h(r_{jk})$$

Any linked diagram whose contribution can be written as a product of integrals,

as in the above example, is called *reducible diagram.* In bosonic systems reducible and unlinked diagrams are both factorisable. It has been demonstrated [Fan74] that , up to the $\frac{1}{A}$ order, no unlinked and reducible diagrams contribute to the TBDF eq. (2.9). An example illustrating how the simplifying procedure works is shown in Appendix A.1.
After the simplification of the unlinked and reducible diagrams, the expression of the TBDF, eq. (2.9), is composed by linked and irreducible diagrams containing two external points labeled 1 and 2:

$$g(r_{12}) = f^2(r_{12}) \sum_{all\ orders} Y_{irr}(r_{12}) \tag{2.18}$$

These diagrams can be classified as *simple* or *composite.* A composite diagram is a diagram formed by parts that are connected only in the two external points 1 and 2. Examples of composite diagrams are given in fig. 2.4. The diagrams which are not composite are named simple and can be classified as *nodal* and *elementary.* A nodal diagram contains al least one point where all the possible paths going from one external point to the other one have to pass through it. These points are called *nodes.* Examples of nodals diagrams are given in fig. 2.4. The remaining diagrams with no nodes are called elementary. The sum of all the irreducible diagrams, composite, nodal and elementary gives the distribution function. For the evaluation of the TBDF it is useful to use a theorem stating that a nodal diagram can be constructed by integrating on the node the two functions representing the parts of the diagram joined at the node. In general
all the nodal diagrams can be obtained as the folding product ot two generic functions $a(r_{ij})$, and $b(r_{kj})$ representing the diagrammatic links between points i and k and k and j respectively.
The folding product is defined as:

$$\Big(a(r_{ik})|b(r_{jk})\Big) \equiv \rho \int d\boldsymbol{r}_k a(r_{ik}) b(r_{kj}) \tag{2.19}$$

Let us indicate with $N(r_{j2})$ the sum of all the nodal diagrams having j and 2 as external points. If we now perform the folding integral of $h(r_{1j})$ with $N(r_{j2})$, we get all the diagrams of $N(r_{12})$. In reality, in this folding integral, the three-point diagrams with two h functions, like the A diagram of fig. 2.2, is excluded and it has to be added by hand. Then the sum of nodal diagrams having 1 and 2 as

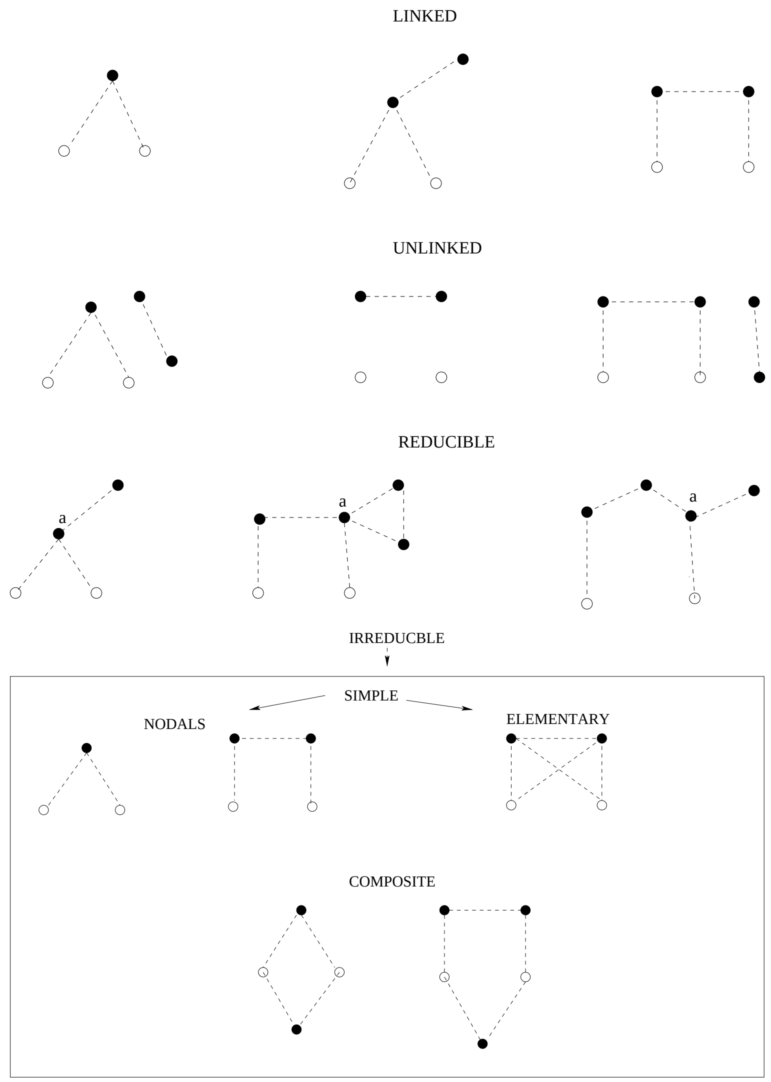

Figure 2.4: Classification of the Mayer diagrams. In the reducible diagrams a indicates the articulation point.

external points is given by

$$N(r_{12}) = \Big(h(r_{1j})|N(r_{j2})\Big) + \Big(h(r_{1j})|h(r_{j2})\Big) \tag{2.20}$$

The definition of composite diagrams, implies that their contribution to the TBDF can be expressed in terms of simple diagrams. Let us write $S(r)$ for their contribution. For example, the sum of all the composite diagrams that can be separated in only two simple diagrams is related to $S^2(r)$. Each term of the $S^2(r)$ sum is given by the product of two simple diagrams. The exchange of all the particles of one subdiagrams with those of the other one, produces the same composite diagram. So $S^2(r)$ must be multiplied by $\frac{1}{2}$ to avoid this double counting. In analogy, the $S^3(r)$ terms should be multiplied by $\frac{1}{3!}$ and so on. The total sum of composite diagrams can be written as:

$$\frac{S^2(r)}{2!} + \frac{S^3(r)}{3!} + \frac{S^4(r)}{4!} + \ldots = e^{S(r)} - S(r) - 1 \tag{2.21}$$

where the last equality appears because our system has an infinite number of particles. The procedure illustrated above, indicates how to construct the composite diagrams from the simple diagrams. If we remember that $S(r) = N(r) + E(r)$, where we have used $E(r)$ to denote the contribution of the elementary diagrams, from the TBDF definition, eq. (2.18) we obtain the following expression:

$$g(r_{12}) = f^2(r_{12})e^{N(r_{12})+E(r_{12})} = 1 + X(r_{12}) + N(r_{12}) \tag{2.22}$$

where we have used $X(r_{12})$ to represent the contribution of the non nodal diagrams. It is evident from eq. (2.22) that the TBDF can be expressed in terms of nodal and elementary diagrams only. The use of the $X(r_{12})$ function is established in the literature but it is not necessary. All the nodal diagrams can be calculated in closed form as a folding product of $X(r_{1j})$ with $X(r_{j2})$ or $X(r_{1j})$ with $N(r_{j2})$:

$$N(r_{12}) = \Big(X(r_{1j})|X(r_{j2}) + N(r_{j2})\Big) \tag{2.23}$$

The set of equations (2.23) is known as HyperNetted Chain (HNC) equations. The HNC equations are a non linear set of integral equations. We solve it by using an iterative procedure. We begin the procedure by using the following ansatz

$$X(r_{12}) = f^2(r_{12}) - 1 \quad N(r_{12}) = 0$$

We then use eq. (2.23) in order to obtain the nodal diagrams $N(r_{12})$ and we repeat the process until the convergence is reached. It is evident that this procedure allows us to consider the contribution of all the nodal diagrams, but it does not include that of the elementary ones. There is not a closed expression which allows the evaluation of all the elementary diagrams. The contribution of these diagrams should be calculated by evaluating individually each diagram. If the contribution of the elementary diagrams is not evaluated, we indicate the set of the equations as HNC/0. If we add the contribution of the first order elementary diagram we call the set of eqs. as HNC/1 and so on.

2.3 Fermions

The method described above, gives a correct representation of the ground state of bosonic systems. To describe a fermionic system, it is necessary to take into account the Pauli exclusion principle. Now in the trial wave function

$$\Psi(x_1, ..., x_A) = \prod_{i<j} f(r_{ij})\Phi(x_1, ..., x_A) \tag{2.24}$$

$\Phi(x_1, ..., x_A)$ is a Slater determinant that describes the non interacting system (IPM)

$$\Phi(x_1, ..., x_A) = \frac{1}{\sqrt{A!}} \begin{vmatrix} \phi_1(x_1) & \phi_1(x_2) & \dots & \phi_1(x_A) \\ \phi_2(x_1) & \phi_2(x_2) & \dots & \phi_2(x_A) \\ \vdots & \vdots & \ddots & \vdots \\ \phi_A(x_1) & \phi_A(x_2) & \dots & \phi_A(x_A) \end{vmatrix} \tag{2.25}$$

where for an infinite fermionic system, the single particle wave functions can be written as:

$$\phi_i(x_j) = \frac{1}{\sqrt{V}} \exp\,[i\boldsymbol{k}_i \cdot \boldsymbol{r}_j]\chi_{s_i}(j)\chi_{t_i}(j). \tag{2.26}$$

We have indicated with χ_s and χ_t the Pauli spinors describing the spin and isospin functions. As in the bosonic case, we shall work in the thermodynamic limit, $A, V \to \infty$ keeping $\rho = A/V$ constant. At this point it is convenient to study some properties of Φ^2 which will become useful for the evaluation of the TBDF. First, we can see that Φ^2 can be written as a determinant

$$|\Phi(1, 2, \dots, A)|^2 = \begin{vmatrix} \rho_0(x_1, x_1) & \rho_0(x_1, x_2) & \dots & \rho_0(x_1, x_A) \\ \rho_0(x_2, x_1) & \rho_0(x_2, x_2) & \dots & \rho_0(x_2, x_A) \\ \vdots & \vdots & \ddots & \vdots \\ \rho_0(x_A, x_1) & \rho_0(x_A, x_2) & \dots & \rho_0(x_A, x_A) \end{vmatrix} \tag{2.27}$$

whose elements are given by

$$\rho_0(x_i, x_j) = \sum_\alpha \phi^*_\alpha(x_i)\phi_\alpha(x_j) \tag{2.28}$$

where the sum runs over all the occupied single particle states of the system. Thanks to the orthogonality of the single particle wave functions the following property holds

$$\int dx_j \rho_0(x_i, x_j)\rho_0(x_j, x_k) = \rho_0(x_i, x_k) \tag{2.29}$$

where both a spatial integration and a trace on spin and isospin variables is denoted by dx_j. Now we define the sub-determinant as:

$$\Delta_p(1, ..., p) = \begin{vmatrix} \rho_0(x_1, x_1) & \rho_0(x_1, x_2) & \dots & \rho_0(x_1, x_p) \\ \rho_0(x_2, x_1) & \rho_0(x_2, x_2) & \dots & \rho_0(x_2, x_p) \\ \vdots & \vdots & \ddots & \vdots \\ \rho_0(x_p, x_1) & \rho_0(x_p, x_2) & \dots & \rho_0(x_p, x_p) \end{vmatrix} \qquad p \leq A \tag{2.30}$$

The sub-determinant defined above has the following property

$$\int dx_{p+1} \Delta_{p+1}(1, ..., p+1) = (A-p)\Delta_p(1, ..., p) \tag{2.31}$$

by iteration we obtain

$$\int dx_{p+1} ... dx_A \Delta_A(1, ..., A) = (A-p)!\Delta_p(1, ..., p) \tag{2.32}$$

Consequently, the following property holds

$$\Delta_p = 0 \qquad\qquad p > A \tag{2.33}$$

By making the thermodynamic limit, we obtain that

$$\rho_0(x_i, x_j) = \frac{\rho}{\nu}\ell(k_F r_{ij}) \sum_{s,t} \chi_s^*(i)\chi_t^*(i)\chi_s(j)\chi_t(j) \tag{2.34}$$

In the above equation, ν indicates the spin-isospin degeneration of the system, 4 in the nuclear matter case, and $k_F = (6\pi^2\rho/\nu)^{1/3}$ is the Fermi momentum. In this particular case, $\ell(x)$ is the Slater function [Fan79], and has the following explicit expression:

$$\ell(x) = \frac{3}{x^3}(\sin x - x\cos x). \tag{2.35}$$

Taking into account the properties presented above, we obtain the following expression for the uncorrelated TBDF

$$g_{2,0}(1, 2) \;\; = \;\; \frac{A(A-1)}{\rho^2 A!} \int dx_3 .... dx_A |\Phi|^2 \tag{2.36}$$

$$= \frac{A(A-1)}{\rho^2 A!}(A-2)!\Delta_2(1,2) \tag{2.37}$$

$$= 1 - \frac{1}{\nu}\ell^2(k_F r_{12}) \tag{2.38}$$

In the above equation a trace on the spin and isospin variables of the external particles is understood. This trace gives the $1/\nu$ factor of the final result, with $\nu = 4$ for symmetric nuclear matter. The above expression shows the need of

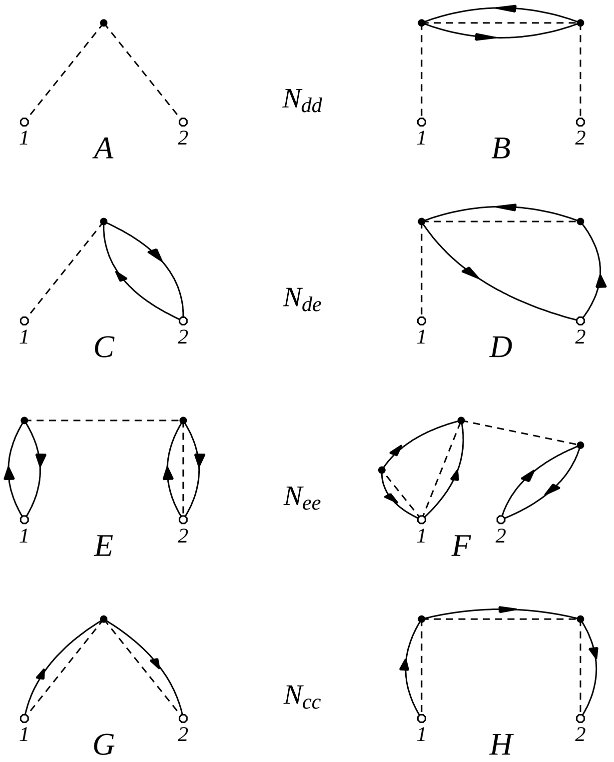

Figure 2.5: Graphical representation of some nodal diagrams for a fermionic system. The oriented lines indicate the statistical correlations. The subscripts *dd*,*de*,*ee*,*cc* represent the different type of diagrams classified with respect to the type of correlations reaching the external points 1 and 2.

inserting a new graphical symbol in the Mayer diagrams in order to identify the presence, and the role, of $\rho_0(x_i, x_j)$. Since ρ_0 forms closed non overlapping loops and we perform the trace in the spin and isospin trace for a permutation of n particles

$$(-1)^{n-1}\rho(x_1,x_2)\rho(x_2,x_3)\ldots\rho(x_{n-1},x_n)\rho(x_n,x_1) =$$
$$(-1)^{n-1}\left(\frac{\rho}{\nu}\right)^n \ell(k_F r_{12})\ell(k_F r_{23})\ldots\ell(k_F r_{n-1n})\ell(k_F r_{n1})$$

$$\begin{aligned} \sum_{s_1,\ldots,s_n} \chi^*_{s_1}(1)\chi^*_{s_2}(2)\ldots\chi^*_{s_n}(n)\chi_{s_n}(1)\chi_{s_1}(2)\ldots\chi_{s_{n-1}}(n) \\ \sum_{t_1,\ldots,t_n} \chi^*_{t_1}(1)\chi^*_{t_2}(2)\ldots\chi^*_{t_n}(n)\chi_{t_n}(1)\chi_{t_1}(2)\ldots\chi_{t_{n-1}}(n) &= \\ -\nu\left(-\frac{\rho}{\nu}\ell(k_F r_{12})\right)\left(-\frac{\rho}{\nu}\ell(k_F r_{13})\right)\ldots\left(-\frac{\rho}{\nu}\ell(k_F r_{n-1n})\right)\left(-\frac{\rho}{\nu}\ell(k_F r_{n1})\right) \end{aligned}$$

where we have included the sign of the permutation. So the new diagrammatic symbol is an oriented line and in the CBF jargon it is called *statistical correlation*, since its presence is due to the Pauli exclusion principle and has to be distinguished from the dynamical correlation $f(r_{ij})$ related to the short-range behavior of the potential. We assign a value of $-\ell(k_F r_{ij})/\nu$ for a statistical line joining the particles i and j since the ρ factor is included in the integration and a factor $-\nu$ in every closed statistical loop. The expression of the correlated TBDF reads:

$$g(x_1,x_2) = \frac{A(A-1)\int dx_3....dx_A \Phi^*(x_1,...,x_A)\prod_{i<j} f(r_{ij})\prod_{k<l} f(r_{kl})\Phi(x_1,....,x_A)}{\rho^2\int dx_1....dx_A|\Psi(x_1,...,x_A)|^2} \tag{2.39}$$

In analogy to the bosonic case, we define $f^2(r_{ij}) = 1 + h(r_{ij})$ then the eq. (2.39) becomes:

$$g(x_1,x_2) = \frac{A(A-1)\int dx_3....dx_A(1+\sum_{i<j} h_{ij} + \sum_{i<j<k} h_{ij}h_{jk} + ...)|\Phi(x_1,....,x_A)|^2}{\rho^2\int dx_1....dx_A(1+\sum_{i<j} h_{ij} + \sum_{i<j<k} h_{ij}h_{jk} + ...)|\Phi(x_1,....,x_A)|^2} \tag{2.40}$$

Then the generical cluster term of TBDF contains both dynamical correlations and statistical correlations. The evaluation of the TBDF requires the calculation of the linked and irreducible diagrams, classified as nodal and elementary, in analogy to the bosonic case. In fig. 2.5 we give a graphical representation of the nodal diagrams classified with respect to the type of correlation reaching the external points 1 and 2. In the A and B diagrams only dynamical correlations reach the external points. These diagrams are labeled with the *dd*(dynamical-dynamical) subscripts (N_{dd}). The C and D diagrams have a dynamical correlation reaching the external point 1 and two statistical correlation lines reaching the external point 2. In this case, we label the nodal diagram with a *de*(dynamical-exchange) subscript (N_{de}). The E and F diagrams, obviously, are labeled by a *ee*(exchange-

exchange) subscript. Finally, the last two diagrams have a statistical correlation which starts from the external point 1 and arrives to the external point 2, forming a open loop. We label these diagrams with the cc(cyclic-cyclic) subscript.
By inserting eq. (2.30) in eq. (2.40) we obtain for the numerator and the denominator of the TBDF:

$$\mathcal{N} = \frac{A(A-1)}{\rho^2} f^2(r_{12}) \int dx_3....dx_A \left(1 + \sum_{i<j} h_{ij} + \sum_{i<j<k} h_{ij}h_{jk} + ...\right) \Delta_A \quad (2.41)$$

$$\mathcal{D} = \int dx_1....dx_A \left(1 + \sum_{i<j} h_{ij} + \sum_{i<j<k} h_{ij}h_{jk} + ...\right) \Delta_A \quad (2.42)$$

The above expressions describe the TBDF with respect to the number of correlations h. We rewrite these sums by grouping the terms containing the same number of points involved, p, and we indicate them as $X^{(p)}(1,2,3,..,p)$. For example

$$X^{(3)}(1,2;i) \quad = \quad h_{1i} + h_{2i} + h_{1i}h_{2i}$$

By using the above definition the numerator and denominator can be rewritten as:

$$\begin{aligned} \mathcal{N} \quad = \quad & \frac{A(A-1)}{\rho^2} f^2(r_{12}) \int dx_3...dx_A \Delta_A \left(1 + \sum_{i=3}^{A} X^{(3)}(1,2;i)\right. \\ & \left. + \sum_{j>i=3}^{A} X^{(4)}(1,2;i,j) + ...\right) \end{aligned}$$

$$\mathcal{D} \quad = \quad \int dx_1...dx_A \Delta_A \left(1 + \sum_{j>i=1}^{A} X^{(2)}(i,j) + \sum_{k>j>i=1}^{A} X^{(3)}(i,j,k) + ...\right)$$

The TBDF can be written as:

$$\begin{aligned} g(x_1,x_2) \quad = \quad & \frac{A(A-1)}{\rho^2} f^2(r_{12}) \int dx_3...dx_A \Delta_A \left(1 + \right. \\ & \left. \sum_{p=3}^{A} \frac{(A-2)!}{(p-2)!(A-p)!} X^{(p)}(1,2;\ldots,p)\right) \cdot \\ & \left[\int dx_1...dx_A \Delta_A \left(1 + \sum_{p=2}^{A} \frac{A!}{p!(A-p)!} X^{(p)}(1,\ldots,p)\right)\right]^{-1} \end{aligned}$$

The factors $\frac{(A-2)!}{(p-2)!(A-p)!}$ and $\frac{A!}{p!(A-p)!}$ take into account the fact that permutations of the p internal points do not change the contribution of the diagram. By using eq. (2.31), it is possible to integrate over all the variables of Δ_A not involved in X^p.

$$\begin{aligned}&\int dx_3....dx_A \frac{(A-2)!}{(p-2)!(A-p)!} X^{(p)}(1,2;...p)\Delta_A = \\ &\int dx_3....dx_p X^{(p)}(1,2;...p)\Delta_p (A-p)! \frac{(A-2)!}{(p-2)!(A-p)!}\end{aligned} \tag{2.43}$$

If we eliminate the factor $A!$ in the numerator and denominator of $g(x_1, x_2)$, they assume the following expressions

$$\begin{aligned}\mathcal{N} &= \frac{f^2(r_{12})}{\rho^2}\left[\Delta_2(1,2) + \sum_{p=3}^{A} \frac{1}{(p-2)!}\int dx_3...dx_p X^{(p)}(1,2;...,p)\Delta_p\right] \\ \mathcal{D} &= \sum_{p=1}^{A} \frac{1}{p!}\int dx_1...dx_p X^{(p)}(...p)\Delta_p\end{aligned} \tag{2.44}$$

Each cluster term (diagram) can be divided in linked and unlinked parts. Let $\mathcal{L}_n(1, 2, i_3, ..., i_n)$ be the linked part containing the external points 1 and 2. In this diagram each internal point $i_3, .., i_n$ is connected to the points 1 and 2 by at least one continous path of dynamical and/or statistical correlations. Let $\mathcal{U}_{p-n}(i_{n+1}, ..., i_p)$ be the unlinked part containing $p - n$ points not connected to 1 and 2, and to no other point of $\mathcal{L}_n$. Any permutation of the internal point of $\mathcal{L}_n$ does not change the contribution of the diagram. The same it happens when the internal points of $\mathcal{U}_{p-n}$ are interchanged. This means that every diagram of the numerator with p internal points can be separated in $\mathcal{L}_n$ and $\mathcal{U}_{p-n}$ in $\frac{(p-2)!}{(n-2)!(p-n)!}$ ways, each of them giving the same contribution. By considering the separation in linked and unlinked diagrams, the numerator can be rewritten as:

$$\begin{aligned}\mathcal{N} = &\frac{f^2(r_{12})}{\rho^2}\left[\Delta_2(1,2) + \sum_{p=3}^{A}\sum_{n=3}^{p} \frac{1}{(p-2)!}\frac{(p-2)!}{(n-2)!(p-n)!}\right. \\ &\left.\int dx_3...dx_n \mathcal{L}_n(1,2,...,n)\int dx_{n+1}...dx_p \mathcal{U}_{p-n}(n+1,...,p)\right] = \\ &f^2(r_{12})\left[\Delta_2(1,2) + \sum_{n+q=3}^{A}\sum_{n=3}^{p+q}\frac{1}{(n-2)!}\int dx_3...dx_n \mathcal{L}_n(1,2,...,n)\right] \\ &\left[\frac{1}{q!}\int dx_{q+1}....dx_{q+n}\mathcal{U}_q(n+1,...,q+n)\right]\end{aligned} \tag{2.45}$$

where in the second equality we have defined $q = p - n$.
Because of eq. (2.33) we can extend up to infinity the sums of (2.45). We have then

$$\begin{aligned}\mathcal{N} &= \frac{f^2(r_{12})}{\rho^2}\left[\Delta_2(1,2) + \sum_{n=3}^{\infty}\frac{1}{(n-2)!}\int dx_3...dx_n \mathcal{L}_n(1,2;...,n)\right] \\ &\left[\sum_{q=1}^{\infty}\frac{1}{q!}\int dx_{q+1}...dx_{q+n}\mathcal{U}_q(n+1,...,q+n)\right] \qquad (2.46)\end{aligned}$$

In the denominator the points (1,2) are integrated, therefore the diagrams we have defined as linked are not present. Only the unlinked diagrams $\mathcal{U}$ contribute to the denominator:

$$\mathcal{D} = f^2(r_{12})\left[\sum_{n=1}^{\infty}\frac{1}{n!}\int dx_1...dx_n \mathcal{U}_n(1,...,n)\right] \qquad (2.47)$$

This expression is identical to that of the unlinked terms of the numerator. In the calculation of the TBDF the denominator cancels the unlinked diagrams of the numerator. We can write

$$g(x_1,x_2) = g(r_{12}) = \frac{f^2(r_{12})}{\rho^2}\left[\Delta_2(1,2) + \sum_{p=3}^{\infty}\frac{1}{(p-2)!}\int dx_3...dx_p \mathcal{L}_p(1,2;...,p)\right] \qquad (2.48)$$

In the above equation the sum on the linked diagrams implies both reducible and irreducible diagrams. The reducible diagrams in the fermionic systems are defined in analogy to the bosonic case. They are diagrams containing a point, the articulation point, which allows the factorization in two subdiagrams. An example of reducible diagrams is given in fig. 2.6. like in the bosonic case, the factorization of the reducible diagrams in two or more sudiagrams is possible because we deal with a translational invariant system, therefore only relative distances between the particles are important.
The mechanism which allows the elimination of the reducible diagrams is very different from that of the boson systems, and it is exact, not limited to $\frac{1}{A}$ terms. The rigorous proof of the cancellation of these diagrams is presented in [Fan74]. We give here the basic idea of the cancellation mechanism. This discussion will become useful when in the finite fermion system we shall present the vertex correction. In the upper part of fig. 2.6 two reducible diagrams are shown. They differ only for the presence of a statistical loop. For the properties of $\rho_0(x_1,x_2)$

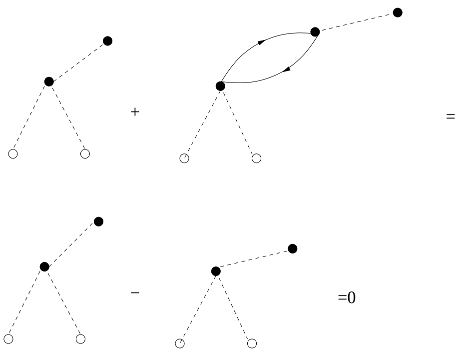

Figure 2.6: Example of cancellation in FHNC diagrams. The statistical loop produce a minus sign, so that the resulting contribution is zero.

this statistical loop does not modify the global contribution of the diagram, but it changes the sign. As it is shown in the lower part of the figure, the global contribution given by the sum of the two diagrams is zero. For a given reducible diagram, in a system composed by an infinite number of particles, it is always possible to find another reducible diagram which has a single additional exchange loop. This is the basic mechanism of the exact cancellation of the reducible diagrams in fermionic systems.

Let us be N_{yz} the sum of all the nodal diagrams of the type specified by the subscripts yz ($y, z = e, d, c$), and X_{yz} the sum of all non-nodal diagrams of the $yz-$type. Indicating with Z_{xy} the generic diagram (X_{xy} or N_{xy}), the Pauli exclusion principle allows only folding products given in Table 2.1:

$Z_{dd}(1,j)$ $Z_{ed}(1,j)$	$Z_{dd}(j,2)$	$Z_{de}(j,2)$	$Z_{ed}(j,2)$	$Z_{ee}(j,2)$
$Z_{de}(1,j)$ $Z_{ee}(1,j)$	$Z_{dd}(j,2)$	$Z_{de}(j,2)$		
$Z_{cc}(1,j)$	$Z_{cc}(j,2)$,	$-l(r_{j2}k_F)/\nu$		

Table 2.1: For each type of nodal diagram we show the allowed folding products depending on the Pauli principle.

The generalization of eq. (2.23) takes into account the above diagrammatic rules and it produces the following set of non-linear integral equations

$$
\begin{aligned}
N_{dd}(r_{12}) &= \Big(X_{dd}(r_{13}) + X_{de}(r_{13})|N_{dd}(r_{32}) + X_{dd}(r_{32})\Big) \\
&+ \Big(X_{dd}(r_{13})|N_{ed}(r_{32}) + X_{ed}(r_{32})\Big) \\
N_{de}(r_{12}) &= \Big(X_{dd}(r_{13}) + X_{de}(r_{13})|N_{de}(r_{32}) + X_{de}(r_{32})\Big) \\
&+ \Big(X_{dd}(r_{13})|N_{ee}(r_{32}) + X_{ee}(r_{32})\Big)
\end{aligned}
$$

$$
\begin{aligned}
N_{ee}(r_{12}) &= \Big(X_{ed}(r_{13}) + X_{ee}(r_{13}) | N_{de}(r_{32}) + X_{de}(r_{32})\Big) \\
&+ \Big(X_{ed}(r_{13}) | N_{ee}(r_{32}) + X_{ee}(r_{32})\Big) \\
N_{cc}(r_{12}) &= \Big(X_{cc}(r_{13}) | N_{cc}(r_{32}) + X_{cc}(r_{32}) - \ell(k_F r_{32})/\nu\Big) \qquad (2.49)
\end{aligned}
$$

The equations for the non-nodal diagrams are

$$
\begin{aligned}
X_{dd}(r_{12}) &= g_{dd}(r_{12}) - N_{dd}(r_{12}) - 1 \qquad (2.50) \\
X_{de}(r_{12}) &= g_{dd}(r_{12})[N_{de}(r_{12}) + E_{de}(r_{12})] - N_{de}(r_{12}) \\
X_{ee}(r_{12}) &= g_{dd}(r_{12})\{N_{ee}(r_{12}) + E_{ee}(r_{12}) + [N_{de}(r_{12} + E_{de}(r_{12})]^2 \\
&\quad -\nu[N_{cc}(r_{12}) + E_{cc}(r_{12}) - \frac{1}{\nu}\ell(k_F r_{12})]^2\} - N_{ee}(r_{12}) \\
X_{cc}(r_{12}) &= g_{dd}(r_{12})[N_{cc}(r_{12}) + E_{cc}(r_{12}) - \frac{1}{\nu}\ell(k_F r_{12})] - N_{cc}(r_{12}) + \frac{1}{\nu}\ell(k_F r_{12})
\end{aligned}
$$

Finally, the partial TBDF are defined as:

$$
\begin{aligned}
g_{dd}(r_{12}) &= f^2(r_{12}) e^{N_{dd}(r_{12}) + E_{dd}(r_{12})} \\
g_{de}(r_{12}) &= N_{de}(r_{12}) + X_{de}(r_{12}) \\
g_{ed}(r_{12}) &= g_{de}(r_{12}) \qquad (2.51) \\
g_{ee}(r_{12}) &= g_{ee,dir}(r_{12}) + g_{ee,exc}(r_{12}) = N_{ee}(r_{12}) + X_{ee}(r_{12}) \\
g_{ee,dir}(r_{12}) &= g_{dd}(r_{12})\Big[N_{ee}(r_{12}) + E_{ee}(r_{12}) + \Big(N_{de}(r_{12}) + E_{de}(r_{12})\Big)^2\Big] \\
g_{ee,exc}(r_{12}) &= -\nu g_{dd}(r_{12})\Big(N_{cc}(r_{12}) + E_{cc}(r_{12}) - \frac{1}{\nu}\ell(k_F r_{12})\Big)^2 \\
g_{cc}(r_{12}) &= N_{cc}(r_{12}) + X_{cc}(r_{12}) - \frac{1}{\nu}\ell(k_F r_{12})
\end{aligned}
$$

2.4 The state dependent correlations

Up to now we have treated only the case of scalar state independent correlations (Jastrow correlations). We shall discuss now what happens when state dependent correlation functions are used. The correlation function we consider has the structure:

$$
\mathcal{F}(1, ..., A) = \mathcal{S}\Big(\prod_{j>i=1}^{A} F_{ij}\Big) = \mathcal{S}\Big(\prod_{j>i=1}^{A}\sum_{p=1}^{6} f_p(r_{ij}) O^p_{ij}\Big) \qquad (2.52)
$$

where the operators are defined as:

$$
O^{p=1,6}_{ij} = 1, \boldsymbol{\tau}_i \cdot \boldsymbol{\tau}_j, \boldsymbol{\sigma}_i \cdot \boldsymbol{\sigma}_j, (\boldsymbol{\sigma}_i \cdot \boldsymbol{\sigma}_j)(\boldsymbol{\tau}_i \cdot \boldsymbol{\tau}_j), S_{ij}, S_{ij}(\boldsymbol{\tau}_i \cdot \boldsymbol{\tau}_j). \qquad (2.53)
$$

where $S_{ij} = 3(\boldsymbol{\sigma}_i \cdot \hat{\boldsymbol{r}}_{ij})(\boldsymbol{\sigma}_j \cdot \hat{\boldsymbol{r}}_{ij}) - \boldsymbol{\sigma}_i \cdot \boldsymbol{\sigma}_j$ is the tensor operator. In eq. (2.52) we have indicated with $\mathcal{S}$ the symmetrization operator. In general, for $j \neq k$ one has $[O^p_{ij}, O^q_{ik}] \neq 0$. Therefore it is necessary the $\mathcal{S}$ operator to garantee the antisymmetrization of the wave function $\Psi(1, ..., A)$.

We are interested in the calculation of expectation value of two-body operators which also depends on the operator (2.53). In general, we can express these operators as

$$B(1, \ldots, A) = \sum_{j>i=1}^{A} \left(\sum_{p=1}^{6} B^p(r_{ij}) O^p_{ij} \right) \tag{2.54}$$

Since the operator is symmetric under the exchange of the particles, the expression of its expectation value can be written as

$$< B >= \frac{A(A-1) \sum_{p=1}^{6} \int dx_1 dx_2 \ldots dx_A \Psi^*(1, \ldots, A) B^p(r_{12}) O^p_{12} \Psi(1, \ldots, A)}{2 \int dx_1 dx_2 \ldots dx_A \Psi^*(1, \ldots, A) \Psi(1, \ldots, A)} \tag{2.55}$$

This suggests to define a state dependent TBDF as:

$$g_p(x_1, x_2) = \frac{A(A-1) \int dx_3 \ldots dx_A \Psi^*(1, \ldots, A) O^p_{12} \Psi(1, \ldots, A)}{\rho^2 \int dx_1 dx_2 \ldots dx_A \Psi^*(1, \ldots, A) \Psi(1, \ldots, A)} \quad p = 1, \ldots, 6 \tag{2.56}$$

where it is understood that the spin and isospin traces are done also for the external particles 1 and 2. We we can write the expectation value of B as

$$< B >= \frac{1}{2} \rho^2 \sum_{p=1}^{6} \int dx_1 dx_2 B^p(r_{12}) g_p(x_1, x_2) \tag{2.57}$$

For the state dependent TBDF we can write:

$$g_p(x_1, x_2) = \frac{A(A-1) \int dx_3 \ldots dx_A \mathcal{S}\Big(\prod_{j>i=1}^{A} F_{ij} \Big) O^p_{12} \mathcal{S}\Big(\prod_{j>i=1}^{A} F_{ij} \Big) \Delta_A(1, \ldots, A)}{\rho^2 \int dx_1 dx_2 \ldots dx_A \mathcal{S}\Big(\prod_{j>i=1}^{A} F_{ij} \Big) \mathcal{S}\Big(\prod_{j>i=1}^{A} F_{ij} \Big) \Delta_A(1, \ldots, A)} \tag{2.58}$$

where we have adopted the convention that Δ_A include all the state dependent operators related to the internal coordinates. In order to perform a cluster expansion we found convenient to write

$$F_{ij} = \sum_{p=1}^{6} f_p(r_{ij}) O_{ij}^p = f_1(r_{ij}) \Big(1 + \sum_{p=2}^{6} \frac{f_p(r_{ij})}{f_1(r_{ij})} O_{ij}^p \Big) = f_1(r_{ij}) \Big(1 + H_{ij} \Big) \qquad (2.59)$$

Since $f_1(r)$ has no operator dependence, the symmetry operator does not act on it. We can write the correlation function as:

$$\mathcal{F}(1, ..., A) = \mathcal{S}\Big(\prod_{j>i=1}^{A} F_{ij} \Big) = \Big(\prod_{j>i=1}^{A} f_1(r_{ij}) \Big) \mathcal{S}\Big(\prod_{j>i=1}^{A} (1 + H_{ij}) \Big) \qquad (2.60)$$

When the H_{ij} are zero we get back the expression of the purely Jastrow correlation previously treated. The operator terms do not commute, in general, this means that in the cluster expansion the various terms depend also from the ordering of the operators. This is a new feature of the theory which should be considered. Eq. (2.60) indicates that each H_{ij} term can be multiplied by any power of $f_1(r_{ij})$ two-body correlation without changing the operator structure. In the many-body jargon this fact is indicated by saying that the Jastrow correlations dress the operator diagrams.

Although the state-dependent case is more involved than the purely Jastrow case, it is possible to demonstrate that the cancellation between the unlinked diagrams of the numerator and all the diagrams of the denominator is still valid. However, the cluster expansion is not any longer irreducible, since the possible presence of operators in the dynamical correlation makes impossible to cancel the reducible diagrams among them. The general treatment of state dependent correlations for nuclear matter was first proposed by R.Wiringa and V. R. Pandharipande in [Pan79].

2.4.1 Traces

The contribution of each diagram is given by two terms. One is the space integral containing the correlation functions f_p and the statistical correlation functions ℓ. The other term is related to the spin and isospin operators and it can be calculated as a trace of ordered products of operators. In order to evaluate the contribution of this second term, let us analyze the permutations of two particles. The direct term is

$$O_{12}^p \rho_0(1,1) \rho_0(2,2) \;\; =$$

$$\rho^2 \frac{1}{\nu^2} \sum_{s_1,s_2,t_1,t_2} \chi^*_{s_1}(1)\chi^*_{s_2}(2)\chi^*_{t_1}(1)\chi^*_{t_2}(2) O^p_{12} \chi_{t_1}(1)\chi_{t_2}(2)\chi_{s_1}(1)\chi_{s_2}(2) \;=\; \rho^2 C(O^p_{12})$$

where we have inserted an operator to show how the notation works, and we have defined the C trace. In the exchange case we have, by using the definition (2.34):

$$\begin{aligned} O^p_{12}\rho_0(1,2)\rho_0(2,1) &= \\ \rho^2 \frac{\ell^2(k_F r_{12})}{\nu^2} \sum_{s_1,s_2,t_1,t_2} \chi^*_{s_1}(1)\chi^*_{s_2}(2)\chi^*_{t_1}(1)\chi^*_{t_2}(2) O^p_{12} \chi_{t_2}(1)\chi_{t_1}(2)\chi_{s_2}(1)\chi_{s_1}(2) &= \\ \rho^2 \ell^2(k_F r_{12}) C\Big(\frac{1}{4}(1+\boldsymbol{\sigma}_1\cdot\boldsymbol{\sigma}_2)(1+\boldsymbol{\tau}_1\cdot\boldsymbol{\tau}_2) O^p_{12}\Big) & \end{aligned}$$

All the traces can be written in terms of C traces adding the corresponding spin isospin exchange operators [Pan79]. For symmetrical nuclear matter, the spin and isospin indices are saturated. For this reason the C traces of operators linear in τ_i or σ_i are zero. For the calculation of the traces of operator products, it is quite convenient to use the Pauli identity:

$$(\boldsymbol{\alpha}_1 \cdot \mathbf{A})(\boldsymbol{\alpha}_1 \cdot \mathbf{B}) = \mathbf{A}\cdot\mathbf{B} + i\boldsymbol{\alpha}_1 \cdot (\mathbf{A}\times\mathbf{B}) \tag{2.61}$$

where $\boldsymbol{\alpha} = \boldsymbol{\sigma}$, $\boldsymbol{\tau}$ and A and B are generic vector operators. By using this identity, we can separate the linear part in τ_i or σ_i from the term independent from spin and isospin. Following [Pan79], we calculate the operator traces for infinite systems. The types of C traces that we need to calculate are essentially:
a) Products of operators acting on the same pair $O^{p>1}_{ij} O^{q>1}_{ij} \cdots O^{r>1}_{ij}$.
b) Single-operator rings $O^{p>1}_{12} O^{q>1}_{23} .....O^{r>1}_{n-1n} O^{s>1}_{n1}$.
c) Multiple operators i.e. the situation when more than two operators reach at an internal point.

2.4.1a Products of operators

We analyze the algebra of the products of operators O^p_{12} acting on the same pair (12) of coordinates. These products can be found in the energy diagrams containing the operator contribution of the interaction. As we have already mentioned, in spin and isospin saturated systems, such as nuclear matter, all operator linear in σ_i and/or τ_i have zero C trace, this is:

$$C(O^p_{12}) = \delta_{p,1} \tag{2.62}$$

We shall consider now the product of two operators $O_{12}^{p>1}O_{12}^{q>1}$. Using eq. (2.61) we obtain:

$$\begin{aligned}(\boldsymbol{\sigma}_1\cdot\boldsymbol{\sigma}_2)(\boldsymbol{\sigma}_1\cdot\boldsymbol{\sigma}_2) &= 3-2\boldsymbol{\sigma}_1\cdot\boldsymbol{\sigma}_2\\ (\boldsymbol{\tau}_1\cdot\boldsymbol{\tau}_2)(\boldsymbol{\tau}_1\cdot\boldsymbol{\tau}_2) &= 3-2\boldsymbol{\tau}_1\cdot\boldsymbol{\tau}_2\\ S_{12}\boldsymbol{\sigma}_1\cdot\boldsymbol{\sigma}_2 &= S_{12}\\ S_{12}\cdot S_{12} &= 6+2\boldsymbol{\sigma}_1\cdot\boldsymbol{\sigma}_2-2S_{12}\end{aligned} \tag{2.63}$$

The C traces of these operators can be written as:

$$C\Big(O_{12}^{p}O_{12}^{q}\Big) = A^p\delta_{pq} \tag{2.64}$$

where the values of A^p are given in tab. 2.2. Moreover from eq. (2.63), it is

p	1	2	3	4	5	6
A^p	1	3	3	9	6	18

Table 2.2: The A^p matrix.

evident that $O_{12}^{p>1}O_{12}^{q>1}$ can be written as sum of operators O_{12}^{r} multiplied by a coefficient. Taking into account all the possible combinations we have:

$$O_{12}^{p}O_{12}^{q} = \sum_r K^{pqr}O_{12}^{r} \tag{2.65}$$

where K^{pqr} is a matrix that can be obtained from eq. (2.63) and whose values are given in appendix A.3.1. By using eqs. (2.64) and (2.65) we can solve the general problem of calculating the expectation values of a product of operators which is reduced to the evaluation of products of K-matrices. For example for three operators we have

$$C\Big(O_{12}^{p}O_{12}^{q}O_{12}^{r}\Big) \;=\; \sum_{ms} K^{pqm}C\Big(O_{12}^{m}O_{12}^{s}\Big) = K^{pqr}A^r$$

Because the operators $O^{p=1,6}$ acting on the same two points commute their order does not matter, therefore we find that $K^{pqr}A^r = K^{prq}A^r = K^{qrp}A^p$.....

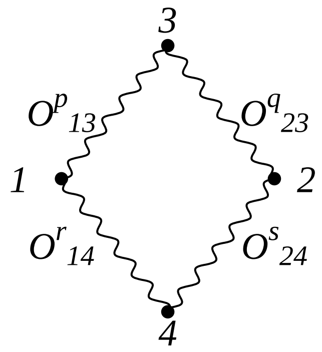

Figure 2.7: Graphical representation of a Single Operator Ring (SOR). A SOR is a diagram where operators form a loop such as only two operators reach the same particle in the loop.

2.4.1b Single operator rings

The order of the operators is also unimportant to calculate the expectation value of a single-operator ring (SOR), see fig.2.7. This can be demonstrated by noting that

$$C\Big(O_{12}^{p_1}O_{23}^{p_2}\dots[O_{ij}^{p_i},O_{jk}^{p_j}]\dots O_{n-1n}^{p_{n-1}}O_{n1}^{p_n}\Big)=0 \tag{2.66}$$

where we have indicated with [,] the commutator, which is zero. Indeed the non commuting terms in eq. (2.66) are linear in τ_j and/or σ_j and their contribution is zero. Let us call O_{12}^p and O_{23}^q two operators acting on the same point 2. Summing over spin and isospin states for the particle 2, and integrating on the azimuthal angle ϕ of $\boldsymbol{r}_{13}$ we obtain

$$\sum_{\sigma_2\tau_2}\int d\phi_2 O_{12}^p O_{23}^q=\sum_r\int d\phi_2 \xi_{123}^{pqr}O_{13}^r \tag{2.67}$$

where ξ_{123}^{pqr} are functions of the three angles in the triangle $1\hat{2}3$ and have the following properties

$$\begin{aligned}
\xi_{123}^{33p} &= \delta_{3p}\\
\xi_{123}^{35p} &= \delta_{5p}\frac{1}{2}(3(\hat{r}_{13}\cdot\hat{r}_{23})^2-1)\\
\xi_{123}^{53p} &= \delta_{5p}\frac{1}{2}(3(\hat{r}_{12}\cdot\hat{r}_{13})^2-1)\\
\xi_{123}^{55p} &= \delta_{3p}(3(\hat{r}_{12}\cdot\hat{r}_{23})^2-1)+\\
&\quad \delta_{5p}\frac{1}{2}\Big[-9((\hat{r}_{13}\cdot\hat{r}_{23})(\hat{r}_{12}\cdot\hat{r}_{13})(\hat{r}_{12}\cdot\hat{r}_{23})-\\
&\quad 3((\hat{r}_{13}\cdot\hat{r}_{23})^2+(\hat{r}_{12}\cdot\hat{r}_{13})^2+(\hat{r}_{12}\cdot\hat{r}_{23})^2)+2\Big]
\end{aligned}$$

$$\begin{aligned} \xi_{123}^{22p} &= \delta_{2p} \\ \xi_{123}^{(k_1+1)(k_2+1)(k_3+1)} &= \xi_{123}^{k_1k_2k_3}(k_i = 1, 3, 5) \end{aligned} \quad (2.68)$$

In Appendix A.2 we show the derivation of these expressions.

2.4.1c Multiple-operators diagrams

Another type of diagrams which occurs in the calculations of the energy is illustrated in fig. 2.8. This diagram presents the case of the product:

$$\mathcal{S}\Big(O_{1m}^a O_{1n}^b O_{mn}^p O_{mn}^q\Big)$$

Its expectation value depends on the ordering of the operators. It is possible to prove that:
The C part of a product of operators of the type $O_{ij}^{p=1,6}$ *is unchanged by a cyclic permutation of the operators.* That is

$$C\Big(O_{ab}^p[\prod O_{ij}^p]\Big) = C\Big([\prod O_{ij}^p]O_{ab}^p\Big) \quad (2.69)$$

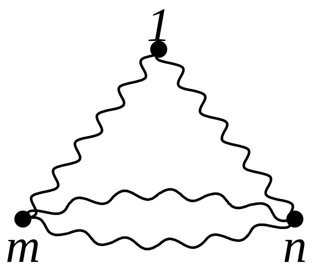

Figure 2.8: Graphical representation of a operator diagram appearing in the energy calculation.

Consequently we have to consider only two different orderings of operators. A first one where the O_{mn}^p and O_{mn}^q are close to each other, and a second one where the two operators are separated by operators of the type O_{m1}^a or O_{n1}^b. In the first case we calculate the expectation value by applying eqs. (2.65) and (2.68). We have:

$$\int d\phi_1 C\Big(O_{mn}^p O_{mn}^q O_{1m}^a O_{1n}^b\Big) = \sum_r K^{pqr} A^r \int d\phi_1 \xi_{m1n}^{abr} \quad (2.70)$$

For the second case we have

$$\int d\phi_1 C\Big(O_{mn}^p O_{m1}^a O_{mn}^q O_{n1}^b\Big) = \sum_r L^{pqr} A^r \int d\phi_1 \xi_{m1n}^{abr} \quad (2.71)$$

where

$$L^{pqr} = \pm K^{pqr} A^r$$

We apply the + sign if

$$C\Big(O^p_{mn}[O^q_{mn}, O^a_{m1}]O^b_{n1}\Big) = 0$$

and the − sign if

$$C\Big(O^p_{mn}\{O^q_{mn}, O^a_{m1}\}O^b_{n1}\Big) = 0$$

where we have indicated with the symbols [,] and {, } the commutator and anti-commutator respectively. The values of matrix L^{pqr} are given in appendix A.3.1.

Another important trace is that of

$$\mathcal{S}\Big(O^a_{1m}O^b_{1m}O^p_{mn}O^q_{mn}\Big)$$

which represent two SOR's that linked in the point m. Again, we have two different orderings depending if the O^p_{mn} and O^q_{mn} are close together or not. In the first case, we obtain

$$C\Big(O^p_{mn}O^q_{mn}O^a_{1m}O^b_{1m}\Big) = A^p\delta_{p,q}A^a\delta_{a,b} \tag{2.72}$$

and in the second, by using the fact that

$$\sum_{\sigma_n\tau_n} O^p_{mn}O^a_{1m}O^q_{mn} = \delta_{p,q}A^p(1 + D_{pa})O^a_{1m} \tag{2.73}$$

we obtain

$$C\Big(O^p_{mn}O^a_{1m}O^q_{mn}O^b_{1m}\Big) = A^p\delta_{p,q}(1 + D_{pa})A^a\delta_{a,b} \tag{2.74}$$

with the matrix D, given in [Pan79].

2.4.2 The Single Operator Chain (SOC) equations

In the Jastrow case, the FHNC equations form a closed set of equations which allow to calculate all the nodal diagrams, and all the composite diagrams formed by the nodal diagrams. As we have already pointed out, from this set of equations the elementary diagrams are excluded. They should be calculated one by one as in the ordinary perturbation expansion.

When operator dependent correlations are used, it is not possible to construct a set of hypernetted equations which allows the calculation of all the nodal and composite diagrams in a closed form. This is due to the non commutativity of the various operators which makes their ordering relevant for the evaluation of the various cluster terms.

However, by assuming the Single Operator Chain (SOC) approximation, it is possible to formulate a closed set of FHNC equations. The SOC approximation consists in considering only those diagrams where a single correlation operator is present between two particles of the diagrams. The two particles can be connected by any number of scalar correlation, this is what we have previously defined as a dressing, but only a $p > 1$ operator should appear.

By using this approximation, we can construct diagrams with arbitrary number of particles. The values of these diagrams will depend only on the number of particles and on the type of operators, and it will be independent of their ordering. The operator between the particle pair can come from the correlation function or from the hamiltonian, see q. (2.54) or in from an exchange line whose contribution is considered by inserting the spin-isospin exchange operator

$$\frac{1}{4}(1 + \boldsymbol{\sigma}_1 \cdot \boldsymbol{\sigma}_2)(1 + \boldsymbol{\tau}_1 \cdot \boldsymbol{\tau}_2).$$

In the present case, we call the nodal functions N contributing to g^p as $N_{xy,p}(r_{ij})$. The subscript p refers to the correspondent operator acting between the i and j external points. The label xy refers to the type of nodal diagram following the same classification used in FHNC: $xy = dd,\ de,\ ed,\ ee,\ cc$. In analogy to the Jastrow case we call $X_{xy,p}(r_{ij})$ the sum of the non nodal diagrams. The set of operators considered is given by eq. (2.53). We denote with the subscripts $\sigma, \tau, \sigma\tau, t, t\tau$ the spin, isospin, spin-isospin, tensor, tensor-isospin dependence of a nodal or non nodal diagram. The method to generate the chain functions N is the same as that used in the traditional FHNC theory: the N functions are generated by folding a X function with a N function or two X functions. Of course the folding integrals are constraint by the Pauli exclusion principle. In fig 2.9 we represent the folding of a simple $X_{dd,\sigma}(r_{13})$ diagram with other $X_{dd,\sigma}(r_{23})$

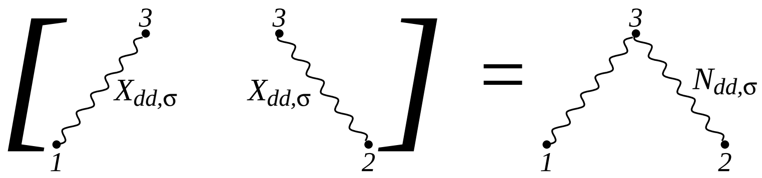

Figure 2.9: Example of folding two X σ-diagrams generating a nodal σ-diagram N.

diagram obtaining a $N_{dd,\sigma}(r_{12})$ diagram. The general expression reads:

$$N_{dd,\sigma}(r_{12}) = \Big(X_{dd,\sigma}(r_{13})|X_{dd,\sigma}(r_{23})\Big) \tag{2.75}$$

Then the folding of two σ-diagrams produces a σ-diagram. The operator dependence generated by the convolution of two diagrams is given by eqs. (2.68). So the σ-chains whose correlations can be either O^σ or O^t contribute to N_σ and N_t respectively, the τ-chains having O^τ correlations give N_τ, and the chains having $O^{\sigma\tau}$ and $O^{t\tau}$ correlations contribute to $N_{\sigma\tau}$ and $N_{t\tau}$. The sum of all the τ-chains connecting 1 and 2 is given by $N_{\tau,xy}(1,2)O^\tau(1,2)$, where N_τ satisfies the integral equations:

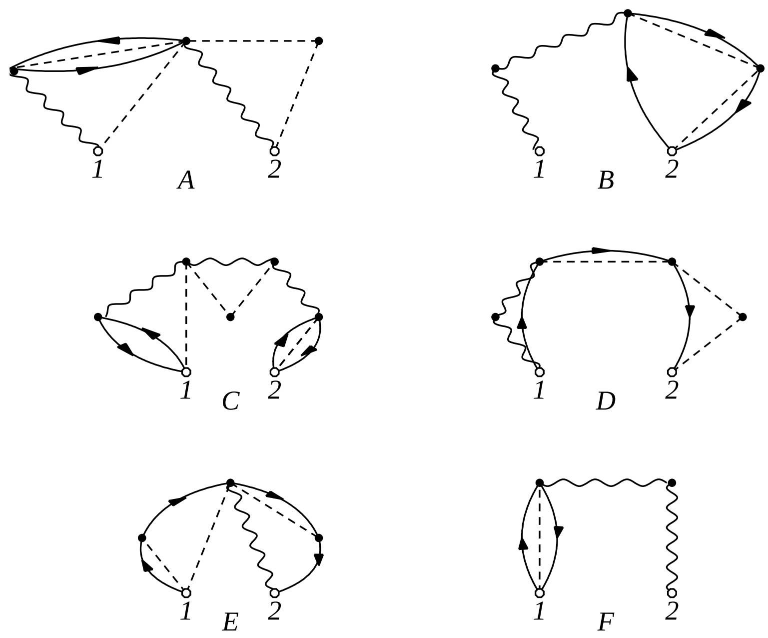

Figure 2.10: Graphical representation of some nodal diagrams in the FHNC/SOC scheme.

$$N_{dd,\tau}(r_{12}) \;=\; \Big(X_{dd,\tau}(r_{13}) + X_{de,\tau}(r_{13})|X_{dd,\tau}(r_{23}) + N_{dd,\tau}(r_{23})\Big) +$$

$$\Big(X_{dd,\tau}(r_{13})|N_{ed,\tau}(r_{23})+N_{ed,\tau}(r_{23})\Big) \tag{2.76}$$

Generalizing eq. (2.76) we can write:

$$N_{xy,r}(r_{12}) \quad = \quad \sum_{x',y'}\sum_{p,q}\Big(X_{xx',p}(r_{13})\xi^{pqr}_{132}|X_{y'y,q}(r_{23})+N_{y'y,q}(r_{23})\Big) \tag{2.77}$$

where $xy = dd, de, ee$, $x'y' = dd, de, ed$, and p, q, r indicate the operator dependence. The expressions of the partial state dependent TBDF's are:

$$\begin{aligned}
g^p(r_{12}) &= g^p_{dd}(r_{12})+2g^p_{de}(r_{12})+g^p_{ee}(r_{12}) && (2.78)\\
g^p_{dd}(r_{12}) &= h_p(r_{12})h^c(r_{12}) = X_{dd,p}(r_{12})+N_{dd,p}(r_{12}) && (2.79)\\
g^p_{de}(r_{12}) &= \Big(h_p(r_{12})N_{de}+f_1^2(r_{12})N_{de,p}(r_{12})\Big)h_c(r_{12})\\
&= X_{de,p}(r_{12})+N_{de,p}(r_{12}) && (2.80)\\
g^p_{ee}(r_{12}) &= \Big[h_p(r_{12})\Big(N_{de}(r_{12})N_{ed}(r_{12})+N_{ee}(r_{12})\Big)\\
&\quad +f_1^2(r_{12})\Big(-\nu L^2(r_{12})\Delta^p+N_{ee,p}(r_{12}) && (2.81)\\
&\quad +2N_{de,p}(r_{12})N_{de}(r_{12})\Big)\Big]h_c(r_{12}) = X_{ee,p}(r_{12})+N_{ee,p}(r_{12})
\end{aligned}$$

where the equations are in the FHNC/0 approximation, i.e. we neglect all the elementary diagrams. In the above eqs. $N_{dd,ed,de,ee}(r_{12})$ indicate the scalar nodal functions, $p > 1$, the function Δ^p is 1 for $p = 1, 2, 3, 4$ and zero for $p = 5, 6$, and

$$h_p(r_{12}) = 2f_p(r_{12})f_1(r_{12})+f_1^2(r_{12})N_{dd,p}(r_{12}) \tag{2.82}$$

$$h_c(r_{12}) = e^{N_{dd}(r_{12})} \tag{2.83}$$

$$L(r_{12}) = N_{cc}(r_{12})-\ell(k_F r_{12})/\nu \tag{2.84}$$

The $N_{cc,p}$ nodal functions are separated in two parts [Pan79], $N_{cc,a}$ and $N_{cc,b}$ (see the diagrams D and E of fig. 2.10), which have the correlation $2f_pf_1$ or $N_{dd,p}$ in the first and last links, respectively. We have:

$$\begin{aligned}
X_{cx,p}(r_{12}) &= \Big(h_pL(r_{12})+f_1^2(r_{12})N_{cx,p}(r_{12})\Big)h^c(r_{12})\\
&\quad -N_{cx,p}(r_{12}) && (2.85)\\
X_{cc}(r_{12}) &= \Big(f_1^2(r_{12})h^c(r_{12})-1\Big)L(r_{12}) && (2.86)
\end{aligned}$$

$$N_{ca,r}(r_{12}) = \sum_{p,q}\left(X_{ca,p}(r_{13})\xi_{132}^{pqr}\Delta^q|X_{cc}(r_{23}) + L(r_{23})\right) \tag{2.87}$$

$$N_{cb,r}(r_{12}) = \sum_{p,q}\left(\Delta^p X_{cc}(r_{13})\xi_{132}^{pqr}|X_{cb,q}(r_{23}) + N_{cb,q}(r_{23})\right) \tag{2.88}$$

where $x = a, b$. Eq. (2.82) is the generalized correlation in the operator case. In particular it contains the single operator correlation dressed by all the scalar correlations. All the diagrams generated by these links are called FHNC/SOC diagrams because they represent a generalization of the Jastrow case. We give a graphical representation of the nodal FHNC/SOC diagrams in fig. 2.10. The diagram A is a $N_{dd,p}(r_{12})$ nodal diagram; the diagrams B and C are examples of $N_{de,p}(r_{12})$ and $N_{ee,p}(r_{12})$ diagrams respectively. Finally, the diagrams D and E are $N_{cc,p}(r_{12})$: we note that the diagram E has an operator correlation on the right side and a operator dependence coming from the exchange loop on the left side; the position of the operators is inverted in the diagram D.

Chapter 3

Finite systems

3.1 FHNC for nuclei

Our goal is to apply the FHNC theory developed for infinite systems to the study of the finite nuclear systems. In analogy to the infinite systems we define the trial wave function as:

$$\Psi(x_1, ..., x_A) = F(x_1, ..., x_A)\Phi(x_1, ..., x_A) \tag{3.1}$$

where for the Jastrow case we have

$$F(x_1, ..., x_A) = \prod_{i<j=1}^{A} f(r_{ij}) \tag{3.2}$$

In the present case the single particle wave functions are not anymore plane waves, but they are solutions of the one-body Schrödinger equation

$$h(x)\phi_i(x) = \epsilon_i\phi_i(x) \tag{3.3}$$

with the hamiltonian

$$h(x) = -\frac{\hbar^2}{2m}\nabla^2 + U(x) \tag{3.4}$$

where $U(x)$ is a one-body potential. The total wave function $\Phi(x_1, ..., x_A)$ is the Slater determinant composed by the wave functions $\phi(x)$.
In analogy to the infinite case the aim is the solution of the variational equation

$$\delta < H >= \delta\frac{< \Psi|H|\Psi >}{< \Psi|\Psi >} = 0 \tag{3.5}$$

Also in this case we perform a cluster expansion, therefore we define OBDF and TBDF in analogy to eqs. (2.9) and by making the cluster expansion of the TBDF we obtain a sum of terms having two external points 1 and 2 (open circle), some internal points (solid circle) connected by the dynamical or statistical correlations which we represent with a dashed line and a oriented line respectively. The definition of the uncorrelated one-body density matrix $\rho_0(x_i, x_j)$ is

$$\rho_0(x_i, x_j) = \sum_{\alpha} \phi^*_\alpha(x_i)\phi_\alpha(x_j) \tag{3.6}$$

Since the system is not infinite, translational invariance is lost and the statistical correlation will depend on more spatial degrees of freedom than the interparticle distance only. For this reason i finite fermionic systems the cluster expansion is no longer irreducible. We shall discuss this point more extensively in the next section.

The simplest case to treat is that of nuclei which have both the proton and neutron shells closed. Because of their spherical symmetry the spatial part of the statistical correlation function depend only on three of the six possible degrees of freedom. For the i and j pair we choose r_i, r_j and r_{ij}, i.e. the distances of the particles from the origin of coordinates and their mutual distance. Our goal is to extend the FHNC/SOC computational scheme to study nuclei with protons and neutrons in a jj coupling scheme, however, we begin our presentation by analyzing the Jastrow correlations case with doubly closed shell nuclei with the same number of protons and neutrons in ls coupling scheme. In this case, we have an isospin saturated system and, since we assume for the single particle wave function the form

$$\Phi(x_i) = R_{nl}(r_i)Y_{lm}(\hat{\boldsymbol{r}}_i)\chi_{s_i}(i)\chi_{t_i}(i)$$

we can write

$$\rho_0(x_i, x_j) = \rho_0(\boldsymbol{r}_i, \boldsymbol{r}_j)\sum_{s,t}\chi^*_s(i)\chi^*_t(i)\chi_s(j)\chi_t(j)$$

with

$$\rho_0(\boldsymbol{r}_i, \boldsymbol{r}_j) = \frac{1}{4\pi}\sum_{nl}(2l+1)R_{nl}(r_i)R_{nl}(r_j)P_l(\hat{\boldsymbol{r}}_i \cdot \hat{\boldsymbol{r}}_j)$$

In the previous eqs. we have indicated with R_{nl} the radial part of the wave function, with Y_{lm} the spherical harmonics and with $P_l(x)$ the Legendre polynomial of grade l.

3.1.1 The vertex corrections

We have seen in the section 1.3 that only connected irreducible diagrams contribute to the cluster expansion of the TBDF in a infinite fermionic system. The disconnected diagrams are exactly canceled by the denominator, and the total contribution of the reducible diagrams is zero due to their mutual cancellation. This last cancellation is a consequence of the translational invariance of systems with infinite number of particles.

The arguments used in 1.3 to show that the unlinked diagrams of the numerator are canceled by the denominator can be repeated also in the finite systems case. The basic point is that all the sums of the various cluster terms can be formally extended up to infinity, since the property (2.33) of the sub-determinant Δ_p ensures that diagrams with a number of particles greater than that of the system do not contribute. By formally extending to infinity the sums of linked and unlinked diagrams of the numerator and the denominator of the TBDF, all the steps of the demonstration presented in section 1.3 can be exactly repeated, showing that, like in the infinite system case, only the linked diagrams contribute to the calculation of the TBDF.

In finite systems the situation changes with the reducible diagrams since their cancellation does not hold any more. In fig. 3.1 we represent two generic dia-

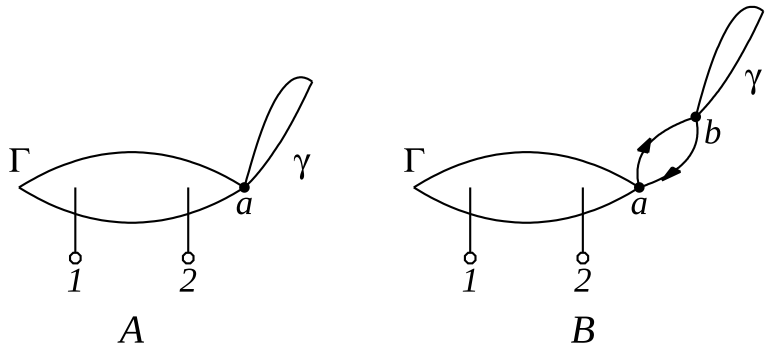

Figure 3.1: Both the diagrams A and B consist of two parts: a first part, labeled Γ, contains the two external points and the other one, γ, contains only internal points. In the diagram A the parts Γ and γ are connected by the articulation point a. In the diagram B they are connected by a closed exchange loop. In the infinite systems their contribution is zero since the exchange loop gives a minus sign due to translational invariance. In finite system there is no translational invariance and therefore these diagrams do not cancel each other.

grams A and B both composed by two parts: a first one containing the external points 1 and 2 and a second one containing only internal points. As we have

discussed in section 1.3, in infinite systems, the contribution of each diagram can be written as the simple product of the contributions of each subdiagrams. We call factorizability this property descending from the translational invariance of the system. Furthermore, since the exchange loop of the B diagram between the a and b articulation points contributes only for a global change of sign, the contribution of the B diagram cancels that of the diagram A. In the finite system, the factorization is not possible since the translational invariance is lost. For this reason, there is not anymore cancellation of all the reducible diagrams.
It is possible to recover the irreducibility of the expansion by introducing the so-called vertex corrections $C(a)$. A graphical representation of this idea is given in fig. 3.2. Every connected diagram can be thought as composed by two parts.

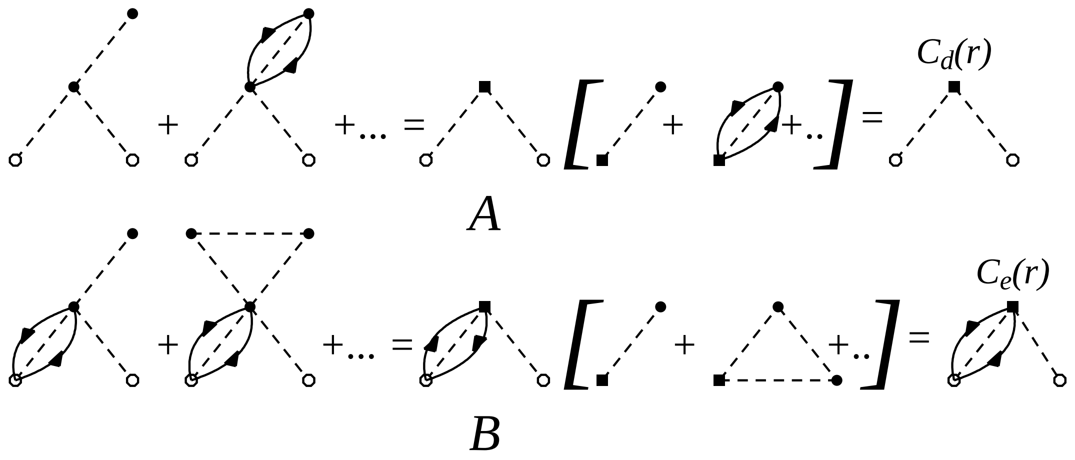

Figure 3.2: We illustrate the idea of vertex correction by giving a graphical representation of few diagrams in the Jastrow case. The diagrams A show a set of reducible diagrams. In those diagrams we can factorize an irreducible diagram which multiplies a set of diagrams having an external point only. The last set of diagrams is the OBD. In the diagrams B, due to the Pauli exclusion principle, we need to exclude the diagrams of the OBD where the articulation point is exchanged. Then we have two types of vertex correction. A first one coinciding with the OBD and labeled as $C_d(\boldsymbol{r})$ and a second one labeled as $C_e(\boldsymbol{r})$ having only the direct diagrams of the OBD.

A first one contains the external points and represents the irreducible part of the diagram. A second part contains any internal points only, and represents the diagrams linked to the irreducible part in the articulation point. The total contribution of these connected diagrams can be written as the folding integral of the irreducible a function $C(a)$ which takes into account the sum of all the factorized diagrams. Since the Pauli principle allows each point to be reached by no more than two exchange lines, we have two types of correlation functions depending on the type of correlation reaching the articulation point. When the articulation point is of type d, i.e. reached only by the dynamical correlations, the Pauli principle is not active, therefore the vertex correction function $C_d(a)$, contains both dynamical and statistical correlations. The vertex correction $C_d(a)$ has an external point, a, which is dressed by the sum of all the possible correlations. This is exactly the definition of the correlated one-body density (OBD). When the articulation points are of type e, i.e. reached by statistical correlations, for the Pauli principle the vertex corrections $C_e(a)$, can contain only the dynamical correlations in the articulation point a. We indicate with $U_d(a)$ the sum of the all diagrams connected and irreducible connected to the point a by dynamical correlations only, and with $U_e(a)$ the sum of the connected and irreducible diagrams where the point a is reached by statistical correlation. In analogy to what we have done in section 1.2, we can construct all the composite diagrams by iterating each diagram. The correct factors multiplying each power term to avoid the double counting allows us to write

$$\begin{aligned} C_e(a) &= 1 + U_d(a) + \frac{1}{2!}U_d^2(a) + \frac{1}{3!}U_d^3(a) + \cdots \\ &= e^{U_d(a)} \end{aligned} \tag{3.7}$$

The iteration of U_e diagrams is not possible because of the Pauli principle. For this reason C_e is formed by all the diagrams connected by a dynamical correlation at any power, as it is shown in eq. (3.7). In addition, we have to multiply by the sum of all the diagrams reaching the point a with an exchange line. We have

$$C_d(a) = e^{U_d(a)}\Big(\rho_0(a) + U_e(a)\Big) = C_e(a)\Big(\rho_0(a) + U_e(a)\Big) = \rho_1(a) \tag{3.8}$$

The construction of the functions $U_{d,e}(1)$ is done by integrating the nodal and non nodal functions $N(1,2)$ and $X(1,2)$ over the coordinate 2. In this procedure we need to take care of possible overcounting problems. We give an example of them by using fig. 3.3. Here we consider only the dd type of diagrams. The diagrams A and B are a product of a $X_{dd}(1,2)$ diagram with a $N_{dd}(1,2)$ diagram and a $N_{dd}(1,2)$ diagram with another $N_{dd}(1,2)$ diagram respectively. In the diagrammatic representation the integration on 2 is represented by changing the white point into a black one. It is evident that after integration on the point 2 the diagrams A and B provide the same contribution. Both diagrams belong to the set $X_{dd}(1,2)$ of the composite diagrams of the TBDF. Then, when we integrate, the

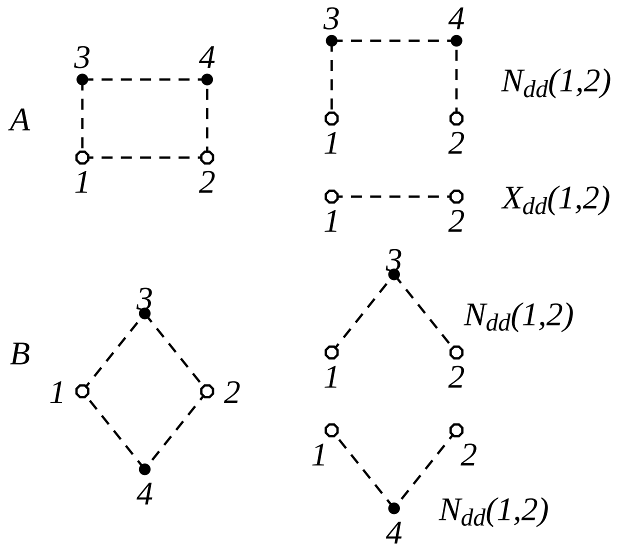

Figure 3.3: Example of double counting in the calculation of the OBD. We show two diagrams A and B generating the same contribution after the integration on the point 2. The diagrams A is thought as product of a $X_{dd}(1,2)$ diagram and a $N_{dd}(1,2)$ diagram. The diagram B is the product of two $N_{dd}(1,2)$ identical diagrams.

$X_{dd}(1,2)$ function on the coordinate 2 we double count the contribution of these diagrams. It is necessary to subtract the contribution of the diagrams coming from the product of two N_{dd} diagrams. The resultant expression is:

$$U_d(1) = \int d\boldsymbol{r}_2 (X_{dd}(1,2) - \frac{1}{2} N_{dd}(1,2) N_{dd}(1,2)\Big) \tag{3.9}$$

where the factor $\frac{1}{2}$ takes into account the symmetry of the diagram. The complete expressions of the $U_{d,e}(1)$ functions are:

$$\begin{aligned}
U_d(1) &= \int d\boldsymbol{r}_2 \Big\{ \Big[X_{dd}(1,2) - E_{dd}(1,2) - S_{dd}(1,2)[g_{dd}(1,2) - 1] \Big] C_d(2) \\
&+ \Big[X_{de}(1,2) - E_{de}(1,2) - S_{dd}(1,2) g_{de}(1,2) \\
&- S_{de}(1,2)[g_{dd}(1,2) - 1] \Big] C_e(2) \Big\} \qquad (3.10) \\
U_e(1) &= \int d\boldsymbol{r}_2 \Big\{ \Big[X_{ed}(1,2) - E_{ed}(1,2) \\
&- S_{dd}(1,2) g_{de}(1,2) - S_{ed}(1,2)[g_{dd}(1,2) - 1] \Big] C_d(2) \\
&+ \Big[X_{ee}(1,2) - E_{ee}(1,2) - S_{dd}(1,2) g_{ee}(1,2) \\
&- S_{ee}(1,2)[g_{dd}(1,2) - 1] - S_{ed}(1,2) g_{de}(1,2)
\end{aligned}$$

$$
-S_{de}(1,2)g_{ed}(1,2)+4S_{cc}(1,2)g_{cc}(1,2)\Big]C_e(2)
$$
$$
-4\rho_0(1,2)[N_{cc}^{\rho x}(1,2)+N_{cc}^{\rho\rho}(1,2)-\rho_0(1,2)]\Big\} \qquad (3.11)
$$

with

$$
S_{xy}(1,2)=\frac{1}{2}N_{xy}(1,2)+E_{xy}(1,2) \qquad (3.12)
$$

and $x,\ y=d,\ e,\ c.$

3.2 The renormalized FHNC equations (RFHNC)

In doubly closed shell nuclei with the same number of protons and neutrons, the closed form used in infinite systems to generate the FHNC equations is modified in two points. The first one is that the different pieces contributing to the TBDF do not depend only on the relative distance of the two interacting particles but also on their distances from the center of the nucleus. The second one is that the equations of the nodal diagrams are modified by the presence of the vertex corrections. Now the equations for the nodal $N_{dd}(1,2)$, $N_{de}(1,2)$, $N_{ee}(1,2)$ diagrams read:

$$
\begin{aligned}
N_{dd}(1,2) &= \Big(X_{dd}(1,3)C_d(3)+X_{de}(1,3)C_e(3)|N_{dd}(3,2)+X_{dd}(3,2)\Big)\\
&+ \Big(X_{dd}(1,3)C_e(3)|N_{ed}(3,2)+X_{ed}(3,2)\Big) &\qquad (3.13)\\
N_{de}(1,2) &= \Big(X_{dd}(1,3)C_d(3)+X_{de}(1,3)C_e(3)|N_{de}(3,2)+X_{de}(3,2)\Big)\\
&+ \Big(X_{dd}(1,3)C_e(3)|N_{ee}(3,2)+X_{ee}(3,2)\Big) &\qquad (3.14)\\
N_{ee}(1,2) &= \Big(X_{ed}(1,3)C_d(3)+X_{ee}(1,3)C_e(3)|N_{de}(3,2)+X_{de}(3,2)\Big)\\
&+ \Big(X_{ed}(1,3)C_e(3)|N_{ee}(3,2)+X_{ee}(3,2)\Big) &\qquad (3.15)
\end{aligned}
$$

In analogy to the infinite system case, the nodals $N_{cc}(1,2)$ diagrams are generated by the folding products of $X_{cc}(1,2)$ or of $\rho_0(1,2)$. In the finite system case, the presence of the vertex corrections generates the possibility of having nodal diagrams where there are two consecutive statistical correlations $\rho_0(i,j)$. In order to explain better the point we remember that:

$$\int d\boldsymbol{r}_3 \rho_0(\boldsymbol{r}_1, \boldsymbol{r}_3)\rho_0(\boldsymbol{r}_3, \boldsymbol{r}_2) = \rho_0(\boldsymbol{r}_1, \boldsymbol{r}_2) \tag{3.16}$$

The above expression is a direct consequence of the orthogonality of the single particle wave functions, and it holds in both infinite and finite systems.

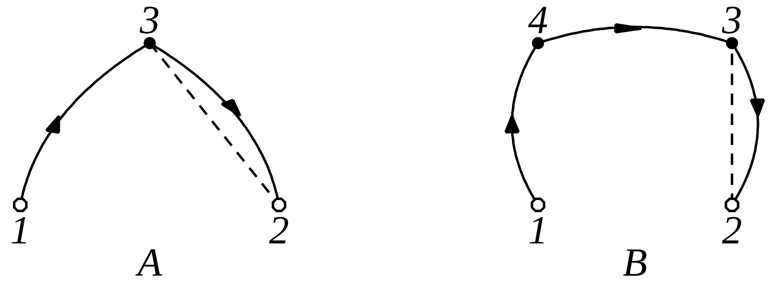

Figure 3.4: Two $N_{cc}(1,2)$ diagrams. In infinite systems they give the same contributions since the integration over 4 in the diagram B recover the diagram A. In finite systems there are the $C(i)$ functions in 3 and 4. For this reason the integration in 4 of the diagram B does not reproduce the result of A.

Now in fig. 3.4 we have represented two nodal diagrams N_{cc} having two different features: in the diagram A the point 3 is reached by a statistical correlation on the side left and a dynamical correlation on right side. In the diagram B only two statistical correlations reach the point 4. In absence of vertex corrections, the two diagrams give the same contribution due to eq. (3.16). For this reason in infinite systems the diagram B is not considered in order to exclude the overcounting. In the finite system case the points 3 and 4 of the diagram B are corrected by the C functions. The integration over 4 cannot be represented anymore by eq.(3.16) and therefore it does not produce the same result of the diagram A. The integral equations are more complicated and we need to classify the nodal function N_{cc} in four different types: $N_{cc}^{xx}(1,2), N_{cc}^{x\rho}(1,2), N_{cc}^{\rho x}(1,2), N_{cc}^{\rho\rho}(1,2)$. The superscripts x and ρ indicate the type of correlation reaching the two external points, x for the dynamical correlation, ρ for the statistical one. The integral equations are:

$$\begin{aligned}
N_{cc}^{xx}(1,2) &= \Big(X_{cc}(1,3)C_e(r_3)|X_{cc}(3,2) + N_{cc}^{xx}(3,2) + N_{cc}^{\rho x}(3,2)\Big) && (3.17)\\
N_{cc}^{x\rho}(1,2) &= \Big(X_{cc}(1,3)C_e(r_3)| - \rho_0(3,2) + N_{cc}^{x\rho}(3,2) + N_{cc}^{\rho\rho}(3,2)\Big) && (3.18)\\
N_{cc}^{\rho x}(1,2) &= -\Big(\rho_0(1,3)C_e(r_3)|X_{cc}(3,2) + N_{cc}^{xx}(3,2)\Big) \\
&\quad -\Big(\rho_0(1,3)[C_e(r_3) - 1]|N_{cc}^{\rho x}(3,2)\Big) && (3.19)\\
N_{cc}^{\rho\rho}(1,2) &= -\Big(\rho_0(1,3)C_e(r_3)|N_{cc}^{x\rho}(3,2)\Big)
\end{aligned}$$

$$-\Big(\rho_0(1,3)[C_e(r_3)-1]|N_{cc}^{\rho\rho}(3,2)-\rho_0(3,2)\Big) \tag{3.20}$$

where

$$N_{cc}(1,2)=N_{cc}^{xx}(1,2)+N_{cc}^{x\rho}(1,2)+N_{cc}^{\rho x}(1,2)+N_{cc}^{\rho\rho}(1,2). \tag{3.21}$$

The full set of eqs.(3.15-3.21) is called Renormalized FHNC equations since they express in terms of irreducible quantities and vertex corrections a cluster expansion that is not irreducible.

3.3 The finite systems with $N \neq Z$

The previous equations hold only for systems with the same number of protons and neutrons and when they are treated as identical particles identified only by their third isospin component. If one of these two hypotheses is not fulfilled, $N \neq Z$ or different radial single particle wave functions for protons and neutrons it is necessary to consider separately the two hadronic densities. Let's consider single particle wave functions of the type

$$\Phi(x_i)=R_{nl}^{t_i}(r_i)Y_{lm}(\hat{\boldsymbol{r}}_i)\chi_{s_i}(i)\chi_{t_i}(i)$$

then we can write

$$\rho_0(x_i,x_j)=\sum_{s,t}\rho_0^t(\boldsymbol{r}_i,\boldsymbol{r}_j)\chi_s^*(i)\chi_t^*(i)\chi_s(j)\chi_t(j)$$

with

$$\rho_0^\alpha(\boldsymbol{r}_i,\boldsymbol{r}_j)=\frac{1}{4\pi}\sum_{nl}(2l+1)R_{nl}^\alpha(r_i)R_{nl}^\alpha(r_j)P_l(\hat{\boldsymbol{r}}_i\cdot\hat{\boldsymbol{r}}_j)$$

where $\alpha=p,n$. Since we have to distinguish two types of statistical correlations also the nodal diagrams related to them, will depend on the isospin. Therefore, we get the following set of integral equations for the nodal diagrams

$$\begin{aligned}
N_{dd}(1,2) &= \sum_{\gamma=p,n}\Big(X_{dd}(1,3)C_d^\gamma(3)+X_{de}^\gamma(1,3)C_e(3)|N_{dd}(3,2)+X_{dd}(3,2)\Big)\\
&+ \sum_{\gamma=p,n}\Big(X_{dd}(1,3)C_e(3)|N_{ed}^\gamma(3,2)+X_{ed}^\gamma(3,2)\Big) \qquad (3.22)\\
N_{de}^\beta(1,2) &= \sum_{\gamma=p,n}\Big(X_{dd}(1,3)C_d^\gamma(3)+X_{de}^\gamma(1,3)C_e(3)|N_{de}^\beta(3,2)+X_{de}^\beta(3,2)\Big)
\end{aligned}$$

$$
\begin{aligned}
& + \sum_{\gamma=p,n} \left(X_{dd}(1,3) C_e(3) | N_{ee}^{\gamma\beta}(3,2) + X_{ee}^{\gamma\beta}(3,2) \right) && (3.23) \\
N_{ee}^{\alpha\beta}(1,2) &= \sum_{\gamma=p,n} \left(X_{ed}^{\alpha}(1,3) C_d^{\gamma}(3) + X_{ee}^{\alpha\gamma}(1,3) C_e(3) | N_{de}^{\beta}(3,2) + X_{de}^{\beta}(3,2) \right) \\
& + \sum_{\gamma=p,n} \left(X_{ed}^{\alpha}(1,3) C_e(3) | N_{ee}^{\gamma\beta}(3,2) + X_{ee}^{\gamma\beta}(3,2) \right) && (3.24) \\
N_{cc}^{(x)\alpha}(1,2) &= \left(X_{cc}^{\alpha}(1,3) C_e(3) | N_{cc}^{\alpha}(3,2) + X_{cc}^{\alpha}(3,2) - \rho_0^{\alpha}(3,2) \right) && (3.25) \\
N_{cc}^{(\rho)\alpha}(1,2) &= -\left(\rho_0^{\alpha}(1,3) C_e(3) | N_{cc}^{(x)\alpha}(3,2) + X_{cc}^{\alpha}(3,2) \right) \\
& - \left(\rho_0^{\alpha}(1,3)(C_e(3) - 1) | N_{cc}^{(\rho)\alpha}(3,2) - \rho_0^{\alpha}(3,2) \right) && (3.26) \\
N_{cc}^{\alpha}(1,2) &= N_{cc}^{(x)\alpha}(1,2) + N_{cc}^{(\rho)\alpha}(1,2) && (3.27)
\end{aligned}
$$

The expressions of the non-nodal, composite and elementary diagrams are

$$
\begin{aligned}
X_{dd}(1,2) &= f^2(r_{12}) e^{N_{dd}(1,2)+E_{dd}(1,2)} - 1 - N_{dd}(1,2) = g_{dd}(1,2) - 1 - N_{dd}(1,2) \\
X_{de}^{\beta}(1,2) &= g_{dd}(1,2) \Big[N_{de}^{\beta}(1,2) + E_{de}^{\beta}(1,2) \Big] - N_{de}^{\beta}(1,2) \\
X_{ee}^{\alpha\beta}(1,2) &= g_{dd}(1,2) \Big[N_{ee}^{\alpha\beta}(1,2) + E_{ee}^{\alpha\beta}(1,2) \\
& + (N_{ed}^{\alpha}(1,2) + E_{ed}^{\alpha}(1,2))(N_{de}^{\beta}(1,2) + E_{de}^{\beta}(1,2)) \\
& - 2\delta_{\alpha\beta}(N_{cc}^{\alpha}(1,2) + E_{cc}^{\alpha}(1,2) - \rho_0^{\alpha}(1,2)) \\
& (N_{cc}^{\beta}(1,2) + E_{cc}^{\beta}(1,2) - \rho_0^{\beta}(1,2)) \Big] - N_{ee}^{\alpha\beta}(1,2) \\
X_{cc}^{\alpha}(1,2) &= g_{dd}(1,2) \Big[N_{cc}^{\alpha}(1,2) + E_{cc}^{\alpha}(1,2) - \rho_0^{\alpha}(1,2) \Big] - N_{cc}^{\alpha}(1,2) + \rho_0^{\alpha}(1,2)
\end{aligned}
$$

3.4 The ls and jj representations

Until now we have used single particle wave function in ls coupling scheme. This corresponds to a single particle hamiltonian of the type

$$
h_i^{\alpha=p,n}(\boldsymbol{r}) = -\frac{\hbar^2}{2m} \nabla_i^2 + U_i^{\alpha=p,n}(r) \tag{3.28}
$$

which does not contain spin-orbit interaction. If the one-body potential of eq.(3.28) contains a spin-orbit interaction term, the single particle wave functions are eigenvectors of j^2, the squared angular momentum and of j_z. These wave functions can be written as:

$$
\phi_{nljm}^{\alpha}(i) = R_{nlj}^{\alpha}(r_i) \sum_{\mu,s} < l\mu \frac{1}{2} s | jm > Y_{l\mu}(\hat{r}_i) \chi_s(i) \chi_\alpha(i) \tag{3.29}
$$

where $< | >$ is the Clebsh-Gordan coefficient. In this case, the uncorrelated OBD can assume the form

$$\rho_0(i,j) = \sum_{s,s',\alpha} \rho_0^{ss'\alpha}(\mathbf{r}_i,\mathbf{r}_j)\chi_s(i)\chi_{s'}(j)\chi_\alpha(i)\chi_\alpha(j) \tag{3.30}$$

with

$$\rho_0^{ss'\alpha}(\mathbf{r}_i,\mathbf{r}_j) = \sum_{nlj} R^\alpha_{nlj}(r_i)R^\alpha_{nlj}(r_j) \sum_{\mu\mu' m} < l\mu\frac{1}{2}s|jm>< l\mu'\frac{1}{2}s'|jm> Y^*_{l\mu}(\hat{r}_i)Y_{l\mu'}(\hat{r}_j)$$

In the jj representation, it is useful to consider separately the uncorrelated density for pairs of particles having parallel or antiparallel spin. We define

$$\rho^\alpha_{0,P}(\mathbf{r}_1,\mathbf{r}_2) = \frac{1}{8\pi}\sum_{nlj}(2j+1)R^\alpha_{nlj}(r_1)R^\alpha_{nlj}(r_2)P_l(\cos\theta_{12}) \tag{3.31}$$

$$\rho^\alpha_{0,A}(\mathbf{r}_1,\mathbf{r}_2) = \frac{1}{4\pi}\sum_{nlj}(-1)^{j-l-1/2}R^\alpha_{nlj}(r_1)R^\alpha_{nlj}(r_2)\sin\theta_{12}P'_l(\cos\theta_{12}) \tag{3.32}$$

where $\cos\theta_{12} = \hat{r}_1\cdot\hat{r}_2$, $P_l(x)$ is the Legendre polynomial of lth degree, and $P'_l(x)$ is its first derivative with respect to x. The equation (3.31) corresponds to pairs of nucleons with parallel spins and this is the only statistical correlation appearing in ls coupling. The function defined in the equation (3.32) is a new statistical correlation between nucleons with antiparallel spins, due to the jj coupling. Sometimes we shall also use the symbol ρ_{oj} to indicate the antiparallel correlation (3.32).
The following properties hold

$$\rho^\alpha_{0,P}(\mathbf{r}_i,\mathbf{r}_j) = \rho_0^{\frac{1}{2}\frac{1}{2}\alpha}(\mathbf{r}_i,\mathbf{r}_j) = \rho_0^{-\frac{1}{2}-\frac{1}{2}\alpha}(\mathbf{r}_i,\mathbf{r}_j) \tag{3.33}$$

$$\rho^\alpha_{0,A}(\mathbf{r}_i,\mathbf{r}_j) = \rho_0^{\frac{1}{2}-\frac{1}{2}\alpha}(\mathbf{r}_i,\mathbf{r}_j) = -\rho_0^{-\frac{1}{2}\frac{1}{2}\alpha}(\mathbf{r}_i,\mathbf{r}_j) \tag{3.34}$$

$$\rho^\alpha_{0,P}(\mathbf{r}_i,\mathbf{r}_j) = \rho^\alpha_{0,P}(\mathbf{r}_j,\mathbf{r}_i) \tag{3.35}$$

$$\rho^\alpha_{0,A}(\mathbf{r}_i,\mathbf{r}_j) = -\rho^\alpha_{0,A}(\mathbf{r}_j,\mathbf{r}_i) \tag{3.36}$$

In order to treat systems in jj representation we have to modify the FHNC equations to take into account the presence of this new statistical correlation. The only diagrams affected by this change are those having an exchange part. Their expressions are given in [Ari96]. We have to point out that by far the most important contributions to the TBDF, and to the energy, are given by the parallel statistical correlation function. For this reason in the following we shall calculate the parallel terms without approximation, and we shall calculate the leading terms of the antiparallel statistical correlation function.

3.5 FHNC/SOC equations for finite systems

3.5.1 Calculation of spin and isospin traces

When a nucleus has different number of protons and neutrons, the system is not saturated in the isospin. In this case, the traces of operators linearly dependent on the isospin operator are not zero. For this reason it is useful to separate the operators in their spin and isospin part:

$$F(i,j)=\sum_{k=1}^{3}\sum_{l=0}^{1} f_{2k-1+l}(r_{ij})O_{ij}^{2k-1+l}=\sum_{l=0}^{1}(\boldsymbol{\tau}_i\cdot\boldsymbol{\tau}_j)^l\sum_{k=1}^{3} f_{2k-1+l}(r_{ij})P_{ij}^{k} \qquad (3.37)$$

with $P_{ij}^{k=1,2,3}=1,\boldsymbol{\sigma}_i\cdot\boldsymbol{\sigma}_j,S_{ij}$.
We know the that uncorrelated density matrix forms nonoverlapping closed loops. Those loops include some operator dependence when the traces are evaluated. Let us consider a n-particle loop:

$$\begin{aligned}
&\rho_0(x_n,x_1)\rho_0(x_1,x_2)\ldots\rho_0(x_{n-1},x_n)=\\
&\quad\sum_{(\alpha_i)(s_i)(s'_i)}\rho_0^{s_1s'_1\alpha_1}(\boldsymbol{r}_n,\boldsymbol{r}_1)\rho_0^{s_2s'_2\alpha_2}(\boldsymbol{r}_1,\boldsymbol{r}_2)\ldots\rho_0^{s_ns'_n\alpha_n}(\boldsymbol{r}_{n-1},\boldsymbol{r}_n)\cdot\\
&\quad\chi^*_{s_1}(n)\chi^*_{s_2}(1)\ldots\chi^*_{s_n}(n-1)\chi_{s'_1}(1)\chi_{s'_2}(2)\ldots\chi_{s'_n}(n)\cdot\\
&\quad\chi^*_{\alpha_1}(n)\chi^*_{\alpha_2}(1)\ldots\chi^*_{\alpha_n}(n-1)\chi_{\alpha_1}(1)\chi_{\alpha_2}(2)\ldots\chi_{\alpha_n}(n)\\
&\quad=\sum_{(\alpha_i)(s_i)(s'_i)}2\rho_0^{s_1s'_1\alpha_1}(\boldsymbol{r}_n,\boldsymbol{r}_1)\rho_0^{s_2s'_2\alpha_2}(\boldsymbol{r}_1,\boldsymbol{r}_2)\ldots\rho_0^{s_ns'_n\alpha_n}(\boldsymbol{r}_{n-1},\boldsymbol{r}_n)\cdot\\
&\quad\chi^*_{s_1}(1)\chi^*_{s_2}(2)...\chi^*_{s_n}(n)[\frac{1}{2^n}(1+\boldsymbol{\sigma}_n\cdot\boldsymbol{\sigma}_{n-1})...(1+\boldsymbol{\sigma}_2\cdot\boldsymbol{\sigma}_1)]\chi_{s'_1}(1)\chi_{s'_2}(2)...\chi_{s'_n}(n)\\
&\chi^*_{\alpha_1}(1)\chi^*_{\alpha_2}(2)...\chi^*_{\alpha_n}(n)[\frac{1}{2^{n-1}}(1+\boldsymbol{\tau}_n\cdot\boldsymbol{\tau}_{n-1})..(1+\boldsymbol{\tau}_2\cdot\boldsymbol{\tau}_1)]\chi_{\alpha_1}(1)\chi_{\alpha_2}(2).....\chi_{\alpha_n}(n)
\end{aligned} \qquad (3.38)$$

From the above expression, we can see that every loop generates a factor 2, and a loop with n particles generates $n-1$ exchange operators

$$\sum_{k=1}^{2}\sum_{l=0}^{1} O_{12}^{2k-1+l} = \sum_{l=0}^{1}(\boldsymbol{\tau}_1\cdot\boldsymbol{\tau}_2)^l \sum_{k=1}^{3}\Delta^k P_{ij}^k \tag{3.39}$$

forming a chain with $\Delta^k = 1-\delta_{k,3}$. We have also an additional 2^{i-n} factor. After these manipulations we have pieces of the form:

$$\frac{1}{2}\sum_{s_1,s_2,\alpha} \rho_0^{s_1,s_2,\alpha}(\boldsymbol{r}_i,\boldsymbol{r}_j)\chi_\alpha^*(j)\chi_\alpha(j)\chi_{s_1}^*(j)\chi_{s_2}(j)$$

that may be written as

$$\sum_\alpha \rho_{0,P}^\alpha(\boldsymbol{r}_i,\boldsymbol{r}_j)\chi_\alpha^*(j)\chi_\alpha(j)\frac{1}{2}\sum_s \chi_s^*(j)\chi_s(j) \tag{3.40}$$

$$+\quad \sum_\alpha \rho_{0,A}^\alpha(\boldsymbol{r}_i,\boldsymbol{r}_j)\chi_\alpha^*(j)\chi_\alpha(j)\frac{1}{2}\sum_s (-1)^{s-1/2}\chi_s^*(j)\chi_{-s}(j) \tag{3.41}$$

The first term is analogous to that of the ls case. The second one is the new statistical link caused by the jj coupling. The behavior in the isospin space is identical to the one previously discussed in the ls coupling. In order to evaluate the diagrams which appear in the calculation of the energy, we give the rules to calculate the operator traces. We distinguish the spin part from the isospin one.

We call $C(O^p)$ the normalized spin trace of the spin operator O^p in the parallel term of eq.(3.41). In analogy to the infinite case we define, only for the spin operator the matrices A, I and J:

$$C(P_{ij}^q P_{ij}^r) = A^q \delta_{qr} \tag{3.42}$$

$$C(P_{ij}^q P_{ij}^r) = \sum_m I^{qrm} P_{ij}^m \tag{3.43}$$

$$\int d\phi_k C(P_{ij}^q P_{ik}^r P_{ij}^s P_{jk}^{s'}) = \sum_m J^{qrm}\int d\phi_k \xi_{ikj}^{ss'm} \tag{3.44}$$

with $A^p = 1,3,6$ for $p=1,2,3$. I is the analogous to K in the infinite case

$$I^{ij1} = \begin{pmatrix} 1 & 0 & 0 \\ 0 & 3 & 0 \\ 0 & 0 & 6 \end{pmatrix} \quad I^{ij2} = \begin{pmatrix} 0 & 1 & 0 \\ 1 & -2 & 0 \\ 0 & 0 & 2 \end{pmatrix} \quad I^{ij3} = \begin{pmatrix} 0 & 0 & 1 \\ 0 & 0 & 1 \\ 1 & 1 & -2 \end{pmatrix} \tag{3.45}$$

and J represents the role of the L of the infinite case

$$J^{ij1} = \begin{pmatrix} 1 & 0 & 0 \\ 0 & 3 & 0 \\ 0 & 0 & 6 \end{pmatrix} \quad J^{ij2} = \begin{pmatrix} 0 & 3 & 0 \\ 3 & 6 & 0 \\ 0 & 0 & -6 \end{pmatrix} \quad J^{ij3} = \begin{pmatrix} 0 & 0 & 6 \\ 0 & 0 & -6 \\ 6 & -6 & 12 \end{pmatrix} \tag{3.46}$$

To evaluate the spin part of the SOR traces, it is convenient to consider that

$$\sum_{\sigma_k \tau_k} \int d\phi_k P^q_{ik} P^r_{kj} = \sum_m \int d\phi_k \xi^{qrm}_{ikj} P^m_{ij} \tag{3.47}$$

with:

$$\begin{aligned}
\xi^{1qr}_{132} &= \xi^{q1r}_{132} = \xi^{qr1}_{132} = \delta_{q1}\delta_{r1} && (3.48)\\
\xi^{22q}_{132} &= \delta_{q2} && (3.49)\\
\xi^{23q}_{132} &= \delta_{q3}\frac{1}{2}(3(\hat{r}_{12}\cdot\hat{r}_{23})^2 - 1) && (3.50)\\
\xi^{32q}_{132} &= \delta_{q3}\frac{1}{2}(3(\hat{r}_{12}\cdot\hat{r}_{13})^2 - 1) && (3.51)\\
\xi^{33q}_{132} &= \delta_{q2}(3(\hat{r}_{13}\cdot\hat{r}_{23})^2 - 1) \\
&+ \delta_{q3}\frac{1}{2}(2 - 3((\hat{r}_{12}\cdot\hat{r}_{13})^2 + (\hat{r}_{12}\cdot\hat{r}_{23})^2 + (\hat{r}_{13}\cdot\hat{r}_{23})^2) \\
&+ 9\hat{r}_{12}\cdot\hat{r}_{13}\hat{r}_{12}\cdot\hat{r}_{23}\hat{r}_{13}\cdot\hat{r}_{23}) && (3.52)
\end{aligned}$$

Now there is an additional trace corresponding to the antiparallel statistical function. We define

$$C_j(O^p_{12}) = \frac{1}{4}\sum_{s_1,s_2}(-1)^{s_1+s_2}\chi^*_{s_1}(1)\chi^*_{s_2}(2)O^p_{12}\chi_{-s_1}(1)\chi_{-s_2}(2)$$

and we have:

$$\begin{aligned}
C_j(1) &= 0 && (3.53)\\
C_j(\boldsymbol{\sigma}_1\cdot\boldsymbol{\sigma}_2) &= 1 && (3.54)\\
C_j(S_{12}) &= 0 && (3.55)
\end{aligned}$$

We see that the contribution of the identity operator is zero and the contribution of the spin operator is one, just the opposite of the case of parallel spins. Equation (3.55) has been obtained supposing the spherical symmetry of the system.

In order to calculate the isospin traces, we consider that:

$$(\boldsymbol{\tau}_i \cdot \boldsymbol{\tau}_j)^n = a_n + (1 - a_n)\boldsymbol{\tau}_i \cdot \boldsymbol{\tau}_j \tag{3.56}$$

with $a_{n+1} = 3(1 - a_n)$ and $a_0 = 1$. Let us begin with the simplest trace

$$\chi_n^{\alpha\beta} = \chi_\alpha^*(1)\chi_\beta^*(2)\,(\boldsymbol{\tau}_1 \cdot \boldsymbol{\tau}_2)^n\,\chi_\alpha(1)\chi_\beta(2) \tag{3.57}$$

since $\chi_0^{\alpha\beta} = 1$ and $\chi_1^{\alpha\beta} = 2\delta_{\alpha\beta} - 1$, we can easily see that

$$\chi_n^{\alpha\beta} = 2a_n - 1 + 2(1 - a_n)\delta_{\alpha\beta} \tag{3.58}$$

The rest of the isospin traces involves three particles. The result can be expressed as:

$$\begin{aligned}
&\chi_{l_1 l_2 l_3 l_4 l_5}^{\alpha\beta\gamma}(i) = \\
&\chi_\alpha^*(1)\chi_\beta^*(2)\chi_\gamma^*(3)(\boldsymbol{\tau}_1 \cdot \boldsymbol{\tau}_2)^{l_1}(\boldsymbol{\tau}_i \cdot \boldsymbol{\tau}_3)^{l_2}(\boldsymbol{\tau}_1 \cdot \boldsymbol{\tau}_2)^{l_3}(\boldsymbol{\tau}_i \cdot \boldsymbol{\tau}_3)^{l_4}(\boldsymbol{\tau}_1 \cdot \boldsymbol{\tau}_2)^{l_5}\chi_\alpha(1)\chi_\beta(2)\chi_\gamma(3) \\
&= b_1' + b_2'\delta_{\alpha\beta} + b_3'\delta_{\alpha\gamma} + b_4'\delta_{\beta\gamma} + b_5'\delta_{\alpha\beta}\delta_{\alpha\gamma}\delta_{\beta\gamma}
\end{aligned} \tag{3.59}$$

and considering that:

$$\delta_{\alpha\beta}\delta_{\alpha\gamma}\delta_{\beta\gamma} = \frac{1}{2}\left(\delta_{\alpha\beta} + \delta_{\alpha\gamma} + \delta_{\beta\gamma} - 1\right) \tag{3.60}$$

we can write:

$$\chi_{l_1 l_2 l_3 l_4 l_5}^{\alpha\beta\gamma}(i) = b_1 + b_2\delta_{\alpha\beta} + b_3\delta_{\alpha\gamma} + b_4\delta_{\beta\gamma} \tag{3.61}$$

with $b_1 = b_1' - b_5'/2$ and $b_i = b_i' + b_5'/2$ for $i = 2, 3, 4$. In the above eqs. all the l indices can assume the values zero or one. Let us then discuss the different cases for l_2 and l_4. First we consider $l_2 = l_4 = 0$. We have

$$\chi_{l_1 0 l_3 0 l_5}^{\alpha\beta\gamma}(i) = \chi_{l_1 + l_3 + l_5}^{\alpha\beta} \tag{3.62}$$

For the cases when one of the indices is one and the other is zero, it is convenient to define:

$$\chi_{l_1 l_2}^{\alpha\beta\gamma}(i) = \chi_\alpha^*(1)\chi_\beta^*(2)\chi_\gamma^*(3)(\boldsymbol{\tau}_1 \cdot \boldsymbol{\tau}_2)^{l_1}(\boldsymbol{\tau}_i \cdot \boldsymbol{\tau}_3)(\boldsymbol{\tau}_1 \cdot \boldsymbol{\tau}_2)^{l_2}\chi_\alpha(1)\chi_\beta(2)\chi_\gamma(3) \tag{3.63}$$

then

$$\begin{aligned}\chi^{\alpha\beta\gamma}_{l_1 l_2}(i) &= a_{l_1}a_{l_2}\chi^{\alpha\beta\gamma}_{00}(i) + \left(a_{l_1}(1-a_{l_2}) + (1-a_{l_1})a_{l_2}\right)\chi^{\alpha\beta\gamma}_{10}(i) + \\ &\quad (1-a_{l_1})(1-a_{l_2})\chi^{\alpha\beta\gamma}_{11}(i)\end{aligned} \tag{3.64}$$

The values of $\chi^{\alpha\beta\gamma}_{l_1 l_2}(i)$ are given in tab. 3.1.

		$\chi^{\alpha\beta\gamma}_{l_1 l_2}(1)$				$\chi^{\alpha\beta\gamma}_{l_1 l_2}(2)$			
l_1	l_2	b_1	b_2	b_3	b_4	b_1	b_2	b_3	b_4
0	0	–1	0	2	0	–1	0	0	2
1	0	–1	0	0	2	–1	0	2	0
1	1	–1	0	–2	4	–1	0	4	–2

Table 3.1: The $\chi^{\alpha\beta\gamma}_{l_1 l_2}(i)$ values.

Using all this we can get

$$\chi^{\alpha\beta\gamma}_{l_1 0 l_3 1 l_5}(i) = \chi^{\alpha\beta\gamma}_{l_1+l_3 l_5}(i) \tag{3.65}$$

$$\chi^{\alpha\beta\gamma}_{l_1 1 l_3 0 l_5}(i) = \chi^{\alpha\beta\gamma}_{l_1 l_3+l_5}(i) \tag{3.66}$$

Finally we must analyze the case when $l_2 = l_4 = 1$. A first simplification to this is

$$\chi^{\alpha\beta\gamma}_{l_1 1 l_3 1 l_5}(i) = a_{l_3}\left(3\chi^{\alpha\beta}_{l_1+l_5} - 2\chi^{\alpha\beta\gamma}_{l_1 l_5}(i)\right) + (1-a_{l_3})\chi^{\alpha\beta\gamma}_{l_1 1 1 1 l_5}(i) \tag{3.67}$$

After that we can write:

$$\begin{aligned}\chi^{\alpha\beta\gamma}_{l_1 1 1 1 l_5}(i) &= a_{l_1}a_{l_5}\chi^{\alpha\beta\gamma}_{01110}(i) + \left(a_{l_1}\ (1-a_{l_5}) + (1-a_{l_1})a_{l_5}\right)\chi^{\alpha\beta\gamma}_{11110}(i) + \\ &\quad (1-a_{l_1})\,(1-a_{l_5})\,\chi^{\alpha\beta\gamma}_{11111}(i)\end{aligned} \tag{3.68}$$

where the numerical values of the $\chi^{\alpha\beta\gamma}_{l_1 000 l_2}(i)$ are given in tab. 3.2.

		$\chi^{\alpha\beta\gamma}_{l_1 111 l_2}(1)$				$\chi^{\alpha\beta\gamma}_{l_1 111 l_2}(2)$			
l_1	l_2	b_1	b_2	b_3	b_4	b_1	b_2	b_3	b_4
0	0	–1	–2	0	4	–1	–2	4	0
1	0	–7	4	4	0	–7	4	0	4
1	1	11	–14	8	–4	11	–14	–4	8

Table 3.2: The $\chi^{\alpha\beta\gamma}_{l_1 000 l_2}(i)$ values.

The last set of traces to be analyzed is

$$\eta^{\alpha\beta\gamma}_{l_1 l_2 l_3 l_4 l_5}(i) = \chi^*_\alpha(1)\chi^*_\beta(2)\chi^*_\gamma(3)(\boldsymbol{\tau}_1\cdot\boldsymbol{\tau}_2)^{l_1}(\boldsymbol{\tau}_i\cdot\boldsymbol{\tau}_3)^{L_2}(\boldsymbol{\tau}_1\cdot\boldsymbol{\tau}_2)^{l_3}(\boldsymbol{\tau}_{3-i}\cdot\boldsymbol{\tau}_3)^{L_4}(\boldsymbol{\tau}_1\cdot\boldsymbol{\tau}_2)^{l_5}\chi_\alpha(1)\chi_\beta(2)\chi_\gamma(3) \tag{3.69}$$

with $i = 1, 2$ and $L_2 = \delta_{i1} l_2 + \delta_{i2} l_4$ and $L_4 = \delta_{i1} l_4 + \delta_{i2} l_2$. Since:

$$\eta^{\alpha\beta\gamma}_{l_1 0 l_3 0 l_5}(i) = \chi^{\alpha\beta}_{l_1+l_3+l_5} \tag{3.70}$$

$$\eta^{\alpha\beta\gamma}_{l_1 1 l_3 0 l_5}(1) = \chi^{\alpha\beta\gamma}_{l_1 l_3+l_5}(1) \tag{3.71}$$

$$\eta^{\alpha\beta\gamma}_{l_1 1 l_3 0 l_5}(2) = \chi^{\alpha\beta\gamma}_{l_1+l_3 l_5}(1) \tag{3.72}$$

$$\eta^{\alpha\beta\gamma}_{l_1 0 l_3 1 l_5}(1) = \chi^{\alpha\beta\gamma}_{l_1+l_3 l_5}(2) \tag{3.73}$$

$$\eta^{\alpha\beta\gamma}_{l_1 0 l_3 1 l_5}(2) = \chi^{\alpha\beta\gamma}_{l_1 l_3+l_5}(2) \tag{3.74}$$

we have only to analyze the case when $l_2 = l_4 = 1$. We can write

$$\begin{aligned} \eta^{\alpha\beta\gamma}_{l_1 1 l_3 1 l_5}(i) = {} & a_{l_1} a_{l_3}\left(a_{l_5}\eta^{\alpha\beta\gamma}_{01010}(i) + (1-a_{l_5})\eta^{\alpha\beta\gamma}_{01011}(i)\right) + \\ & (1-a_{l_1})a_{l_3}\left(a_{l_5}\eta^{\alpha\beta\gamma}_{11010}(i) + (1-a_{l_5})\eta^{\alpha\beta\gamma}_{11011}(i)\right) + \\ & a_{l_1}(1-a_{l_3})\left(a_{l_5}\eta^{\alpha\beta\gamma}_{01110}(i) + (1-a_{l_5})\eta^{\alpha\beta\gamma}_{01111}(i)\right) + \\ & (1-a_{l_1})(1-a_{l_3})\left(a_{l_5}\eta^{\alpha\beta\gamma}_{11110}(i) + (1-a_{l_5})\eta^{\alpha\beta\gamma}_{11111}(i)\right) \end{aligned} \tag{3.75}$$

The values of the $\eta^{\alpha\beta\gamma}_{l_1 1 l_3 1 l_5}(i)$ are given in tab. 3.3.

			$\eta^{\alpha\beta\gamma}_{l_1 1 l_3 1 l_5}(1)$				$\eta^{\alpha\beta\gamma}_{l_1 1 l_3 1 l_5}(2)$			
l_1	l_3	l_5	b_1	b_2	b_3	b_4	b_1	b_2	b_3	b_4
0	0	0	–1	2	0	0	–1	2	0	0
1	0	0	5	–4	4	–4	5	–4	–4	4
0	1	0	5	4	–4	–4	5	4	–4	–4
0	0	1	5	–4	–4	4	5	–4	4	–4
1	1	0	11	–2	0	–8	11	–2	–8	0
1	0	1	–13	14	0	0	–13	14	0	0
0	1	1	11	–2	–8	0	11	–2	0	–8
1	1	1	–7	16	–4	–4	–7	16	–4	–4

Table 3.3: The $\eta^{\alpha\beta\gamma}_{l_1 1 l_3 1 l_5}(i)$ values.

3.5.2 The FHNC/SOC equations for non saturated isospin systems

Before treating the operator case and for the sake completeness we give the complete expression of the nodal functions N and of the functions X including the vertex correction for the case of scalar correlations:

$$
\begin{aligned}
g_{dd}^{\alpha\beta}(1,2) &= f_1^2(r_{12})e^{N_{dd}^{\alpha\beta}(1,2)+E_{dd}^{\alpha\beta}(1,2)} \\
&= 1+N_{dd}^{\alpha\beta}(1,2)+X_{dd}^{\alpha\beta}(1,2) && (3.76)\\
g_{de}^{\alpha\beta}(1,2) &= g_{dd}^{\alpha\beta}(1,2)\Big[N_{de}^{\alpha\beta}(1,2)+E_{de}^{\alpha\beta}(1,2)\Big] \\
&= N_{de}^{\alpha\beta}(1,2)+X_{de}^{\alpha\beta}(1,2) && (3.77)\\
g_{ee}^{\alpha\beta}(1,2) &= g_{ee,dir}^{\alpha\beta}(1,2)+2\delta_{\alpha\beta}g_{ee,exc}^{\alpha\beta}(1,2)+2\delta_{\alpha\beta}g_{ee,excj}^{\alpha\beta}(1,2) \\
&= N_{ee}^{\alpha\beta}(1,2)+X_{ee}^{\alpha\beta}(1,2) && (3.78)\\
g_{ee,dir}^{\alpha\beta}(1,2) &= g_{dd}(1,2)\Big[N_{ee}^{\alpha\beta}(1,2)+E_{ee}^{\alpha\beta}(1,2) \\
&+ (N_{ed}^{\alpha\beta}(1,2)+E_{ed}^{\alpha\beta}(1,2))(N_{de}^{\alpha\beta}(1,2)+E_{de}^{\alpha\beta}(1,2))\Big] && (3.79)\\
g_{ee,exc}^{\alpha\beta}(1,2) &= -g_{dd}(1,2)(N_{cc}^{\alpha}(1,2)+E_{cc}^{\alpha}(1,2)-\rho_0^{\alpha}(1,2))\cdot \\
&\quad (N_{cc}^{\beta}(1,2)+E_{cc}^{\beta}(1,2)-\rho_0^{\beta}(1,2)) && (3.80)\\
g_{ee,excj}^{\alpha\beta}(1,2) &= -g_{dd}(1,2)(N_{ccj}^{\alpha}(1,2)+E_{ccj}^{\alpha}(1,2)-\rho_{0j}^{\alpha}(1,2))\cdot \\
&\quad (N_{ccj}^{\beta}(1,2)+E_{ccj}^{\beta}(1,2)-\rho_{0j}^{\beta}(1,2)) && (3.81)\\
g_{cc}^{\alpha}(1,2) &= g_{dd}(1,2)[N_{cc}^{\alpha}(1,2)+E_{cc}^{\alpha}(1,2)-\rho_0^{\alpha}(1,2)] \\
&= N_{cc}^{\alpha}(1,2)+X_{cc}^{\alpha}(1,2)-\rho_0^{\alpha}(1,2) && (3.82)\\
g_{ccj}^{\alpha}(1,2) &= g_{dd}(1,2)[N_{ccj}^{\alpha}(1,2)+E_{cc}^{\alpha}(1,2)-\rho_{0j}^{\alpha}(1,2)] \\
&= N_{ccj}^{\alpha}(1,2)+X_{ccj}^{\alpha}(1,2)-\rho_{0j}^{\alpha}(1,2) && (3.83)
\end{aligned}
$$

where we have used $\rho_0^{\alpha}(1,2)=\rho_{0P}^{\alpha}(1,2)$ and $\rho_{0j}^{\alpha}(1,2)=\rho_{0A}^{\alpha}(1,2)$.

Nodal diagrams

$$
N_{xy}^{\alpha\beta}(1,2)=\sum_{\gamma=p,n}\sum_{x'y'=d,e}(X_{xx'}^{\alpha\gamma}(1,3)V_{x'y'}^{\gamma}(3)|N_{y'y}^{\gamma\beta}(3,2)+X_{y'y}^{\gamma\beta}(3,2)) \qquad (3.84)
$$

with $(x'y')=dd,de,ed$ and $V_{xy}^{\gamma}(i)=\begin{cases} C_d^{\gamma}(i) & \text{for} \quad (xy)=dd \\ C_e^{\gamma}(i) & \qquad \text{otherwise}\end{cases}$

$$
N_{cc}^{(x)\alpha}(1,2) = (X_{cc}^{\alpha}(1,3)C_e^{\alpha}(3)|N_{cc}^{\alpha}(3,2)+X_{cc}^{\alpha}(3,2)-\rho_0^{\alpha}(3,2))
$$

$$
\begin{aligned}
& - \quad (X^{\alpha}_{ccj}(1,3)C^{\alpha}_{e}(3)|N^{\alpha}_{ccj}(3,2) + X^{\alpha}_{ccj}(3,2) - \rho^{\alpha}_{0j}(3,2)) \quad (3.85)\\
N^{(\rho)\alpha}_{cc}(1,2) &= -(\rho^{\alpha}_{0}(1,3)C^{\alpha}_{e}(3)|N^{(x)\alpha}_{cc}(3,2) + X^{\alpha}_{cc}(3,2))\\
&- \quad (\rho^{\alpha}_{0}(1,3)(C^{\alpha}_{e}(3)-1)|N^{(\rho)\alpha}_{cc}(3,2) - \rho^{\alpha}_{0}(3,2))\\
&+ \quad (\rho^{\alpha}_{0j}(1,3)C^{\alpha}_{e}(3)|N^{(x)\alpha}_{ccj}(3,2) + X^{\alpha}_{ccj}(3,2))\\
&+ \quad (\rho^{\alpha}_{0j}(1,3)(C^{\alpha}_{e}(3)-1)|N^{(\rho)\alpha}_{ccj}(3,2) - \rho^{\alpha}_{0j}(3,2)) \quad (3.86)\\
N^{(x)\alpha}_{ccj}(1,2) &= (X^{\alpha}_{ccj}(1,3)C^{\alpha}_{e}(3)|N^{\alpha}_{cc}(3,2) + X^{\alpha}_{cc}(3,2) - \rho^{\alpha}_{0}(3,2))\\
&+ \quad (X^{\alpha}_{cc}(1,3)C^{\alpha}_{e}(3)|N^{\alpha}_{ccj}(3,2) + X^{\alpha}_{ccj}(3,2) - \rho^{\alpha}_{0j}(3,2)) \quad (3.87)\\
N^{(\rho)\alpha}_{ccj}(1,2) &= -(\rho^{\alpha}_{0j}(1,3)C^{\alpha}_{e}(3)|N^{(x)\alpha}_{cc}(3,2) + X^{\alpha}_{cc}(3,2))\\
&- \quad (\rho^{\alpha}_{0j}(1,3)(C^{\alpha}_{e}(3)-1)|N^{(\rho)\alpha}_{cc}(3,2) - \rho^{\alpha}_{0}(3,2))\\
&- \quad (\rho^{\alpha}_{0}(1,3)C^{\alpha}_{e}(3)|N^{(x)\alpha}_{ccj}(3,2) + X^{\alpha}_{ccj}(3,2))\\
&- \quad (\rho^{\alpha}_{0}(1,3)(C^{\alpha}_{e}(3)-1)|N^{(\rho)\alpha}_{ccj}(3,2) - \rho^{\alpha}_{0j}(3,2)) \quad (3.88)
\end{aligned}
$$

where we have defined $N^{(x)\alpha}_{cc}(1,2) = N^{xx\alpha}_{cc}(1,2) + N^{x\rho\alpha}_{cc}(1,2)$ and $N^{(\rho)\alpha}_{cc}(1,2) = N^{\rho x\alpha}_{cc}(1,2) + N^{\rho\rho\alpha}_{cc}(1,2)$

Vertex corrections

$$
\begin{aligned}
U^{\alpha}_{d}(1) &= \int d\mathbf{r}_2 \sum_{\beta=p,n} \{C^{\beta}_{d}(2)[X^{\alpha\beta}_{dd}(1,2) - E^{\alpha\beta}_{dd}(1,2) - S^{\alpha\beta}_{dd}(1,2)(g^{\alpha\beta}_{dd}(1,2)-1)]\\
&+C^{\beta}_{e}(2)[X^{\alpha\beta}_{de}(1,2) - E^{\alpha\beta}_{de}(1,2) - S^{\alpha\beta}_{de}(1,2)(g^{\alpha\beta}_{dd}(1,2)-1)\\
&-S^{\alpha\beta}_{dd}(1,2)g^{\alpha\beta}_{de}(1,2)]\} + E^{\alpha}_{d}(1) \quad (3.89)\\
U^{\alpha}_{e}(1) &= \int d\mathbf{r}_2 \{ \sum_{\beta=p,n} \{C^{\beta}_{d}(2)[X^{\alpha\beta}_{ed}(1,2) - E^{\alpha\beta}_{ed}(1,2) -\\
&S^{\alpha\beta}_{ed}(1,2)(g^{\alpha\beta}_{dd}(1,2)-1) + S_{dd}(1,2)g^{\alpha}_{ed}(1,2)]\\
&+C^{\beta}_{e}(2)[X^{\alpha\beta}_{ee}(1,2) + (2\delta_{\alpha\beta}-1)(g^{\alpha\beta}_{ee,exc}(1,2) + g^{\alpha\beta}_{ee,excj}(1,2))\\
&-E^{\alpha\beta}_{ee}(1,2) - (2\delta_{\alpha\beta}-1)(E^{\alpha\beta}_{ee,exc}(1,2) + E^{\alpha\beta}_{ee,excj}(1,2))\\
&-S^{\alpha\beta}_{ee}(1,2)(g_{dd}(1,2)-1) - S^{\alpha}_{ed}(1,2)g^{\beta}_{de}(1,2) - S^{\beta}_{de}(1,2)g^{\alpha}_{ed}(1,2)]\\
&-S_{dd}(1,2)(g^{\alpha\beta}_{ee}(1,2) + (2\delta_{\alpha\beta}-1)(g^{\alpha\beta}_{ee,exc}(1,2) + g^{\alpha\beta}_{ee,excj}(1,2))]\\
&+2\delta_{\alpha\beta}[C^{\beta}_{e}(2)[S^{\alpha}_{cc}(1,2)g^{\beta}_{cc}(1,2) + S^{\alpha}_{ccj}(1,2)g^{\beta}_{ccj}(1,2)]\\
&-\rho^{\alpha}_{0}(1,2)(N^{(\rho)\beta}_{cc}(1,2) - \rho^{\beta}_{0}(1,2)) - \rho^{\alpha}_{0j}(1,2)(N^{(\rho)\beta}_{ccj}(1,2) - \rho^{\beta}_{0j}(1,2)]\}\\
&+E^{\alpha}_{e}(1) \quad (3.90)
\end{aligned}
$$

with:

$$
C^{\alpha}_{e}(1) = e^{U^{\alpha}_{d}(1)}
$$

$$\begin{aligned}\rho_1(1) = C_d^\alpha(1) &= C_e^\alpha(1)[U_e^\alpha(1) + \rho_0^\alpha(1)] \\ S_{xy}^{\alpha\beta}(1,2) &\equiv \frac{1}{2}N_{xy}^{\alpha\beta}(1,2) + E_{xy}^{\alpha\beta}(1,2)\end{aligned}$$

where $(x,y) = dd$, de, ed, ee, cc and the subscript j refers to the open antiparallel loop. We have seen that in the non saturated isospin systems the treatment of the operator correlations have been modified in order to separate the isospin dependence from the spin part of the operators. In particular we need to calculate explicitly the isospin part since in this case we have a non zero contribution from the linear isospin operators. This affects the form of the chain equations in the calculation of the $N_{xy,p}^{\alpha\beta}(1,2)$ functions. In generating of the chains we have the folding product of a function $X_{xy,p}(1,3)$ with another function $X_{xy,q}(3,2)$ or the folding product of a function $X_{xy,p}(1,3)$ with a function $N_{xy,q}(1,3)$ and eventually that of a function $X_{xy,p}(1,3)$ or $N_{xy,q}(1,3)$ with $\rho_0(3,2)$. In addition to the combinations available in the infinite case we have the possibility of the presence of only an isospin operator on left (O_{13}^τ) or on right (O_{32}^τ) with no zero contribution. Then the explicit expression of direct nodals diagrams are:

$$\begin{aligned}N_{xy,2k_1-1}^{\alpha\beta}(1,2) &= \sum_{k_2k_3=1}^{3}\sum_{\gamma=p,n}[N_{xy,2k_1-1,2k_2-1,2k_3-1}^{\alpha\beta\gamma}(1,2) \\ &+ (2\delta_{\alpha\gamma}-1)N_{xy,2k_1-1,2k_2,2k_3-1}^{\alpha\beta\gamma}(1,2) \\ &+ (2\delta_{\beta\gamma}-1)N_{xy,2k_1-1,2k_2-1,2k_3}^{\alpha\beta\gamma}(1,2)] \qquad (3.91) \\ N_{xy,2k_1}^{\alpha\beta}(1,2) &= \sum_{k_2,k_3=1}^{3}\sum_{\gamma=p,n}N_{xy,2k_1,2k_2,2k_3}^{\alpha\beta\gamma}(1,2) \qquad (3.92)\end{aligned}$$

with:

$$\begin{aligned}N_{xy,pqr}^{\alpha\beta\gamma}(1,2) &= (X_{xd,q}^{\alpha\gamma}(1,3)\xi_{132}^{k_2k_3k_1}C_{d,qr}^{\gamma}(3)|X_{dy,r}^{\gamma\beta}(3,2) + N_{dy,r}^{\gamma\beta}(3,2)) + \\ &\quad (X_{xe,q}^{\alpha\gamma}(1,3)\xi_{132}^{k_2k_3k_1}C_{e,qr}^{\gamma}(3)|X_{dy,r}^{\gamma\beta}(3,2) + N_{dy,r}^{\gamma\beta}(3,2)) + \\ &\quad (X_{xd,q}^{\alpha\gamma}(1,3)\xi_{132}^{k_2k_3k_1}C_{e,qr}^{\gamma}(3)|X_{ey,r}^{\gamma\beta}(3,2) + N_{ey,r}^{\gamma\beta}(3,2)) \qquad (3.93)\end{aligned}$$

where we have supposed that $p = 2k_1 - 1 + l_1, q = 2k_2 - 1 + l_2, r = 2k_3 - 1 + l_3$, and finally $(xy) = (dd,\ de,\ ed,\ ee)$.
The expressions of the nodal cc diagrams are:

$$\begin{aligned}N_{cc,p}^{\alpha}(1,2) &= N_{cc,p}^{(x)\alpha}(1,2) + N_{cc,p}^{(\rho)\alpha}(1,2) \quad p = 1,...,6 \qquad (3.94) \\ N_{ccj,p}^{\alpha}(1,2) &= N_{ccj,p}^{(x)\alpha}(1,2) + N_{ccj,p}^{(\rho)\alpha}(1,2) \quad p = 1,2 \qquad (3.95)\end{aligned}$$

The above equation indicates that the antiparallel contribute loops only to the first two channels of the interaction.

$$
\begin{aligned}
N^{(y)}_{cc(j),2k_1-1}(1,2) &= \sum_{k_2,k_3=1}^{3}\sum_{\gamma=p,n}[N^{(y)\alpha\gamma}_{cc(j),2k_1-1,2k_2-1,2k_3-1}(1,2) \\
&\quad +(2\delta_{\alpha\gamma}-1)(N^{(y)\alpha\gamma}_{cc(j),2k_1-1,2k_2,2k_3-1}(1,2)+ \\
&\quad N^{(y)\alpha\gamma}_{cc(j),2k_1-1,2k_2-1,2k_3}(1,2)] && (3.96) \\
N^{(y)\alpha}_{cc(j),2k_1}(1,2) &= \sum_{k_2,k_3=1}^{3}\sum_{\gamma=p,n} N^{(y)\alpha\gamma}_{cc(j),2k_1,2k_2,2k_3}(1,2) && (3.97)
\end{aligned}
$$

with $y=x,\rho$
and

$$
\begin{aligned}
N^{(x)\alpha\gamma}_{cc,pqr}(1,2) &= (X^{\alpha}_{cc,q}(1,3)\xi^{k_2k_3k_1}_{132}C^{\gamma}_{e,qr}(3)\frac{\Delta^{k_3}}{2}|X^{\gamma}_{cc}(3,2)+N^{\gamma}_{cc}(3,2)-\rho^{\gamma}_{0}(3,2))+ \\
&\quad (1-\delta_{r,1})(X^{\alpha}_{cc}(1,3)\frac{\Delta^{k_2}}{2}\xi^{k_2k_3k_1}_{132}C^{\gamma}_{e,qr}(3)|X^{\gamma}_{cc,r}(3,2)+N^{\gamma}_{cc,r}(3,2)) \\
&&& (3.98) \\
N^{(\rho)\alpha\gamma}_{cc,pqr}(1,2) &= -(\rho^{\alpha}_{0}(1,3)\frac{\Delta^{k_2}}{2}\xi^{k_2k_3k_1}_{132}C^{\gamma}_{e,qr}(3)|X^{\gamma}_{cc,r}(3,2)+N^{(x)\gamma}_{cc,r}(3,2) \\
&\quad -(\rho^{\alpha}_{0}(1,3)\frac{\Delta^{k_2}}{2}\xi^{k_2k_3k_1}_{132}(C^{\gamma}_{e,qr}-1)|N^{(\rho)\gamma}_{cc,r}(3,2)-\delta_{r,1}\rho^{\gamma}_{0}(3,2)) && (3.99) \\
N^{(x)\alpha\gamma}_{cc,pst}(1,2) &= (X^{\alpha}_{ccj,s}(1,3)C^{\gamma}_{e,st}(3)\frac{1}{2}|X^{\gamma}_{ccj}(3,2)+N^{\gamma}_{ccj}(3,2)-\rho^{\gamma}_{0j}(3,2))+ \\
&\quad (1-\delta_{t,1})(X^{\alpha}_{ccj}(1,3)C^{\gamma}_{e,st}(3)\frac{1}{2}|X^{\gamma}_{ccj,t}(3,2)+N^{\gamma}_{ccj,t}(3,2)) && (3.100) \\
N^{(\rho)\alpha\gamma}_{cc,pst}(1,2) &= (\rho^{\alpha}_{0j}(1,3)C^{\gamma}_{e,st}(3)\frac{1}{2}|X^{\gamma}_{ccj,t}(3,2)+N^{\gamma}_{ccj,t}(3,2))+ \\
&\quad (\rho^{\alpha}_{0j}(1,3)(C^{\gamma}_{e,st}(3)-1)\frac{1}{2}|N^{\gamma}_{ccj,t}(3,2)-\delta_{t,1}\rho^{\gamma}_{0j}(3,2)) && (3.101) \\
N^{(x)\alpha\gamma}_{ccj,pst}(1,2) &= (X^{\alpha}_{cc,s}(1,3)C^{\gamma}_{e,st}(3)\frac{1}{2}|X^{\gamma}_{ccj}(3,2)+N^{\gamma}_{ccj}(3,2)-\rho_{0j}(3,2))+ \\
&\quad (1-\delta_{t,1})(X^{\alpha}_{cc}(1,3)C^{\gamma}_{e,st}(3)\frac{1}{2}|X^{\gamma}_{ccj,t}(3,2)+N^{\gamma}_{ccj,t}(3,2)+ \\
&\quad (X^{\alpha}_{ccj,s}(1,3)C^{\gamma}_{e,st}(3)\frac{1}{2}|X^{\gamma}_{cc}(3,2)+N^{\gamma}_{cc}(3,2)-\rho^{\gamma}_{0}(3,2))+ \\
&\quad (1-\delta_{t,1})(X^{\alpha}_{ccj}(1,3)C^{\gamma}_{e,st}(3)\frac{1}{2}|X^{\gamma}_{cc,t}(3,2)+N^{\gamma}_{cc,t}(3,2)) && (3.102) \\
N^{(\rho)\alpha\gamma}_{ccj,pst}(1,2) &= -(\rho^{\alpha}_{0}(1,3)C^{\gamma}_{e,st}(3)\frac{1}{2}|X^{\gamma}_{ccj,t}(3,2)+N^{\gamma}_{ccj,t}(3,2)) \\
&\quad -(\rho^{\alpha}_{0}(1,3)(C^{\gamma}_{e,st}(3)-1)\frac{1}{2}|N^{\gamma}_{ccj,t}(3,2)-\delta_{t,1}\rho^{\gamma}_{0j}(3,2))
\end{aligned}
$$

$$
\begin{aligned}
&-(\rho_{0j}^{\alpha}(1,3)C_{e,st}^{\gamma}(3)\frac{1}{2}|X_{cc,t}^{\gamma}(3,2)+N_{cc,t}^{\gamma}(3,2)) \\
&-(\rho_{0j}^{\alpha}(1,3)(C_{e,st}^{\gamma}(3)-1)\frac{1}{2}|N_{cc,t}^{\gamma}(3,2)-\delta_{t,1}\rho_{0}^{\gamma}(3,2))
\end{aligned} \tag{3.103}
$$

with $(s,t)=1,2$.

The two-body distribution functions have essentially the same expressions than in the infinite case. The formulae are:

$$
\begin{aligned}
g_{dd,p}^{\alpha\beta}(1,2) &= \frac{2f_p(r_{12})}{f_1(r_{12})}g_{dd}^{\alpha\beta}(1,2)+g_{dd}^{\alpha\beta}(1,2)N_{dd,p}^{\alpha\beta}(1,2) \\
&= X_{dd,p}^{\alpha\beta}(1,2)+N_{dd,p}^{\alpha\beta}(1,2) && (3.104)\\
g_{de,p}^{\alpha\beta}(1,2) &= \frac{2f_p(r_{12})}{f_1(r_{12})}g_{de}^{\alpha\beta}(1,2)+g_{dd}^{\alpha\beta}(1,2)N_{de,p}^{\alpha\beta}(1,2) \\
&+ g_{de}^{\alpha\beta}(1,2)N_{dd,p}^{\alpha\beta}(1,2)=X_{de,p}^{\alpha\beta}(1,2)+N_{de,p}^{\alpha\beta}(1,2) && (3.105)\\
g_{ee,p}^{\alpha\beta}(1,2) &= g_{ee,dir,p}^{\alpha\beta}(1,2)+g_{ee,exc,p}^{\alpha\beta}(1,2)+g_{ee,excj,p}^{\alpha\beta}(1,2) \\
&= X_{ee,p}^{\alpha\beta}(1,2)+N_{ee,p}^{\alpha\beta}(1,2) && (3.106)\\
g_{ee,dir,p}^{\alpha\beta}(1,2) &= \frac{2f_p(r_{12})}{f_1(r_{12})}g_{ee,dir}^{\alpha\beta}(1,2)+g_{dd}^{\alpha\beta}(1,2)N_{ee,p}^{\alpha\beta}(1,2) \\
&+ g_{de}^{\alpha\beta}(1,2)N_{ed,p}^{\alpha\beta}(1,2)+g_{ed}^{\alpha\beta}(1,2)N_{de,p}^{\alpha\beta}(1,2) \\
&+ g_{ee,dir}^{\alpha\beta}(1,2)N_{dd,p}^{\alpha\beta}(1,2) && (3.107)\\
g_{ee,exc,p}^{\alpha\beta}(1,2) &= \Delta^k g_{ee,exc}^{\alpha\beta}(1,2) && (3.108)\\
g_{ee,excj,p}^{\alpha\beta}(1,2) &= \Delta^k g_{ee,excj}^{\alpha\beta}(1,2) && (3.109)\\
g_{cc(j)}^{\alpha}(1,2) &= \frac{2f_p(r_{12})}{f_1(r_{12})}g_{cc(j)}^{\alpha}(1,2)+g_{cc(j)}^{\alpha}(1,2)N_{dd,p}^{\alpha\alpha}(1,2) \\
&+ g_{dd}^{\alpha\alpha}(1,2)N_{cc(j),p}^{\alpha}=X_{cc(j),p}^{\alpha}(1,2)+N_{cc(j),p}^{\alpha}(1,2) && (3.110)
\end{aligned}
$$

with $p>1$ and $p=2k-1+l$.

Vertex Corrections

$$
C_{e,pq}^{\alpha}(1)=C_{e}^{\alpha}(1)\Big(1+\delta_{pq,11}U_{d,op}^{\alpha}(1)\Big) \tag{3.111}
$$

$$
C_{d,pq}^{\alpha}(1)=C_{e,pq}^{\alpha}(1)\Big(\rho_0^{\alpha}(1)+U_{e}^{\alpha}(1)\Big)+\delta_{pq,11}C_{e}^{\alpha}(1)\Big(U_{e,op}^{\alpha}(1)+U_{ej,op}^{\alpha}(1)\Big) \tag{3.112}
$$

$$
\begin{aligned}
U_{x,op}^{\alpha}(1) &= \sum_{k_1=1}^{3}A^k\sum_{\beta=p,n}\Big[(1-\delta_{k_1 1})U_{x,2k_1-1,2k_1-1}^{\alpha\beta}(1) \\
&+ \chi_1^{\alpha\beta}\Big(U_{x,2k_1-1,2k_1}(1)+U_{x,2k_1,2k_1-1}(1)\Big)
\end{aligned}
$$

$$
\begin{aligned}
&+ \quad \chi_2^{\alpha\beta} U^{\alpha\beta}_{x,2k_1,2k_1}(1)\Big] && (3.113)\\
U^{\alpha}_{ej,op}(1) &= -\sum_{k_1k_2=1}^{3} I^{k_1k_2 2} \sum_{\beta=p,n} \Big[(1-\delta_{k_1 1})(1-\delta_{k_2 1})U^{\alpha\beta}_{ej,2k_1-1,2k_2-1}(1)\\
&+ \quad \chi_1^{\alpha\beta}\Big(U_{ej,2k_1-1,2k_2}(1) + U_{ej,2k_1,2k_2-1}(1)\Big)\\
&+ \quad \chi_2^{\alpha\beta} U^{\alpha\beta}_{ej,2k_1,2k_2}(1)\Big] && (3.114)
\end{aligned}
$$

where $x = d, e$, $p = 2k_1 - 1 + l_1$ and $q = 2k_2 - 1 + l_2$ and

$$
\begin{aligned}
U^{\alpha\beta}_{d,pq}(1) &= \int d\mathbf{r}_2 \frac{f_p(r_{12})}{f_1^2(r_{12})}\Big[\Big(g^{\alpha\beta}_{dd}(1,2)C^{\beta}_{e}(2) + g^{\alpha\beta}_{de}(1,2)C_{e,pq}(2)\Big)h^{\alpha\beta}_{q}(1,2)\\
&+ \quad g^{\alpha\beta}_{dd}(1,2)C^{\beta}_{e,pq}(2)2f_1(r_{12})N^{\alpha\beta}_{de,q}(1,2)\Big] && (3.115)\\
U^{\alpha\beta}_{e,pq}(1) &= \int d\mathbf{r}_2 \frac{f_p(r_{12})}{f_1^2(r_{12})}\Big[\Big(g^{\alpha\beta}_{ed}(1,2)C^{\beta}_{d,pq}(2) + g^{\alpha\beta}_{ee,dir}(1,2)C^{\beta}_{e,pq}(2)\Big)h^{\alpha\beta}_{q}(1,2)\\
&+ \quad g^{\alpha\beta}_{dd}(1,2)2f_1(r_{12})\Big(C^{\beta}_{d,pq}(2)N^{\alpha}_{ed,q}(1,2) + C^{\beta}_{e,pq}(2)\Big(N^{\alpha\beta}_{ee,q}(1,2)\\
&+ \quad N^{\alpha\beta}_{de,q}(1,2)N^{\alpha\beta}_{ed}(1,2) + N^{\alpha\beta}_{ed,q}(1,2)N^{\alpha\beta}_{de}(1,2)\Big)\Big)\Big]\\
&+ \quad 2\Delta^k \int d\mathbf{r}_2 f_p(r_{12}) f_1(r_{12}) g^{\alpha\beta}_{ee,exc}(1,2)C^{\beta}_{e,pq}(2) && (3.116)\\
U^{\alpha\beta}_{ej,pq} &= 2\Delta^k \int d\mathbf{r}_2 f_p(r_{12}) f_1(r_{12}) g^{\alpha\beta}_{ee,excj}(1,2)C^{\beta}_{e,pq}(2). && (3.117)
\end{aligned}
$$

with $h^{\alpha\beta}_{q}(1,2) = f_q(r_{12}) + 2f_1(r_{12})N^{\alpha\beta}_{dd,q}(1,2)$.

Chapter 4

The calculation of the energy

4.1 Kinetic energy and V_{12}^6 part

In this chapter we calculate the expectation value of the energy:

$$< H >= \frac{< \Psi|H|\Psi >}{< \Psi|\Psi >} \tag{4.1}$$

with the hamiltonian:

$$H = -\sum_{i=1}^{A} \frac{\hbar^2}{2m}\nabla_i^2 + \sum_{i<j=1}^{A} V_{ij} + \sum_{i<j<k=1}^{A} V_{ijk} \tag{4.2}$$

where the two-body interaction is given by

$$V_{ij} = \sum_{p=1}^{6} v^p(r_{ij})O_{ij}^p. \tag{4.3}$$

The explicit expression of the three-body interaction V_{ijk} will be given in section 3.3.

The trial wave function is:

$$|\Psi >= \mathcal{S}\prod_{i<j} F_{ij}|\Phi > \tag{4.4}$$

where

$$F_{ij} = \sum_{p=1}^{6} f_p(r_{ij})O_{ij}^p = \sum_{l=0}^{1}(\boldsymbol{\tau}_i \cdot \boldsymbol{\tau}_j)^l \sum_{k=1}^{3} f_{2k-1+l}(r_{ij})P_{ij}^k \tag{4.5}$$

with $P^k_{ij} = 1, \boldsymbol{\sigma}_i \cdot \boldsymbol{\sigma}_j, S_{ij}$.
The function $|\Phi >$ is a Slater determinant composed by single particle wave function generated by a spherical Woods-Saxon potential. We consider different potentials for protons and neutrons, containing spin-orbit terms.
We clarify here some conventions we shall use henceforth in the formulae. We understand a sum on the repeated, α, β, and eventually γ superscripts which indicate proton and neutron. The p, q, r, s labels may assume values from 1 up to 6, and are used to identify the different operator channels as in eq. (2.53). Since we use the expression (4.5) to write the operators, all the labels l can assume the values 0 or 1, and the labels k the values 1, 2, 3. We indicate with $[,]$ the commutator and with $\{,\}$ the anticommutator.
We evaluate the expectation value of the kinetic energy, by separating it in three parts:

$$\langle T \rangle = T_{JF} = T_\phi + T_F - T_{c.m.}, \tag{4.6}$$

with

$$T_\phi = -\frac{\hbar^2}{4m}\Big(< \Phi^* F^2 \sum_i \nabla_i^2 \Phi > - < \sum_i (\nabla_i \Phi^*) F^2 (\nabla_i \Phi) > \Big) \tag{4.7}$$

and

$$T_F = -\frac{\hbar^2}{4m} < \Phi^* \Big[F \Big(\sum_i \nabla_i^2 F \Big) - \sum_i (\nabla_i F)^2 \Big] \Phi > \tag{4.8}$$

A derivation of the above equations is done in Appendix A.4. For the calculation of the kinetic energy term, it is useful to define the following quantities

$$\rho^\alpha_{T1}(\boldsymbol{r}_1) = \sum_i \phi_i^{\alpha*}(\boldsymbol{r}_1) \nabla_1^2 \phi_i^\alpha(\boldsymbol{r}_1) - \sum_i \nabla_1 \phi_i^{\alpha*}(\boldsymbol{r}_1) \cdot \nabla_1 \phi_i^\alpha(\boldsymbol{r}_1) \tag{4.9}$$

$$\rho^{\alpha\beta}_{T2}(\boldsymbol{r}_1, \boldsymbol{r}_2) = \rho^\alpha_0(\boldsymbol{r}_1, \boldsymbol{r}_2) \nabla_1^2 \rho^\beta_0(\boldsymbol{r}_1, \boldsymbol{r}_2) - \nabla_1 \rho^\alpha_0(\boldsymbol{r}_1, \boldsymbol{r}_2) \cdot \nabla_1 \rho^\beta_0(\boldsymbol{r}_1, \boldsymbol{r}_2) \tag{4.10}$$

$$\rho^\alpha_{T3}(\boldsymbol{r}_1, \boldsymbol{r}_2) = \sum_s \chi_s^*(2) \chi_\alpha^*(2) \nabla_1^2 \rho^\alpha_0(\boldsymbol{r}_1, \boldsymbol{r}_2) \chi_s(1) \chi_\alpha(1) \tag{4.11}$$

$$\rho^\alpha_{T4}(\boldsymbol{r}_1, \boldsymbol{r}_2) = -\rho^\alpha_0(\boldsymbol{r}_1, \boldsymbol{r}_2) \nabla_1 \cdot \nabla_2 \rho^\alpha_0(\boldsymbol{r}_1, \boldsymbol{r}_2) + \nabla_1 \rho^\alpha_0(\boldsymbol{r}_1, \boldsymbol{r}_2) \cdot \nabla_2 \rho^\alpha_0(\boldsymbol{r}_1, \boldsymbol{r}_2) \tag{4.12}$$

where we have indicated with $\phi_i^\alpha(\boldsymbol{r}_i)$ the single particle wave function. The explicit expression of the above densities in our jj coupled single particle basis, are given in Appendix A.5. The contribution of the center of mass term is calculated as

$$\begin{aligned} T_{c.m.} &= -\frac{\hbar^2}{2mA} < \Psi_0^* \Big(\sum_i \nabla_i \Big)^2 \Psi_0 > \\ &= -\frac{\hbar^2}{4mA} \sum_{\alpha=p,n} \Big(\int d\boldsymbol{r}_1 \rho^{\alpha}_{T1}(\boldsymbol{r}_1) - \int d\boldsymbol{r}_1 d\boldsymbol{r}_2 \rho^{\alpha}_{T4}(\boldsymbol{r}_1, \boldsymbol{r}_2) \Big) \end{aligned} \quad (4.13)$$

The distinction between T_ϕ and T_F is related to the fact that in the first operator ∇ acts on the uncorrelated wave function, while in T_F it acts on the correlation. The structure of this second operator is such that it is convenient to evaluate its expectation value together with the two-body potential energy $\langle v \rangle = V_2$. The contribution of $T_F + V_2 = W$ is also called *interaction energy* [Fab98]. It is possible to express W in terms of

$$\begin{aligned} H^{pqr}_{JF}(r_{12}) &= \frac{1}{f_1^2(r_{12})} \Big(-\frac{\hbar^2}{2m} \delta_{q1} \Big\{ f_p(r_{12}) \nabla^2 f_r(r_{12}) - \nabla f_p(r_{12}) \cdot \nabla f_r(r_{12}) \Big\} \\ &\quad + f_p(r_{12}) v^q(r_{12}) f_r(r_{12}) \Big). \end{aligned} \quad (4.14)$$

There are various types of correlation linking the interacting points which we label as $\boldsymbol{r}_1$ and $\boldsymbol{r}_2$. We found convenient to separate the contribution of W in four parts

$$W = W_0 + W_s + W_c + W_{cs}, \quad (4.15)$$

We indicate with W_0 is the sum of the diagrams with only scalar chains between the interacting points. With W_s we indicate the sum of diagrams having single operator rings (SOR) touching the interacting points and scalar chains. The term W_c contains all the diagrams with one single operator chain (SOC) between the interacting points and W_{cs} contains both SOR at the interacting points and SOC between them.

The W_0 term is given by

$$\begin{aligned} W_0 &= \frac{1}{2} \int d\mathbf{r}_1 d\mathbf{r}_2 H^{2k_1-1+l_1, 2k_2-1+l_2, 2k_3-1+l_3}_{JF}(r_{12}) \Big[I^{k_1k_2k_3} A^{k_3} \rho^{\alpha\beta}_{2,dir}(1,2) \chi^{\alpha\beta}_{l_1+l_2+l_3} \\ &\quad + I^{k_4k_1k_5} I^{k_2k_3k_5} A^{k_5} \Delta^{k_4} \rho^{\alpha\beta}_{2,exc}(1,2) \Big(\chi^{\alpha\beta}_{l_1+l_2+l_3} + \chi^{\alpha\beta}_{l_1+l_2+l_3+1} \Big) \\ &\quad + I^{k_4k_1k_5} I^{k_2k_3k_6} I^{k_5k_62} \Delta^{k_4} \rho^{\alpha\beta}_{2,excj}(1,2) \Big(\chi^{\alpha\beta}_{l_1+l_2+l_3} + \chi^{\alpha\beta}_{l_1+l_2+l_3+1} \Big) \Big] \end{aligned} \quad (4.16)$$

k	1	2	3
A^k	1	3	6

Table 4.1: The A^k matrix.

	Direct	Exchange
$k_4k_1k_2k_3k_5$	$I^{k_1k_2k_3}A^{k_3}A^{k_4}\delta_{k_4k_5}$	$I^{k_6k_1k_7}I^{k_2k_3k_7}A^{k_7}(1+D_{k_6k_4})A^{k_4}\delta_{k_4k_5}$
$k_4k_1k_2k_5k_3$	$I^{k_1k_2k_3}A^{k_3}(1+D_{k_3k_4})A^{k_4}\delta_{k_4k_5}$	$I^{k_6k_1k_7}I^{k_2k_3k_7}A^{k_7}(1+D_{k_7k_4})A^{k_4}\delta_{k_4k_5}$
$k_1k_4k_2k_3k_5$	$I^{k_1k_2k_3}A^{k_3}(1+D_{k_1k_4})A^{k_4}\delta_{k_4k_5}$	$I^{k_6k_1k_7}I^{k_2k_3k_7}A^{k_7}(1+D_{k_7k_4})A^{k_4}\delta_{k_4k_5}$
$k_1k_4k_2k_5k_3$	$I^{k_1k_2k_3}A^{k_3}(1+D_{k_2k_4})A^{k_4}\delta_{k_4k_5}$	$I^{k_6k_1k_7}I^{k_2k_3k_7}A^{k_7}(1+D_{k_2k_4})A^{k_4}\delta_{k_4k_5}$

Table 4.2: Spin traces with parallel particles for the operators in eq. (4.20).

The densities in the above equation are defined as:

$$\begin{aligned}
\rho_{2,dir}^{\alpha\beta}(1,2) &= C_{d,22}^{\alpha}(1)(C_{d,22}^{\beta}(2)g_{dd}^{\alpha\beta}(1,2)+C_{e,22}^{\beta}(2)g_{de}^{\alpha\beta}(1,2)) \\
&+ C_{e,22}^{\alpha}(1)C_{d,22}^{\beta}(2)g_{ed}^{\alpha\beta}(1,2)+C_{e,22}^{\alpha}(1)C_{e,22}^{\beta}(2)g_{ee,dir}^{\alpha\beta}(1,2) \quad (4.17) \\
\rho_{2,exc}^{\alpha\beta}(1,2) &= C_{e,22}^{\alpha}(1)C_{e,22}^{\beta}(2)g_{ee,exc}^{\alpha\beta}(1,2) \quad (4.18) \\
\rho_{2,excj}^{\alpha\beta}(1,2) &= C_{e,22}^{\alpha}(1)C_{e,22}^{\beta}(2)g_{ee,excj}^{\alpha\beta}(1,2) \quad (4.19)
\end{aligned}$$

where we have used the functions $C_{x,22}^{\gamma}(i)$ $(x=d,e)$, defined in the previous chapter, in order to include only state–independent vertex corrections so the ρ functions consider all the direct and exchange central dressing that can arrive to the external points. The values of the A^k coefficients are given in table 4.1. The values of $I^{k_1k_2k_3}$ and $J^{k_1k_2k_3}$ are given in Appendix A.3.1 and $\Delta^k=1-\delta_{k,3}$. The $\chi_l^{\alpha\beta}$ functions give the isospin traces and were defined in equation (3.57).

We now discuss the effects of one SOR attached to one of the interacting particles, IP. The operator structure that we must analyze in W_s, for the direct case is:

$$\frac{1}{2}\{k_1,k_4\}k_2\frac{1}{2}\{k_3,k_5\}=\frac{1}{4}\left(k_4k_1k_2k_3k_5+k_4k_1k_2k_5k_3+k_1k_4k_2k_3k_5+k_1k_4k_2k_5k_3\right) \quad (4.20)$$

with k_1, k_2 and k_3 operators acting on 1 and 2, k_4 and k_5 operators acting on 1 and 3 or 2 and 3. The symbol $\{,\}$ indicates the anticommutator. In the exchange case an additional k_6 operator must be included on the left. For the part with parallel spin, in IP, following [Pan79] for the spin trace, we get the results given in tab. 4.2: The traces of the part with antiparallel particles in the IP produces are given in tab 4.3: The part with antiparallel particles in 13 or 23 forces the

$k_6k_4k_1k_2k_3k_5$	$I^{k_6k_1k_7}I^{k_2k_3k_8}I^{k_7k_82}(1+D_{k_6k_4})A^{k_4}\delta_{k_4k_5}$
$k_6k_4k_1k_2k_5k_3$	$I^{k_6k_1k_7}I^{k_2k_3k_8}I^{k_7k_82}(1+D_{k_7k_4})A^{k_4}\delta_{k_4k_5}$
$k_6k_1k_4k_2k_3k_5$	$I^{k_6k_1k_7}I^{k_2k_3k_8}I^{k_7k_82}(1+D_{k_7k_4})A^{k_4}\delta_{k_4k_5}$
$k_6k_1k_4k_2k_5k_3$	$I^{k_6k_1k_7}I^{k_2k_3k_8}I^{k_7k_82}(1+D_{k_2k_4})A^{k_4}\delta_{k_4k_5}$

Table 4.3: Spin traces with antiparralel particle for the operators in eq. (4.20).

operator k_4 to be on the left handside. This produces the traces given in tab. 4.4. where in our notation the matrix D is:

$$D_{k_1,k_2} = \begin{pmatrix} 0 & 0 & 0 \\ 0 & -4/3 & -4/3 \\ 0 & -4/3 & -4/3 \end{pmatrix} \tag{4.21}$$

Henceforth, we understand saturated all the indices appearing in the tables. All the isospin parts of the above operators can be written in terms of $\chi^{\alpha\beta\gamma}_{l_1l_2l_3l_4l_5}(i)$ (see equation (3.59)). By using the above definitions we can write:

$$\begin{aligned} W_s \;=\; & \frac{1}{2}\int d\mathbf{r}_1 d\mathbf{r}_2 H_{JF}^{2k_1-1+l_1,2k_2-1+l_2,2k_3-1+l_3}(r_{12})\Big[I^{k_1k_2k_3}A^{k_3} \qquad (4.22)\\ & \Big\{\rho^{\alpha\beta}_{2,dir}(1,2)\left(M^{\alpha\beta k_1k_2k_3}_{d,l_1,l_2,l_3}(1)+M^{\alpha\beta k_1k_2k_3}_{d,l_1,l_2,l_3}(2)\right)+\\ & \left(g^{\alpha\beta}_{dd}(1,2)C^{\beta}_{d,22}(2)+g^{\alpha\beta}_{de}(1,2)C^{\beta}_{e,22}(2)\right)C^{\alpha}_{e,22}(1)M^{\alpha\beta k_1k_2k_3}_{e,l_1,l_2,l_3}(1)+\\ & \left(g^{\alpha\beta}_{dd}(1,2)C^{\alpha}_{d,22}(1)+g^{\alpha\beta}_{ed}(1,2)C^{\alpha}_{e,22}(1)\right)C^{\beta}_{e,22}(2)M^{\alpha\beta k_1k_2k_3,}_{e,l_1,l_2,l_3}(2)+\\ & \left(g^{\alpha\beta}_{dd}(1,2)C^{\beta}_{d,22}(2)+g^{\alpha\beta}_{de}(1,2)C^{\beta}_{e,22}(2)\right)C^{\alpha}_{e,22}(1)M^{\alpha\beta k_1k_2k_3}_{ej,l_1,l_2,l_3}(1)+\\ & \left(g^{\alpha\beta}_{dd}(1,2)C^{\alpha}_{d,22}(1)+g^{\alpha\beta}_{ed}(1,2)C^{\alpha}_{e,22}(1)\right)C^{\beta}_{e,22}(2)M^{\alpha\beta k_1k_2k_3}_{ej,l_1,l_2,l_3}(2)\Big\}+\\ & I^{k_5k_1k_6}I^{k_2k_3k_6}A^{k_5}\Delta^{k_5}\rho^{\alpha\beta}_{2,exc}(1,2)\left(M^{\alpha\beta k_2k_5k_6}_{d,l_1,l_2,l_3,l_5}(1)+M^{\alpha\beta k_2k_5k_6}_{d,l_1,l_2,l_3,l_5}(2)\right)+\\ & I^{k_5k_1k_6}I^{k_2k_3k_7}I^{k_6k_72}\Delta^{k_5}\rho^{\alpha\beta}_{2,excj}(1,2)\left(M^{\alpha\beta k_2k_5k_6}_{d,l_1,l_2,l_3,l_5}(1)+M^{\alpha\beta k_2k_5k_6}_{d,l_1,l_2,l_3,l_5}(2)\right)\Big] \end{aligned}$$

with

$$\begin{aligned} M^{\alpha\beta k_1k_2k_3}_{x,l_1,l_2,l_3}(i) \;=\; & \frac{1}{4}\Big(M^{\alpha\beta k_4}_{x,0,l_1+l_2+l_3,0}(i)+(1+D_{k_3k_4})M^{\alpha\beta k_4}_{x,0,l_1+l_2,l_3}(i)+ \qquad (4.23)\\ & (1+D_{k_1k_4})M^{\alpha\beta k_4}_{x,l_1,l_2+l_3,0}(i)+(1+D_{k_2k_4})M^{\alpha\beta k_4}_{x,l_1,l_2,l_3}(i)\Big)\\ M^{\alpha\beta k_1k_2k_3}_{ej,l_1,l_2,l_3}(i) \;=\; & \frac{1}{4}\Big(M^{\alpha\beta k_4k_8}_{ej,0,0,l_1+l_2+l_3}(i)+(1+D_{k_3k_4})M^{\alpha\beta k_4k_8}_{ej,0,l_1+l_2,l_3}(i)+ \qquad (4.24) \end{aligned}$$

$k_4k_1k_2k_3k_5$	$I^{k_1k_2k_3}A^{k_3}I^{k_4k_52}$
$k_4k_1k_2k_5k_3$	$I^{k_1k_2k_3}A^{k_3}I^{k_4k_52}(1+D_{k_3k_4})$
$k_4k_1k_5k_2k_3$	$I^{k_1k_2k_3}A^{k_3}I^{k_4k_52}(1+D_{k_1k_4})$
$k_4k_5k_1k_2k_3$	$I^{k_1k_2k_3}A^{k_3}I^{k_4k_52}$

Table 4.4: Spin traces in 13 or 23 with antiparallel particles.

$$(1+D_{k_1k_4})M^{\alpha\beta k_4k_8}_{ej,0,l_1,l_2+l_3}(i)+M^{\alpha\beta k_4k_8}_{ej,0,l_1+l_2+l_3,0}(i)\Big)$$

$$\begin{aligned} M^{\alpha\beta k_2k_5k_6}_{d,l_1,l_2,l_3,l_5}(i) &= \frac{1}{4}\Big((1+D_{k_5k_4})M^{\alpha\beta k_4}_{d,l_5,l_1+l_2+l_3,0}(i)+(1+D_{k_6k_4})M^{\alpha\beta k_4}_{d,l_5,l_1+l_2,l_3}(i)+ \\ &(1+D_{k_6k_4})M^{\alpha\beta k_4}_{d,l_5+l_1,l_2+l_3,0}(i)+(1+D_{k_2k_4})M^{\alpha\beta k_4}_{d,l_5+l_1,l_2,l_3}(i)\Big) \end{aligned} \quad (4.25)$$

$$\begin{aligned} M^{\alpha\beta k_4}_{x,l_1,l_2,l_3}(i) &= A^k\Big((1-\delta_{k_4,1})\chi^{\alpha\beta\gamma}_{l_10l_20l_3}(i)U^{\mu\gamma}_{x,2k_4-1,2k_4-1}(i)+ \\ &\chi^{\alpha\beta\gamma}_{l_11l_20l_3}(i)U^{\mu\gamma}_{x,2k_4,2k_4-1}(i)+\chi^{\alpha\beta\gamma}_{l_10l_21l_3}(i)U^{\mu\gamma}_{x,2k_4-1,2k_4}(i)+ \\ &\chi^{\alpha\beta\gamma}_{l_11l_21l_3}(i)U^{\mu\gamma}_{x,2k_4,2k_4}(i)\Big) \end{aligned} \quad (4.26)$$

$$\begin{aligned} M^{\alpha\beta k_4k_8}_{ej,l_1,l_2,l_3}(i) &= I^{k_4k_82}\Big(\chi^{\alpha\beta\gamma}_{l_10l_20l_3}(i)U^{\mu\gamma}_{ej,2k_4-1,2k_8-1}(i)+\chi^{\alpha\beta\gamma}_{l_11l_20l_3}(i)U^{\mu\gamma}_{ej,2k_4,2k_8-1}(i)+ \\ &\chi^{\alpha\beta\gamma}_{l_10l_21l_3}(i)U^{\mu\gamma}_{ej,2k_4-1,2k_8}(i)+\chi^{\alpha\beta\gamma}_{l_11l_21l_3}(i)U^{\mu\gamma}_{ej,2k_4,2k_8}(i)\Big) \end{aligned} \quad (4.27)$$

with $i=1,2$, $x=d,e$, $\mu=\alpha$ for $i=1$ and $\mu=\beta$ for $i=2$ and the expressions for $U^{\alpha\beta}_{x,pq}(i)$ and $U^{\alpha\beta}_{dj,pq}(i)$ are given in formulae (3.115) to (3.117).

The structure of the W_c term is more involved. We calculate separately the various terms according to the direct or exchange nature of the correlations reaching the external points.

$$W_c = W_c(dd)+W_c(ed)+W_c(de)+W_c(ee)+W_c(cc) \quad (4.28)$$

The operator structure that we must analyze in the case direct dd is:

$$\begin{aligned} &\frac{1}{4}\Big[\frac{1}{4}\{k_1,k_4\}k_2\{k_3,k_5\}+\frac{1}{4}\{k_1,k_5\}k_2\{k_3,k_5\}+ \\ &\frac{1}{6}\left(\{\{k_4,k_5\},k_1\}+k_4k_1k_5+k_5k_1k_4\right)k_2k_3+ \end{aligned}$$

	Direct	Exchange
$k_4k_1k_2k_3k_5$	$I^{k_1k_2k_7}I^{k_3k_6k_7}A^{k_7}$	$I^{k_1k_2k_7}I^{k_7k_3k_8}J^{k_9k_6k_8}$
$k_4k_1k_2k_5k_3$	$I^{k_1k_2k_7}J^{k_3k_6k_7}$	$I^{k_1k_2k_7}I^{k_3k_8k_9}J^{k_9k_6k_7}$
$k_1k_4k_2k_3k_5$	$I^{k_2k_3k_7}J^{k_1k_6k_7}$	$I^{k_2k_3k_7}I^{k_8k_1k_9}J^{k_9k_6k_7}$
$k_1k_4k_2k_5k_3$	$I^{k_3k_1k_7}J^{k_2k_6k_7}$	$I^{k_3k_8k_7}I^{k_7k_1k_9}J^{k-2k_6k_9}$
$k_4k_5k_1k_2k_3$	$I^{k_1k_2k_7}I^{k_3k_6k_7}A^{k_7}$	$I^{k_8k_6k_7}I^{k_1k_2k_9}I^{k_7k_9k_3}A^{k_3}$
$k_1k_4k_5k_2k_3$	$I^{k_1k_2k_7}I^{k_3k_6k_7}A^{k_7}$	$I^{k_8k_6k_7}I^{k_1k_2k_9}I^{k_7k_9k_3}A^{k_3}$
$k_4pk_5k_2k_3$	$I^{k_2k_3k_7}J^{k_1k_6k_7}$	$I^{k_2k_3k_7}I^{k_7k_8k_9}J^{k_1k_6k_9}$
$k_1k_2k_3k_4k_5$	$I^{k_1k_2k_7}I^{k_3k_6k_7}A^{k_7}$	$I^{k_8k_6k_7}I^{k_1k_2k_9}I^{k_7k_9k_3}A^{k_3}$
$k_1k_2k_4k_5k_3$	$I^{k_1k_2k_7}I^{k_3k_6k_7}A^{k_7}$	$I^{k_8k_6k_7}I^{k_1k_2k_9}I^{k_7k_9k_3}A^{k_3}$
$k_1k_2k_4k_3k_5$	$I^{k_1k_2k_7}J^{k_3k_6k_7}$	$I^{k_8k_1k_7}I^{k_7k_2k_9}J^{k_3k_6k_9}$

Table 4.5: The traces obtained for the $W_c(dd)$ term.

$$\left.\frac{1}{6}k_1k_2\left(\{\{k_4,k_5\},k_3\}+k_4k_3k_5+k_5k_3k_4\right)\right] \tag{4.29}$$

the k_1, k_2 and k_3 operators act on the 1 and 2 particles, k_4 depends on 1 and 3 k_5 on 2 and 3. The calculation of this term is done following the lines of 2.4.1b, specifically the result of eq. (2.71). The results of the various terms of (4.29) are given in tab. 4.5. Here we did not write the factors ξ since will be included later in the nodal diagrams terms N defined as in eq. (2.77). The above results are invariant about the position of k_4 and k_5. The isospin traces are given by the coefficients $\eta^{\alpha\beta\gamma}_{l_1l_2l_3l_4l_5}(i)$ calculated in equation (3.69)

By using the above definitions we can write:

$$\begin{aligned}
W_c(dd) \;=\;& \frac{1}{24}\int d\mathbf{r}_1 d\mathbf{r}_2 H_{JF}^{2k_1-1+l_1,2k_2-1+l_2,2k_3-1+l_3}(r_{12})\Big[\rho^{\alpha\beta}_{2,dir}(1,2)\Big\{\\
& I^{k_1k_2k_5}I^{k_3k_4k_5}A^{k_5}M^{\alpha\beta k_4}_{1,dd,l_1,l_2,l_3}(1,2)+I^{k_1k_2k_5}J^{k_3k_4k_5}M^{\alpha\beta k_4}_{2,dd,l_1,l_2,l_3}(1,2)+\\
& I^{k_2k_3k_5}J^{k_1k_4k_5}M^{\alpha\beta k_4}_{3,dd,l_1,l_2,l_3}(1,2)+\frac{3}{2}I^{k_3k_1k_5}J^{k_2k_4k_5}M^{\alpha\beta k_4}_{dd,l_1,l_2,l_3}(1,2)\Big\}+\\
& \Delta^{k_5}\rho^{\alpha\beta}_{2,exc}(1,2)\sum_{l_5=0}^{1}\Big\{\frac{3}{2}\Big(I^{k_1k_2k_6}I^{k_6k_3k_7}J^{k_5k_4k_7}M^{\alpha\beta k_4}_{dd,l_5,l_1+l_2+l_3,0}(1,2)+\\
& I^{k_1k_2k_6}I^{k_3k_5k_7}J^{k_7k_4k_6}M^{\alpha\beta k_4}_{dd,l_5,l_1+l_2,l_3}(1,2)+\\
& I^{k_2k_3k_6}I^{k_5k_1k_7}J^{k_7k_4k_6}M^{\alpha\beta k_4}_{dd,l_5+l_1,l_2+l_3,0}(1,2)+\\
& I^{k_3k_5k_6}I^{k_6k_1k_7}J^{k_2k_4k_7}M^{\alpha\beta k_4}_{dd,l_5+l_1,l_2,l_3}(1,2)\Big)+\\
& I^{k_5k_4k_6}I^{k_1k_2k_7}I^{k_6k_7k_3}A^{k_3}M^{\alpha\beta k_4}_{4,dd,l_1,l_2,l_3,l_5}(1,2)+\\
& I^{k_2k_3k_6}I^{k_6k_5k_7}J^{k_1k_4k_7}M^{\alpha\beta k_4}_{dd,l_5,l_1,l_2+l_3}(1,2)+
\end{aligned}$$

$$I^{k_5 k_1 k_6} I^{k_6 k_2 k_7} J^{k_3 k_4 k_7} M^{\alpha\beta k_4}_{dd,l_5+l_1+l_2,l_3,0}(1,2) \Big\} \Big] \tag{4.30}$$

with

$$M^{\alpha\beta k_1}_{dd,l_1,l_2,l_3}(1,2) = \frac{1}{2}\left(M^{\alpha\beta k_1}_{dd,l_1,l_2,l_3}(1,2;1) + M^{\alpha\beta k_1}_{dd,l_1,l_2,l_3}(1,2;2)\right) \tag{4.31}$$

$$\begin{aligned} M^{\alpha\beta k_1}_{1,dd,l_1,l_2,l_3}(1,2) &= \frac{3}{2} M^{\alpha\beta k_1}_{dd,0,l_1+l_2+l_3,0}(1,2) + M^{\alpha\beta k_1}_{dd,0,0,l_1+l_2+l_3}(1,2) + \\ & M^{\alpha\beta k_1}_{dd,l_1,0,l_2+l_3}(1,2) + M^{\alpha\beta k_1}_{dd,l_1+l_2+l_3,0,0}(1,2) + \\ & M^{\alpha\beta k_1}_{dd,l_1+l_2,0,l_3}(1,2) \end{aligned} \tag{4.32}$$

$$M^{\alpha\beta k_1}_{2,dd,l_1,l_2,l_3}(1,2) = \frac{3}{2} M^{\alpha\beta k_1}_{dd,0,l_1+l_2,l_3}(1,2) + M^{\alpha\beta k_1}_{dd,l_1+l_2,l_3,0}(1,2) \tag{4.33}$$

$$M^{\alpha\beta k_1}_{3,dd,l_1,l_2,l_3}(1,2) = \frac{3}{2} M^{\alpha\beta k_1}_{dd,l_1,l_2+l_3,0}(1,2) + M^{\alpha\beta k_1}_{dd,0,l_1,l_2+l_3}(1,2) \tag{4.34}$$

$$\begin{aligned} M^{\alpha\beta k_1}_{4,dd,l_1,l_2,l_3,l_5}(1,2) &= M^{\alpha\beta k_1}_{dd,l_5,0,l_1+l_2+l_3}(1,2) + M^{\alpha\beta k_1}_{dd,l_5+l_1,0,l_2+l_3}(1,2) + \\ & M^{\alpha\beta k_1}_{dd,l_5+l_1+l_2+l_3,0,0}(1,2) + M^{\alpha\beta k_1}_{dd,l_5+l_1+l_2,0,l_3}(1,2) \end{aligned} \tag{4.35}$$

and

$$\begin{aligned} M^{\alpha\beta k_1}_{xy,l_1,l_2,l_3}(1,2;i) = \sum_{k_2,k_3=1}^{3} \sum_{\gamma=p,n} \Big[& (1-\delta_{k_1 1}) \eta^{\alpha\beta\gamma}_{l_1,0,l_2,0,l_3}(i) N^{\alpha\beta\gamma}_{xy,2k_1-1,2k_2-1,2k_3-1}(1,2) \\ & + \eta^{\alpha\beta\gamma}_{l_1,1,l_2,0,l_3}(i) N^{\alpha\beta\gamma}_{xy,2k_1-1,2k_2,2k_3-1}(1,2) \\ & + \eta^{\alpha\beta\gamma}_{l_1,0,l_2,1,l_3}(i) N^{\alpha\beta\gamma}_{xy,2k_1-1,2k_2-1,2k_3}(1,2) \\ & + \eta^{\alpha\beta\gamma}_{l_1,1,l_2,1,l_3}(i) N^{\alpha\beta\gamma}_{xy,2k_1,2k_2,2k_3}(1,2) \Big] \end{aligned} \tag{4.36}$$

where we have used the xy labels since this last equation is valid not only for the dd diagrams but also for the ed, de and ee ones.

We have calculated, so far, diagrams where only dynamical correlations reach the external points 1 and 2. The statistical correlations, labeled with e, are treated by using the spin-isospin exchange operator

$$\tfrac{1}{4}\Big[1 + \boldsymbol{\sigma}_1 \cdot \boldsymbol{\sigma}_2\Big]\Big[1 + \boldsymbol{\tau}_1 \cdot \boldsymbol{\tau}_2\Big] = \Pi^{\sigma\tau}$$

This means that in the evaluation of the spin-isospin traces also operators coming from $\Pi^{\sigma\tau}$ should be considered. The role of these operators is somehow different from that of the operators coming from the interaction or from the dynamical correlation. In the last case the operators can have any position in the trace, while in the former case they should be positioned where the operators $\Pi^{\sigma\tau}$ acts.

In our case, we assume that $\Pi^{\sigma\tau}$ acts on the bra $< \Phi|$ state, therefore only to the left handside of the sequence of operators coming from interaction and dynamical correlations. Because of cyclic properties of the traces, the results are identical to those obtained if we would have considered $\Pi^{\sigma\tau}$ acting on the ket $|\Phi >$ state. In the ed part the operator structure of the spin-tensor terms is

$$\frac{1}{2}k_4\left[\frac{1}{2}k_1k_2\{k_3,k_5\}+\frac{1}{2}\{k_1,k_5\}k_2k_3\right] \tag{4.37}$$

where k_4 is the operator coming from $\Pi^{\sigma\tau}$. The different terms have already been calculated in the evaluation of the dd part (see table 4.5). We obtain

$$\begin{aligned} W_c(ed) &= \frac{1}{8}\int d\mathbf{r}_1 d\mathbf{r}_2 H_{JF}^{2k_1-1+l_1,2k_2-1+l_2,2k_3-1+l_3}(r_{12})\cdot \\ &\quad (g_{dd}^{\alpha\beta}(1,2)C_{d,22}^{\beta}(2)+g_{de}^{\alpha\beta}(1,2)C_{e,22}^{\beta}(2))C_{e,22}^{\alpha}(1) \\ &\quad \Big\{I^{k_1k_2k_5}I^{k_3k_4k_5}A^{k_5}(M_{ed,0,l_1+l_2+l_3,0}^{\alpha\beta k_4}(1,2;1)+M_{ed,0,0,l_1+l_2+l_3}^{\alpha\beta k_4}(1,2;1))+ \\ &\quad I^{k_1k_2k_5}J^{k_3k_4k_5}M_{ed,0,l_1+l_2,l_3}^{\alpha\beta k_4}(1,2;1)+I^{k_2k_3k_5}J^{k_1k_4k_5}M_{ed,0,l_1,l_2+l_3}^{\alpha\beta k_4}(1,2;1)\Big\} \end{aligned} \tag{4.38}$$

The de term of eq. (4.28) has the same operator structure as the ed term if k_4 and k_5 are interchanged. The result is:

$$\begin{aligned} W_c(de) &= \frac{1}{8}\int d\mathbf{r}_1 d\mathbf{r}_2 H_{JF}^{2k_1-1+l_1,2k_2-1+l_2,2k_3-1+l_3}(r_{12}) \\ &\quad (g_{dd}^{\alpha\beta}(1,2)C_{d,22}^{\alpha}(1)+g_{ed}^{\alpha\beta}(1,2)C_{e,22}^{\alpha}(1))C_{e,22}^{\beta}(2) \\ &\quad \Big\{I^{k_1k_2k_5}I^{k_3k_4k_5}A^{k_5}(M_{de,0,l_1+l_2+l_3,0}^{\alpha\beta k_4}(1,2;2)+M_{de,0,0,l_1+l_2+l_3}^{\alpha\beta k_4}(1,2;2))+ \\ &\quad I^{k_1k_2k_5}J^{k_3k_4k_5}M_{de,0,l_1+l_2,l_3}^{\alpha\beta k_4}(1,2;2)+I^{k_2k_3k_5}J^{k_1k_4k_5}M_{de,0,l_1,l_2+l_3}^{\alpha\beta k_4}(1,2;2)\Big\} \end{aligned} \tag{4.39}$$

The operator structure ee term is such that only the terms $1/2\{k_4,k_5\}k_1k_2k_3$ are present, so we can write

$$W_c(ee) = \frac{1}{2}\int d\mathbf{r}_1 d\mathbf{r}_2 H_{JF}^{2k_1-1+l_1,2k_2-1+l_2,2k_3-1+l_3}(r_{12})C_{e,22}^{\alpha}(1)g_{dd}^{\alpha\beta}(1,2)C_{e,22}^{\beta}(2)$$

$$I^{k_1k_2k_5}I^{k_3k_4k_5}A^{k_5}\left[\frac{1}{2}\left(M_{ee,l_1l_2l_3}^{k_1\alpha\beta}(1,2;1)+M_{ee,l_1l_2l_3}^{k_1\alpha\beta}(1,2;2)\right)\right] \tag{4.40}$$

To calculate the $W_c(cc)$ term of the eq. (4.28) we found useful to consider separately the situations where the $p>1$ operator structure appears on the left, or on the right part of the folding integrals. Specifically we define non-nodal diagrams

	Traces
$k_4k_6k_5k_1k_2k_3$	$I^{k_2k_3k_7}I^{k_1k_7k_8}J^{k_6k_8k_9}$
$k_4k_6k_1k_5k_2k_3$	$I^{k_2k_3k_7}I^{k_6k_1k_8}J^{k_7k_8k_9}$
$k_4k_6k_1k_2k_5k_3$	$I^{k_1k_2k_7}I^{k_6k_7k_8}J^{k_8k_3k_9}$
$k_4k_6k_1k_2k_3k_5$	$I^{k_2k_3k_7}I^{k_6k_1k_8}I^{k_7k_8k_9}A^{k_9}$
$k_6lk_4k_5k_1k_2k_3$	$I^{k_2k_3k_7}I^{k_7k_6k_8}I^{k_1k_8k_9}A^{k_9}$
$k_6k_4k_1k_5k_2k_3$	$I^{k_2k_3k_7}I^{k_7k_6k_8}J^{k_1k_8k_9}$
$k_6k_4k_1k_2k_5k_3$	$I^{k_1k_2k_7}I^{k_3k_6k_8}J^{k_8k_7k_9}$
$k_6k_4k_1k_2k_3k_5$	$I^{k_2k_3k_7}I^{k_1k_7k_8}J^{k_6k_8k_9}$

Table 4.6: Tensor-spin traces for the eq. (4.45).

as:

$$X^{Z\alpha}_{cc,p}(1,2) = \left(2f_1(r_{12})f_p(r_{12}) + N^{\alpha\alpha}_{dd,p}(1,2)\right) g^{\alpha}_{cc}(1,2) + \left(g^{\alpha\alpha}_{dd}(1,2) - 1\right) N^{Z\alpha}_{cc,p}(1,2) \tag{4.41}$$

where the label Z can be L (for left) and R (for right). By using eqs. (3.96) and (3.97) we define the left and right nodal diagrams as:

$$N^{L\alpha\gamma}_{cc,pqr}(1,2) = \left(X^{L\alpha}_{cc,q}(1,3)\xi^{k_2k_3k_1}_{132}C^{\gamma}_{e,qr}(3)\frac{\Delta^{k_3}}{2}\Big|X^{\gamma}_{cc}(3,2) + N^{\gamma}_{cc}(3,2) - \rho^{0,\gamma}_1(3,2)\right) \tag{4.42}$$

$$N^{R\alpha\gamma}_{cc,pqr}(1,2) = \left(X^{\alpha}_{cc}(1,3)\frac{\Delta^{k_2}}{2}\xi^{k_2k_3k_1}_{132}C^{\gamma}_{e,qr}(3)\Big|X^{R\gamma}_{cc,r}(3,2) + N^{R\gamma}_{cc,r}(3,2)\right) \tag{4.43}$$

The above equations (4.41),(4.42),(4.43) form a set of hypernetted equations which can be solved iteratively. For example, one may start by setting the nodal diagrams equal to zero in eq. (4.41). The (cc) nodal diagrams to be used in the evaluation of $W_c(cc)$ are those where the left and right nodal diagrams are subtracted:

$$N^{int,\alpha}_{cc,p}(1,2) = N^{\alpha}_{cc,p}(1,2) - N^{R\alpha}_{cc,p}(1,2) - N^{L\alpha}_{cc,p}(1,2) \tag{4.44}$$

The operator structure of the spin-tensor terms to the right diagrams is:

$$\frac{1}{4}\{k_6,k_4\}\left[\frac{1}{2}\{k_1,k_5\}k_2k_3 + \frac{1}{2}k_1k_2\{k_3,k_5\}\right] \tag{4.45}$$

The terms related to the diagrams L are obtained by exchanging k_4 and k_5. The various possibilities are given in tab. 4.6. By putting together the various terms we obtain

$$\begin{aligned}
W_c(cc) &= -\frac{1}{8}\int d\mathbf{r}_1 d\mathbf{r}_2 H_{JF}^{2k_1-1+l_1,2k_2-1+l_2,2k_3-1+l_3}(r_{12}) \\
& C_{e,22}^{\alpha}(1) g_{cc}^{\alpha}(1,2) C_{e,22}^{\beta}(2) \Delta^{k_4} \\
& \sum_{l_4=0}^{1} \Big\{ 8 I^{k_2k_3k_6} I^{k_1k_6k_7} J^{k_7k_4k_5} \chi_{l_1+l_2+l_3+l_4+l_5} N_{cc,2k_5-1+l_5}^{int,\beta}(1,2) + \\
& I^{k_2k_3k_6} I^{k_1k_6k_7} J^{k_7k_4k_5} \left(M_{cc,0,l_4,l_1+l_2+l_3}^{\beta k_5}(1,2) + M_{cc,l_4,l_1+l_2+l_3,0}^{\beta k_5}(1,2) \right) + \\
& I^{k_2k_3k_6} I^{k_4k_1k_7} J^{k_6k_7k_5} M_{cc,0,l_4+l_1,l_2+l_3}^{\beta k_5}(1,2) + \\
& I^{k_1k_2k_6} I^{k_4k_6k_7} J^{k_7k_3k_5} M_{cc,0,l_4+l_1+l_2,l_3}^{\beta k_5}(1,2) + \\
& I^{k_2k_3k_6} I^{k_4k_1k_7} I^{k_6k_7k_5} A^{k_5} M_{cc,0,l_4+l_1+l_2+l_3,0}^{\beta k_5}(1,2) + \\
& I^{k_2k_3k_6} I^{k_6k_4k_7} I^{k_1k_7k_5} A^{k_5} M_{cc,l_4,0,l_1+l_2+l_3}^{\beta k_5}(1,2) + \\
& I^{k_2k_3k_6} I^{k_6k_4k_7} J^{k_1k_7k_5} M_{cc,l_4,l_1,l_2+l_3}^{\beta k_5}(1,2) + \\
& I^{k_1k_2k_6} I^{k_4k_3k_7} J^{k_7k_6k_5} M_{cc,l_4,l_1+l_2,l_3}^{\beta k_5}(1,2) \Big\}
\end{aligned} \tag{4.46}$$

with

$$M_{cc,l_1,l_2,l_3}^{\alpha k_1}(1,2) = \frac{1}{2}\left(M_{cc,l_1,l_2,l_3}^{R\alpha k_1}(1,2;1) + M_{cc,l_1,l_2,l_3}^{L\alpha k_1}(1,2;2) \right) \tag{4.47}$$

In the above equation the left and right functions are defined as in eq. (4.36) by substituting the nodal diagrams N with the left and right nodal diagrams of eqs. (4.42) and (4.43).

We evaluate the last term of eq. (4.28) by using the prescription adopted in [Fab98]:

$$W_{cs} \sim \frac{W_s W_c}{W_0}$$

This approximated treatment of W_{cs} has been adopted to simplify the calculation of the W_{cs}, which has a large number of operators. On the other hand, nuclear matter estimations show that its contribution is at least two orders of magnitude smaller than those of the other W terms.

In nuclear matter the above approximation has been compared with the results obtained in [Pan79] where a more complicated and refined approximations are used. The two results agree up to second decimal digit.

Now, we calculate the part of the kinetic energy (4.6) where the ∇ operator acts

on the uncorrelated wave function Φ. In eq. (4.7) we called T_ϕ this term. We found convenient to separate it in three parts:

$$T_\phi = T_\phi^{(1)} + T_\phi^{(2)} + T_\phi^{(3)}. \tag{4.48}$$

In the $T_\phi^{(1)}$ term the kinetic energy operator acts on a nucleon not involved in any exchange loop. In the $T_\phi^{(2)}$ the nucleon is involved in a two-body exchange loop and in $T_\phi^{(3)}$ in a many-body exchange loop. As in eq. (4.28) the (0) label indicate terms with only scalar chains between interacting points, the (s) label the diagrams with SOR touching the interacting points and the (c) the diagrams containing SOC between the interacting points.
The terms with j label contains exchange lines with antiparallel spins. For the $T_\phi^{(1)}$ term we obtain

$$T_\phi^{(1)} = -\frac{\hbar^2}{4m} \sum_{\alpha=p,n} \int d\mathbf{r}_1 \rho_{T1}^\alpha(\mathbf{r}_1) C_{e,11}^\alpha(\mathbf{r}_1) \tag{4.49}$$

with $\rho_{T1}^\alpha(\mathbf{r}_1)$ is given in eq. (4.9). We separate the remaining terms in five parts:

$$T_\phi^{(n)} = T_{\phi,0}^{(n)} + T_{\phi,s}^{(n)} + T_{\phi,0j}^{(n)} + T_{\phi,sj}^{(n)} + T_{\phi,c}^{(n)} \qquad n = 2,3 \tag{4.50}$$

We define the function:

$$h_{pq}^{\alpha\beta}(1,2) = \Big(f_p(r_{12}) f_q(r_{12}) g_{dd}^{\alpha\beta}(1,2) - \delta_{p,1}\delta_{q,1} \Big) C_{e,22}^\alpha(1) C_{e,22}^\beta(2) \tag{4.51}$$

and we obtain:

$$\begin{aligned}
T_{\phi,0}^{(2)} &= \frac{\hbar^2}{4m} \int d\mathbf{r}_1 d\mathbf{r}_2 \rho_{T2}^{\alpha\beta}(1,2) \Big[h_{2k_1-1+l_1,2k_2-1+l_2}^{\alpha\beta}(1,2) \Delta^{k_3} I^{k_1k_2k_3} A^{k_3} \qquad (4.52)\\
&\quad \Big[\chi_{l_1+l_2}^{\alpha\beta} \chi_{l_1+l_2+1}^{\alpha\beta} \Big] +_{\alpha\beta} C_{e,22}^\alpha(1) \Big(C_{e,22}^\beta(2) - 1 \Big) \Big] \\
T_{\phi,0j}^{(2)} &= -\frac{\hbar^2}{4m} \int d\mathbf{r}_1 d\mathbf{r}_2 \rho_{T2A}^{\alpha\beta}(1,2) \Big[h_{2k_1-1+l_1,2k_2-1+l_2}^{\alpha\beta}(1,2) \Delta^{k_3} I^{k_1k_2k_4} I^{k_4k_3 2} \cdot \\
&\quad \Big[\chi_{l_1+l_2}^{\alpha\beta} + \chi_{l_1+l_2+1}^{\alpha\beta} \Big] + 2\delta_{\alpha\beta} C_{e,22}^\alpha(1) \Big(C_{e,22}^\beta(2) - 1 \Big) \Big] \qquad (4.53)\\
T_{\phi,0}^{(3)} &= -\frac{\hbar^2}{2m} \int d\mathbf{r}_1 d\mathbf{r}_2 \rho_{T3}^{\alpha}(1,2) \Big[h_{2k_1-1+l_1,2k_2-1+l_2}^{\alpha\beta}(1,2) \Delta^{k_3} I^{k_1k_2k_3} A^{k_3} \cdot
\end{aligned}$$

$$
\begin{aligned}
& N^{\beta}_{cc}(1,2)\Big[\chi^{\alpha\beta}_{l_1+l_2}+\chi^{\alpha\beta}_{l_1+l_2+1}\Big]2\delta_{\alpha,\beta}C^{\alpha}_{e,22}(1) \\
& \Big(C^{\beta}_{e,22}(2)N^{(x)\beta}_{cc}(1,2)+N^{(\rho)\beta}_{cc}(1,2)\Big(C^{\beta}_{e,22}(2)-1\Big)\Big)\Big] \qquad (4.54)
\end{aligned}
$$

$$
\begin{aligned}
T^{(3)}_{\phi,0j} &= \frac{\hbar^2}{2m}\int d\mathbf{r}_1 d\mathbf{r}_2 \rho^{\alpha}_{T3A}(1,2)\Big[h^{\alpha\beta}_{2k_1-1+l_1,2k_2-1+l_2}(1,2)N^{\beta}_{ccj}(1,2)\cdot \\
& \Delta^{k_3}I^{k_1k_2k_4}I^{k_4k_32}\Big[\chi^{\alpha\beta}_{l_1+l_2}+\chi^{\alpha\beta}_{l_1+l_2+1}\Big]2\delta_{\alpha,\beta}C^{\alpha}_{e,22}(1) \\
& \Big(C^{\beta}_{e,22}(2)N^{(x)\beta}_{ccj}(1,2)+N^{(\rho)\beta}_{ccj}(1,2)\Big(C^{\beta}_{e,22}(2)-1\Big)\Big)\Big] \qquad (4.55)
\end{aligned}
$$

$$
\begin{aligned}
T^{(2)}_{\phi,s} &= \frac{\hbar^2}{4m}\int d\mathbf{r}_1 d\mathbf{r}_2 \rho^{\alpha\beta}_{T2}(1,2)\Big[h^{\alpha\beta}_{2k_1-1+l_1,2k_2-1+l_2}(1,2)\Delta^{k_3}I^{k_1k_2k_3}A^{k_3}\times \\
& \sum_{l_3=0}^{1}\Big(M^{\alpha\beta k_1k_2k_3}_{d,l_1,l_2,l_3}(1)+M^{\alpha\beta k_1k_2k_3}_{d,l_1,l_2,l_3}(2)\Big)+ \\
& 2\delta_{\alpha\beta}C^{\alpha}_{e,22}(1)\Big(U^{\alpha}_{d,op}(1)\Big(C^{\beta}_{e,22}(2)-1\Big)+C^{\alpha}_{e,22}(1)U^{\beta}_{d,op}(2)\Big)\Big] \qquad (4.56)
\end{aligned}
$$

$$
\begin{aligned}
T^{(2)}_{\phi,sj} &= -\frac{\hbar^2}{4m}\int d\mathbf{r}_1 d\mathbf{r}_2 \rho^{\alpha\beta}_{T2A}(1,2)\Big[h^{\alpha\beta}_{2k_1-1+l_1,2k_2-1+l_2}(1,2)\Delta^{k_3}I^{k_1k_2k_4}I^{k_4k_32}\times \\
& \sum_{l_3=0}^{1}\Big(M^{\alpha\beta k_1k_2k_3}_{d,l_1,l_2,l_3}(1)+M^{\alpha\beta k_1k_2k_3}_{d,l_1,l_2,l_3}(2)\Big)+ \\
& 2\delta_{\alpha\beta}C^{\alpha}_{e,22}(1)\Big(U^{\alpha}_{d,op}(1)\Big(C^{\beta}_{e,22}(2)-1\Big)+C^{\alpha}_{e,22}(1)U^{\beta}_{d,op}(2)\Big)\Big] \qquad (4.57)
\end{aligned}
$$

$$
\begin{aligned}
T^{(3)}_{\phi,s} &= -\frac{\hbar^2}{2m}\int d\mathbf{r}_1 d\mathbf{r}_2 \rho^{\alpha}_{T3}(1,2)\Big[h^{\alpha\beta}_{2k_1-1+l_1,2k_2-1+l_2}(1,2)\Delta^{k_3}I^{k_1k_2k_3}A^{k_3} \\
& N^{\beta}_{cc}(1,2)\sum_{l_3=0}^{1}\Big(M^{\alpha\beta k_1k_2k_3}_{d,l_1,l_2,l_3}(1)+M^{\alpha\beta k_1k_2k_3}_{d,l_1,l_2,l_3}(2)\Big)+ \\
& 2\delta_{\alpha\beta}C^{\alpha}_{e,22}(1)\Big(N^{\beta}_{cc}(1,2)C^{\beta}_{e,22}(2)U^{\beta}_{d,op}(2)+ \\
& U^{\alpha}_{d,op}(1)\Big(N^{(x)\beta}_{cc}(1,2)C^{\beta}_{e,22}(2)+N^{(\rho)\beta}_{cc}(1,2)\Big(C^{\beta}_{e,22}(2)-1\Big)\Big)\Big)\Big] \qquad (4.58)
\end{aligned}
$$

$$
\begin{aligned}
T^{(3)}_{\phi,sj} &= \frac{\hbar^2}{2m}\int d\mathbf{r}_1 d\mathbf{r}_2 \rho^{\alpha}_{T3A}(1,2)\Big[h^{\alpha\beta}_{2k_1-1+l_1,2k_2-1+l_2}(1,2)\Delta^{k_3}I^{k_1k_2k_4}I^{k_4k_32}\times \\
& N^{\beta}_{cc}(1,2)\sum_{l_3=0}^{1}\Big(M^{\alpha\beta k_1k_2k_3}_{d,l_1,l_2,l_3}(1)+M^{\alpha\beta k_1k_2k_3}_{d,l_1,l_2,l_3}(2)\Big)+ \\
& 2\delta_{\alpha\beta}C^{\alpha}_{e,22}(1)\Big(N^{\beta}_{ccj}(1,2)C^{\beta}_{e,22}(2)U^{\beta}_{d,op}(2)+ \\
& U^{\alpha}_{d,op}(1)\Big(N^{(x)\beta}_{ccj}(1,2)C^{\beta}_{e,22}(2)+N^{(\rho)\beta}_{ccj}(1,2)\Big(C^{\beta}_{e,22}(2)-1\Big)\Big)\Big)\Big] \qquad (4.59)
\end{aligned}
$$

where the one-body densities $\rho_{T2,P}$,$\rho_{T2,A}$ and $\rho_{T3,P}$,$\rho_{T3.A}$ are defined in Appendix A.5.

Let us study now the structure of the $T^{(2)}_{\phi,c}$ term. In this case the external points

	Traces
$k_6k_4k_1k_2k_5$	$I^{k_1k_2k_7}J^{k_6k_8k_7}$
$k_6k_4k_1k_5k_2$	$I^{k_2k_6k_7}J^{k_7k_8k_1}$
$k_6k_1k_4k_2k_5$	$I^{k_6k_1k_7}J^{k_7k_8k_2}$
$k_6k_1k_4k_5k_2$	$I^{k_2k_6k_7}I^{k_7k_1k_8}A^{k_8}$
$k_6k_4k_5k_1k_2$	$I^{k_6k_8k_7}I^{k_7k_1k_2}A^{k_2}$
$k_6k_1k_4k_5k_2$	$I^{k_6k_8k_7}I^{k_7k_1k_2}A^{k_2}$
$k_6k_4k_1k_5k_2$	$I^{k_2k_6k_7}J^{k_1k_8k_7}$
$k_6k_1k_2k_4k_5$	$I^{k_6k_8k_7}I^{k_7k_1k_2}A^{k_2}$
$k_6k_1k_4k_5k_2$	$I^{k_6k_8k_7}I^{k_7k_1k_2}A^{k_2}$
$k_6k_1k_4k_2k_5$	$I^{k_6k_1k_7}J^{k_2k_8k_7}$

Table 4.7: Tensor-spin traces for the operators of eq. (4.61).

are exchanged. An exchange operator (n) contributes. Moreover there is a couple of operators in the external particles (p, q) and two operators in the chain (s_1, s_2). The operator structure is:

$$\frac{n}{4}\left[\frac{1}{4}\{k_1, k_4\}\{k_2, k_5\} + \frac{1}{4}\{k_1, k_5\}\{k_2, k_4\} + \frac{1}{6}\Big(\{\{k_4, k_5\}, k_1\}\right. \tag{4.60}$$

$$\left. +k_4k_1k_5 + k_5k_1k_4\Big)k_2 + \frac{1}{6}k_1\Big(\{\{k_4, k_5\}, k_2\} +k_4k_2k_5 + k_5k_2k_4\Big)\right] \tag{4.61}$$

The various contributions of the spin-tensor part are given in tab. 4.7. Then

$$\begin{aligned} T_{\phi,c}^{(2)} &= -\frac{\hbar^2}{48m}\int d\mathbf{r}_1 d\mathbf{r}_2 \rho_{T2}^{\alpha\beta}(1,2) f_{2k_1-1+l_1}(r_{12}) f_{2k_2-1+l_2}(r_{12}) \cdot \\ &\Delta^{k_3} C_{e,22}^{\alpha}(1) C_{e,22}^{\beta}(2) g_{dd}^{\alpha\beta}(1,2) \sum_{l_3=0}^{1}\Big\{\frac{3}{2}\Big(I^{k_1k_2k_5}J^{k_3k_4k_5}M_{dd,l_3,l_1+l_2,0}^{\alpha\beta k_4}(1,2) \\ &+I^{k_2k_3k_5}J^{k_5k_4k_1}M_{dd,l_3,l_1,l_2}^{\alpha\beta k_4}(1,2) + I^{k_3k_1k_5}J^{k_5k_4k_2}M_{dd,l_3+l_1,l_2,0}^{\alpha\beta k_4}(1,2) \\ &+I^{k_3k_1k_5}I^{k_5k_2k_4}A^{k_4}M_{dd,l_3+l_1,0,l_2}^{\alpha\beta k_4}(1,2)\Big) + I^{k_2k_3k_5}J^{k_1k_4k_5}M_{dd,l_3,l_1,l_2}^{\alpha\beta k_4}(1,2) \\ &+I^{k_3k_4k_5}I^{k_5k_1k_2}A^{k_2}M_{4,dd,l_1,0,l_2,l_3}^{\alpha\beta k_4}(1,2) + I^{k_3k_1k_5}J^{k_2k_4k_5}M_{dd,l_3+l_1,l_2,0}^{\alpha\beta k_4}(1,2)\Big\} \end{aligned} \tag{4.62}$$

4.2 Spin-orbit and Coulomb terms

The contribution of the Coulomb interaction is:

$$< v_{Coul} >= \frac{1}{< \Psi^* \Psi >} < \Psi^* \sum_{i \neq j} \delta(\boldsymbol{r}_1 - \boldsymbol{r}_i) \delta(\boldsymbol{r}_2 - \boldsymbol{r}_i) \Big(\frac{1 + \tau_{i,z}}{2} \Big) \Big(\frac{1 + \tau_{j,z}}{2} \Big) \frac{e^2}{r_{12}} \Psi > \tag{4.63}$$

where $(1 + \tau_{i(j),z})/2$ are the projection operators on the proton states. The Coulomb interaction is added in the scalar channel of the equations of the sect. 3.1 in all the proton-proton terms. The FHNC/SOC computational scheme described above is not modified by the inclusion of the Coulomb interaction. The contribution of the spin-orbit terms of the potential, p=7,8, has been calculated by making an approximation. In eq. (4.15) we consider only the W_0 term. This corresponds in considering only those diagrams containing scalar chains between interacting points. By using the conventions of sect. 3.1 where $l_i = 0, 1$ we obtain

$$\begin{aligned} < v^{7+l_2} >_{W_0} \;\; = \;\; & -9 \int d\boldsymbol{r}_1 d\boldsymbol{r}_2 \frac{f_{5+l_1}(r_{12}) v^{7+l_2}(r_{12}) f_{5+l_3}(r_{12})}{f_1^2(r_{12})} \\ & g_{dd}^{\alpha\beta}(1,2) \Big\{ C_d^{\alpha}(1) C_d^{\beta}(2) \chi_{l_1+l_2+l_3}^{\alpha\beta} \\ & -2 \Big[N_{cc}^{\alpha}(1,2) - \rho_0^{\alpha}(1,2) \Big] \Big[N_{cc}^{\beta}(1,2) - \rho_0^{\beta}(1,2) \Big] \\ & C_e^{\alpha}(1) C_e^{\beta}(2) (\chi_{l_1+l_2+l_3}^{\alpha\beta} + \chi_{l_1+l_2+l_3+1}^{\alpha\beta}) \Big\} \end{aligned} \tag{4.64}$$

4.3 The three-body potential

The three-body potential used in our calculation is composed by two parts [Car83]:

$$V_3 = v_{ijk}^{2\pi} + v_{ijk}^R \tag{4.65}$$

We call $v_{ijk}^{2\pi}$ the Fujita-Niyazawa term (see fig. 4.1) which exchanges two pions with intermediate excitation of a Δ. This is the long range part of the three–body interaction and gives an attractive contribution. The v_{ijk}^R term is a repulsive term of shorter range. The explicit expressions of these two terms are:

$$\begin{aligned} v_{123}^{2\pi} \;\; = \;\; & A_{2\pi} \sum_{cycl} \Big(\{X_{31}, X_{32}\} \{\boldsymbol{\tau}_3 \cdot \boldsymbol{\tau}_1, \boldsymbol{\tau}_3 \cdot \boldsymbol{\tau}_2\} \\ & + \frac{1}{4} [X_{31}, X_{32}] [\boldsymbol{\tau}_3 \cdot \boldsymbol{\tau}_1, \boldsymbol{\tau}_3 \cdot \boldsymbol{\tau}_2] \Big) \end{aligned} \tag{4.66}$$

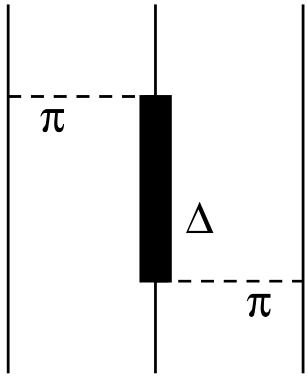

Figure 4.1: Fujita-Niyazawa term.

$$v_{123}^{R} = U_0 \sum_{cycl} T_{\pi}^{2}(r_{31}) T_{\pi}^{2}(r_{32}) \tag{4.67}$$

with

$$Y_{\pi}(r) = \frac{e^{-\mu r}}{\mu r}(1 - e^{-cr^2}) \tag{4.68}$$

$$T_{\pi}(r) = \frac{e^{-\mu r}}{\mu r}[1 + \frac{3}{\mu r} + \frac{3}{(\mu r^2)}](1 - e^{-cr^2})^2 \tag{4.69}$$

$$X_{ij} = T_{\pi}(r_{ij}) \boldsymbol{\sigma}_i \cdot \boldsymbol{\sigma}_j + T_{\pi}(r_{ij}) S_{ij} \tag{4.70}$$

where S_{ij} indicates the tensor operator and the values of the constants are $\mu \sim 0.7 fm^{-1}$, and $c = 2 fm^{-2}$. The $A_{2\pi}$, and U_0 parameters are adjusted to provide a good fit to the binding energies of three-body nuclei and nuclear matter [Car83]. The symbols $\{,\}$ and $[,]$ indicate the anticommutator and commutator, respectively.

We evaluate the contribution of the three-body interaction as the sum of the five diagrams presented in fig. 4.2 calculated in FHNC/SOC approximation. The diagrams 2.1-3 are related to $v_{123}^{2\pi}$ and 3.1-2 to v_{123}^{R} (see fig. 4.2).
In diagram 2.1 the pairs of nucleon connected by operators X_{ij} (pairs 31 and 32) are dressed at all orders by Jastrow scalar correlations, whereas the remaining pair (e.g. the pair 12) is dressed by all the operator correlations (in SOC approximation).
The anticommutator terms in $v_{123}^{2\pi}$ contains linear terms in σ_3 and τ_3. The contribution of τ_3 is different from zero for nuclei with $N \neq Z$. On the other hand, the contribution of the terms linear in σ_3 are zero in any case. This means that the contribution of the diagram 2.1 is analogous to that of the case $N = Z$. Only the

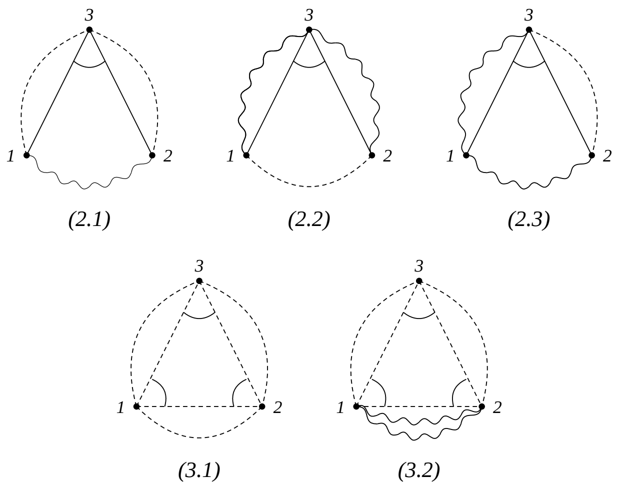

Figure 4.2: Cluster diagrams considered for the three-body force expectation value. The 2.1, 2.2, 2.3 diagrams are related to the $< v^{2\pi}_{ijk} >$ part of the force, and the 3.1 and 3.2 diagrams are related to $< v^{R}_{ijk} >$. The points denote the particle coordinates. The dashed, wavy, and double-wavy lines represent generalized scalar, operator and single-operator ring correlation bonds, respectively.

anticommuator terms contribute. The contribution is provided only by the $\sigma\tau$ ($p = 4$) and ($p = 6$) components. The explicit expressions of the various terms contributing are:

$$
\begin{aligned}
v^{k_3,\alpha\beta}_{eff,dd}(1,2) &= \sum_{\gamma} 4A_{2\pi} \int d\mathbf{r}_3 [g^{\alpha\gamma}_{dd}(1,3) C^{\gamma}_{d}(3) g^{\gamma\beta}_{dd}(3,2) \\
&+ g^{\alpha\gamma}_{dd}(1,3) C^{\gamma}_{e}(3) g^{\gamma\beta}_{ed}(3,2) \\
&+ g^{\alpha\gamma}_{de}(1,3) C^{\gamma}_{e}(3) g^{\gamma\beta}_{dd}(3,2)] \xi^{k_1k_2k_3}_{132} X^{k_1}(r_{13}) X^{k_2}(r_{32}) \qquad (4.71) \\
v^{k_3,\alpha\beta}_{eff,de}(1,2) &= \sum_{\gamma} 4A_{2\pi} \int d\mathbf{r}_3 [g^{\alpha\gamma}_{dd}(1,3) C^{\gamma}_{e}(3) g^{\gamma\beta}_{de}(3,2) \\
&+ g^{\alpha\gamma}_{dd}(1,3) C^{\gamma}_{e}(3) (g^{\gamma\beta}_{ee}(3,2) + (2\delta_{\gamma\beta} - 1) g^{\gamma\beta}_{ee,exc}(3,2)) \\
&+ g^{\alpha\gamma}_{de}(1,3) C^{\gamma}_{e}(3) g^{\gamma\beta}_{de}(3,2)] \xi^{k_1k_2k_3}_{132} X^{k_1}(r_{13}) X^{k_2}(r_{32}) \qquad (4.72) \\
v^{k_3,\alpha\beta}_{eff,ed}(1,2) &= \sum_{\gamma} 4A_{2\pi} \int d\mathbf{r}_3 [g^{\alpha\gamma}_{ed}(1,3) C^{\gamma}_{e}(3) g^{\gamma\beta}_{dd}(3,2) \\
&+ g^{\alpha\gamma}_{ed}(1,3) C^{\gamma}_{e}(3) g^{\gamma\beta}_{ed}(3,2) \\
&+ (g^{\alpha\gamma}_{ee}(1,3) + (2\delta_{\alpha\gamma} - 1) g^{\alpha\gamma}_{ee,exc}(1,3)) C^{\gamma}_{e}(3) g^{\gamma\beta}_{dd}(3,2)] \qquad (4.73) \\
&\cdot \xi^{k_1k_2k_3}_{132} X^{k_1}(r_{13}) X^{k_2}(r_{32}) \qquad (4.74) \\
v^{k_3,\alpha\beta}_{eff,ee}(1,2) &= \sum_{\gamma} 4A_{2\pi} \int d\mathbf{r}_3 [g^{\alpha\gamma}_{ed}(1,3) C^{\gamma}_{e}(3) g^{\gamma\beta}_{de}(3,2) \\
&+ g^{\alpha\gamma}_{ed}(1,3) C^{\gamma}_{e}(3) (g^{\gamma\beta}_{ee}(3,2) + (2\delta_{\gamma\beta} - 1) g^{\gamma\beta}_{ee,exc}(3,2))
\end{aligned}
$$

$$
\begin{aligned}
&+ \quad (g_{ee}^{\alpha\gamma}(1,3) + (2\delta_{\alpha\gamma} - 1) g_{ee,exc}^{\alpha\gamma}(1,3)) \\
&\cdot \quad C_e^{\gamma}(3) g_{de}^{\gamma\beta}(3,2)] \xi_{132}^{k_1 k_2 k_3} X^{k_1}(r_{13}) X^{k_2}(r_{32})
\end{aligned} \tag{4.75}
$$

$$
\begin{aligned}
v_{eff,cc}^{k_3,\alpha}(1,2) &= \sum_{\beta} 4A_{2\pi} \int d\mathbf{r}_3 2\delta_{\alpha\beta} [g_{cc}^{\alpha}(1,3) \frac{C_e^{\beta}(3)}{2} g_{cc}^{\beta}(3,2)] \\
&\cdot \quad \xi_{132}^{k_1 k_2 k_3} X^{k_1}(r_{13}) X^{k_2}(r_{32})
\end{aligned} \tag{4.76}
$$

The mean value of $v_{123}^{2\pi}$ is:

$$
\begin{aligned}
< v_{123}^{2\pi} >_{2.1} &= \frac{1}{2} \sum_{\alpha\beta} \int d\mathbf{r}_1 \int d\mathbf{r}_2 \frac{f_{2k_1-1+l_1}(r_{12}) f_{2k_2-1+l_2}(r_{12})}{f_1^2(r_{12})} \\
&\cdot \quad I^{k_1 k_3 k_2} A^{k_2} \chi_{l_1+l_2+1}^{\alpha\beta} \{ \\
&\quad\ v_{eff,dd}^{k_3,\alpha\beta} (g_{dd}^{\alpha\beta}(1,2) C_d^{\alpha}(1) C_d^{\beta}(2) + g_{de}^{\alpha\beta}(1,2) C_d^{\alpha}(1) C_e^{\beta}(2) \\
&+ \quad g_{ed}^{\alpha\beta}(1,2) C_e^{\alpha}(1) C_d^{\beta}(2) + g_{ee,dir}^{\alpha\beta}(1,2) C_e^{\alpha}(1) C_e^{\beta}(2)) \\
&+ \quad v_{eff,de}^{k_3,\alpha\beta} (g_{dd}^{\alpha\beta}(1,2) C_d^{\alpha}(1) C_e^{\beta}(2) + g_{ed}^{\alpha\beta}(1,2) C_e^{\alpha}(1) C_e^{\beta}(2)) \\
&+ \quad v_{eff,ed}^{k_3,\alpha\beta} (g_{dd}^{\alpha\beta}(1,2) C_e^{\alpha}(1) C_d^{\beta}(2) + g_{de}^{\alpha\beta}(1,2) C_e^{\alpha}(1) C_e^{\beta}(2)) \\
&+ \quad v_{eff,ee}^{k_3,\alpha\beta} (g_{dd}^{\alpha\beta}(1,2) C_e^{\alpha}(1) C_e^{\beta}(2)) \} \\
&- \quad \frac{1}{2} \int d\mathbf{r}_1 \int d\mathbf{r}_2 f_{2k_1-1+l_1}(r_{12}) f_{2k_2-1+l_2}(r_{12}) g_{dd}^{\alpha\beta}(1,2) C_e^{\alpha}(1) C_e^{\beta}(2) \\
&\cdot \quad I^{k_1 k_3 k_4} I^{k_4 k_2 k_5} A^{k_5} (\chi_{l_1+l_2+1}^{\alpha\beta} + \chi_{l_1+l_2+2}^{\alpha\beta}) \Delta^{k_5} \\
&\cdot \quad \{ v_{eff,dd}^{k_3,\alpha\beta}(1,2) [N_{cc}^{\alpha}(1,2) - \rho_1^{0,\alpha}(1,2)][N_{cc}^{\beta}(1,2) - \rho_1^{0,\beta}(1,2)] \\
&+ \quad 2 v_{eff,cc}^{k_3,\alpha}(1,2) [N_{cc}^{\beta}(1,2) - \rho_1^{0,\beta}(1,2)] \}
\end{aligned} \tag{4.77}
$$

where

$$
\begin{aligned}
g_{ee}^{\alpha\beta}(i,j) &= g_{dd}^{\alpha\beta}(i,j)[N_{ee}^{\alpha\beta}(i,j) + N_{ed}^{\alpha\beta}(i,j) N_{de}^{\alpha\beta}(i,j)] \\
&- \quad g_{dd}^{\alpha\beta}(i,j)[N_{cc}^{\alpha}(i,j) - \rho_0^{\alpha}(i,j)][N_{cc}^{\beta}(i,j) - \rho_0^{\beta}(i,j)].
\end{aligned}
$$

The (2.2) diagram contains two wiggly lines which indicate the contribution of the correlation of pairs (13)(23). Its operator structure is :

$$
\begin{aligned}
&\tfrac{1}{4}(\tfrac{1}{2}\{O_{13}^{p}, O_{23}^{s_1}\}(O_{13}^{q} O_{23}^{s_2})_{\pm} + \tfrac{1}{2}(O_{13}^{q}, O_{23}^{s_2})_{\pm}\{O_{13}^{p} O_{23}^{s_1}\} \\
&\quad + O_{13}^{p}(O_{13}^{q}, O_{23}^{s_2})_{\pm} O_{23}^{s_1} + O_{23}^{s_1}(O_{13}^{q}, O_{23}^{s_2})_{\pm} O_{13}^{p})
\end{aligned} \tag{4.78}
$$

	Traces
$k_3k_4(k_1,k_2)_\pm$	$R^{k_3k_4k_1k_2} \pm A^{k_3}\delta_{k_3k_1}\ A^{k_4}\delta_{k_2k_4}$
$k_4k_3(k_1,k_2)_\pm$	$A^{k_3}\delta_{k_3k_1}\ A^{k_4}\delta_{k_2k_4} \pm R^{k_4k_3k_2k_1}$
$(k_1,k_2)_\pm k_3k_4$	$R^{k_1k_2k_3k_4} \pm A^{k_3}\delta_{k_3k_1}\ A^{k_4}\delta_{k_2k_4}$
$(k_1,k_2)_\pm k_4k_3$	$A^{k_3}\delta_{k_3k_1}\ A^{k_4}\delta_{k_2k_4} \pm R^{k_1k_2k_3k_4}$
$k_3(k_1,k_2)_\pm k_4$	$A^{k_3}\delta_{k_3k_1}\ A^{k_4}\delta_{k_2k_4} \pm R^{k_3k_2k_1k_4}$
$k_4(k_1,k_2)_\pm k_3$	$R^{k_4k_1k_2k_3} \pm A^{k_3}\delta_{k_3k_1}\ A^{k_4}\delta_{k_2k_4}$

Table 4.8: Tensor-spin traces of the operator of eq. (4.78).

where

$$(O_{13}^q, O_{23}^{s_2})_\pm = O_{13}^q O_{23}^{s_2} \pm O_{23}^{s_2} O_{13}^q$$

We write the operators in this form

$$\begin{aligned}
(O_{13}^q, O_{23}^{s_2})_\pm &= (P_{13}^{k_1}, P_{23}^{k_2})_\pm (\boldsymbol{\tau}_1 \cdot \boldsymbol{\tau}_3, \boldsymbol{\tau}_2 \cdot \boldsymbol{\tau}_3)_\pm \\
(O_{13}^p, O_{23}^{s_1})_\pm &= \frac{1}{2}\{P_{13}^{k_3}, P_{23}^{k_4}\}\{(\boldsymbol{\tau}_1 \cdot \boldsymbol{\tau}_3)^{l_1}, (\boldsymbol{\tau}_2 \cdot \boldsymbol{\tau}_3))^{l_2}\} \\
&+ \frac{1}{2}[P_{13}^{k_3}, P_{23}^{k_4}][(\boldsymbol{\tau}_1 \cdot \boldsymbol{\tau}_3)^{l_1}, (\boldsymbol{\tau}_2 \cdot \boldsymbol{\tau}_3)^{l_2}]
\end{aligned}$$

By defining the $R^{k_1k_2k_3k_4}$ matrix as [Wir80]:

$$R^{k_1k_2k_3k_4} = C(O_{13}^{k_1} O_{23}^{k_2} O_{13}^{k_3} O_{23}^{k_4}) \tag{4.79}$$

and by using the A^k matrices defined in table 4.1 we get the results of tab. 4.8: with $p = 2k_3 - 1 + l_1$, $q = 2k_1$, $s_1 = 2k_4 - 1 + l_2$, $s_2 = 2k_2$. Including the isopin traces we get:

$$\begin{aligned}
\tfrac{1}{8}(R^{k_3k_4k_1k_2} \pm A^{k_4}\delta_{k_4k_1}A^{k_4}\delta_{k_4k_2}[\chi^{\alpha\beta\gamma}_{l_1l_2110}(1) \pm \chi^{\alpha\beta\gamma}_{l_1l_2011}(1) \pm \chi^{\alpha\beta\gamma}_{0l_2l_1+110}(1) \\
+\chi^{\alpha\beta\gamma}_{0l_2l_111}(1) + \chi^{\alpha\beta\gamma}_{11l_1l_20}(1) \pm \chi^{\alpha\beta\gamma}_{01l_1+1l_20}(1) \pm \chi^{\alpha\beta\gamma}_{110l_2l_1}(1) \\
+\chi^{\alpha\beta\gamma}_{011l_2l_1}(1) \pm 2\chi^{\alpha\beta\gamma}_{l_1+110l_20}(1) + 2\chi^{\alpha\beta\gamma}_{l_111l_20}(1) + 2\chi^{\alpha\beta\gamma}_{0l_211l_1}(1) \\
\pm 2\chi^{\alpha\beta\gamma}_{0l_201l_1+1}(1)]
\end{aligned} \tag{4.80}$$

	Traces
$k_3k_4[k_1,k_2]$	$J^{k_3k_1s_3} - I^{k_3k_1s_3}A^{s_3}$
$k_4k_3[k_1,k_2]$	$-J^{k_3k_1s_3} + I^{k_3k_1s_3}A^{s_3}$
$[k_1,k_2]k_3k_4$	$J^{k_3k_1s_3} - I^{k_3k_1s_3}A^{s_3}$
$[k_1,k_2]k_4k_3$	$-J^{k_3k_1s_3} + I^{k_3k_1s_3}A^{s_3}$
$k_3[k_1,k_2]k_4$	$-J^{k_3k_1s_3} + I^{k_3k_1s_3}A^{s_3}$
$k_4[k_1,k_2]k_3$	$J^{k_3k_1s_3} - I^{k_3k_1s_3}A^{s_3}$

Table 4.9: Tensor-spin traces of the operators of eq. (4.84).

If we indicate the above expression as $\Sigma^{\alpha\beta\gamma}_{k_1k_2k_3k_4,l_1l_2}$, the contribution of diagram 2.2 can be written as:

$$\begin{aligned} < v^{2\pi}_{123} >_{2.2} \;&=\; A_{2\pi}\int d\mathbf{r}_1 d\mathbf{r}_2 d\mathbf{r}_3 \frac{f_{2k_3-1+l_1}(r_{13})}{f_1(r_{13})} X^{k_3}(r_{13}) \frac{f_{2k_4-1+l_2}(r_{23})}{f_1(r_{23})} X^{k_4}(r_{32}) \\ &\quad \Sigma^{\alpha\beta\gamma}_{k_1k_2k_3k_4,l_1l_2}\rho^{\alpha\beta\gamma}_3(1,2,3) \end{aligned} \tag{4.81}$$

where the sum over all the indices is understood and:

$$\begin{aligned} \rho^{\alpha\beta\gamma}_3(1,2,3) \;&=\; \sum_{xyzx'y'z'=d,e} g^{\alpha\gamma}_{xx'}(1,3)V^{\gamma}_{x'y'}(3)g^{\gamma\beta}_{y'y}(3,2)V^{\beta}_{yz}(2)g^{\beta\alpha}_{zz'}(2,1)V^{\alpha}_{z'x}(1) \\ &- \; g^{\gamma}_{cc}(1,3)V^{\gamma}_{cc}(3)g^{\beta}_{cc}(3,2)V^{\beta}_{cc}(2)g^{\alpha}_{cc}(2,1)V^{\alpha}_{cc}(1) \end{aligned} \tag{4.82}$$

with

$$V^{\alpha}_{xy}(i) = \begin{cases} C^{\alpha}_d(i) & \text{if} \quad \text{(xy)} \equiv \text{(dd)} \\ C^{\alpha}_e(i) & \quad\text{otherwise} \end{cases} \tag{4.83}$$

In diagram (2.3) the correlations link the pairs (12)(13): then the operator structure is:

$$\begin{aligned} &\tfrac{1}{4}(\tfrac{1}{2}\{O^p_{13},O^{s_1}_{23}\}[O^q_{13}O^{s_2}_{23}] + \tfrac{1}{2}[O^q_{13},O^{s_2}_{23}]\{O^p_{13}O^{s_1}_{23}\} \\ &\quad +O^p_{13}[O^q_{13},O^{s_2}_{23}]O^{s_1}_{23} + O^{s_1}_{23}[O^q_{13},O^{s_2}_{23}]O^p_{13}) \end{aligned} \tag{4.84}$$

with the spin traces given in tab. 4.9. By including the isospin traces we obtain:

$$\begin{aligned} &\tfrac{1}{8}(J^{k_3k_1s_3} - I^{k_3k_1s_3}A^{s_3})[\eta^{\alpha\beta\gamma}_{l_1l_2110}(2) - \eta^{\alpha\beta\gamma}_{l_1l_2011}(2) - \eta^{\alpha\beta\gamma}_{0l_2l_1+110}(2) \\ &\quad +\eta^{\alpha\beta\gamma}_{0l_2l_111}(2) + \eta^{\alpha\beta\gamma}_{11l_1l_20}(1) - \eta^{\alpha\beta\gamma}_{01l_1+1l_20}(1) - \eta^{\alpha\beta\gamma}_{110l_2l_1}(1) \\ &\quad +\eta^{\alpha\beta\gamma}_{011l_2l_1}(1) - 2\eta^{\alpha\beta\gamma}_{l_1+110l_20}(1) + 2\eta^{\alpha\beta\gamma}_{l_111l_20}(1) + 2\eta^{\alpha\beta\gamma}_{0l_211l_1}(1) \end{aligned}$$

$$-2\eta^{\alpha\beta\gamma}_{0l_2 0 1 l_1+1}(1)] \tag{4.85}$$

If we indicate with $\Xi^{\alpha\beta\gamma}_{k_1k_2k_3k_4,l_1l_2}$ the above trace we can be write the contribution of the (2.3) diagram as:

$$\begin{aligned} < v^{2\pi}_{123} >_{2.3} &= C_{2\pi}\int d\mathbf{r}_1 d\mathbf{r}_2 d\mathbf{r}_3 \frac{f_{2k_3-1+l_1}(r_{13})}{f_1(r_{13})} X^{k_3}(r_{13}) \frac{f_{2k_4-1+l_2}(r_{12})}{f_1(r_{12})} X^{k_4}(r_{32}) \\ & \rho^{\alpha\beta\gamma}_3(1,2,3)\Xi^{\alpha\beta\gamma}_{k_1k_2k_3k_4,l_1l_2} \end{aligned} \tag{4.86}$$

Finally ,the expressions of diagrams (3.1) and (3.2) are:

$$< v^R_{123} >_{3.1} = \frac{1}{6}\int d\mathbf{r}_1 d\mathbf{r}_2 d\mathbf{r}_3 v^R_{123}\rho^{\alpha\beta\gamma}_3(1,2,3) \tag{4.87}$$

$$\begin{aligned} < v^R_{123} >_{3.2} &= \frac{1}{2}\int d\mathbf{r}_1 d\mathbf{r}_2 d\mathbf{r}_3 \frac{f_{2k_1-1+l_1}(r_{12}) f_{2k_2-1+l_2}(r_{12})}{[f_1(r_{12})]^2} \\ &\cdot \quad I^{k_1k_2k_3} A^{k_3} \chi^{\alpha\beta}_{l_1+l_2+l_3}[\rho^{\alpha\beta\gamma}_{3,dir}(1,2,3)\delta_{k_1,k_2} + \rho^{\alpha\beta\gamma}_{3,exc}(1,2,3)] \end{aligned} \tag{4.88}$$

Chapter 5

Specific applications and results

5.1 The single particle wave functions

The formalism presented in the previous section has been applied to the ^{12}C, ^{16}O, ^{40}Ca, ^{48}Ca and ^{208}Pb nuclei. In order to calculate the uncorrelated total function $\Phi(1, ..., A)$ we have used a complete basis of single particle wave functions $\phi_\alpha(x_i)$, solutions of the one-body Schrödinger equation

$$h_i \phi(x_i) = \epsilon_i \phi(x_i) \tag{5.1}$$

with

$$h_i = -\frac{\hbar^2}{2m}\nabla_i + U(r_i) \tag{5.2}$$

where $U(r_i)$ is a Wood-Saxon potential of the form

$$U(r) = \frac{V_0}{1 + e^{\frac{r-R_0}{a_0}}} + \left[\frac{\hbar c}{m_\pi c^2}\right]^2 \frac{V_{ls}}{a_{ls} r} \frac{e^{\frac{r-R_{ls}}{a_{ls}}}}{(1 + e^{\frac{r-R_{ls}}{a_{ls}}})^2} \boldsymbol{l} \cdot \boldsymbol{\sigma} - V_C(r) \tag{5.3}$$

where m_π is the pion mass and the term

$$V_C = \left\{ \begin{array}{ll} \frac{(Z-1)e^2}{r} & r \geq R \\ \frac{(Z-1)e^2}{2R}[3 - \frac{r^2}{R^2}] & r \leq R \end{array} \right. \tag{5.4}$$

is the Coulomb potential generated by a homogeneous charge distribution. In principle V_0, V_{ls}, R_0, R_{ls}, a_0, a_{ls} are variational parameters whose values should be fixed in the minimization process of the energy. In [Fab00] the results of a complete minimization done on both single particle wave functions and correla-

tion have shown a relatively scarce sensitivity on the variation of the mean-field potential. A change of about 50% of the value of V_0, changes of about 5% the ^{16}O binding energy. In order to limit the number of calculations we did not make the minimization on the mean-field potential potential and we keep fixed the values of the parameters for each nucleus considered.
We have chosen a set of parameters taken from the literature [Ari96]. The values of these parameters, given in table 5.1, have been fixed to reproduce the charge root mean square radii and the single particle energies around the Fermi surface.

	^{12}C	^{16}O	^{40}Ca	^{48}Ca	^{208}Pb
V_0^p	-62.00	-52.50	-57.5	-59.50	-60.40
V_{ls}^p	-3.20	-7.00	-11.11	-8.55	-6.75
a_0^p	0.57	0.53	0.53	0.53	0.79
a_{ls}^p	0.57	0.53	0.53	0.53	0.79
R_0^p	2.86	3.20	4.10	4.36	7.46
R_{ls}^p	2.86	3.20	4.10	4.36	7.46
R_{Coul}	2.86	3.20	4.10	4.36	7.46
V_0^n	-62.00	-52.50	-55.00	-50.00	-4.32
V_{ls}^n	-3.15	-6.54	-8.50	-7.74	-6.08
a_0^n	0.57	0.53	0.53	0.53	0.66
a_{ls}^n	0.57	0.53	0.53	0.53	0.66
R_0^n	2.86	3.20	4.10	4.36	7.46
R_{ls}^n	2.86	3.20	4.10	4.36	7.46

Table 5.1: The parameters of the single particle Wood-Saxon potential. The superscripts p and n indicate protons and neutrons respectively. The values of V_0 and V_{ls} are expressed in MeV, the other parameters in fm.

5.2 The interactions

In the calculation of the energy we have used realistic nucleon-nucleon interactions together with a three-body phenomenological interaction. We have adopted nucleon-nucleon potentials of Argonne-Urbana type which are local and non-relativistic. In our calculation we have used th Argonne AV8' potential [Pud97] which is the simplified version of the charge-dependent Argonne AV18 potential [Wir95]. The AV8' potential considers only the first eight channels, up to the spin-orbit isospin included. The parameters of AV8' potential are slightly mod-

$R(fm)$	$R'(fm)$	$a(fm^{-1})$	$a'(fm^-1)$	$\mu(fm^{-1})$	$c(fm^{-2})$
.5	.36	.2	.17	.7	2

k	1	2	3	4	5	6	7	8
α^k	2575.3125	-466.5625	-366.5625	402.8125	0	0	0	0
β^k	0	0	0	0	0	0	-1650	-550
I^k	-5.7024	.8987	.7629	-.2791	.0525	-.2325	0	0
J^k	0	0	0	3.4876	0	0	0	0
J'^k	0	0	0	0	0	3.4876	0	0

Table 5.2: The parameters used in the U14 model.

ified with respect to the those of AV18 in order to simulate the effects of the missing channels.
In addition to this potential we also use the Urbana U14 potential [Lag81A] truncated to the first eight channels. We also used the truncated version of the Urbana U14' potential, a parametrization of the U14 potential whose parameters have been changed to deal with the Friedman-Pandharipande three-body force [Fri80].

The two-nucleon interactions are separated in short, intermediate and long range components

$$v_8 = v_S + v_I + v_\pi \tag{5.5}$$

The short-range interaction has the form

$$v_S(i,j) = \sum_{p=1,8} v_S^p(r_{ij}) O_{ij}^p \tag{5.6}$$

with

$$\begin{aligned} v_S^p(r_{ij}) &= \alpha^p W(r_{ij}) + \beta^p W'(r_{ij}) && (5.7)\\ W(r_{ij}) &= \frac{1}{1+e^{\frac{r_{ij}-R}{a}}} && (5.8)\\ W'(r_{ij}) &= \frac{1}{1+e^{\frac{r_{ij}-R'}{a'}}} && (5.9) \end{aligned}$$

The intermediate range attraction v_I is modeled on the two-pion exchange interaction:

$$v_I(i,j) = \sum_{p=1,8} I^p T_\pi^2(r_{ij}) O_{ij}^p \tag{5.10}$$

with $T_\pi(r)$ was defined in eq. (4.69). Finally the long range term is based on the one-pion exchange contribution which is defined as:

$$v_{\pi,ij} = \sum_{p=1,8} \Big\{ J'^p T_\pi(r_{ij}) + J^p Y_\pi(r_{ij}) \Big\} O_{ij}^p \tag{5.11}$$

with $Y_\pi(r)$ was defined in eq. (4.68). The parameters used in the U14 potential are given in table 5.2. This is the basic idea underlying the construction of all the interactions we used.
It is more difficult to show the parameters of the AV8' potential since they are expressed in the total spin and isospin channels. For details, see [Pud97][Wir95].

Associated to each two-nucleon potential there is a three-body force. Specifically, the AV8' is linked to the Urbana UIX interaction [Pud97], the U14 to the UVII [Sch86] and the U14' to the Friedman-Pandharipande (FP) [Fri80] force. The Urbana interactions are parametrized by following the Tucson model we have already presented in sect. 4.1. The parameters of these two interactions are given in table 5.4.
We present below the FP model. Also in this case, the three-body interaction is separated in a repulsive TNR, and an attractive part TNA. In analogy to the Tucson model, the TNR component has the form:

$$TNR = \sum_{cyc} U_0 T_\pi^2(r_{ij}) T_\pi^2(r_{jk}), \tag{5.12}$$

In the FP model its effect is considered by introducing a density dependence in the intermediate range term of the two-body interaction v_I of U14,

$$U14 + TNR = v_S + v_I e^{-\gamma_1 \rho} + v_\pi \tag{5.13}$$

where γ_1=0.15 fm^3 and ρ is the average uncorrelated density defined as:

$$\rho = [3\pi^2]^{\frac{1}{3}} \Big[\frac{\int dr_1 \rho_0(\boldsymbol{r}_1)^{\frac{4}{3}}}{\int dr_1 \rho_0(\boldsymbol{r}_1)} \Big]^3 \tag{5.14}$$

The attractive conribution TNA is assumed to have the form:

$$TNA = \gamma_2[\rho]^2 e^{-\gamma_3 \rho}\Big\{3 - 2\Big[\Big(\rho_p - \rho_n\Big)/\rho\Big]^2\Big\} \tag{5.15}$$

where we have indicated with $\rho_{p,n}$ the average uncorrelated one-body densities for the protons and neutrons respectively. The values of the parameters $\gamma_{1,2,3}$ are given in table 5.3

$\gamma_1(fm^3)$	$\gamma_2(fm^6)$	$\gamma_3(fm^3)$
.15	-700	13.6

Table 5.3: Parameters used in the Friedman-Pandharipande model.

	UVII	UIX
$A_{2\pi}$	-.03330	-.02930
$C_{2\pi}$	-.008325	-.007325700
U_0	-.003700	.004800
$\mu(fm^{-1})$	.7	.7
$c(fm^{-2})$	2	2

Table 5.4: Parameters used in the Tucson models UVII and UIX. All the parameters are defined in chapter 4.

The UIX and UVII interactions have been fixed to reproduce together with they respective two-body forces, the ^3H binding energy. The parameters of the FP have been fixed to reproduce the empirical saturation point of nuclear matter, with variational CBF calculations.

5.3 The correlation functions

In our calculations the search for the energy minimum is done making variations of the two-body correlation functions. A first possibility is to use $f_p(r_{12})$ with specific functional dependences based on a set of parameters. In refs. [Co92, Co94, Ari96] gaussian correlations have been used. A better choice, from the physics point of view, and also in terms of number of parameters to change, is to fix the correlation functions consistently with the interaction.
The basic idea is to force the $f_p(r)$ functions to reach their asymptotic values, the unity for the scalar correlation, and zero for the other ones, after certain values

called healing distances. The values of these distances, d^p, are the variational parameters.
The energy expectation value $E(d^p)$ is calculated and minimized with respect to variations of d^p. In principle one should solve the full set of FHNC/SOC equations by arbitrary changing d^p. This approach would be computationally extremely heavy. In practice we obtain the function $f_p(r,d^p)$ by minimizing the two-body cluster contribution of the energy for a fixed value of d^p. The $f_p(r,d^p)$ obtained in this manner are then used to solve the FHNC/SOC equations. If we consider only the two-body cluster contributions, the energy is given by the W_0 and $T_\Phi^{(1,2)}$ terms since all the nodal functions are zero and, as a consequence, also the contribution of the SOR's. The expression of the energy in the two-body approximation is given by the sum of the following terms.

$$\begin{aligned}
T_{F,2} &= -\frac{\hbar^2}{4m}\int d\boldsymbol{r}_1 d\boldsymbol{r}_2 \Big(f_{2k_1-1+l_1}(r_{12})\nabla^2 f_{2k_2-1+l_2}(r_{12}) \\
&\quad -\nabla f_{2k_1-1+l_1}(r_{12})\cdot\nabla f_{2k_2-1+l_2}(r_{12})\Big) \\
&\quad \Big\{ \Big[\rho_0^{s_1 s_2\alpha}(\boldsymbol{r}_1,\boldsymbol{r}_1)\rho_0^{s_3 s_4\beta}(\boldsymbol{r}_2,\boldsymbol{r}_2)\chi^*_{s_1}(1)\chi^*_{s_2}(2)P^{k_1}P^{k_2}\chi_{s_3}(1)\chi_{s_4}(2) \\
&\quad \chi^*_\alpha(1)\chi^*_\beta(2)(\boldsymbol{\tau}_1\cdot\boldsymbol{\tau}_2)^{l_1+l_2}\chi_\alpha(1)\chi_\beta(2)\Big] \\
&\quad -\Big[\rho_0^{s_1 s_2\alpha}(\boldsymbol{r}_1,\boldsymbol{r}_2)\rho_0^{s_3 s_4\beta}(\boldsymbol{r}_1,\boldsymbol{r}_2)\chi^*_{s_1}(1)\chi^*_{s_2}(2)P^{k_1}P^{k_2}P^{k_3}\chi_{s_3}(1)\chi_{s_4}(2) \\
&\quad \chi^*_\alpha(1)\chi^*_\beta(2)(\boldsymbol{\tau}_1\cdot\boldsymbol{\tau}_2)^{l_1+l_2+l_3}\chi_\alpha(1)\chi_\beta(2)\Big]\Big\} \qquad (5.16) \\
T^{(1)}_{\Phi,2} &= -\frac{\hbar^2}{4m}\int d\boldsymbol{r}_1 \rho_{T1}^{s_1 s_2\alpha}(\boldsymbol{r}_1)\int d\boldsymbol{r}_2 \rho_0^{s_3 s_4\beta}(\boldsymbol{r}_2)\Big(f_{2k_1-1+l_1}(r_{12}) f_{2k_2-1+l_2}(r_{12}) \\
&\quad -\delta_{2k_1-1+l-1,1}\delta_{2k_2-1+l_2,1}\Big) \\
&\quad \chi^*_{s_1}(1)\chi^*_{s_2}(2)P^{k_1}P^{k_2}\chi_{s_3}(1)\chi_{s_4}(2) \\
&\quad \chi_\alpha(1)\chi_\beta(2)(\boldsymbol{\tau}_1\cdot\boldsymbol{\tau}_2)^{l_1+l_2}\chi_\alpha(1)\chi_\beta(2) \qquad (5.17) \\
T^{(2)}_{\Phi,2} &= \frac{\hbar^2}{4m}\int d\boldsymbol{r}_1 d\boldsymbol{r}_2 \rho_{T2}^{s_1 s_2 s_3 s_4\alpha\beta}(\boldsymbol{r}_1,\boldsymbol{r}_2)\Big(f_{2k_1-1+l_1}(r_{12}) f_{2k_2-1+l_2}(r_{12}) \\
&\quad -\delta_{2k_1-1+l_1,1}\delta_{2k_2-1+l_2,1}\Big) \\
&\quad \chi^*_{s_1}(1)\chi^*_{s_2}(2)P^{k_1}P^{k_2}P^{k_3}\chi_{s_3}(1)\chi_{s_4}(2) \\
&\quad \chi^*_\alpha(1)\chi^*_\beta(2)(\boldsymbol{\tau}_1\cdot\boldsymbol{\tau}_2)^{l_1+l_2+l_3}\chi_\alpha(1)\chi_\beta(2) \qquad (5.18) \\
V_2 &= \frac{1}{2}\int d\boldsymbol{r}_1 d\boldsymbol{r}_2 \Big(f_{2k_1-1+l_1}(r_{12}) v^{2k_2-1+l_2}(r_{12}) f_{2k_3-1+l_3}(r_{12})\Big)
\end{aligned}$$

$$\Big\{\Big[\rho_0^{s_1 s_2\alpha}(\boldsymbol{r}_1,\boldsymbol{r}_1)\rho_0^{s_3 s_4\beta}(\boldsymbol{r}_2,\boldsymbol{r}_2)\chi^*_{s_1}(1)\chi^*_{s_2}(2)P^{k_1}P^{k_2}P^{k_3}\chi_{s_3}(1)\chi_{s_4}(2)$$
$$\chi^*_{\alpha}(1)\chi^*_{\beta}(2)(\boldsymbol{\tau}_1\cdot\boldsymbol{\tau}_2)^{l_1+l_2+l_3}\chi_\alpha(1)\chi_\beta(2)\Big]$$
$$-\Big[\rho_0^{s_1 s_2\alpha}(\boldsymbol{r}_1,\boldsymbol{r}_2)\rho_0^{s_3 s_4\beta}(\boldsymbol{r}_1,\boldsymbol{r}_2)\chi^*_{s_1}(1)\chi^*_{s_2}(2)P^{k_1}P^{k_2}P^{k_3}P^{k_4}\chi_{s_3}(1)\chi_{s_4}(2)$$
$$\chi^*_{\alpha}(1)\chi^*_{\beta}(2)(\boldsymbol{\tau}_1\cdot\boldsymbol{\tau}_2)^{l_1+l_2+l_3+l_4}\chi_\alpha(1)\chi_\beta(2)\Big]\Big\} \quad (5.19)$$

In the above expressions a sum over the α and β indices is understood. By considering only the first four channel. We have

$$P_{12}^{k=1,2} = 1, \boldsymbol{\sigma}_1\cdot\boldsymbol{\sigma}_2 \quad (5.20)$$

and

$$\begin{aligned}\rho_{T1}^{\alpha s_1 s_2}(\boldsymbol{r}_1,\boldsymbol{r}_1) &= \sum \phi^*_{s_1\alpha}(\boldsymbol{r}_1)\nabla_1^2\phi_{s_2\alpha}(\boldsymbol{r}_1) \\ &\quad -\sum_\alpha \nabla_1\phi^*_{s_1\alpha}(\boldsymbol{r}_1)\cdot\nabla_1\phi_{s_2\alpha}(\boldsymbol{r}_1) \quad (5.21)\\ \rho_{T2}^{\alpha\beta s_1 s_2 s_3 s_4}(\boldsymbol{r}_1,\boldsymbol{r}_2) &= \rho_0^{s_1 s_2\alpha}(\boldsymbol{r}_1,\boldsymbol{r}_2)\nabla_1^2\rho_0^{s_3 s_4\beta}(\boldsymbol{r}_1,\boldsymbol{r}_2) \\ &\quad -\nabla_1\rho_0^{s_1 s_2\alpha}(\boldsymbol{r}_1,\boldsymbol{r}_2)\cdot\nabla_1\rho_0^{s_3 s_4\beta}(\boldsymbol{r}_1,\boldsymbol{r}_2) \quad (5.22)\end{aligned}$$

The total energy in two-body cluster approximation is given by

$$E_2 = T^{(1)}_{\Phi,2} + T^{(2)}_{\Phi,2} + T_{F,2} + V_2 \quad (5.23)$$

The optimal correlations f_p are obtained by solving the Euler-Lagrange equation

$$\frac{\delta E_2}{\delta f_p} = 0 \quad (5.24)$$

with the boundary conditions

$$\begin{aligned} f_1(r>d) &= 1 \quad (5.25)\\ f_{p>1}(r>d) &= 0 \quad (5.26)\\ \frac{\partial f_{q=1,4}}{\partial r}|_{r=d} &= 0 \quad (5.27)\end{aligned}$$

If we perform the variation on eq. (5.23) we obtain four equations, each of them containing terms proportional to 1,$\boldsymbol{\sigma}_1\cdot\boldsymbol{\sigma}_2$,$\boldsymbol{\tau}_1\cdot\boldsymbol{\tau}_2$, $(\boldsymbol{\sigma}_1\cdot\boldsymbol{\sigma}_2)(\boldsymbol{\tau}_1\cdot\boldsymbol{\tau}_2)$. It is possible to decouple the operator dependence of these equations by projecting them over the total spin and isospin S and T of the nucleon pair. The projection operator are related to the operators in the old representation by the following equations:

$$P_{12}^{S=0} = \frac{1}{4}(1 - \boldsymbol{\sigma}_1 \cdot \boldsymbol{\sigma}_2) \tag{5.28}$$

$$P_{12}^{S=1} = \frac{1}{4}(3 + \boldsymbol{\sigma}_1 \cdot \boldsymbol{\sigma}_2) \tag{5.29}$$

$$\Pi_{12}^{T=0} = \frac{1}{4}(1 - \boldsymbol{\tau}_1 \cdot \boldsymbol{\tau}_2) \tag{5.30}$$

$$\Pi_{12}^{T=1} = \frac{1}{4}(3 + \boldsymbol{\tau}_1 \cdot \boldsymbol{\tau}_2) \tag{5.31}$$

The functions v^{ST} and f^{ST} are related to the old functions by

$$x^{ST} = x^1 + (4S-3)x^3 + (4T-3)x^2 + (4S-3)(4T-3)x^4 \tag{5.32}$$

with $x^{ST} = v^{ST}$ or f^{ST}. By using the above equations we can express the operators $\boldsymbol{\sigma}_1 \cdot \boldsymbol{\sigma}_2$ and $\boldsymbol{\tau}_1 \cdot \boldsymbol{\tau}_2$ as

$$\boldsymbol{\sigma}_1 \cdot \boldsymbol{\sigma}_2 = 2(P^1 - P^0) - 1 \tag{5.33}$$

$$\boldsymbol{\tau}_1 \cdot \boldsymbol{\tau}_2 = 2(\Pi^1 - \Pi^0) - 1 \tag{5.34}$$

if we define as f^{ST} the components of the correlations in the (S,T) representation we have

$$F(1,...,A) = \sum_{p=1,4} f^p(r_{12}) O^p(r_{12}) = \sum_{ST=0,1} f^{ST}(r_{12}) P_{12}^S \Pi_{12}^T \tag{5.35}$$

Eq. (5.35) allows us to express all the products of type $O^p O^q ... O^r$ as product of $P^S \Pi^T$. For example, we have

$$\begin{aligned} \sum_{pq=1}^{4} f_p(r_{12}) f_q(r_{12}) O_{12}^p O_{12}^q &= \sum_{T_1 S_1 T_2 S_2 = 0,1} f^{S_1 T_1}(r_{12}) f^{S_2 T_2}(r_{12}) P_{12}^{S_1} \Pi_{12}^{T_1} P_{12}^{S_2} \Pi_{12}^{T_2} \\ &= \sum_{S,T=0,1} [f^{ST}(r_{12})]^2 P_{12}^S \Pi_{12}^T \end{aligned} \tag{5.36}$$

where we have used the properties

$$P^{S_1} P^{S_2} = \delta_{S_1 S_2} P^{S_1} \tag{5.37}$$

$$\Pi^{T_1} \Pi^{T_2} = \delta_{T_1 T_2} \Pi^{T_1} \tag{5.38}$$

The exchange operator can be written with respect to the projection operators as

$$\frac{1}{4}\Big(1+\boldsymbol{\sigma}_1\cdot\boldsymbol{\sigma}_2+\boldsymbol{\tau}_1\cdot\boldsymbol{\tau}_2+(\boldsymbol{\sigma}_1\cdot\boldsymbol{\sigma}_2)(\boldsymbol{\tau}_1\cdot\boldsymbol{\tau}_2)\Big)=\sum_{S,T=0,1}(-)^{T+S}P_{12}^{S}\Pi_{12}^{T} \tag{5.39}$$

By using the above defined quantities we rewrite the terms of the two-body cluster energy as

$$\begin{aligned} T_{F,2} &= -\frac{\hbar^2}{4m}\sum_{s_1s_2s_3s_4\alpha\beta}\int d\boldsymbol{r}_1 d\boldsymbol{r}_2\Big(f^{ST}(r_{12})\nabla^2 f^{ST}(r_{12})-\nabla f^{ST}(r_{12})\cdot\nabla f^{ST}(r_{12})\Big)\\ &\quad\Big\{\Big[\rho_0^{s_1s_2\alpha}(\boldsymbol{r}_1,\boldsymbol{r}_1)\rho_0^{s_3s_4\beta}(\boldsymbol{r}_2,\boldsymbol{r}_2)\chi_{s_1}^*(1)\chi_{s_2}^*(2)P_{12}^{S}\chi_{s_3}(1)\chi_{s_4}(2)\\ &\quad\chi_\alpha^*(1)\chi_\beta^*(2)\Pi_{12}^{T}\chi_\alpha(1)\chi_\beta(2)\Big]\\ &\quad-\Big[\rho_0^{s_1s_2\alpha}(\boldsymbol{r}_1,\boldsymbol{r}_2)\rho_0^{s_3s_4\beta}(\boldsymbol{r}_1,\boldsymbol{r}_2)\chi_{s_1}^*(1)\chi_{s_2}^*(2)P_{12}^{S}(-)^{S+1}\chi_{s_3}(1)\chi_{s_4}(2)\\ &\quad\chi_\alpha^*(1)\chi_\beta^*(2)\Pi_{12}^{T}(-)^{T+1}\chi_\alpha(1)\chi_\beta(2)\Big]\Big\} \qquad (5.40)\\ T_{\Phi,2}^{(1)} &= -\frac{\hbar^2}{4m}\sum_{s_1s_2s_3s_4\alpha\beta}\int d\boldsymbol{r}_1\rho_{T1}^{s_1s_2\alpha}(\boldsymbol{r}_1)\int d\boldsymbol{r}_2\rho_0^{s_3s_4\beta}(\boldsymbol{r}_2)f^{ST}(r_{12})f^{ST}(r_{12})\\ &\quad\chi_{s_1}^*(1)\chi_{s_2}^*(2)P_{12}^{S}\chi_{s_3}(1)\chi_{s_4}(2)\\ &\quad\chi_\alpha(1)\chi_\beta(2)\Pi_{12}^{T}\chi_\alpha(1)\chi_\beta(2) \qquad (5.41)\\ T_{\Phi,2}^{(2)} &= \frac{\hbar^2}{4m}\sum_{s_1s_2s_3s_4\alpha\beta}\int d\boldsymbol{r}_1 d\boldsymbol{r}_2\rho_{T2}^{s_1s_2s_3s_4\alpha\beta}(\boldsymbol{r}_1,\boldsymbol{r}_2)\Big(f^{ST}(r_{12})f^{ST}(r_{12})(-)^{T+S}\Big)\\ &\quad\chi_{s_1}^*(1)\chi_{s_2}^*(2)P_{12}^{S}\chi_{s_3}(1)\chi_{s_4}(2)\\ &\quad\chi_\alpha^*(1)\chi_\beta^*(2)\Pi_{12}^{T}\chi_\alpha(1)\chi_\beta(2) \qquad (5.42)\\ V_2 &= \frac{1}{2}\sum_{s_1s_2s_3s_4\alpha\beta}\int d\boldsymbol{r}_1 d\boldsymbol{r}_2\Big(f^{ST}(r_{12})v^{ST}(r_{12})f^{ST}(r_{12})\Big)\\ &\quad\Big\{\Big[\rho_0^{s_1s_2\alpha}(\boldsymbol{r}_1,\boldsymbol{r}_1)\rho_0^{s_3s_4\beta}(\boldsymbol{r}_2,\boldsymbol{r}_2)\chi_{s_1}^*(1)\chi_{s_2}^*(2)P_{12}^{S}\chi_{s_3}(1)\chi_{s_4}(2)\\ &\quad\chi_\alpha^*(1)\chi_\beta^*(2)\Pi_{12}^{T}\chi_\alpha(1)\chi_\beta(2)\Big]\\ &\quad-\Big[\rho_0^{s_1s_2\alpha}(\boldsymbol{r}_1,\boldsymbol{r}_2)\rho_0^{s_3s_4\beta}(\boldsymbol{r}_1,\boldsymbol{r}_2)(-)^{T+S}\chi_{s_1}^*(1)\chi_{s_2}^*(2)P_{12}^{S}\chi_{s_3}(1)\chi_{s_4}(2)\\ &\quad\chi_\alpha^*(1)\chi_\beta^*(2)\Pi_{12}^{T}\chi_\alpha(1)\chi_\beta(2)\Big]\Big\} \qquad (5.43) \end{aligned}$$

Taking into account that

$$\chi^*_{s_1}(1)\chi^*_{s_2}(2)P^S_{12}\chi_{s_3}(1)\chi_{s_4}(2) = \frac{1}{2}\Big(\delta_{s_1s_3}\delta_{s_2s_4} + (-1)^{S+1}\delta_{s_1s_4}\delta_{s_2s_3}\Big) \quad (5.44)$$

$$\chi^*_{\alpha}(1)\chi^*_{\beta}(2)\Pi^T_{12}\chi_{\alpha}(1)\chi_{\beta}(2) = \frac{1}{2}\Big(1 + (-1)^{T+1}\delta_{\alpha\beta}\Big) \quad (5.45)$$

we obtain

$$\begin{aligned}
E_2 = & \sum_{s_1s_2s_3s_4\alpha\beta}\Big\{\int d\boldsymbol{r}_1 d\boldsymbol{r}_2\Big[\big[\frac{1}{2}\Big(f^{ST}(r_{12})v^{ST}(r_{12})f^{ST}(r_{12})\Big) \\
& -\frac{\hbar^2}{4m}\Big(f^{ST}(r_{12})\nabla^2 f^{ST}(r_{12}) - \nabla f^{ST}(r_{12})\cdot\nabla f^{ST}(r_{12})\Big)\big] \\
& \Big[\rho_0^{s_1s_2\alpha}(\boldsymbol{r}_1,\boldsymbol{r}_1)\rho_0^{s_3s_4\beta}(\boldsymbol{r}_2,\boldsymbol{r}_2) - (-1)^{T+S}\rho_0^{s_1s_2\alpha}(\boldsymbol{r}_1,\boldsymbol{r}_2)\rho_0^{s_3s_4\beta}(\boldsymbol{r}_1,\boldsymbol{r}_2)\Big]\Big] \\
& -\frac{\hbar^2}{4m}\int d\boldsymbol{r}_1\rho_{T1}^{s_1s_2\alpha}(\boldsymbol{r}_1,\boldsymbol{r}_1)\int d\boldsymbol{r}_2\rho_0^{s_3s_4\beta}(\boldsymbol{r}_2,\boldsymbol{r}_2)[f^{ST}(r_{12})]^2) \\
& +\frac{\hbar^2}{4m}\int d\boldsymbol{r}_1 d\boldsymbol{r}_2\rho_{T2}^{s_1s_2s_3s_4\alpha\beta}(\boldsymbol{r}_1,\boldsymbol{r}_2)\Big([f^{ST}(r_{12})]^2(-)^{T+S}\Big)\Big\} \\
& \frac{1}{2}\Big(\delta_{s_1s_3}\delta_{s_2s_4} + (-)^{S+1}\delta_{s_1s_4}\delta_{s_2s_4}\Big)\frac{1}{2}\Big(1 + (-)^{T+1}\delta_{\alpha\beta}\Big) \quad (5.46)
\end{aligned}$$

Now we define

$$\begin{aligned}
P^{ST}(\boldsymbol{r}_1,\boldsymbol{r}_2) = & \frac{\hbar^2}{4m}\frac{4}{2T+1}\Big[\delta_{T1}\big[\Big(\rho_0^p(\boldsymbol{r}_1)\rho_0^p(\boldsymbol{r}_2) + \rho_0^n(\boldsymbol{r}_1)\rho_0^n(\boldsymbol{r}_2)\Big) \\
& +(-1)^S 4\Big(\rho_0^p(\boldsymbol{r}_1,\boldsymbol{r}_2)\rho_0^p(\boldsymbol{r}_1,\boldsymbol{r}_2) + \rho_0^n(\boldsymbol{r}_1,\boldsymbol{r}_2)\rho_0^n(\boldsymbol{r}_1,\boldsymbol{r}_2)\Big)\big] \\
& +\frac{1}{2}\big[\rho_0^p(\boldsymbol{r}_1)\rho_0^n(\boldsymbol{r}_2) + \rho_0^n(\boldsymbol{r}_1)\rho_0^p(\boldsymbol{r}_2) \\
& -(-1)^{T+S}4\Big(\rho_0^p(\boldsymbol{r}_1,\boldsymbol{r}_2)\rho_0^n(\boldsymbol{r}_1,\boldsymbol{r}_2) + \rho_0^n(\boldsymbol{r}_1,\boldsymbol{r}_2)\rho_0^p(\boldsymbol{r}_1,\boldsymbol{r}_2)\Big)\big]\Big] \\
& +\frac{16(-1)^T}{(2S+1)(2T+1)}\big[\delta_{T1}\Big(\rho_{1j}^{0,p}(\boldsymbol{r}_1)\rho_{1j}^{0,n}(\boldsymbol{r}_2) + \rho_{1j}^{0,n}(\boldsymbol{r}_1)\rho_{1j}^{0,p}(\boldsymbol{r}_2)\Big) \\
& +\frac{1}{2}\Big(\rho_{1j}^{0,p}(\boldsymbol{r}_1,\boldsymbol{r}_2)\rho_{1j}^{0,n}(\boldsymbol{r}_1,\boldsymbol{r}_2) + \rho_{1j}^{0,n}(\boldsymbol{r}_1,\boldsymbol{r}_2)\rho_{1j}^{0,p}(\boldsymbol{r}_1,\boldsymbol{r}_2)\Big)\big] \quad (5.47) \\
Q^{ST}(\boldsymbol{r}_1,\boldsymbol{r}_2) = & \sum_{\alpha\beta=p,n}\big[\frac{\hbar^2}{4m}\frac{4}{2T+1}[\delta_{T1}(-1)^S 4\delta_{\alpha\beta} - (-1)^{T+S}4(1-\delta_{\alpha\beta})] \\
& \Big(\rho_0^\alpha(\boldsymbol{r}_1,\boldsymbol{r}_2)\nabla_{12}^2\rho_0^\beta(\boldsymbol{r}_1,\boldsymbol{r}_2) - \nabla_{12}\rho_0^\alpha(\boldsymbol{r}_1,\boldsymbol{r}_2)\nabla_{12}\rho_0^\beta(\boldsymbol{r}_1,\boldsymbol{r}_2)\Big)\big] \\
& +\frac{16(-1)^T}{(2S+1)(2T+1)}\big[[\delta_{T1}\delta_{\alpha\beta} + (1-\delta_{\alpha\beta})\frac{1}{2}] \\
& \Big(\rho_{1j}^{0,\alpha}(\boldsymbol{r}_1,\boldsymbol{r}_2)\nabla_{12}^2\rho_{1j}^{0,\beta}(\boldsymbol{r}_1,\boldsymbol{r}_2) - \nabla_{12}\rho_{1j}^{0,\alpha}(\boldsymbol{r}_1,\boldsymbol{r}_2)\nabla_{12}\rho_{1j}^{0,\beta}(\boldsymbol{r}_1,\boldsymbol{r}_2)\Big)\big]
\end{aligned}$$

$$+\frac{2m}{\hbar^2}P^{ST}(\boldsymbol{r}_1,\boldsymbol{r}_2)v^{ST} \tag{5.48}$$

In the above expression we have explicitly written the sum over the spin and isospin and the expression of ρ_{T2}. By inserting the above equations in eq. (5.46) we obtain

$$\begin{aligned} E_2 &= \int d\boldsymbol{r}_1 d\boldsymbol{r}_2 \Big[Q^{ST}\Big(f^{ST}\Big)^2 - P^{ST}\Big(f^{ST}\nabla^2 f^{ST} - \nabla f^{ST}\nabla f^{ST}\Big)\Big] \\ &= \int d\boldsymbol{r}_{12} d\boldsymbol{r}_2 \Big[Q^{ST}\Big(f^{ST}\Big)^2 - P^{ST}\Big(f^{ST}\nabla^2 f^{ST} - \nabla f^{ST}\nabla f^{ST}\Big)\Big] \\ &= \int d\boldsymbol{r}_{12} \Big[\tilde{Q}^{ST}\Big(f^{ST}\Big)^2 - \tilde{P}^{ST}\Big(f^{ST}\nabla^2 f^{ST} - \nabla f^{ST}\nabla f^{ST}\Big)\Big] \end{aligned} \tag{5.49}$$

In the above expression and in the following ones we understand that all the functions and the operators act on the $\boldsymbol{r}_{12}$ coordinate. We define $\tilde{P}^{ST}$ and $\tilde{Q}^{ST}$ by integrating Q^{ST} and P^{ST} over $\boldsymbol{r}_1$ and $\boldsymbol{r}_2$ by keeping fixed the interparticle distance $\boldsymbol{r}_{12}$. we have

$$\tilde{Q}^{ST} = \int d\boldsymbol{r}_2 Q^{ST}(\boldsymbol{r}_1,\boldsymbol{r}_2,\boldsymbol{r}_{12}) = \frac{2\pi}{r_{12}}\int_0^R r_2 dr_2 \int_{|r_2-r_{12}|}^{|r_2+r_{12}|} r_1 dr_1 Q(\boldsymbol{r}_1,\boldsymbol{r}_2,\boldsymbol{r}_{12}) \tag{5.50}$$

and an analogous expression for $\tilde{P}^{ST}$. In eq. (5.49) we have neglected the term containing ρ_{T1} because we make the minimization by using only two-body terms. The variation of E_2 on f^{ST} gives

$$\begin{aligned} \delta E_2 &= \int d\boldsymbol{r}_{12}\Big\{\tilde{Q}^{ST} 2 f^{ST}\delta f^{ST} \qquad (5.51) \\ &\quad -\tilde{P}^{ST}[\delta f^{ST}\nabla^2 f^{ST} + f^{ST}\nabla^2\delta f^{ST} - 2\nabla f^{ST}\nabla\delta f^{ST}]\Big\} \\ &= \int d\boldsymbol{r}_{12}\delta f^{ST} 4[P^{ST}]^2\Big\{-\nabla^2 F^{ST} + F^{ST}\frac{1}{4\tilde{P}^{ST}}(2\tilde{Q}^{ST} \\ &\quad -\frac{1}{\tilde{P}^{ST}}(\nabla\tilde{P}^{ST})(\nabla\tilde{P}^{ST})\Big\} = 0 \qquad (5.52) \end{aligned}$$

where we have defined $F^{ST} = f^{ST}(\tilde{P}^{ST})^{\frac{1}{2}}$.

The above variation has to be true for each δf^{ST}, this requires the expression included in the braces {...} to be zero. By imposing this condition we obtain the Euler-Lagrange equations

$$-\nabla^2 F^{ST} + \tilde{v}^{ST}F^{ST} = 0 \tag{5.53}$$

with

$$\tilde{v}^{ST} = \frac{1}{4\tilde{P}^{ST}}(2\tilde{Q}^{ST} + \nabla^2\tilde{P}^{ST} - \frac{1}{\tilde{P}^{ST}}\nabla\tilde{P}^{ST}\nabla\tilde{P}^{ST}) \tag{5.54}$$

the eqs. (5.53) are the decoupled differential equations in the representation (ST) with the boundary conditions

$$f^{ST}(r \geq d) = 0 \tag{5.55}$$

$$\frac{\partial f^{ST}}{\partial r}|_{r=d} = 0 \tag{5.56}$$

The solution of the above equations gives the optimal value for f^{ST} and by inverting eqs. (5.32) we obtain the optimal f^p. If we make the substitution

$$u^{ST} = rF^{ST} \tag{5.57}$$

we obtain the like Schrödinger equation

$$-\nabla^2 u^{ST} + \tilde{v}^{ST} u^{ST} = \lambda^{ST} u^{ST} \tag{5.58}$$

where λ are the Lagrange multipliers, chosen in a way that the $\partial u^{ST}/\partial r$ are continous in $r = d$.
The discussion developed above is referred to the first four channels of the correlations. The presence of the tensor terms does not create principle problems but it complicates the expressions of the equations.

A complete minimization would imply the search for for energy minima by changing six healing distances. Nuclear matter calculations [Pan79] indicate that the healing distances of the four central channels are rather similar and also those of the two tensor distances. For this reason we defined a single variational parameter d_c for central channels $p \leq 4$ and another parameter d_t for the remaining tensor channels. In Tab. 5.5, we present the values of the healing distances giving the energy minima for each nucleus, and for both interactions v_8' with UIX and v_{14} with $UVII$. It is remarkable the similarity of these values for all the nuclei but the ^{12}C nucleus. The values of d_c for the two interactions are the same, with the usual exception of ^{12}C , while the d_t values for v_{14} plus $UVII$ are slightly larger than those obtained with v_8' plus UIX. The two-body correlation functions obtained for the v_8' plus UIX interaction are shown in Fig. 5.1 for each channel. In the figure we also show with the diamonds the nuclear matter

		^{12}C	^{16}O	^{40}Ca	^{48}Ca	^{208}Pb
v_8' +	d_c	1.20	2.10	2.15	2.10	2.20
UIX	d_t	3.30	3.70	3.66	3.70	3.60
v_{14} +	d_c	1.40	2.10	2.15	2.10	2.20
$UVII$	d_t	3.30	3.80	3.86	3.90	3.80

Table 5.5: Values, in fm, of the *healing distances*, obtained minimizing the energy functional with the two different interactions we have adopted.

correlations. These last correlations are obtained with the Euler procedure by using the same healing distances used for finite nuclei but with constant density value of the nuclear matter the saturation point. Analogous results have been obtained for the v_{14} plus $UVII$ interaction. The diamonds in the figure, show the nuclear matter correlations obtained with the Euler procedure by using the same healing distances of the $AV8'$ interactions but for constant density. We used $\rho = 0.17\ fm^{-3}$, the density of the nuclear matter saturation point. We would like to point out two features of these results. The first one is that the various correlations are rather similar for all the nuclei considered. Only the ^{12}C results are out of this general trend. This fact indicates that the correlation functions are more sensitive to the characteristics of the nucleon-nucleon interaction than to the shell effects. The second point we want to mention is the difference between the *healing distances* of the central and tensor channels. In the two-body interaction, the tensor channels are active at larger distances with respect to the central channels, and this produces the consequences on the correlation functions we have just pointed out. It is interesting to notice that the *healing* for the tensor channels appears at distances larger than the experimental charge radius of the deuteron.

In this discussion the ^{12}C nucleus remains an anomaly. The f_1 correlation is rather similar to those of the other nuclei, all the other two-body correlations are remarkably different, especially f_3 and f_4 related to the spin and spin-orbit dependent terms.

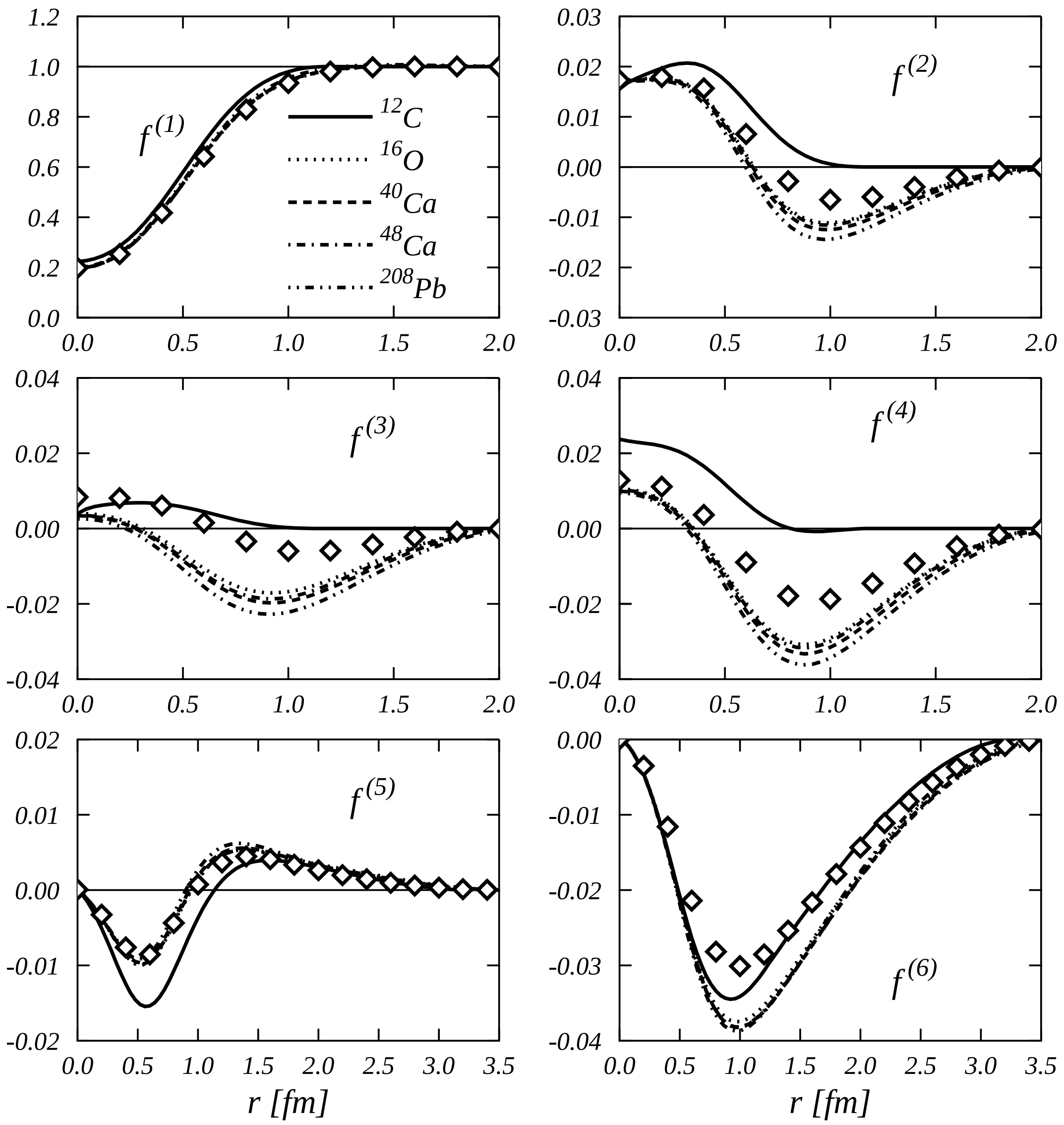

Figure 5.1: Correlation functions of the considered nuclei for each operator channel. The symbols show the nuclear matter correlation functions obtained by using the same interaction model (AV8'+UIX).

5.4 The sum rules

Sum rules are an important tool to verify the accuracy of the calculations. We have evaluated three different types of sum rules

$$
\begin{aligned}
S_1 &= \frac{1}{A}\sum_{\alpha=p,n}\int d\boldsymbol{r}_1 \rho_1^{\alpha}(\boldsymbol{r}_1) = 1 && (5.59)\\
S_2 &= \frac{1}{A(A-1)}\sum_{\alpha\beta=p,n}\int d\boldsymbol{r}_1 d\boldsymbol{r}_2 \rho_{2,1}^{\alpha\beta}(\boldsymbol{r}_1,\boldsymbol{r}_2) = 1 && (5.60)\\
S_{2,\sigma} &= \frac{1}{3A}\sum_{\alpha\beta=p,n}\int d\boldsymbol{r}_1 d\boldsymbol{r}_2 \rho_{2,2}^{\alpha\beta}(\boldsymbol{r}_1,\boldsymbol{r}_2) = -1 && (5.61)
\end{aligned}
$$

with

$$
\rho_{2,q}^{\alpha\beta}(\boldsymbol{r}_1,\boldsymbol{r}_2) =< \Psi^* \sum_{k\neq l=1}^{A} \delta(\boldsymbol{r}_1-\boldsymbol{r}_k)P_k^{\alpha}\delta(\boldsymbol{r}_2-\boldsymbol{r}_l)P_l^{\beta}O_{kl}^{q}\Psi >, \qquad q=1,...,6 \tag{5.62}
$$

where P_k^{α} is the projection operator on the $\alpha = p, n$ state of the k-th nucleon. In the above equation we have used the definition

$$
< X >= \frac{\int dx X}{\int dx |\Psi|^2} \tag{5.63}
$$

where we have indicated with dx the integration over the space coordinates and the sum over the spin and isospin states.
The sum rule S_1 is related to the one-body density and then we have used the subindex 1. The sum rule S_2 is related to the two-body density function and, finally, $S_{2,\sigma}$ is related to the spin two-body density function. This last sum rule is satisfied only when the shells of the considered nucleus are closed and in absence of correlations with tensor components. In the following equations we give the explicit expressions of the sum rules in terms of the quantities used in the $FHNC/SOC$ calculations, and we specify the proton and neutron contributions. We have performed the calculations by considering all the possible correlations in the 1 and 2 coordinates and by dressing them with the scalar correlations. This is the same approximation used to calculate the W_0 part of the two-body energy:

$$
\begin{aligned}
S_1^p &= \frac{1}{Z}\int d\boldsymbol{r}_1 \rho_1^{p}(\boldsymbol{r}_1) = 1 && (5.64)\\
S_1^n &= \frac{1}{N}\int d\boldsymbol{r}_1 \rho_1^{n}(\boldsymbol{r}_1) = 1 && (5.65)
\end{aligned}
$$

$$
\begin{aligned}
S_2^{pp} &= \frac{1}{Z(Z-1)} \int d\boldsymbol{r}_1 d\boldsymbol{r}_2 \rho_{2,1}^{pp}(\boldsymbol{r}_1, \boldsymbol{r}_2) && (5.66)\\
&= \frac{1}{Z(Z-1)} \int d\boldsymbol{r}_1 d\boldsymbol{r}_2 \frac{f_{2k_1-1+l_1}(r_{12}) f_{2k_2-1+l_2}(r_{12})}{f_1^2(r_{12})} \\
&\Big\{ \rho_{2,dir}^{pp}(\boldsymbol{r}_1, \boldsymbol{r}_2) I^{k_1 k_2 1} \chi_{l_1+l_2}^{pp} \\
&+ \Big(\rho_{2,exc}^{pp}(\boldsymbol{r}_1, \boldsymbol{r}_2) A^{k_3} I^{k_1 k_2 k_3} + \rho_{2,excj}^{pp}(\boldsymbol{r}_1, \boldsymbol{r}_2) I^{k_1 k_2 k_4} I^{k_4 k_3 2} \Big) \\
&\Delta^{k_3} \sum_{l_3=0}^{1} \chi_{l_1+l_2+l_3}^{pp} \Big\} = 1 && (5.67)\\
S_2^{pn(np)} &= \frac{1}{ZN} \int d\boldsymbol{r}_1 d\boldsymbol{r}_2 \rho_{2,1}^{pn(np)}(\boldsymbol{r}_1, \boldsymbol{r}_2) \\
&= \frac{1}{ZN)} \int d\boldsymbol{r}_1 d\boldsymbol{r}_2 \frac{f_{2k_1-1+l_1}(r_{12}) f_{2k_2-1+l_2}(r_{12})}{f_1^2(r_{12})} \\
&\Big\{ \rho_{2,dir}^{pn(np)}(\boldsymbol{r}_1, \boldsymbol{r}_2) I^{k_1 k_2 1} \chi_{l_1+l_2}^{pn(np)} \\
&+ \Big(\rho_{2,exc}^{pn(np)}(\boldsymbol{r}_1, \boldsymbol{r}_2) A^{k_3} I^{k_1 k_2 k_3} + \rho_{2,excj}^{pn(np)}(\boldsymbol{r}_1, \boldsymbol{r}_2) I^{k_1 k_2 k_4} I^{k_4 k_3 2} \Big) \\
&\Delta^{k_3} \sum_{l_3=0}^{1} \chi_{l_1+l_2+l_3}^{pn(np)} \Big\} = 1 && (5.68)\\
S_2^{nn} &= \frac{1}{N(N-1)} \int d\boldsymbol{r}_1 d\boldsymbol{r}_2 \rho_{2,1}^{nn}(\boldsymbol{r}_1, \boldsymbol{r}_2) \\
&= \frac{1}{N(N-1)} \int d\boldsymbol{r}_1 d\boldsymbol{r}_2 \frac{f_{2k_1-1+l_1}(r_{12}) f_{2k_2-1+l_2}(r_{12})}{f_1^2(r_{12})} \\
&\Big\{ \rho_{2,dir}^{nn}(\boldsymbol{r}_1, \boldsymbol{r}_2) I^{k_1 k_2 1} \chi_{l_1+l_2}^{nn} \\
&+ \Big(\rho_{2,exc}^{nn}(\boldsymbol{r}_1, \boldsymbol{r}_2) A^{k_3} I^{k_1 k_2 k_3} + \rho_{2,excj}^{nn}(\boldsymbol{r}_1, \boldsymbol{r}_2) I^{k_1 k_2 k_4} I^{k_4 k_3 2} \Big) \\
&\Delta^{k_3} \sum_{l_3=}^{1} \chi_{l_1+l_2+l_3}^{nn} \Big\} = 1 && (5.69)\\
S_{2,\sigma} &= \frac{1}{3A} \sum_{\alpha\beta=p,n} \int d\boldsymbol{r}_1 d\boldsymbol{r}_2 \frac{f_{2k_1-1+l_1}(r_{12}) f_{2k_2-1+l_2}(r_{12})}{f_1^2(r_{12})} \\
&\Big\{ \rho_{2,dir}^{\alpha\beta}(\boldsymbol{r}_1, \boldsymbol{r}_2) I^{k_1 2 k_2} \chi_{l_1+l_2}^{\alpha\beta} \\
&+ \Big(\rho_{2,exc}^{\alpha\beta}(\boldsymbol{r}_1, \boldsymbol{r}_2) A^{k_3} I^{k_1 2 k_4} I^{k_4 k_2 k_3} + \rho_{2,excj}^{\alpha\beta}(\boldsymbol{r}_1, \boldsymbol{r}_2) I^{k_1 2 k_4} I^{k_4 k_2 k_5} I^{k_5 k_3 2} \Big) \\
&\Delta^{k_3} \sum_{l_3=0}^{1} \chi_{l_1+l_2+l_3}^{\alpha\beta} \Big\} = -1 && (5.70)
\end{aligned}
$$

We have indicated with N, Z and A the number of neutrons, protons and the mass number, respectively. The two-body densities $\rho_{2,dir}^{\alpha\beta}(\boldsymbol{r}_1, \boldsymbol{r}_2)$ and $\rho_{2,exc(j)}^{\alpha\beta}(\boldsymbol{r}_1, \boldsymbol{r}_2)$ are defined in eqs. (4.19). The α,β indices may be p or n and the sum over the $k_i = 1, 2, 3$ indices are saturated. Also the indices $l_i = 0, 1$ are saturated. In tables 5.6,

	^{12}C	^{16}O	^{40}Ca	^{48}Ca	^{208}Pb
$S^p_{1,J}$	1.000	1.000	1.000	1.000	0.999
$S^n_{1,J}$	1.000	1.000	1.000	0.999	0.999
$S^p_{1,SOC}$	0.997	1.006	1.008	1.013	1.024
$S^n_{1,SOC}$	0.997	1.006	1.008	1.021	1.027
$S_{2,J}$	1.004	1.003	1.001	1.000	0.998
$S_{2,SOC}$	0.996	1.025	1.022	1.042	1.055
$S_{2,\sigma,J}$	-0.687	-0.964	-0.942	-0.860	-0.897
$S_{2,\sigma,SOC}$	-0.715	-1.055	-1.067	-0.970	-1.000

Table 5.6: Sum rules for each nucleus obtained by using the AV8' interaction. The variational parameter are represented in tables 5.1, 5.5.

5.7 and 5.8, we give the sum rules obtained by using the three interactions AV8', U14 and U14', respectively. In these tables we give the sum rule values obtained with scalar correlation function only, and with the full operator dependence. The general consideration is that the sum rules are better exhausted when only Jastrow correlations are used. For example, the S_1 sum rules are exhausted at the level of the numerical uncertainty for the Jastrow case. For the SOC case the uncertainty increases with the nucleons number reaching the 3% in ^{208}Pb. The S_2 sum rules show a similar behavior, but now for the SOC calculations the maximum uncertainty is of about 5%. We present also the results for the $S_{s,\sigma}$ sum rule, even though we know that this is satisfied only in ^{16}O and ^{40}Ca which are saturated in spin and isospin. In these two nuclei the sum rule violations vary from about 4% in Jastrow calculations up to a 10% in SOC calculations. The differences between Jastrow and SOC sum rules, give an estimate of the validity of the SOC approximation.

	^{12}C	^{16}O	^{40}Ca	^{48}Ca	^{208}Pb
$S^p_{1,J}$	1.000	1.000	1.000	1.000	0.999
$S^n_{1,J}$	1.000	1.000	1.000	0.999	0.999
$S^p_{1,SOC}$	0.999	1.005	1.006	1.017	1.028
$S^n_{1,SOC}$	0.999	1.005	1.005	1.017	1.023
$S_{2,J}$	1.003	1.002	1.001	1.000	0.998
$S_{2,SOC}$	1.001	1.022	1.018	1.041	1.053
$S_{2,\sigma,J}$	-0.697	-0.974	-0.955	-0.870	-0.882
$S_{2,\sigma,SOC}$	-0.729	-1.086	-1.103	-1.003	-1.030

Table 5.7: Sum rules for each nucleus obtained by using the U14 interaction. The variational parameter are represented in tables 5.1, 5.5.

	^{12}C	^{16}O	^{40}Ca	^{48}Ca	^{208}Pb
$S^p_{1,J}$	1.000	1.000	1.000	1.000	0.999
$S^n_{1,J}$	1.000	1.000	1.000	0.999	0.999
$S^p_{1,SOC}$	0.999	1.005	1.006	1.017	1.028
$S^n_{1,SOC}$	0.999	1.005	1.006	1.017	1.022
$S_{2,J}$	1.003	1.002	1.001	1.000	0.998
$S_{2,SOC}$	1.001	1.021	1.017	1.039	1.051
$S_{2,\sigma,J}$	-0.697	-0.977	-0.961	-0.875	-0.887
$S_{2,\sigma,SOC}$	-0.729	-1.083	-1.098	-0.996	-1.026

Table 5.8: Sum rules for each nucleus obtained by using the U14' interaction. The variational parameter are represented in tables 5.1, 5.5.

5.5 The ground state energies and the distribution functions

The most important result of this work is summarized in Tab. 5.9 where we give the values of the binding energies per nucleon, obtained in the two models AV8'+UIX and U14+UVII, for all the five nuclei considered and we compare them with the experimental energies. In the table we present the various terms contributing to the total energy: the kinetic energy T, the two-body interaction, where the contribution of the first six channels V^6_{2-body} and that of the spin-orbit interaction V_{LS} are separately given, the Coulomb interaction V_{Coul} and the three-body force V_{3-body}. In the kinetic energy term the contribution of the center of mass motion, has already been subtracted.

The various terms show some saturation properties. For example the values of kinetic energies per nucleon T increase up to ^{40}Ca and then they remain almost stable around a value of about 40 MeV. An analogous behavior is shown by the V^6_{2-body} terms. The contribution per nucleon increases with increasing number of nucleons up to ^{40}Ca. After that it is evident that saturation appears in heavier systems.

We have mentioned the fact that the spin-orbit terms are not treated consistently in the FHNC/SOC computational scheme, but they are evaluated by using some approximation. In any case, in all the nuclei considered, their contributions are of the order of few percent with respect to the V^6_{2-body} contributions. We have done calculations in ^{16}O and ^{40}Ca switching off the spin-orbit terms in the mean field potential. In this case the spin-orbit partner single particle wave functions are identical. The differences in the total spin-orbit contributions, with respect to the values given in Tab. 5.9 are within the numerical uncertainty.

As it was expected, the results of Tab. 5.9 show that the binding is obtained by a subtle subtraction between the repulsive kinetic energy term and the actractive contribution of the two-body potential. The sum of only these contributions for the AV8' interaction, provide -2.25, -6.20, -8.30, -7.31 and -9.32 MeV for the ^{12}C, ^{16}O, ^{40}Ca, ^{48}Ca and ^{208}Pb nuclei respectively. The sum in the U14 model provide -2.40, -6.56, -9.25, -8.19 and -10.21. It is evident that the U14 interaction is more attractive than the AV8'. That depends on the intrinsic structure of the interaction and its parametrization.

The contribution of the Coulomb term V_{Coul} is evaluated within the complete

FHNC/SOC computational scheme. As expected, the behavior with increasing size of the nucleus does not show saturation because of the long range nature of the interaction. The Coulomb terms behave as expected, their contributions increase with increasing number of protons. The apparent inversion of this trend from ^{40}Ca to ^{48}Ca is due to the representation in terms of energy per nucleon, which in this case is misleading, since the proton number is the same for the two nuclei. In this case it is better to compare the total values of the Coulomb energies, 78.40 MeV for ^{40}Ca and 75.36 for ^{48}Ca. The 3.8% difference between these two values is due to the different structure of the two nuclei. The inclusion of the Coulomb repulsion reduces the nuclear binding energies. The binding energy values, for the AV8'+UIX interaction, without the three-body forces are -1.58, -5.34, -6.34, -5.74 and -5.35 for the ^{12}C, ^{16}O, ^{40}Ca, ^{48}Ca and ^{208}Pb nuclei respectively, all them above the experimental values. For the U14+UVII model we have -1.72, -5.68, -7.24, -6.60 and -6.21 respectively.

In addition to that, there is the contribution of the three-body force. As discussed in chapter 3.4 for the Tucson model, the two terms composing this interactions provide contributions of different sign, one repulsive v^R_{123} and the other one attractive $v^{2\pi}_{123}$. In our calculations the total contribution of the Urbana VII,IX interactions is always globally repulsive.

The comparison with the experimental energies indicates a general underbinding of about 4.0 MeV per nucleon. The behavior of the ^{12}C nucleus is anomalous in this general trend. This nucleus is barely bound in our calculations. Some crucial physics ingredient relevant in ^{12}C while negligible for the other other nuclei is missing in our approach. Probably this has to do with soft deformations of the ^{12}C nucleus which we are unable to treat.

The comparison between the two interactions indicates that the v_{14} plus $UVII$ is more attractive than the v_8' plus UIX. This is a fact already present when the two-body interaction only is considered. The situation is enhanced by the three-body force, more repulsive for the UIX case than for the $UVII$ one. The contributions of the spin-orbit term in the two cases have different sign, they are attractive for v_8' and slightly repulsive for v_{14}. The changes in the total energies go from a minimum of 5% (^{16}O) to a maximum of 18% (^{208}Pb).

In order to study the sensitivity of the results to the various terms of the interactions we have done calculations with the truncated Urbana $U14$ and $U14'$

potentials [Lag81A, Lag81B] by using the values of the the healing distances of table 5.5 fixed for the $AV8'$ potential. We have implemented this interaction with different three-body forces: the Urbana VII and IX models and the FP interaction. The results of these calculations are given in Tables 5.10, 5.11, 5.12, 5.13 and 5.14. Also in these cases the saturation properties of the nuclear interaction are evident, even though the V^6_{2-body} contributions seems slightly less attractive than that of the Argonne $AV8'$ case. The main difference between the two calculations is in the spin-orbit contribution, which for case is much smaller than that of the $AV8'$ interaction, and repulsive, instead than attractive. The values of energy without the three-body terms for the U14+UIX model, are -1.72, -5.68, -7.24, -6.60 and -6.17 for the ^{12}C, ^{16}O, ^{40}Ca, ^{48}Ca and ^{208}Pb nuclei respectively. This interaction is more attractive than the $AV8'$ interaction. We have done calculations with two different three-body interaction, the Urbana IX already used together with the Argonne $AV8'$, and the Urbana VII fixed in [Sch86] to be used with the Urbana $U14$ potential. In both cases the contributions of the three-body interactions are repulsive. It is interesting to see that the Urbana IX produce larger contributions than those obtained with $AV8'$ potential. On the other hand, the Urbana VII potential is less repulsive. The binding energies obtained with the $U14'+FP$ model are in Mev per nucleon, -5.56,-9.24,-10.67,-10.05 and -9.45 for the ^{12}C, ^{16}O, ^{40}Ca, ^{48}Ca and ^{208}Pb, respectively. The difference between the kinetic energy T and the two-body potential V^6_{2-body} is very similary to the $U14{+}UIX$ model, but the contribution of the TNA term of FP interaction is strongly attractive. The contribution of the various terms we have calculated to obtain the nuclear energy, are given in great detail in tables 5.15-5.24 for the two interactions $AV8' + UIX$ and $U14 + UVII$. The meaning of the various terms is explained in the table caption and it will not be repeated here.

The larger contributions to the energy are coming from the (0) approximation of eq. (4.15), i.e. from the diagrams containing all the scalar dressings of the (1,2). The contributions given by the terms depending on antiparallel spin one-body densities, the terms labeled with the j subscripts in the tables, are very small. This is particularly evident in nuclei with saturated l shells such as ^{16}O and ^{40}Ca . The contribution of these terms is slightly larger in ^{48}Ca and ^{208}Pb , but still much smaller than the contributions of the various channels indicates that the spin-isospin ($p = 4$) and tensor-isospin ($p = 6$) are the main responsible of the binding. The tables show that in the three-body forces the repulsive contribution of the UIX interaction is stronger than that of the $UVII$ force.

AV8'+UIX	^{12}C	^{16}O	^{40}Ca	^{48}Ca	^{208}Pb
T	27.13	32.33	41.06	39.64	39.56
V^6_{2-body}	-29.13	-38.15	-48.97	-46.60	-48.43
V_{Coul}	0.67	0.86	1.97	1.57	3.97
V_{LS}	-0.25	-0.38	-0.39	-0.35	-0.45
$T + V^6_{2-body}$	-1.58	-5.34	-6.34	-5.74	-5.35
V_{3-body}	0.67	0.86	1.76	1.61	1.91
$E^{g.s.}$	-0.91	-4.48	-4.58	-4.14	-3.43
U14+UVII	^{12}C	^{16}O	^{40}Ca	^{48}Ca	^{208}Pb
T	24.63	29.25	37.32	36.12	36.07
V^6_{2-body}	-27.08	-35.84	-46.65	-44.40	-46.28
V_{Coul}	0.68	0.88	2.01	1.59	4.00
V_{LS}	0.05	0.03	0.08	0.09	0.04
$T + V^6_{2-body}$	-1.72	-5.68	-7.37	-6.71	-6.32
V_{3-body}	0.54	0.69	1.46	1.32	1.61
$E^{g.s.}$	-1.18	-4.99	-5.77	-5.27	-4.55
E_{exp}	-7.68	-7.97	-8.55	-8.66	-7.86

Table 5.9: Energies per nucleon obtained by using the $AV8' + UIX$ and $U14 + UVII$ interaction models. The units are Mev/nucleon

	AV8'+UIX	U14+UIX	U14+UVII	U14'+FP
T	27.13	24.63	24.63	27.70
V^6_{2-body}	-29.13	-27.08	-27.08	-26.09
V_{Coul}	0.67	0.68	0.68	0.68
V_{LS}	-0.25	0.05	0.05	0.05
$T+V^6_{2-body}$	-2.00	-2.45	-2.45	0.80
V_{3-body}	0.66	1.00	0.54	-4.91
$E^{g.s.}$	-0.91	-0.72	-1.18	-5.56

Table 5.10: We show the various contributions to the energy of the ^{12}C for four different types of interactions: in particular we consider the truncated two-body Argonne potential AV8' with the phenomenological three-body interaction UIX (Tucson model), the two-body truncated Urbana potential U14 with the three-body interactions UIX ,UVII and finally the modified Urbana U14' with the three-body Friedman-Pandharipande (FP) interaction. For each interaction we calculate the total kinetic energy T, the total contribution of the first six channels of the two-body potential V^6_{2-body}, the Coulomb energy V_{Coul}, the (LS) term. We give the result obtained by using two-body interactions only, the total three-body contribution and finally the total ground state energy. The units are Mev/nucleon.

	AV8'+UIX	U14+UIX	U14+UVII	U14'+FP
T	32.33	29.25	29.25	28.82
V^6_{2-body}	-38.15	-35.84	-35.84	-34.04
V_{Coul}	0.86	0.88	0.88	0.87
V_{LS}	-0.38	0.03	0.03	0.04
$T+V^6_{2-body}$	-5.82	-6.59	-6.59	-5.22
V_{3-body}	0.86	1.26	0.69	-4.93
$E^{g.s.}$	-4.48	-4.42	-4.99	-9.24

Table 5.11: The same of table 5.10 for the ^{16}O.

	AV8'+UIX	U14+UIX	U14+UVII	U14'+FP
T	41.06	37.32	37.32	36.51
V^6_{2-body}	-48.97	-46.65	-46.65	-43.41
V_{Coul}	1.97	2.01	2.01	2.00
V_{LS}	-0.39	0.08	0.08	0.11
$T+V^6_{2-body}$	-7.91	-9.33	-9.33	-6.90
V_{3-body}	1.76	2.47	1.46	-5.87
$E^{g.s.}$	-4.58	-4.77	-5.77	-10.67

Table 5.12: The same of table 5.10 for the ^{40}Ca.

	AV8'+UIX	U14+UIX	U14+UVII	U14'+FP
T	39.64	36.12	36.12	35.53
V^6_{2-body}	-46.60	-44.40	-44.40	-41.85
V_{Coul}	1.57	1.59	1.59	1.58
V_{LS}	-0.35	0.09	0.09	0.11
$T+V^6_{2-body}$	-6.96	-8.28	-8.28	-6.32
V_{3-body}	1.61	2.23	1.32	-5.43
$E^{g.s.}$	-4.14	-4.36	-5.27	-10.05

Table 5.13: The same of table 5.10 for the ^{48}Ca.

	AV8'+UIX	U14+UIX	U14+UVII	U14'+FP
T	39.56	36.07	36.07	35.47
V^6_{2-body}	-48.43	-46.28	-46.28	-43.76
V_{Coul}	3.97	4.00	4.00	3.98
V_{LS}	-0.45	0.04	0.04	0.07
$T+V^6_{2-body}$	-8.87	-10.21	-10.21	-8.29
V_{3-body}	1.91	2.55	1.61	-5.21
$E^{g.s.}$	-3.43	-3.61	-4.55	-9.45

Table 5.14: The same of table 5.10 for the ^{208}Pb.

	(0)	(s)	(c)	$(0)+(s)+(c)$
$T_{\Phi}^{(1)}$	16.68			16.68
$T_{\Phi}^{(2)}$	1.77	-0.25	-0.04	1.48
$T_{\Phi}^{(3)}$	-0.05	-0.05		-0.10
T_F	9.60	0.51	0.03	10.14
$T_{\Phi j}^{(2)}$	0.36			0.36
$T_{\Phi j}^{(3)}$	-0.03			-0.03
T_{Fj}	-0.01			-0.01
$T_{c.m.}$	1.07			1.07
v^1	0.95	0.20	-0.30	0.85
v^2	-0.89	0.02	-0.02	-0.89
v^3	-2.87	0.08	-0.04	-2.83
v^4	-12.64	-0.09	0.03	-12.7
v^5	0.08	-0.01	0.01	0.08
v^6	-13.50	-0.43	0.13	-13.8
v_j^1	0.06			0.05
v_j^2	-0.003			-0.003
v_j^3	0.02			0.02
v_j^4	0.13			0.13
v_j^5	0.003			0.003
v_j^6	-0.03			-0.03
UIX				
v_{123}^R				1.568
$v_{123}^{2\pi}$				-0.898

Table 5.15: Contributions of the various terms forming the ^{12}C energy. The various terms are defined in chapt. 3. The T terms of the kinetic energy are defined by eqs. (4.6,4.7,4.8,4.48). The v^p terms indicate the six-channels of the two-body interaction. The three-body terms are defined in eqs. (4.65,4.67,4.70). The subscript j indicate the contribution produced by antiparralel spin densities. The labels (0), (s) and (c) indicate the various approximation of the energy related to the pieces W_0, W_s, and W_c as defined in eq. (4.15). The results have been obtained by using a two-body AV8' potential with a three-body interaction UIX. The units are Mev/nucleon.

	(0)	(s)	(c)	$(0)+(s)+(c)$
$T_\Phi^{(1)}$	16.42			16.42
$T_\Phi^{(2)}$	1.88	-0.18	-0.03	1.66
$T_\Phi^{(3)}$	-0.01	-0.04		-0.05
T_F	7.30	0.35	0.001	7.67
$T_{\Phi j}^{(2)}$	0.37			0.37
$T_{\Phi j}^{(3)}$	-0.03			-0.03
T_{Fj}	0.00			0.00
$T_{c.m.}$	1.07			1.07
v^1	3.01	0.24	-0.41	2.89
v^2	1.95	-0.07	0.12	1.99
v^3	1.75	-0.04	0.05	1.76
v^4	-25.09	-0.15	0.12	-25.12
v^5	0.25	-0.004	0.01	0.26
v^6	-9.05	-0.24	0.30	-8.99
v_j^1	0.05			0.05
v_j^2	-0.01			-0.01
v_j^3	0.003			0.003
v_j^4	0.14			0.14
v_j^5	0.02			0.02
v_j^6	-0.02			-0.02
$UVII$				
v_{123}^R				1.258
$v_{123}^{2\pi}$				-0.716
UIX				
v_{123}^R				1.632
$v_{123}^{2\pi}$				-0.630

Table 5.16: The same of the table 5.15 for the two-body U14 potential with the three-body interactions UVII and UIX.

	(0)	(s)	(c)	$(0)+(s)+(c)$
$T_{\Phi}^{(1)}$	14.42			14.42
$T_{\Phi}^{(2)}$	3.91	-0.27	-0.05	3.59
$T_{\Phi}^{(3)}$	0.43	-0.06		0.37
T_F	13.27	0.98	0.39	14.64
$T_{\Phi j}^{(2)}$	0.001			0.001
$T_{\Phi j}^{(3)}$	0.0			0.0
T_{Fj}	0.0			0.0
$T_{c.m.}$	0.71			0.71
v^1	1.61	0.19	-0.40	1.40
v^2	-1.10	0.03	-0.14	-1.21
v^3	-3.25	0.11	-0.50	-3.64
v^4	-15.24	-0.28	-1.13	-16.65
v^5	0.06	-0.01	0.03	0.08
v^6	-17.17	-0.81	-0.13	-18.11
v_j^1	0.0			0.0
v_j^2	0.0			0.0
v_j^3	0.0			0.0
v_j^4	0.0			0.0
v_j^5	0.0			0.0
v_j^6	0.0			0.0
UIX				
v_{123}^R				1.898
$v_{123}^{2\pi}$				-1.036

Table 5.17: The same of the table 5.15 for the ^{16}O.

	(0)	(s)	(c)	$(0)+(s)+(c)$
$T_\Phi^{(1)}$	14.49			14.49
$T_\Phi^{(2)}$	3.82	-0.22	-0.06	3.54
$T_\Phi^{(3)}$	0.40	-0.04		0.36
T_F	10.57	0.82	0.18	11.57
$T_{\Phi j}^{(2)}$	0.001			0.001
$T_{\Phi j}^{(3)}$	0.0			0.0
T_{Fj}	0.0			0.0
$T_{c.m.}$	0.71			0.71
v^1	4.23	0.38	-0.57	4.04
v^2	2.07	-0.12	0.51	2.46
v^3	2.28	-0.06	0.28	2.50
v^4	-30.36	-0.62	-2.31	-33.29
v^5	0.32	-0.007	0.04	0.35
v^6	-11.73	-0.58	0.39	-11.92
v_j^1	0.0			0.0
v_j^2	0.0			0.0
v_j^3	0.0			0.0
v_j^4	0.0			0.0
v_j^5	0.0			0.0
v_j^6	0.0			0.0
$UVII$				
v_{123}^R				1.570
$v_{123}^{2\pi}$				-0.884
UIX				
v_{123}^R				2.037
$v_{123}^{2\pi}$				-0.778

Table 5.18: The same of the table 5.16 for the ^{16}O.

	(0)	(s)	(c)	$(0)+(s)+(c)$
$T_{\Phi}^{(1)}$	16.09			16.09
$T_{\Phi}^{(2)}$	4.98	-0.31	-0.10	4.57
$T_{\Phi}^{(3)}$	0.78	-0.08		0.70
T_F	17.64	1.83	0.50	19.97
$T_{\Phi j}^{(2)}$	0.011			0.011
$T_{\Phi j}^{(3)}$	0.0			0.0
T_{Fj}	0.0			0.0
$T_{c.m.}$	0.25			0.25
v^1	1.16	0.12	-0.60	0.68
v^2	-1.40	0.05	-0.21	-1.56
v^3	-3.83	0.18	-0.71	-4.36
v^4	-18.18	-0.50	-1.56	-19.89
v^5	0.11	-0.02	0.05	0.14
v^6	-22.26	-1.54	0.17	-23.63
v_j^1	0.0			0.0
v_j^2	0.0			0.0
v_j^3	0.0			0.0
v_j^4	0.0			0.0
v_j^5	0.0			0.0
v_j^6	0.0			0.0
UIX				
v_{123}^R				3.384
$v_{123}^{2\pi}$				-1.627

Table 5.19: The same of the table 5.15 for the ^{40}Ca.

	(0)	(s)	(c)	$(0)+(s)+(c)$
$T_{\Phi}^{(1)}$	16.25			16.25
$T_{\Phi}^{(2)}$	4.85	-0.25	-0.12	4.48
$T_{\Phi}^{(3)}$	0.70	-0.06		0.6
T_F	14.42	1.58	0.19	16.19
$T_{\Phi j}^{(2)}$	0.01			0.01
$T_{\Phi j}^{(3)}$	0.0			0.0
T_{Fj}	0.0			0.0
$T_{c.m.}$	0.25			0.25
v^1	4.46	0.45	-0.84	4.07
v^2	2.68	-0.20	0.79	3.27
v^3	2.94	-0.11	0.45	3.28
v^4	-37.48	-1.15	-3.39	-42.02
v^5	0.39	-0.01	0.07	0.45
v^6	-15.54	-1.14	0.97	-15.71
v_j^1	0.0			0.0
v_j^2	0.0			0.0
v_j^3	0.0			0.0
v_j^4	0.0			0.0
v_j^5	0.0			0.0
v_j^6	0.0			0.0
$UVII$				
v_{123}^R				2.825
$v_{123}^{2\pi}$				-1.361
UIX				
v_{123}^R				3.665
$v_{123}^{2\pi}$				-1.198

Table 5.20: The same of the table 5.16 for the ^{40}Ca.

	(0)	(s)	(c)	$(0)+(s)+(c)$
$T_{\Phi}^{(1)}$	16.38			16.38
$T_{\Phi}^{(2)}$	4.50	-0.29	-0.10	4.11
$T_{\Phi}^{(3)}$	0.68	-0.08		0.60
T_F	16.73	1.64	0.36	18.73
$T_{\Phi j}^{(2)}$	0.21			0.21
$T_{\Phi j}^{(3)}$	-0.02			-0.02
T_{Fj}	-0.008			-0.008
$T_{c.m.}$	0.20			0.20
v^1	0.69	0.05	-0.58	0.16
v^2	-1.29	0.04	-0.18	-1.43
v^3	-3.78	0.18	-0.61	-4.21
v^4	-17.30	-0.42	-1.30	-19.02
v^5	0.11	-0.02	0.04	0.13
v^6	-21.17	-1.40	0.30	-22.27
v_j^1	0.013			0.013
v_j^2	0.0			0.0
v_j^3	0.007			0.007
v_j^4	0.013			0.0013
v_j^5	0.0			0.0
v_j^6	0.0			0.0
UIX				
v_{123}^R				3.097
$v_{123}^{2\pi}$				-1.490

Table 5.21: The same of the table 5.15 for the ^{48}Ca.

	(0)	(s)	(c)	$(0)+(s)+(c)$
$T_{\Phi}^{(1)}$	16.50			16.50
$T_{\Phi}^{(2)}$	4.41	-0.23	-0.11	4.07
$T_{\Phi}^{(3)}$	0.64	-0.06		0.58
T_F	13.65	1.43	0.10	15.18
$T_{\Phi j}^{(2)}$	0.20			0.20
$T_{\Phi j}^{(3)}$	-0.02			-0.02
T_{Fj}	-0.007			-0.007
$T_{c.m.}$	0.20			0.20
v^1	3.82	0.34	-0.82	3.43
v^2	2.45	-0.18	0.68	2.95
v^3	2.85	-0.10	0.38	3.13
v^4	-35.56	-1.00	-2.77	-39.33
v^5	0.36	-0.01	0.06	0.41
v^6	-14.87	-1.05	0.99	-14.93
v_j^1	0.014			0.014
v_j^2	0.0			0.0
v_j^3	0.00			0.00
v_j^4	0.018			0.0018
v_j^5	0.0			0.0
v_j^6	0.003			0.003
$UVII$				
v_{123}^R				2.567
$v_{123}^{2\pi}$				-1.246
UIX				
v_{123}^R				3.330
$v_{123}^{2\pi}$				-1.096

Table 5.22: The same of the table 5.16 for the ^{48}Ca.

	(0)	(s)	(c)	(0) + (s) + (c)
$T_{\Phi}^{(1)}$	16.05			16.05
$T_{\Phi}^{(2)}$	4.16	-0.35	-0.13	3.68
$T_{\Phi}^{(3)}$	0.42	-0.08		0.34
T_F	17.34	1.62	0.55	19.51
$T_{\Phi j}^{(2)}$	0.17			0.17
$T_{\Phi j}^{(3)}$	-0.012			-0.012
T_{Fj}	0.0			0.0
$T_{c.m.}$	0.02			0.02
v^1	-0.03	-0.10	-0.47	-0.6
v^2	-1.29	0.04	-0.19	-1.44
v^3	-3.87	0.18	-0.67	-4.36
v^4	-17.57	-0.41	-1.49	-19.47
v^5	0.11	-0.02	0.04	0.13
v^6	-21.42	-1.37	0.10	-22.69
v_j^1	0.006			0.006
v_j^2	0.0			0.0
v_j^3	0.004			0.004
v_j^4	0.012			0.012
v_j^5	0.0			0.0
v_j^6	-0.005			-0.005
UIX				
v_{123}^R				3.282
$v_{123}^{2\pi}$				-1.368

Table 5.23: The same of the table 5.15 for the ^{208}Pb.

	(0)	(s)	(c)	$(0)+(s)+(c)$
$T_{\Phi}^{(1)}$	16.38			16.38
$T_{\Phi}^{(2)}$	3.98	-0.32	-0.14	3.52
$T_{\Phi}^{(3)}$	0.31	-0.06		0.25
T_F	14.23	1.42	0.29	15.94
$T_{\Phi j}^{(2)}$	0.15			0.15
$T_{\Phi j}^{(3)}$	-0.009			-0.009
T_{Fj}	0.0			0.0
$T_{c.m.}$	0.03			0.03
v^1	3.15	0.16	-0.63	2.68
v^2	2.46	-0.17	0.69	2.98
v^3	2.90	-0.10	0.41	3.21
v^4	-36.11	-1.01	-3.20	-40.32
v^5	0.36	-0.01	0.06	0.41
v^6	-15.05	-1.04	0.80	-15.29
v_j^1	0.006			0.006
v_j^2	0.0			0.0
v_j^3	0.00			0.00
v_j^4	0.014			0.014
v_j^5	0.0			0.0
v_j^6	-0.003			-0.003
$UVII$				
v_{123}^R				2.720
$v_{123}^{2\pi}$				-1.104
UIX				
v_{123}^R				3.529
$v_{123}^{2\pi}$				2.557

Table 5.24: The same of the table 5.16 for the ^{208}Pb.

5.6 The one-body distribution functions

Other interesting information about the nuclear ground states are related to the density distributions. In figs. 5.2-5.6 we show these distributions for protons and neutrons, respectively. The full lines show the uncorrelated distributions, the dotted lines those obtained by using only scalar correlations (f_1), usually called Jastrow, and the dashed lines the results of the complete calculation. The Jastrow results produce distributions which are smaller at the center of the nucleus with respect to the mean-field distributions. This effect is strongly reduced when all the correlations are included in the calculation. These findings are in agreement with the results of ref. [Ari97] where a first-order cluster expansion was used. It is evident the scarce relevance of short-range correlations in reducing the occupation probability of the 3s1/2 proton state in ^{208}Pb. As it is pointed out in [Ang01], the effect of long-range correlations seems to be the main reduction mechanism. To investigate the relative effects of the various correlations on the proton and neutron distributions we study the ratio

$$\Delta_1(r) = \frac{\rho_1(r) - \rho_0(r)}{\rho_0(r)} \tag{5.71}$$

where, $\rho_0(r)$ is the uncorrelated, mean-field, density. The Δ_1 ratios are shown in fig. 5.7. Despite the noticeable differences between proton and neutron distributions, especially in ^{48}Ca and ^{208}Pb, the figure points out that, in these differences, the type of correlation is more relevant than the proton or neutron distribution. A direct comparison with the empirical density distributions is not fully meaningful since the mean-field potential has already been fixed to reproduce at best, these distributions. The only statements we can make is whether the inclusion of the correlations may improve or not the agreement with the data. For this reason we show in fig. 5.8 the ratios

$$\Delta_2(r) = \frac{\rho_1(r) - \rho_{exp}(r)}{\rho_{exp}(0)} \tag{5.72}$$

where the experimental charge distributions have been taken from [Dej87].

The inclusion of correlations lowers the charge density distributions at the center of the nuclei. If scalar correlation only are considered the effect is too large. When all the correlations are included the effect is strongly reduced and the agreement with the empirical densities slightly improves.

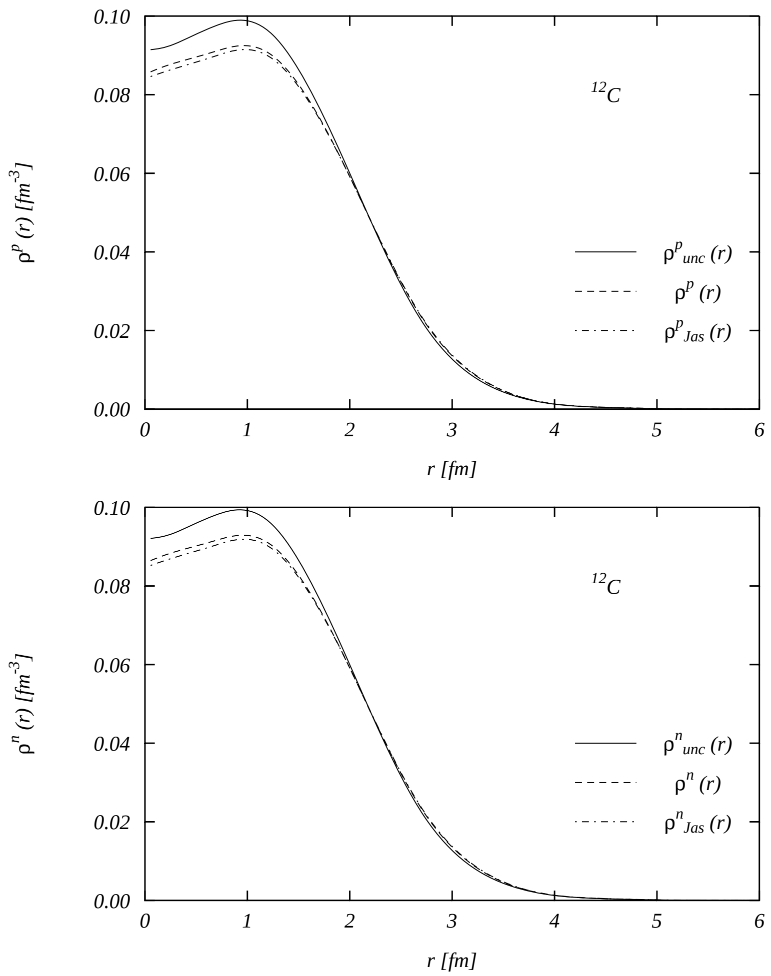

Figure 5.2: One-body proton (up) and neutron (down) densities for the ^{12}C.

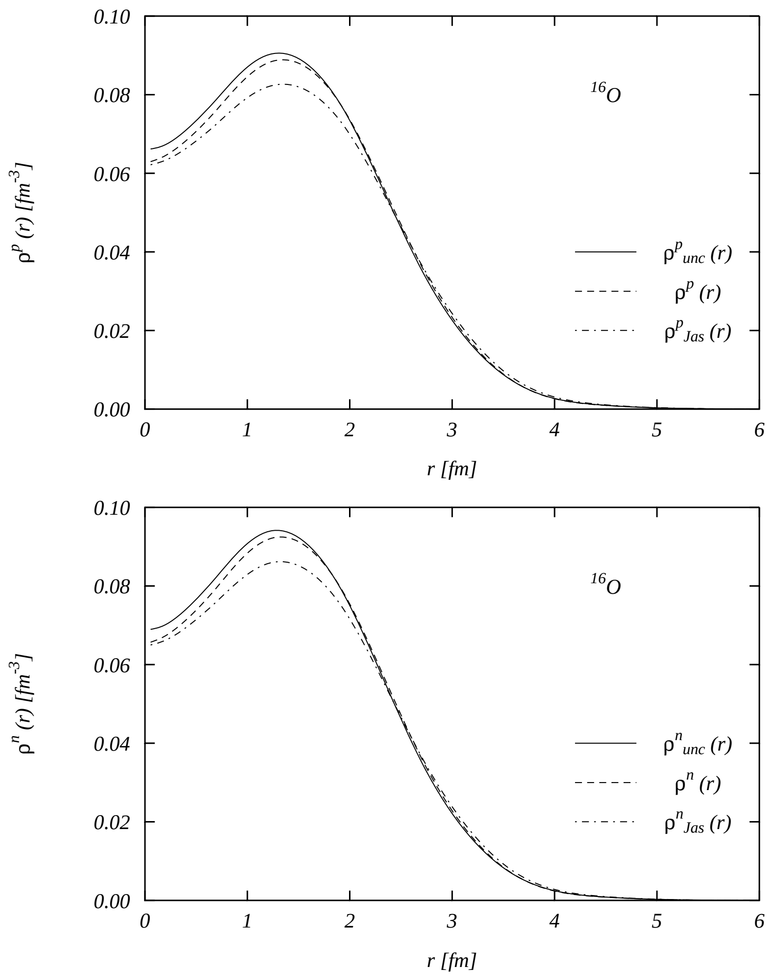

Figure 5.3: One-body proton (up) and neutron (down) densities for the ^{16}O.

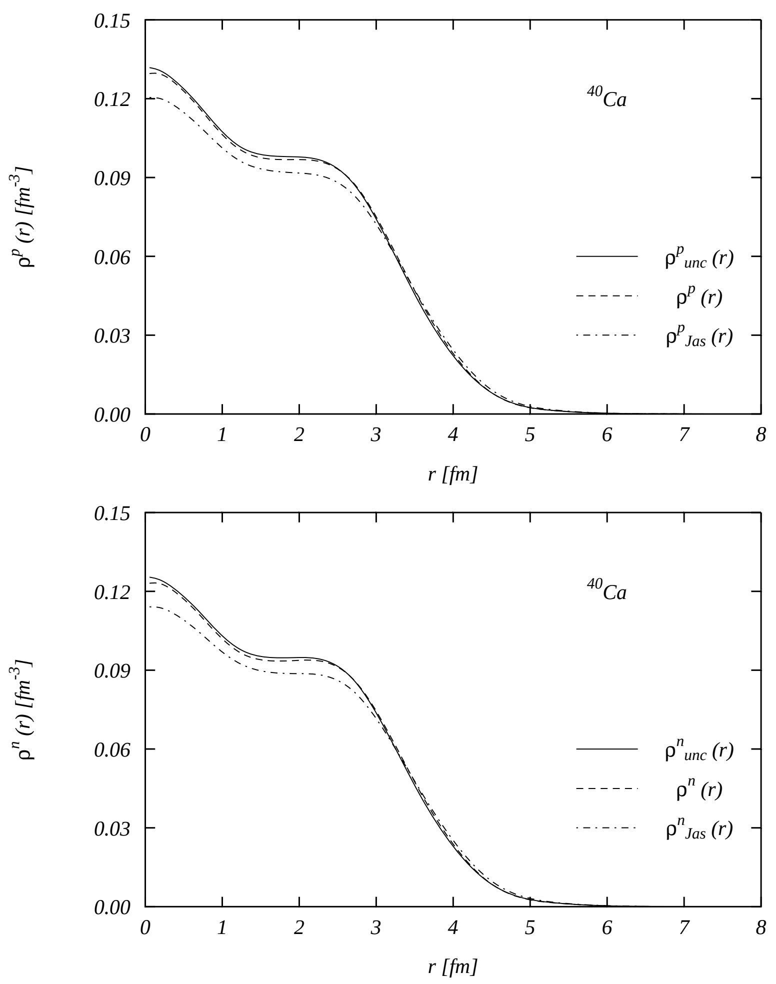

Figure 5.4: One-body proton (up) and neutron (down) densities for the ^{40}Ca.

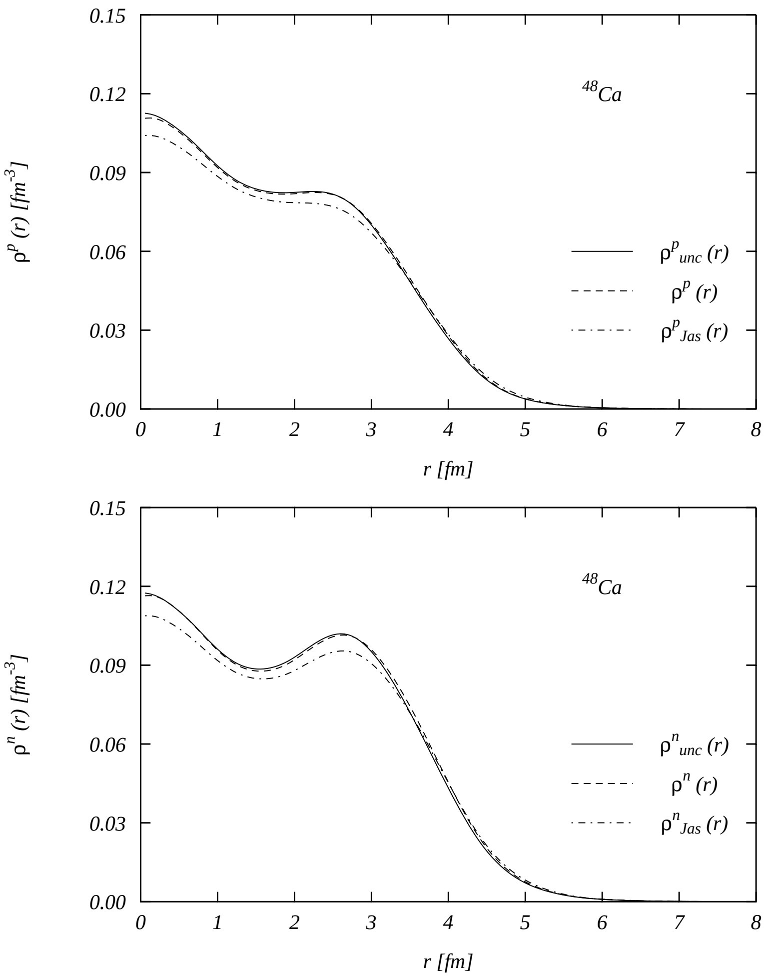

Figure 5.5: One-body proton (up) and neutron (down) densities for the ^{48}Ca.

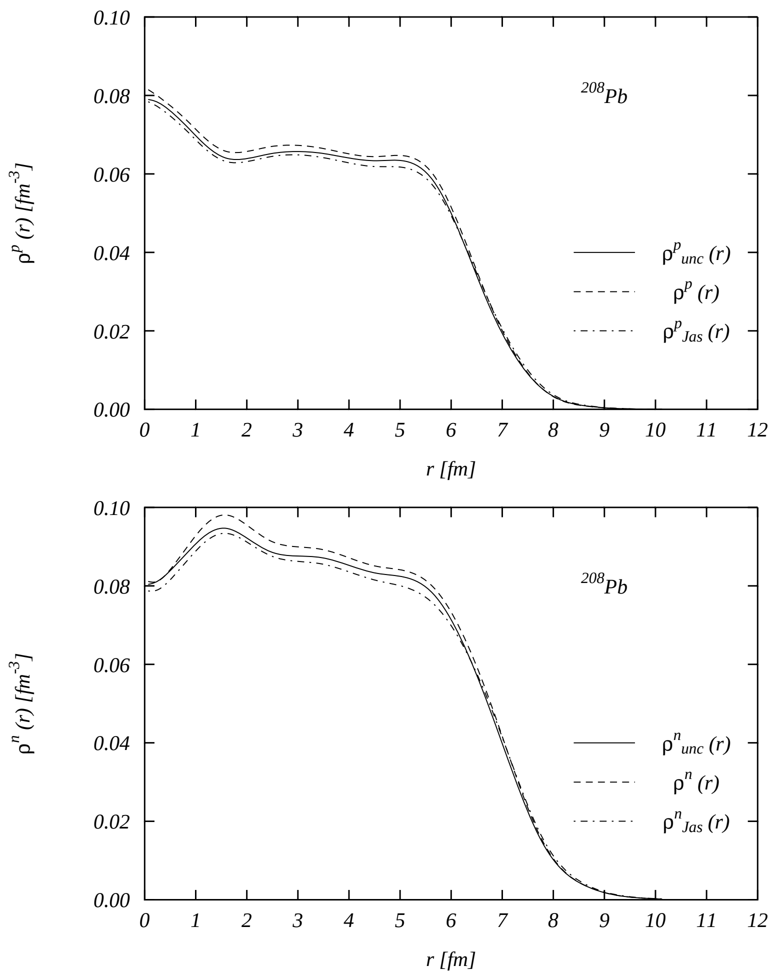

Figure 5.6: One-body proton (up) and neutron (down) densities for the ^{208}Pb.

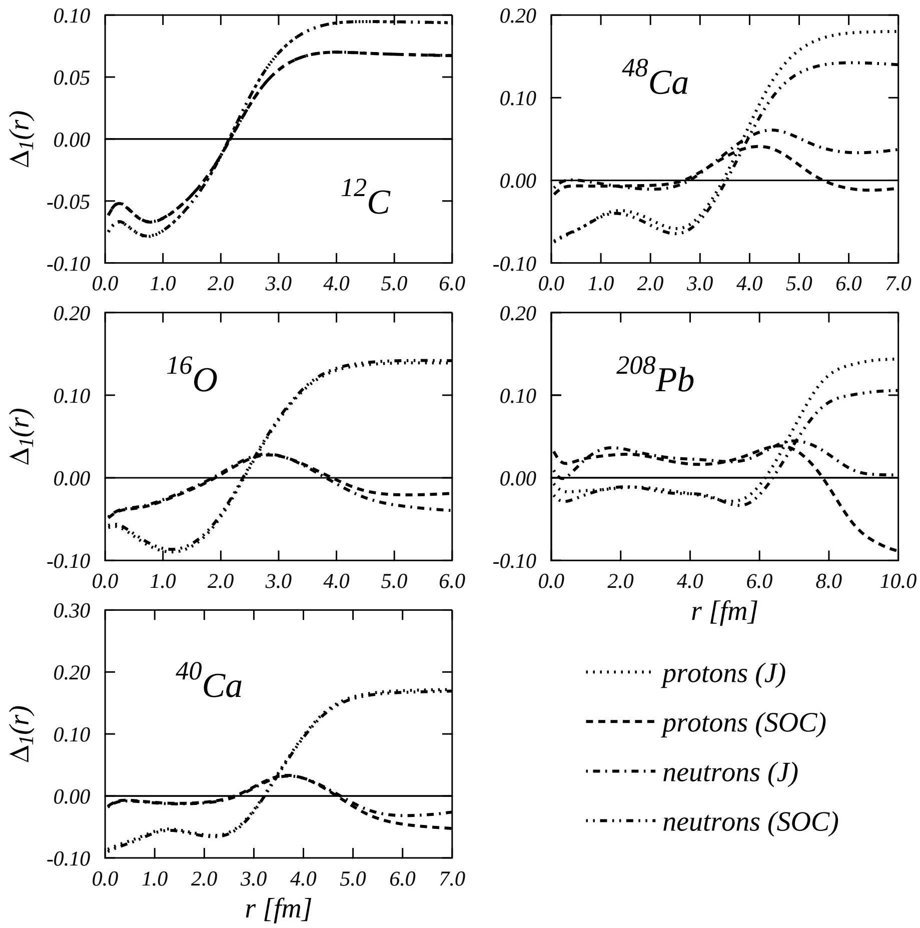

Figure 5.7: Normalised ratios (eq. 5.71) for proton and neutron distributions. The meaning of the lines is given in the legend, where we have indicated with J the results obtained with scalar correlation (f_1) only, and with SOC the results of the full calculation.

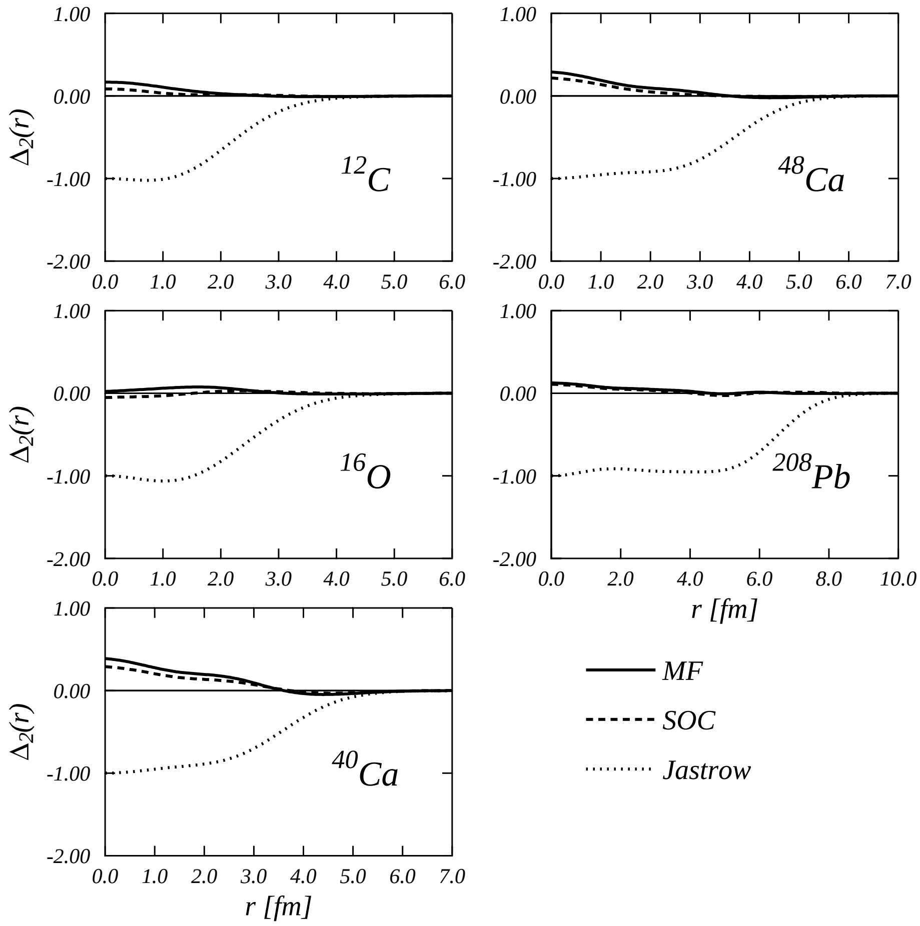

Figure 5.8: Normalised ratios (eq. 5.72) for charge density distributions. The meaning of the lines is given in the legend.

5.7 The two-body distribution functions

It is interesting also to evaluate the two-body distribution functions (TBDF). We define the operator dependent two-body density matrices as:

$$\begin{aligned}\rho^{\alpha\beta}_{2,q}(x_1,x_2) &= A(A-1)\int dx_3...dx_A\, \Psi^*(x_1,x_2,x_3,...,x_A)\mathcal{P}^{+\alpha}(x_1)O^q(x_1,x_2)\mathcal{P}^{\beta}(x_2) \\ &\quad \Psi(x_1,x_2,x_3,...,x_A)/<\Psi|\Psi>\end{aligned} \tag{5.73}$$

where

$$\mathcal{P}^{\alpha} = \begin{array}{ll}(1+t_z)/2 & \text{for protons} \\ (1-t_z)/2 & \text{for neutrons}\end{array} \tag{5.74}$$

The explicit expression of $\rho^{\alpha\beta}_{2,q}(\boldsymbol{r}_1,\boldsymbol{r}_2)$ using FHNC/SOC approximation can be written as

$$\begin{aligned}\rho^{\alpha\beta}_{2,2k_3-1+l_3}(\boldsymbol{r}_1,\boldsymbol{r}_2) &= \frac{f_{2k_1-1+l_1}(r_{12})f_{2k_2-1+l_2}(r_{12})}{f_1^2(r_{12})} \\ &\quad \Big\{ I^{k_1k_3k_2}A^{k_2}\chi^{\alpha\beta}_{l_1+l_2+l_3}\rho^{\alpha\beta}_{2,dir}(\boldsymbol{r}_1,\boldsymbol{r}_2) \\ &\quad +\Big(I^{k_4k_1k_5}I^{k_2k_3k_5}A^{k_5}\rho^{\alpha\beta}_{2,exc}(\boldsymbol{r}_1,\boldsymbol{r}_2) \\ &\quad +I^{k_4k_1k_5}I^{k_2k_3k_6}I^{k_5k_62}\rho^{\alpha\beta}_{2,excj}(\boldsymbol{r}_1,\boldsymbol{r}_2)\Big) \\ &\quad \Delta^{k_4}\sum_{l_4=0}^{1}\chi^{\alpha\beta}_{l_1+l_2+l_3+l_4}\Big\}\end{aligned} \tag{5.75}$$

where a sum is understood on every repeated index. The direct and the exchange two-body densities $\rho^{\alpha\beta}_{2,dir}(\boldsymbol{r}_1,\boldsymbol{r}_2)$ and $\rho^{\alpha\beta}_{2,exc(j)}(\boldsymbol{r}_1,\boldsymbol{r}_2)$ have been defined in eqs. (4.19). We summarize the great amount of information contained in eq. (5.73) by considering its dependence from the relative distance between the particles 1 and 2:

$$\rho^{\alpha\beta}_{2,q}(r_{12}) = \frac{1}{A}\int d\boldsymbol{R}_{12}\rho^{\alpha\beta}_{2,q}(\boldsymbol{r}_1,\boldsymbol{r}_2) \tag{5.76}$$

where $\boldsymbol{R}_{12} = (\boldsymbol{r}_1+\boldsymbol{r}_2)/2$. The details of the calculation of (5.76) are given in Appendix A.6.

In the figures 5.9 to 5.23, we give, for the nuclei considered, the TBDF for every channel. In these figures we also show the uncorrelated distributions and the distributions obtained only with the scalar correlations. We notice that in the particular case where $\alpha = \beta$ we the eq. (5.73) reads:

$$\begin{aligned} \rho^{\alpha\alpha}_{2,q}(x_1, x_2) &= A(A-1)\int dx_3...dx_A\, \Psi^*(x_1, x_2, x_3, ..., x_A)\mathcal{P}^\alpha(x_1)O^q(x_1, x_2)\mathcal{P}^\alpha(x_2) \\ &\quad \Psi(x_1, x_2, x_3, ..., x_A)/ <\Psi|\Psi> \end{aligned} \tag{5.77}$$

Taking into account that in this case also is verified this identity

$$\mathcal{P}^{+\alpha}(x_1)\boldsymbol{\tau}_1 \cdot \boldsymbol{\tau}_2\mathcal{P}^\alpha(x_2) = \mathcal{P}^\alpha(x_1)\mathcal{P}^\alpha(x_2) \tag{5.78}$$

we have

$$\rho^{\alpha\alpha}_{2,2k_3-1}(r_{12}) = \rho^{\alpha\alpha}_{2,2k_3}(r_{12}) \tag{5.79}$$

In the cases of the uncorrelated and central correlations and with independence of the isospin of the external particles, both the tensor and tensor-isospin TBDF are zero since at least two tensor operators are needed to a get a not zero spin trace. In the same cases that mentioned above and when the isospin of the external particles are different also the spin TBDF are zero. This zero is caused by the spin trace on the direct part and by the isospin trace on the exchange part.

As expected, for all the nuclei considered, the different from zero uncorrelated TBDF are not zero in the origin, i.e. there exist a no zero probability to find two particles in the same point. The inclusion of the correlation drops this probability and makes that the distribution is closer to zero in the origin. As a general trend we can mention that for these TBDF the main effect is caused by the central correlation since the inclusion of the operator ones do not modify much the scalar results. This small differences between the two correlated calculations is still valid for the tensor and tensor-isospin TBDF since the size of these functions is quite small.

In the fig. 5.24 we give for each nucleus the uncorrelated TBDF for the scalar channel and in the proton-proton projection. We can see that the adding of the exchange part in the TBDF causes, in general, a dropping in the region close to the origin. Since the exchange part is related to the Pauli principle we can affirm that the dropping is a first sign of correlation of the particles in our system.

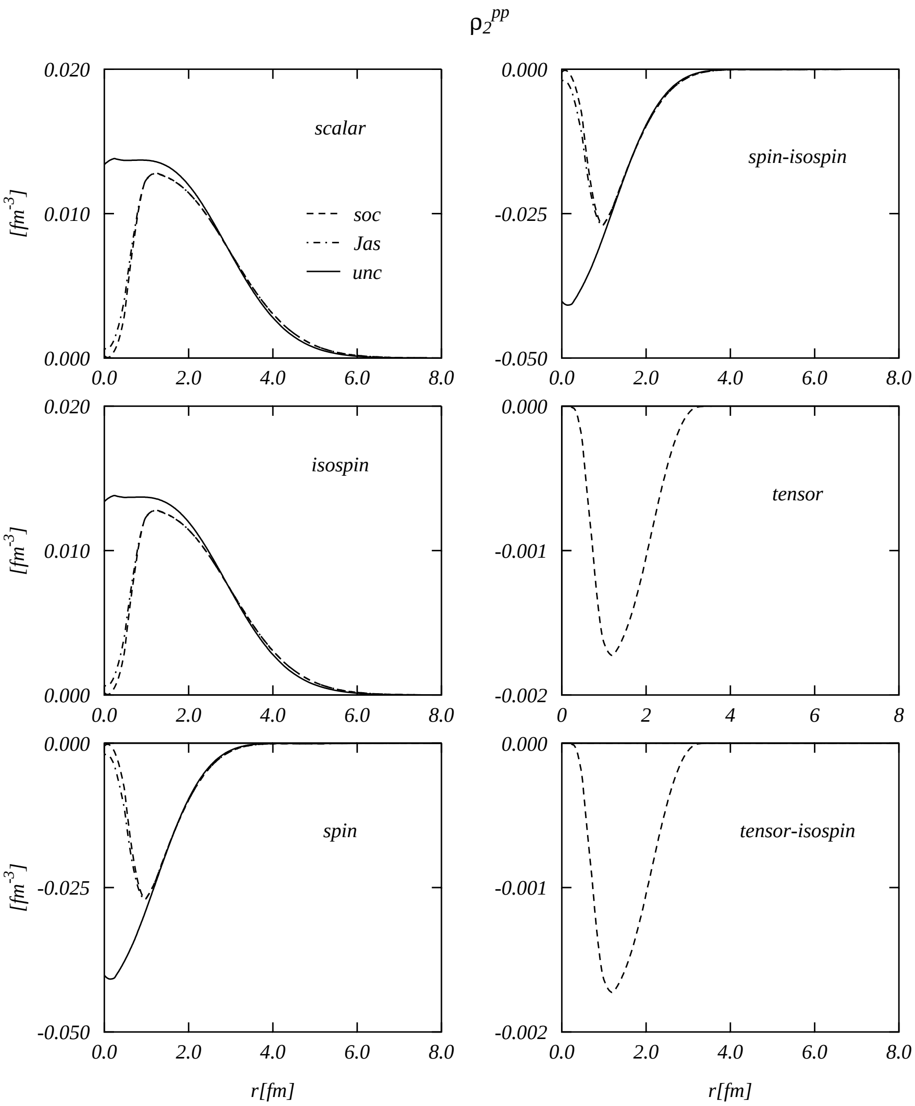

Figure 5.9: Two-body proton-proton distribution functions per channel for the ^{12}C.

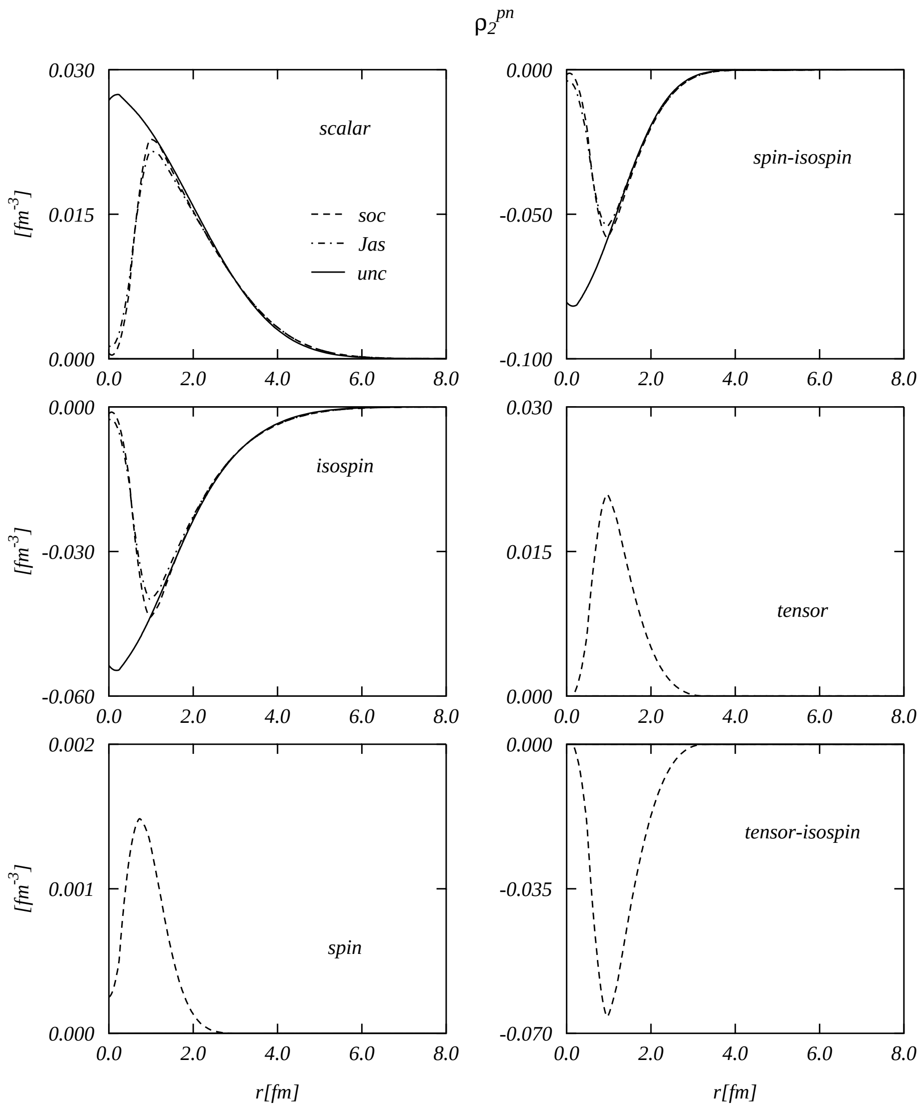

Figure 5.10: Two-body proton-neutron distribution functions per channel for the ^{12}C.

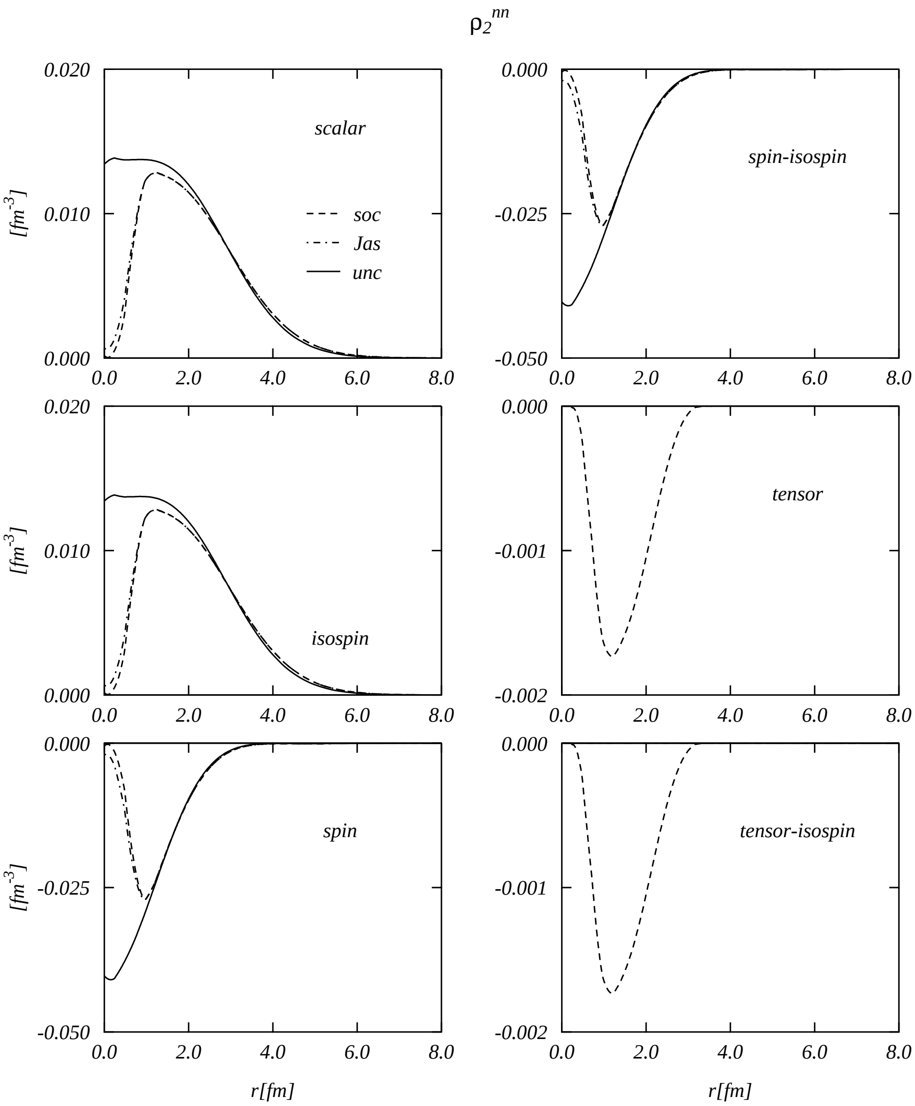

Figure 5.11: Two-body neutron-neutron distribution functions for the ^{12}C.

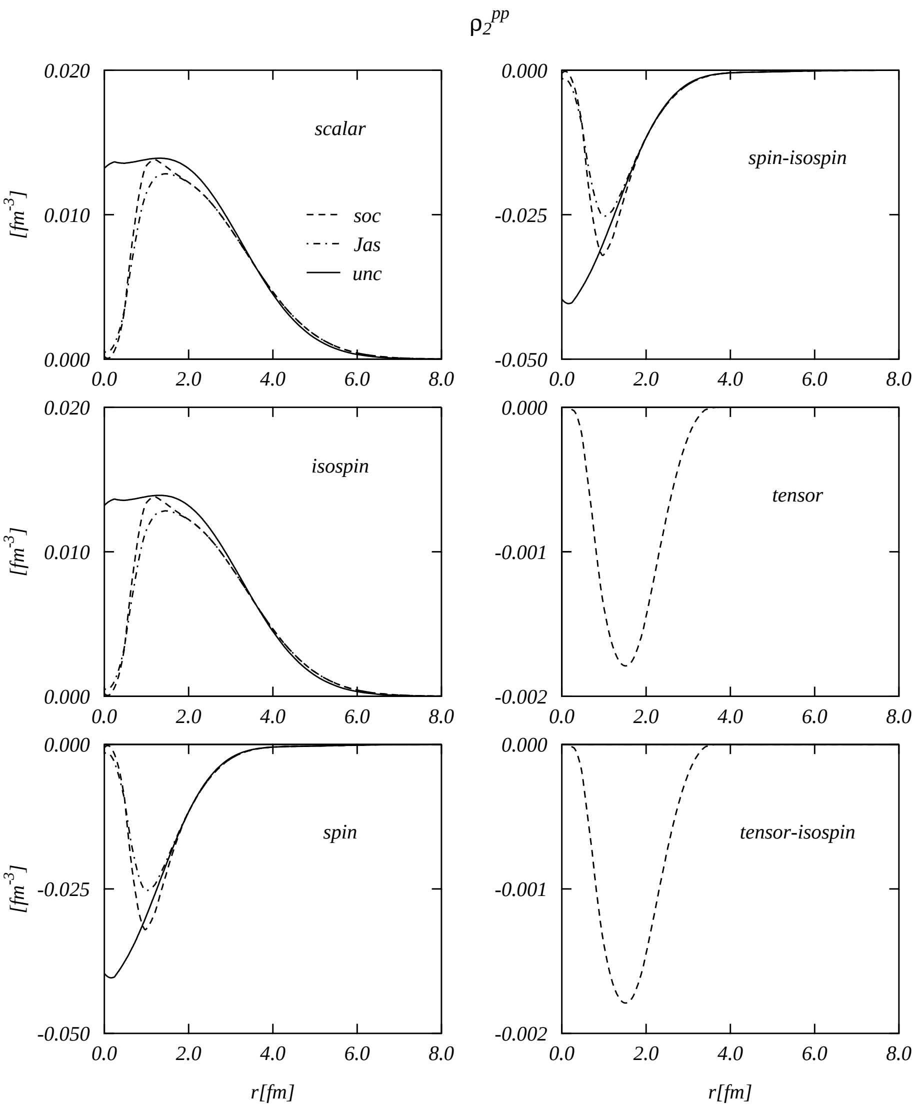

Figure 5.12: Two-body proton-proton distribution functions per channel for the ^{16}O.

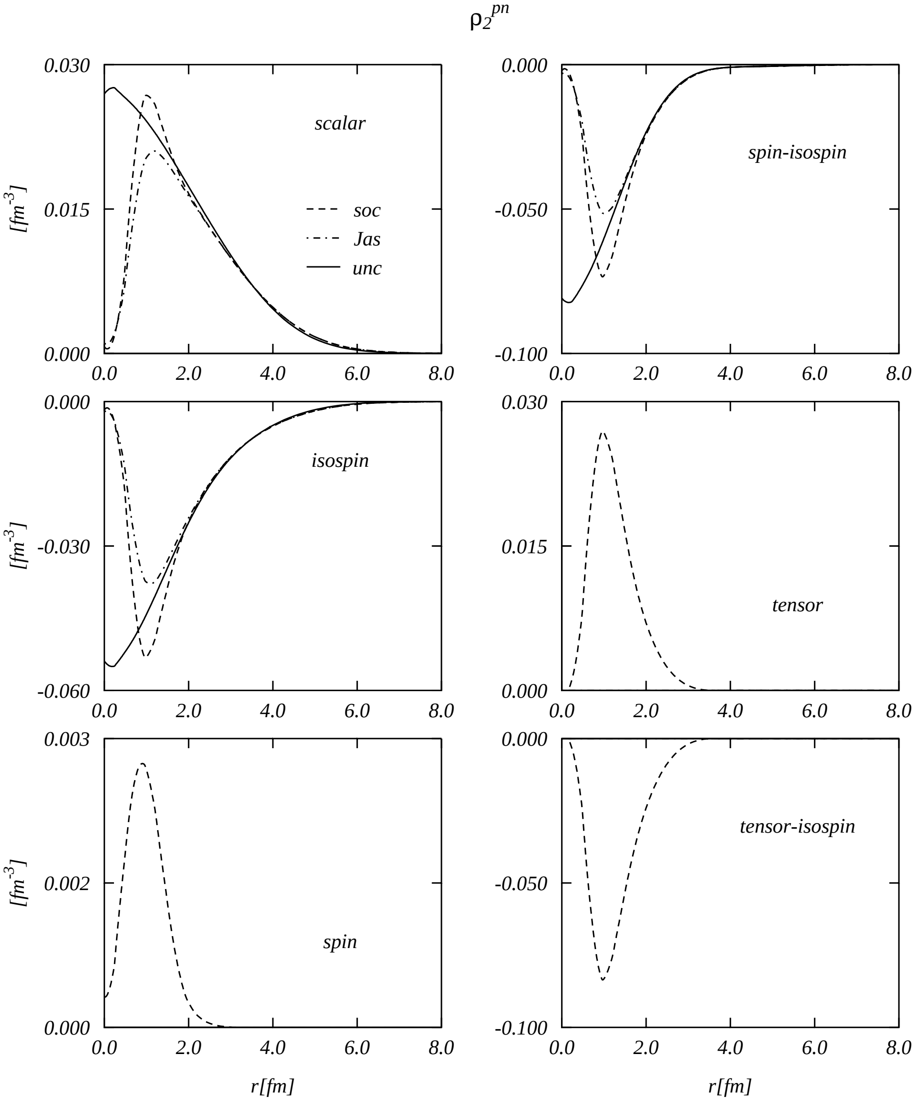

Figure 5.13: Two-body proton-neutron distribution functions per channel for the ^{16}O.

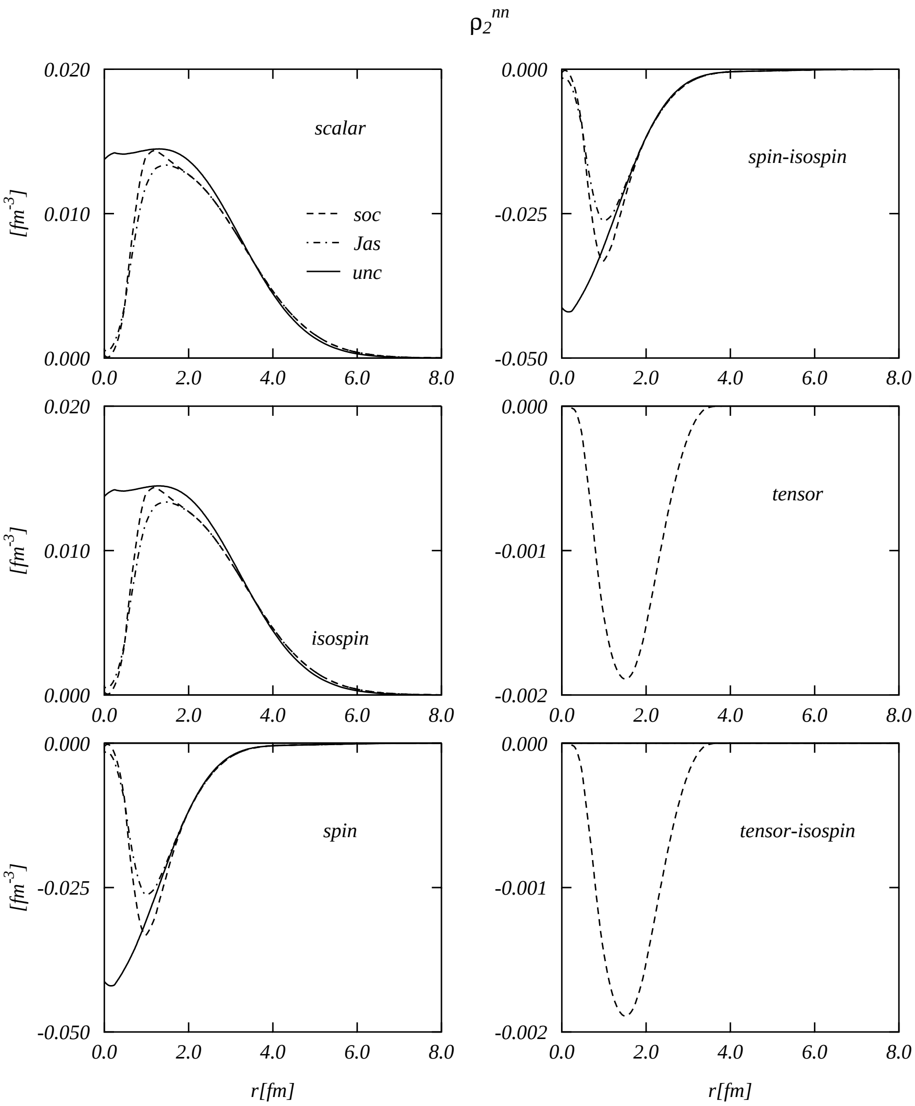

Figure 5.14: Two-body neutron-neutron distribution functions for the ^{16}O.

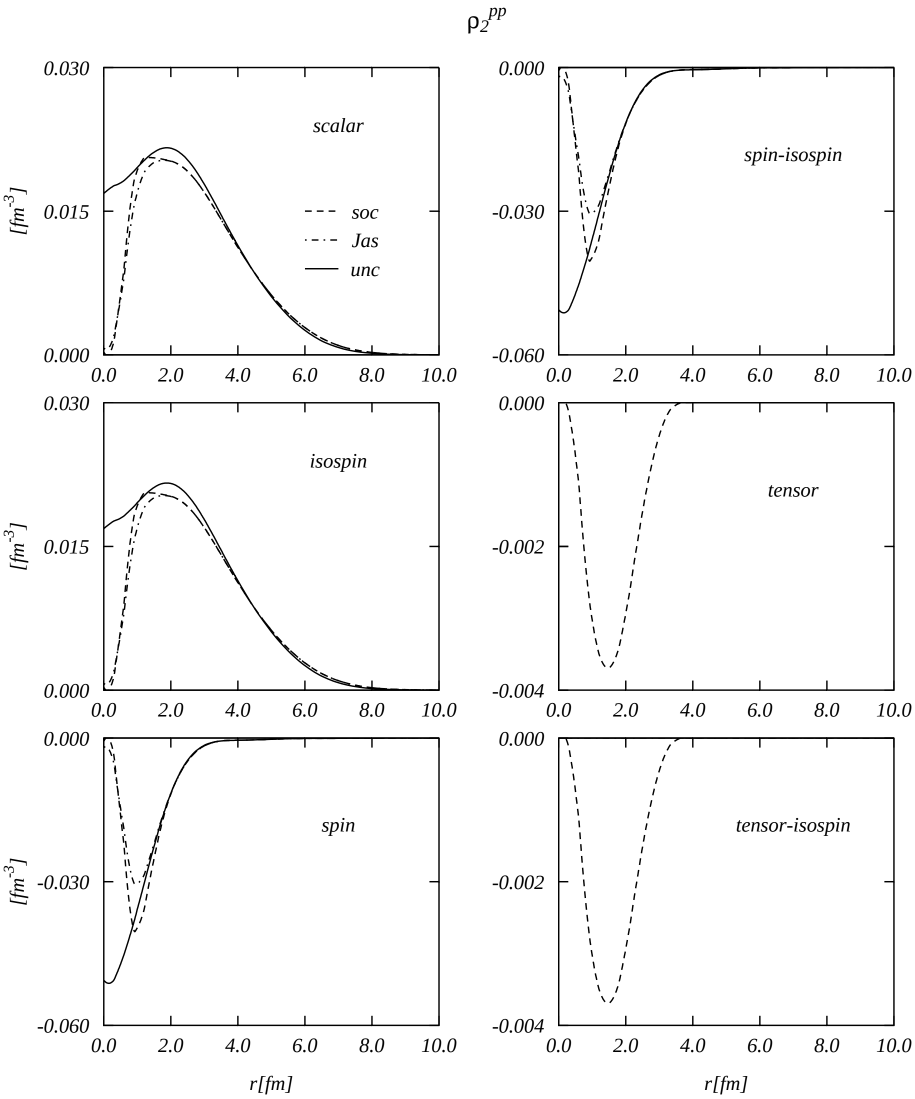

Figure 5.15: Two-body proton-proton distribution functions per channel for the ^{40}Ca.

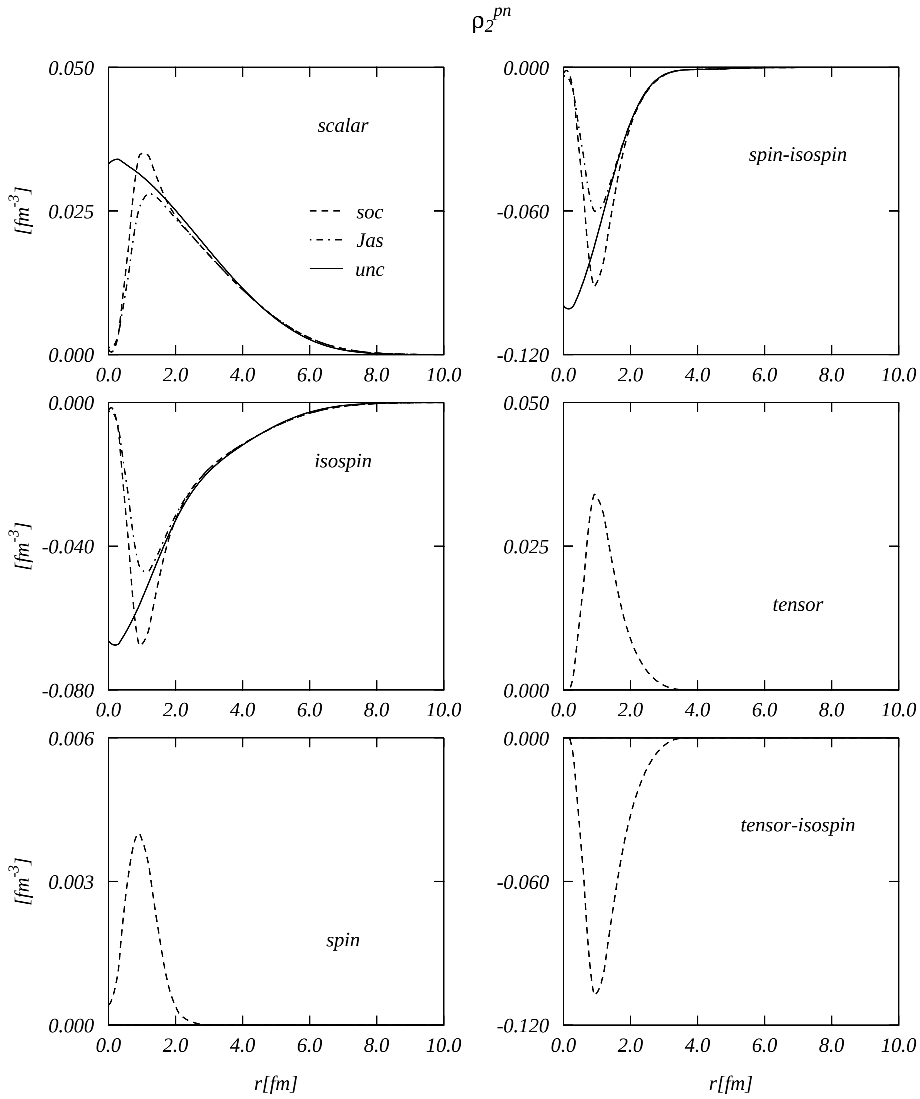

Figure 5.16: Two-body proton-neutron distribution functions per channel for the ^{40}Ca.

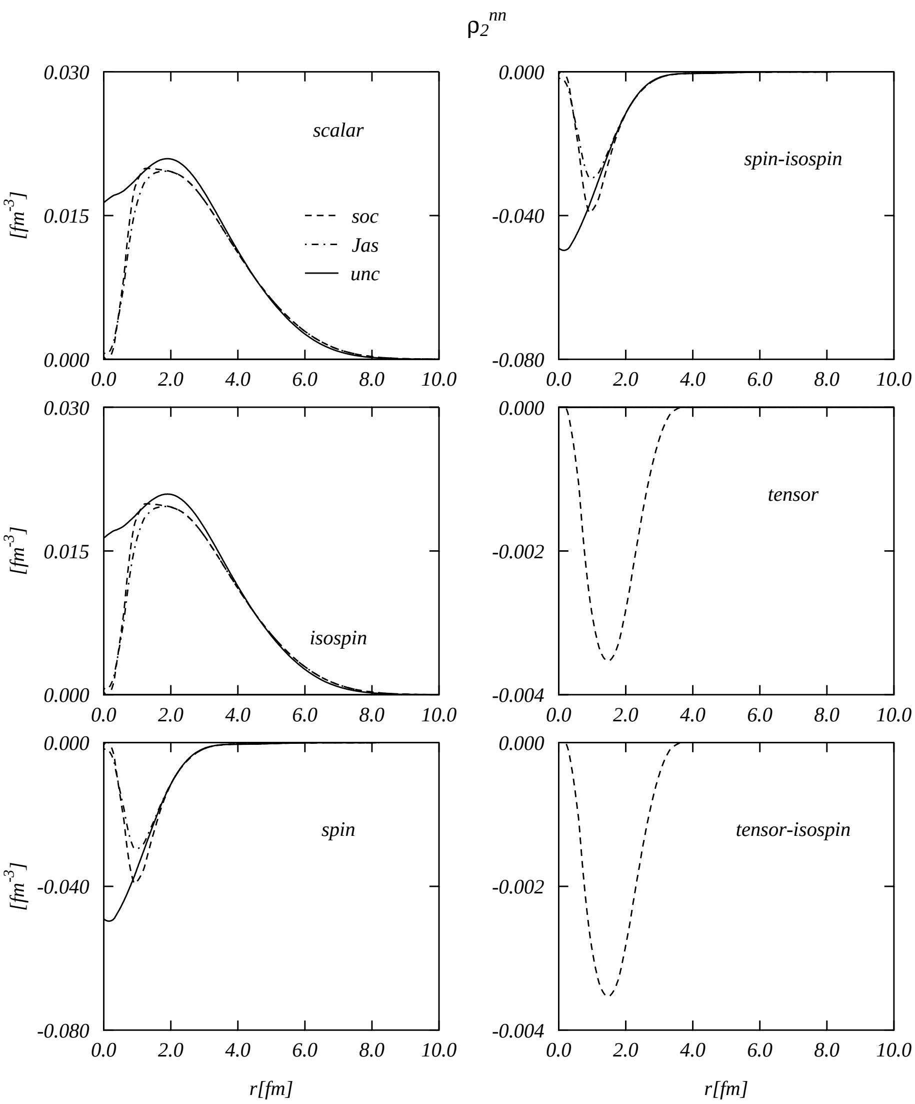

Figure 5.17: Two-body neutron-neutron distribution functions for the ^{40}Ca.

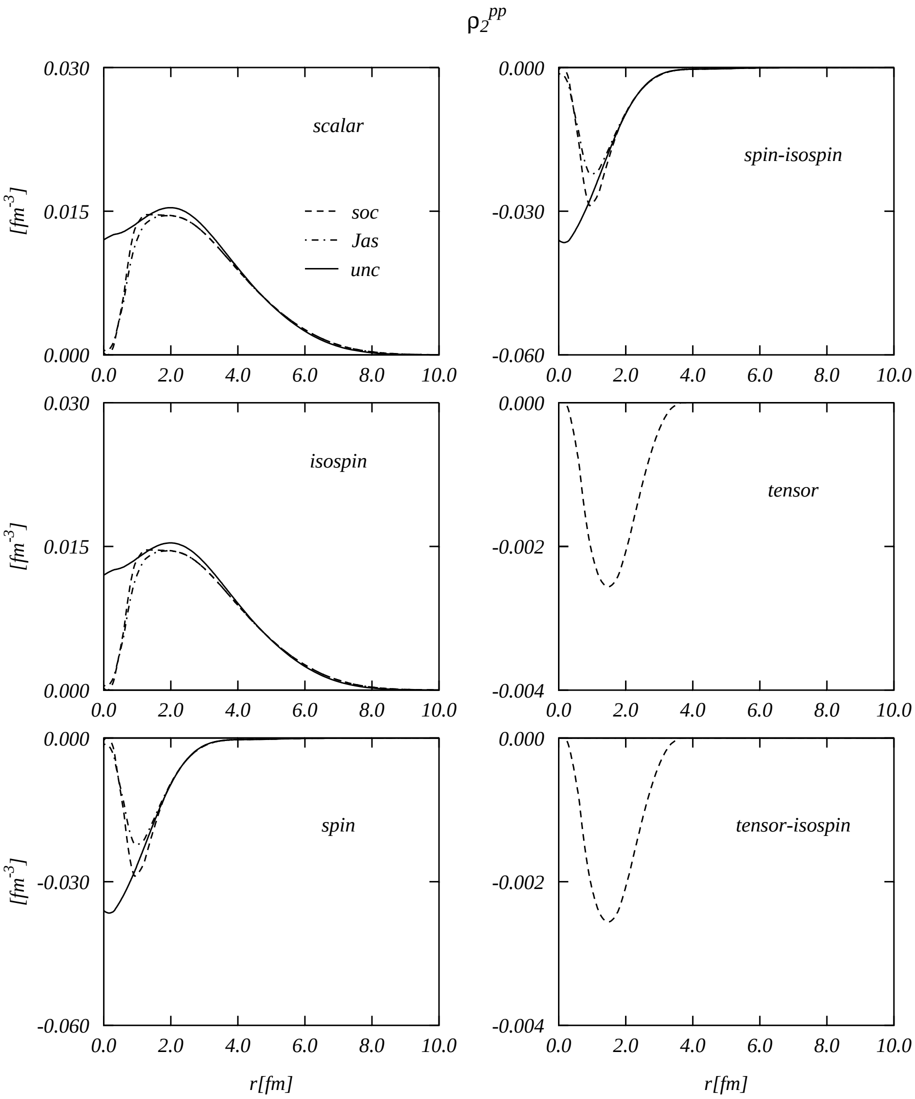

Figure 5.18: Two-body proton-proton distribution functions per channel for the ^{48}Ca.

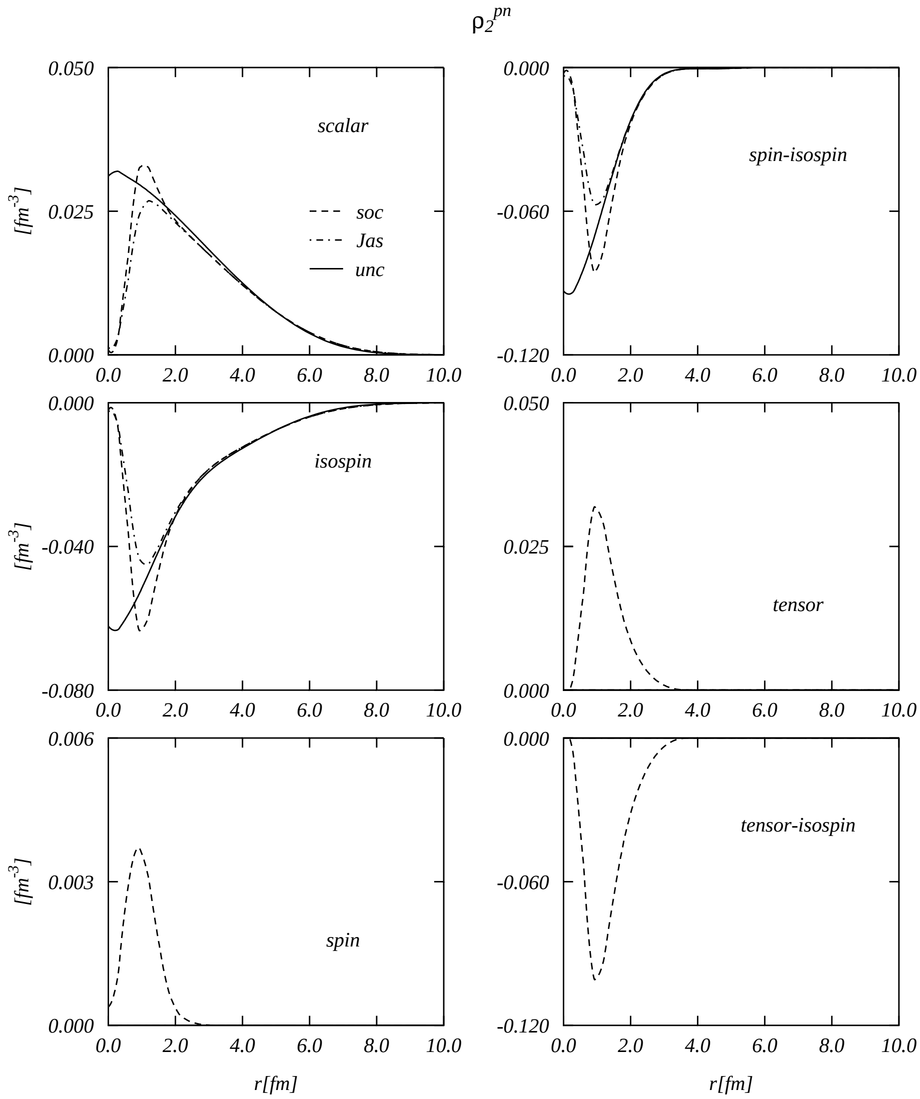

Figure 5.19: Two-body proton-neutron distribution functions per channel for the ^{48}Ca.

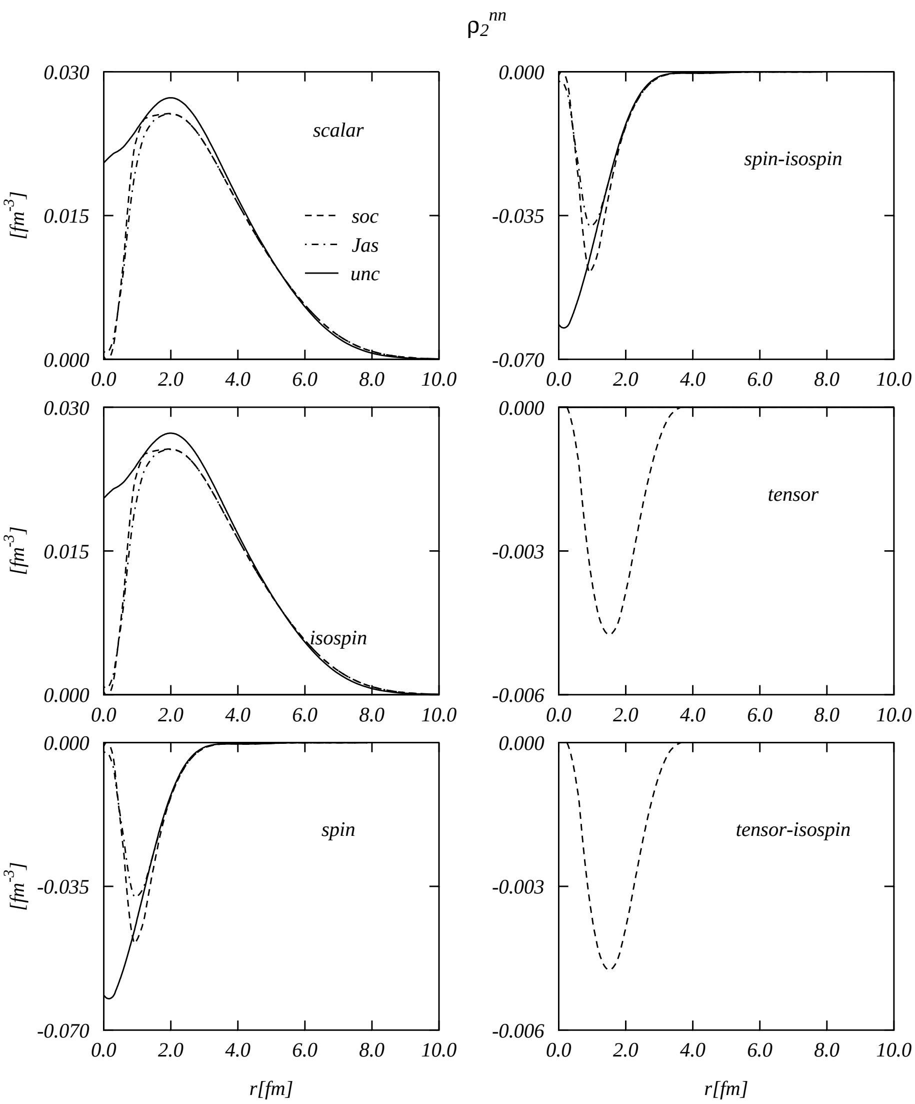

Figure 5.20: Two-body neutron-neutron distribution functions for the ^{48}Ca.

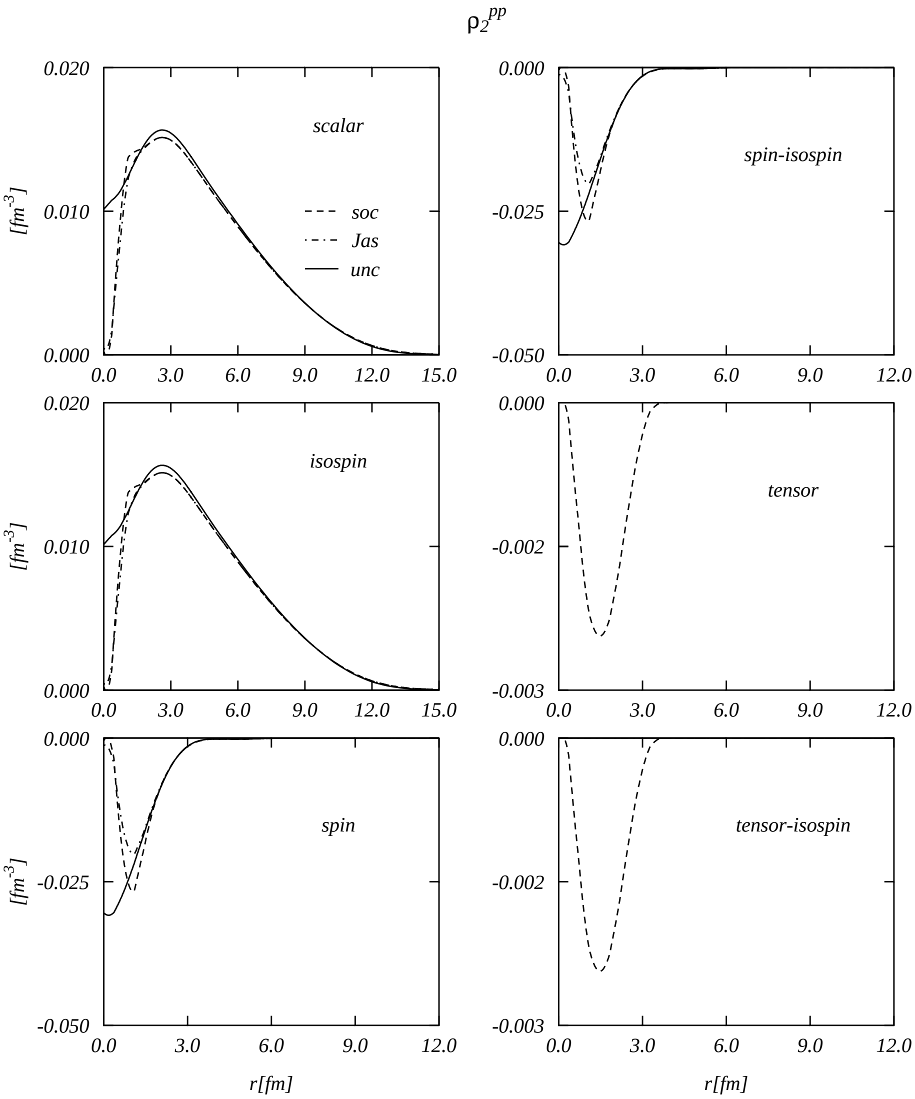

Figure 5.21: Two-body proton-proton distribution functions per channel for the ^{208}Pb.

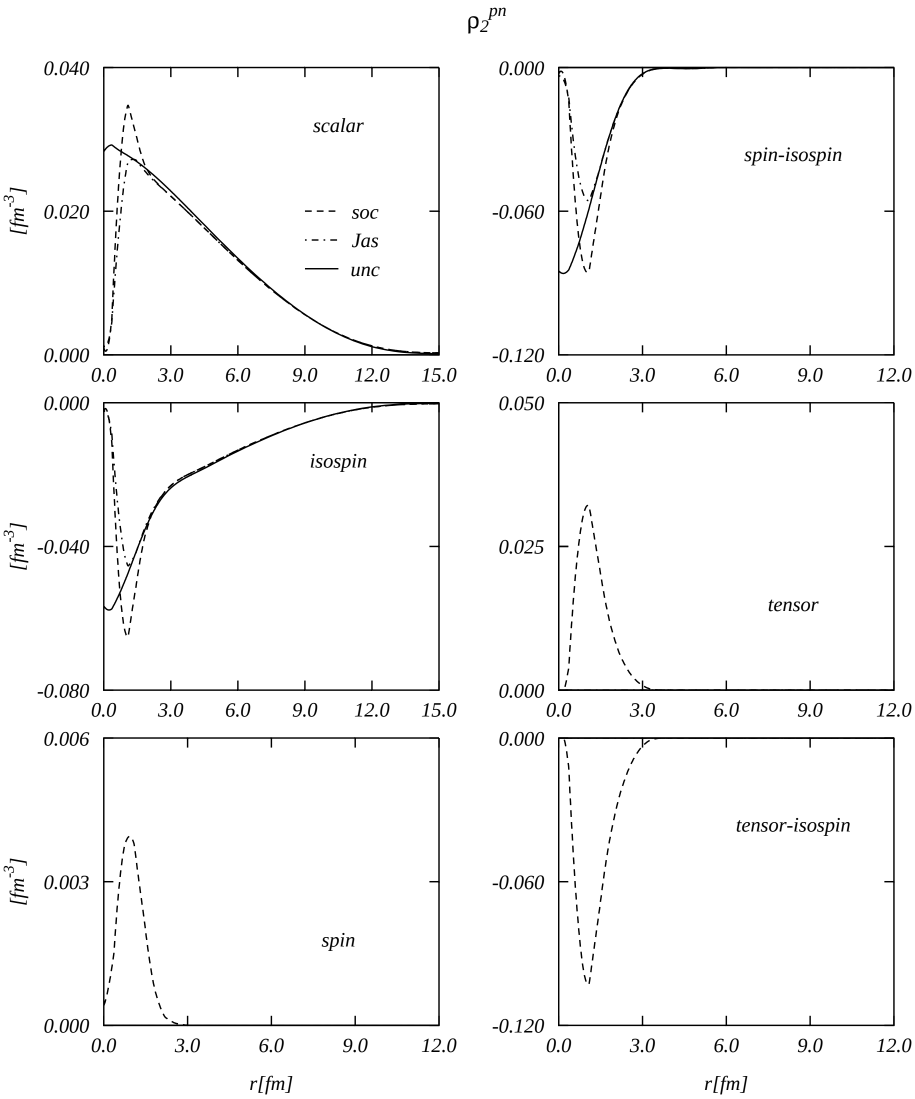

Figure 5.22: Two-body proton-neutron distribution functions per channel for the ^{208}Pb.

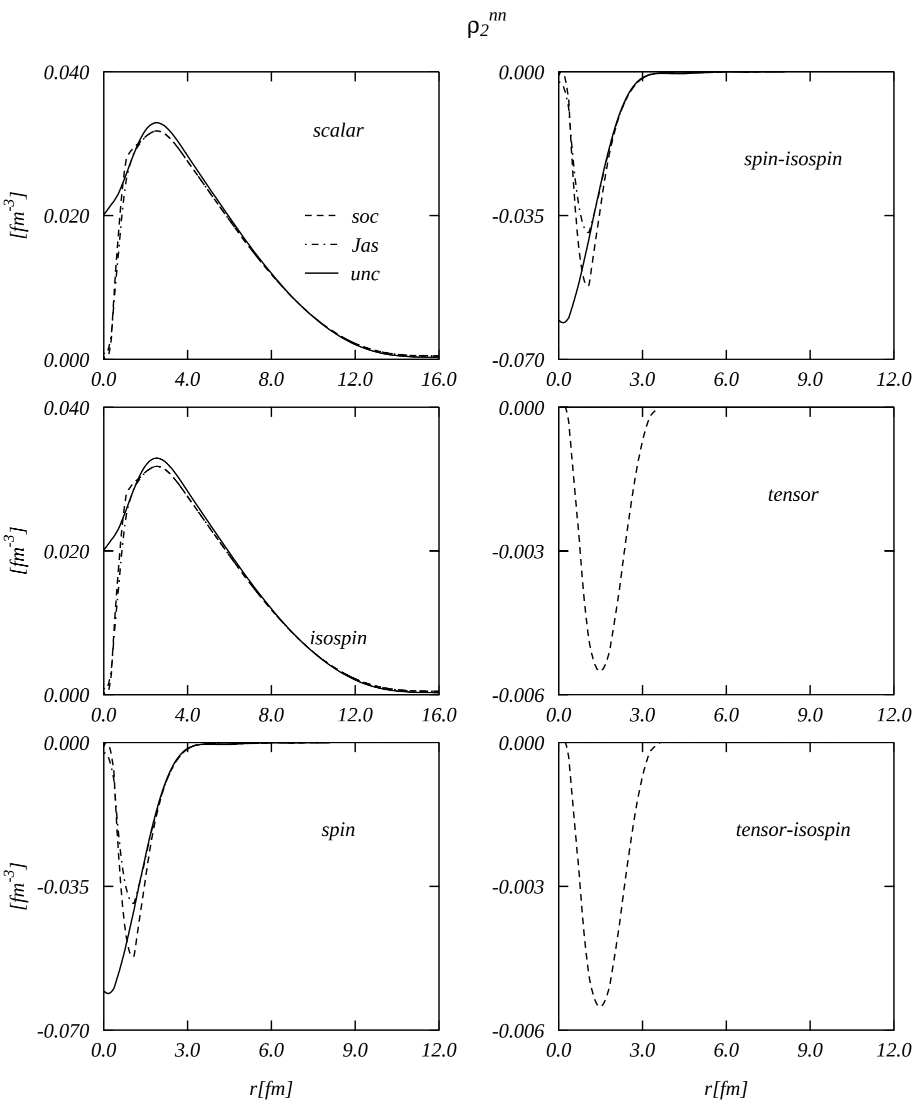

Figure 5.23: Two-body neutron-neutron distribution functions for the ^{208}Pb.

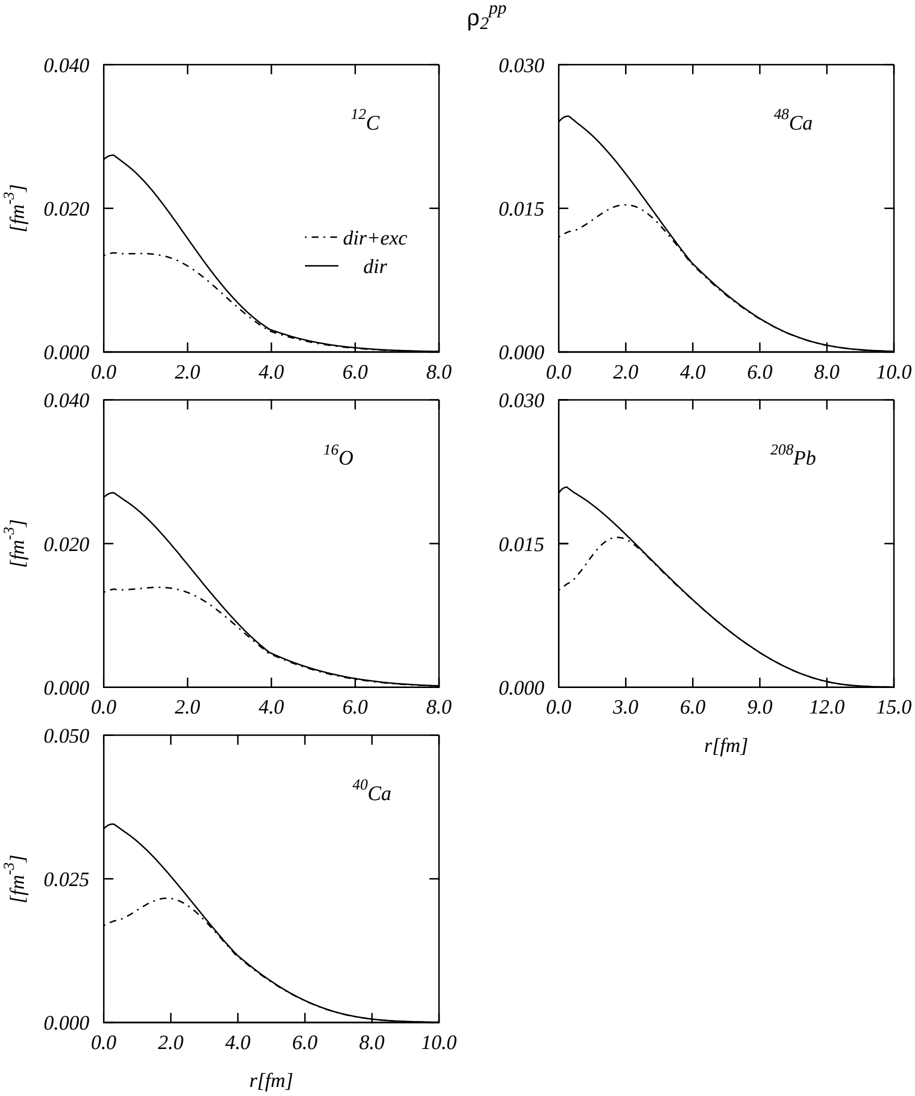

Figure 5.24: Direct and direct plus exchange proton-proton scalar uncorrelated TBDF for each nucleus. The adding of the exchange part drops the TBDF in the origin.

Chapter 6

Conclusions and perspectives

This thesis work can be considered the conclusive step of a project started more than ten years ago. The aim of this project was to extend the FHNC/SOC resummation technique in order to make a description of finite nuclear system whithin the CBF theory framework.

The situation of the project before this thesis work started was that the FHNC/SOC formalism was developed and applied to treat systems degenerated in spin and isospin variables. In this thesis we extended the formalism to treat nuclei with different number of protons and neutrons described by different sets of single particle wave functions. This breaks the isospin degeneracy. In addition to that we considered the set of single particle wave functions in a jj coupling scheme in order to reproduce the full set of magic numbers. In our study we have calculated binding energies and one- and two-body density distributions for the ^{12}C, ^{16}O, ^{40}Ca, ^{48}Ca, and ^{208}Pb nuclei.

Our investigation has been conducted with two-body interactions of Argonne and Urbana type, implemented with three-body interactions. Specifically, we used the Argonne v_8' interaction together with the Urbana UIX three-body force, and the Urbana v_{14} interaction implemented with the three-body $UVII$ force. These two sets of interactions have been fixed to reproduce the properties of the two-body systems and the ^3H binding energy. In addition we have done calculations also with the Urbana v_{14} implemented with the three-body Friedmann-Pandharipande interaction fixed to reproduce the nuclear matter saturation point.

The most important results of our study are shown in Tabs. 5.9-5.14 where the binding energies obtained with the various interactions are compared to the experimental values. Our results show an underbinding of about 3-4 MeV per nucleon with respect to the measured energies. This general trend is a common feature of all the nuclei we have considered but the ^{12}C which is barely bound. The ^{12}C anomaly is evident also by observing the correlations functions, which in the ^{12}C case heal at different distances with respect to those of the other nuclei.

The study of one-body distribution functions shows that the correlations do not considerably modify their shape. The effects of the correlations are more relevant at the center of the nucleus, where this produce a lowering of the uncorrelated densities. The effect is relatively large when only scalar correlations are used, and it is strongly reduced when the other terms of the correlations are included. These results are in agreement with the findings of [Ari97] where a simple first order expansion of the density has been used.

The correlations between two nucleons have been studied by investigating the operator dependent two-body densities. We have observed that the short-range correlations lower the probability of finding two nucleons very closed to each other. It has been quite surprising to observe that, while the scalar two-body densities extend on the full nuclear volume, the spin and tensor ones saturate at 3-f fm.

With this work, microscopic calculations for medium-heavy nuclei have reached the same degree of accuracy of nuclear matter calculations. In reality, in order to match these last type of calculations we should consider the p>8 terms of the two-body interaction and in the correlation. The contribution of these terms on the binding energy has been estimated in [Fab00], by means of a local density interpolation of the nuclear matter results, to be attractive and of the order of 1 MeV per nucleon. A further improvement of the FHNC/SOC computational scheme can be obtained by including three-body correlations. Also the contribution of the elementary diagrams, at least the lowest order ones, should be considered. An estimation of their contributions was done in [Co92].

Straightforward applications and extension of the formalism developed in this work are the evaluation of momentum distributions, natural orbits and quasi-particle wave functions. In a slightly longer term plan the formalism can be extended to describe hypernuclei, as in [Def98], and nuclei with a nucleon more, or less, the closed shell. It would be also interesting to extract from our formalism effective interactions to be used in effective theories such as Hartree-Fock or Random Phase Approximation.

A more ambitious project is to go beyond the Jastrow ansatz $|\Psi>= F|\Phi>$, and enlarge the space where to search for the minimum of the energy functional. This could be done by considering $|\Phi >$ not a single Slater determinant but a combination of them. The coefficients of this combination could be provided, for example, by the RPA. This could be a way of implementing long-range correlations in the CBF theory.

Finally, we should mention the possibility of using the FHNC/SOC computational scheme to study excited states, may be in a correlated RPA theory [Def98].

Chapter 7

Appendices

A.1 Cancellation of reducible diagrams in HNC

With reference to section 2.2, we show here an example of cancellation of a reducible diagram with two unlinked diagrams. Let consider a correlation of the type

$$f_K^2(r_{ij}) = [1 + Kh(r_{ij})] \tag{1}$$

where K is a costant. We define

$$< \mathcal{O}_{12} >_K = \frac{1}{2} \int dx_1 dx_2 g_K(x_1, x_2) O_{12}(x_1, x_2) \tag{2}$$

The expression of $g_K(x_1 x_2)$ is given by the eq. (2.9) with $f_K(r_{ij})$ instead of $f(r_{ij})$. Obviously it holds

$$< O_{12} > = < \mathcal{O}_{12} >_{K=1} \tag{3}$$

We write $g_K(x_1, x_2)$ up to linear terms in $h(r_{ij})$ we have

$$\begin{aligned} g_K(x_1, x_2) \;\; &= \;\; (1 - \frac{1}{A}) f^2(r_{12}) \Big(1 + \frac{2(A-2)}{A} \rho K \int dr_j h(r_{1j}) \\ &+ \frac{(A-2)(A-3)}{2A^2} \rho^2 K \int dr_i dr_j h(r_{ij}) + \cdots \Big) \cdot \\ &\Big(1 + \frac{A(A-1)}{2A^2} \rho^2 K \int dr_i dr_j h(r_{ij}) + \cdots \Big)^{-1} \end{aligned}$$

We make a Taylor's series expansion of $g_K(x_1, x_2)$ up to the first order in K. By considering then $K = 1$ we have

$$\begin{aligned} g_{K=1}(x_1, x_2) &= (1 - \frac{1}{A}) f^2(r_{12})(1 + \frac{2(A-2)}{A}\rho \int dr_j h(r_{1j}) + \\ & \frac{(A-2)(A-3)}{2A^2}\rho^2 \int dr_i dr_j h(r_{ij}) \\ & -\frac{A(A-1)}{2A^2}\rho^2 \int dr_i dr_j h(r_{ij}) + \cdots) \end{aligned}$$

The integral

$$\frac{2(A-2)}{A}\rho \int dr_j h(r_{1j}) = \frac{2(A-2)}{A}\rho \int dr_{1j} h(r_{1j})$$

can be considered as a special type of reducible diagram. On the other hand, the integrals

$$\begin{aligned} \frac{(A-2)(A-3)}{2A^2}\rho^2 \int dr_i dr_j h(r_{ij}) &= \frac{(A-2)(A-3)}{2A}\rho \int dr_{ij} h(r_{ij}) \\ -\frac{A(A-1)}{2A^2}\rho^2 \int dr_i dr_j h(r_{ij}) &= -\frac{A(A-1)}{2A}\rho \int dr_{ij} h(r_{ij}) \end{aligned}$$

are unlinked diagrams since the external points 1 and 2 are not involved in the integration. In the above equations we made use of the translational invariance of the system and the fact that

$$\rho \int dr_i dr_j = \frac{A}{V} \int dR_{ij} \int dr_{ij} = \frac{A}{V} V \int dr_{ij}$$

By summing the three terms we have

$$g_{K=1}(x_1, x_2) = (1 - \frac{1}{A}) f^2(r_{12})[1 - \frac{1}{A}\rho \int dr_{ij} h(r_{ij})] \tag{4}$$

and for $A \to \infty$ the contribution of all the terms linear in h vanishes. This example shows the basic mechanism used in [Fan79] to obtain a formal proof of the fact that unlinked and reducible diagrams cancel up to the $\frac{1}{A}$ order.

A.2 The calculation of the ξ functions

Th first equation (2.68) is a direct consequence of the Pauli identity and of the fact that the trace of linear terms in σ is zero.

$$\sum_{\sigma_j\tau_j}\int d\phi_j(\boldsymbol{\sigma}_i\cdot\boldsymbol{\sigma}_j)(\boldsymbol{\sigma}_j\cdot\boldsymbol{\sigma}_k) \;=\; \sum_{\tau_j}\int d\phi_j(\boldsymbol{\sigma}_i\cdot\boldsymbol{\sigma}_k)$$

Now we analyze the product $\boldsymbol{\sigma}_i\cdot\boldsymbol{\sigma}_j S_{kj}$. We have

$$\begin{aligned}
&\sum_{\sigma_j\tau_j}\int d\phi_j\boldsymbol{\sigma}_i\cdot\boldsymbol{\sigma}_j[3(\boldsymbol{\sigma}_k\hat{r}_{kj}\boldsymbol{\sigma}_j\hat{r}_{kj})-\boldsymbol{\sigma}_k\cdot\boldsymbol{\sigma}_j] \;=\\
&\sum_{\sigma_j\tau_j}\int d\phi_j\Big(3(\boldsymbol{\sigma}_k\cdot\hat{r}_{kj})[(\boldsymbol{\sigma}_i\cdot\hat{r}_{kj})+i\boldsymbol{\sigma}_j\cdot(\boldsymbol{\sigma}_i\times\hat{r}_{kj})]\\
&\qquad -[\boldsymbol{\sigma}_i\cdot\boldsymbol{\sigma}_k+i\boldsymbol{\sigma}_j\cdot(\boldsymbol{\sigma}_i\times\boldsymbol{\sigma}_k)]\Big) \;=\\
&\sum_{\tau_j}\int d\phi_j\Big(3(\boldsymbol{\sigma}_k\cdot\hat{r}_{kj})(\boldsymbol{\sigma}_i\cdot\hat{r}_{kj})-\boldsymbol{\sigma}_i\cdot\boldsymbol{\sigma}_k\Big)
\end{aligned}$$

If we choose

$$\begin{aligned}
\boldsymbol{r}_{ik} &= r_{ik}(0,0,1)\\
\boldsymbol{r}_{kj} &= r_{kj}(\sin\theta\sin\phi,\sin\theta\cos\phi,\cos\theta)\\
\boldsymbol{r}_{ij} &= (r_{kj}\sin\theta\sin\phi, r_{kj}\sin\theta\cos\phi, r_{kj}\cos\theta-r_{ik})=\boldsymbol{r}_{kj}-\boldsymbol{r}_{ik}
\end{aligned}$$

Then

$$\begin{aligned}
S_{ik} &= 2\sigma_{i,z}\sigma_{k,z}-\sigma_{i,x}\sigma_{k,x}-\sigma_{i,y}\sigma_{k,y}\\
\sigma_{i,x}\sigma_{k,x}+\sigma_{i,y}\sigma_{k,y} &= 2\sigma_{i,z}\sigma_{k,z}-S_{ik}=\frac{1}{3}(2\boldsymbol{\sigma}_i\cdot\boldsymbol{\sigma}_k-S_{ik})
\end{aligned}$$

and we have

$$\begin{aligned}
\int d\phi_j(\boldsymbol{\sigma}_k\cdot\hat{r}_{kj})(\boldsymbol{\sigma}_i\cdot\hat{r}_{kj}) &= \int d\phi_j[\sigma_{k,x}\sigma_{i,x}\sin^2\theta\sin^2\phi+\sigma_{k,x}\sigma_{i,y}\sin^2\theta\cos^2\phi\\
&\quad +\sigma_{k,z}\sigma_{i,z}\cos^2\theta\\
&= \frac{1}{2}(\sigma_{k,z}\sigma_{i,x}+\sigma_{k,y}\sigma_{i,y})\int d\phi_j(1-\cos^2\theta)\\
&\quad +\int d\phi_j\sigma_{k,z}\sigma_{i,z}\cos^2\theta\\
&= \frac{1}{6}(2\boldsymbol{\sigma}_i\cdot\boldsymbol{\sigma}_k-S_{ik})\int d\phi_j+\int d\phi_j[\sigma_{k,z}\sigma_{i,z}
\end{aligned}$$

$$
\begin{aligned}
& -\frac{(2\boldsymbol{\sigma}_i \cdot \boldsymbol{\sigma}_k - S_{ik})}{2}] \cos^2\theta \\
= & \frac{1}{6}(2\boldsymbol{\sigma}_i \cdot \boldsymbol{\sigma}_k - S_{ik}) \int d\phi_j + \frac{1}{2} S_{ik} \int d\phi_j \cos^2\theta \\
= & \frac{1}{6}(2\boldsymbol{\sigma}_i \cdot \boldsymbol{\sigma}_k - S_{ik}) \int d\phi_j + \frac{1}{2} S_{ik} \int d\phi_j (\hat{r}_{ik} \cdot \hat{r}_{kj})^2
\end{aligned}
$$

where we have used the fact that $\int_0^{2\pi} d\phi_j \cos^2\phi = \int_0^{2\pi} d\phi_j \sin^2\phi = \frac{1}{2}\int_0^{2\pi} d\phi_j$ and $\cos^2\theta = (\hat{r}_{ik} \cdot \hat{r}_{kj})^2$.

By using the above result we have

$$
\sum_{\tau_j} \int d\phi_j [3(\boldsymbol{\sigma}_k \cdot \hat{r}_{kj})(\boldsymbol{\sigma}_i \cdot \hat{r}_{kj}) - \boldsymbol{\sigma}_k \cdot \boldsymbol{\sigma}_i] = \sum_{\tau_j} \int d\phi_j \frac{1}{2} S_{ik} (3(\hat{r}_{ik} \cdot \hat{r}_{kj})^2 - 1) \tag{5}
$$

and

$$
\sum_{\tau_j} \int d\phi_j [3(\boldsymbol{\sigma}_k \cdot \hat{r}_{ij})(\boldsymbol{\sigma}_i \cdot \hat{r}_{ij}) - \boldsymbol{\sigma}_k \cdot \boldsymbol{\sigma}_i] = \sum_{\tau_j} \int d\phi_j \frac{1}{2} S_{ik} (3(\hat{r}_{ik} \cdot \hat{r}_{ij})^2 - 1) \tag{6}
$$

$$
\begin{aligned}
\sum_{\sigma_j \tau_j} \int d\phi_j S_{ij} S_{kj} = & \sum_{\tau_j} \int d\phi_j [9 \hat{r}_{ij} \cdot \hat{r}_{kj} (\boldsymbol{\sigma}_i \cdot \hat{r}_{ij})(\boldsymbol{\sigma}_k \cdot \hat{r}_{kj}) \\
& -3(\boldsymbol{\sigma}_i \cdot \hat{r}_{ij})(\boldsymbol{\sigma}_k \cdot \hat{r}_{ij}) \\
& -3(\boldsymbol{\sigma}_i \cdot \hat{r}_{kj})(\boldsymbol{\sigma}_k \cdot \hat{r}_{kj}) - \boldsymbol{\sigma}_i \cdot \boldsymbol{\sigma}_k]
\end{aligned} \tag{7}
$$

$$
\begin{aligned}
\int d\phi_j (\boldsymbol{\sigma}_i \cdot \hat{r}_{ij})(\boldsymbol{\sigma}_k \cdot \hat{r}_{kj}) = & (\sigma_{i,x}\sigma_{k,x} + \sigma_{i,y}\sigma_{k,y}) \frac{1}{2} \int d\phi_j \frac{1}{r_{kj}} [1 - (\hat{r}_{ik} \cdot \hat{r}_{kj})^2] \\
& + \int d\phi_j \frac{1}{r_{kj}} \sigma_{i,z}\sigma_{k,z} (\hat{r}_{ij} \cdot \hat{r}_{ik})(\hat{r}_{ij} \cdot \hat{r}_{kj})
\end{aligned}
$$

Then

$$
\begin{aligned}
\int d\phi_j (\hat{r}_{ij} \cdot \hat{r}_{ij})(\boldsymbol{\sigma}_i \cdot \hat{r}_{ij})(\boldsymbol{\sigma}_k \cdot \hat{r}_{kj}) = & \frac{1}{6}(2\boldsymbol{\sigma}_i \cdot \boldsymbol{\sigma}_k - S_{ik}) \int d\phi_j \frac{1}{r_{kj}} (\hat{r}_{ij} \cdot \hat{r}_{kj})^2 \\
& + \frac{1}{2} S_{ik} \int d\phi_j (\hat{r}_{ij} \cdot \hat{r}_{kj})(\hat{r}_{ij} \cdot \hat{r}_{ik})(\hat{r}_{kj} \cdot \hat{r}_{ik})
\end{aligned}
$$

and finally

$$
\sum_{\tau_j} \int d\phi_j S_{ij} S_{kj} = \boldsymbol{\sigma}_i \cdot \boldsymbol{\sigma}_k \sum_{\tau_j} \int d\phi_j [3(\hat{r}_{ij} \cdot \hat{r}_{kj})^2 - 1]
$$

$$+\sum_{\tau_j}\int d\phi_j \frac{1}{2} S_{ik}[9(\hat{r}_{ij}\cdot\hat{r}_{ik}\hat{r}_{ik}\cdot\hat{r}_{kj}\hat{r}_{kj}\cdot\hat{r}_{ij})$$

$$-3(\hat{r}_{ij}\cdot\hat{r}_{kj})^2 - 3(\hat{r}_{ij}\cdot\hat{r}_{ik})^2 - 3(\hat{r}_{kj}\cdot\hat{r}_{ik})^2 + 2] \qquad (8)$$

A.3

A.3.1 The K^{pqr} and L^{pqr} matrices

K^{pqr}

	p \ q	1	2	3	4	5	6		1	2	3	4	5	6
r=1	1	1	0	0	0	0	0	r=2	0	1	0	0	0	0
	2	0	3	0	0	0	0		1	-2	0	0	0	0
	3	0	0	3	0	0	0		0	0	0	3	0	0
	4	0	0	0	9	0	0		0	0	3	-6	0	0
	5	0	0	0	0	6	0		0	0	0	0	2	0
	6	0	0	0	0	0	18		0	0	0	0	0	6
r=3	1	0	0	1	0	0	0	r=4	0	0	0	1	0	0
	2	0	0	0	3	0	0		0	0	1	-2	0	0
	3	1	0	-2	0	0	0		0	1	0	-2	0	0
	4	0	3	0	-6	0	0		1	-2	-2	4	0	0
	5	0	0	0	0	0	6		0	0	0	0	0	2
	6	0	0	0	0	6	-12		0	0	0	0	2	-4
r=5	1	0	0	0	0	1	0	r=6	0	0	0	0	0	1
	2	0	0	0	0	1	0		0	0	0	0	0	1
	3	0	0	0	0	0	3		0	0	0	0	1	-2
	4	0	0	0	0	0	3		0	0	0	0	1	-2
	5	1	1	0	0	-2	0		0	0	1	1	0	-2
	6	0	0	3	3	0	-6		1	1	-2	-2	-2	4

L^{pqr}

	p \ q	1	2	3	4	5	6		1	2	3	4	5	6
r=1	1	1	0	0	0	0	0	r=2	0	3	0	0	0	0
	2	0	3	0	0	0	0		3	6	0	0	0	0
	3	0	0	3	0	0	0		0	0	0	9	0	0
	4	0	0	0	9	0	0		0	0	9	18	0	0
	5	0	0	0	0	6	0		0	0	0	0	-6	0
	6	0	0	0	0	0	18		0	0	0	0	0	-18
r=3	1	0	0	0	3	0	0	r=4	0	0	0	9	0	0
	2	0	0	0	0	9	0		0	0	9	18	0	0
	3	3	0	6	0	0	0		0	9	0	18	0	0
	4	0	9	0	18	0	0		9	18	18	36	0	0
	5	0	0	0	0	0	18		0	0	0	0	0	-18
	6	0	0	0	0	18	36		0	0	0	0	-18	-36
r=5	1	0	0	0	0	6	0	r=6	0	0	0	0	0	18
	2	0	0	0	0	-6	0		0	0	0	0	0	-18
	3	0	0	0	0	0	18		0	0	0	0	18	36
	4	0	0	0	0	0	-18		0	0	0	0	-18	-36
	5	6	-6	0	0	12	0		0	0	18	-18	0	36
	6	0	0	18	-18	0	36		18	-18	36	-36	36	72

A.3.2 The $I^{k_1k_2k_3}$ and $J^{k_1k_2k_3}$ matrices

$$I^{k_1k_21} = \begin{pmatrix} 1 & 0 & 0 \\ 0 & 3 & 0 \\ 0 & 0 & 6 \end{pmatrix} \quad I^{k_1k_22} = \begin{pmatrix} 0 & 1 & 0 \\ 1 & -2 & 0 \\ 0 & 0 & 2 \end{pmatrix} \quad I^{k_1k_23} = \begin{pmatrix} 0 & 0 & 1 \\ 0 & 0 & 1 \\ 1 & 1 & -2 \end{pmatrix} \quad (9)$$

$$J^{k_1k_21} = \begin{pmatrix} 1 & 0 & 0 \\ 0 & 3 & 0 \\ 0 & 0 & 6 \end{pmatrix} \quad J^{k_1k_22} = \begin{pmatrix} 0 & 3 & 0 \\ 3 & 6 & 0 \\ 0 & 0 & -6 \end{pmatrix} \quad J^{k_1k_23} = \begin{pmatrix} 0 & 0 & 6 \\ 0 & 0 & -6 \\ 6 & -6 & 12 \end{pmatrix} \quad (10)$$

A.4 The Jackson-Feenberg expression of the kinetic energy

The kinetic energy operator is:

$$\hat{T} = -\frac{\hbar^2}{2m}\sum_{i=1}^{A}\nabla_i^2 \quad (11)$$

Then the expectation value of $\hat{T}$ is:

$$< T >= \frac{< \Psi|\hat{T}|\Psi >}{< \Psi|\Psi >} \quad (12)$$

If $\Psi = F(1,...,A)\Phi(\mathbf{x}_1,...,\mathbf{x}_A)$ we get:

$$< T >= \frac{< \Phi F| -\frac{\hbar^2}{2m}\sum_{i=1}^{A}\nabla_i^2|F\Phi >}{< \Phi F|F\Phi >} \quad (13)$$

F is the correlation function and Φ the uncorrelated wave function of the system. Expanding the above expression:

$$< T >= -\frac{\hbar^2}{2m}\frac{1}{\mathcal{N}}\sum_{i=1}^{A}\int d\mathbf{x}_1....d\mathbf{x}_A\Phi^*(\mathbf{x}_1,...,\mathbf{x}_A)F\nabla_i^2[F\Phi(\mathbf{x}_1,...,\mathbf{x}_A)]$$

with $\mathcal{N} =< \Psi|\Psi >$. Now

$$\nabla_i^2(F\Phi) \quad = \quad \nabla_i\nabla_i(F\Phi) = \nabla_i[(\nabla_iF)\Phi + F(\nabla_i\Phi)]$$

$$= (\nabla_i^2 F)\Phi + 2(\nabla_i F)\cdot(\nabla_i \Phi) + F\nabla_i^2\Phi$$

then

$$< T >= -\frac{\hbar^2}{2m}\frac{1}{\mathcal{N}}\sum_{i=1}^{A}\int d\mathbf{x}_1...d\mathbf{x}_A[\Phi^* F(\nabla_i^2 F)\Phi + 2\Phi^* F(\nabla_i F)\cdot(\nabla_i\Phi) + \Phi^* F^2\nabla_i^2\Phi] \quad (14)$$

Integrating by parts the term $2\Phi^* F(\nabla_i F)(\nabla_i\Phi)$ we get:

$$\begin{aligned} 2\int \Phi^* F(\nabla_i F)(\nabla_i \Phi) d\mathbf{x}_1, ..., d\mathbf{x}_A &= 2\int' d\mathbf{x}_1, ..., d\mathbf{x}_A \Phi^* F(\nabla_i F)\Phi]_{x_i}^{x_i'} \\ &- 2\int d\mathbf{x}_1, ..., d\mathbf{x}_A \nabla_i(\Phi^* F(\nabla_i F)\Phi \\ &= 0 - 2\int d\mathbf{x}_1, ..., d\mathbf{x}_A[(\nabla_i\Phi^*)F(\nabla_i F)\Phi \\ &+ \Phi^*(\nabla_i F)\Phi + \Phi^*(\nabla_i F)^2\Phi + \Phi^* F(\nabla_i^2 F)\Phi] \end{aligned}$$

where we supposed that the following property holds:

$$\Phi(\mathbf{x}_1, ..., x_i, ...\mathbf{x}_A) - \Phi(\mathbf{x}_1, ..., x_i', ..., \mathbf{x}_A) = 0 \qquad \textit{Periodic condition}$$

The (14) becames:

$$\begin{aligned} < T > &= -\frac{\hbar^2}{2m}\frac{1}{\mathcal{N}}\sum_{i=1}^{A}\int d\mathbf{x}_1, d\mathbf{x}_2, ..., d\mathbf{x}_A[\Phi^* F^2\nabla_i^2\Phi \\ &- \Phi^* F(\nabla_i^2)\Phi - 2(\nabla_i\Phi^*)F(\nabla_i F)\Phi - 2\Phi^*(\nabla_i F)^2\Phi] \end{aligned} \quad (15)$$

We note that:

$$\begin{aligned} \nabla_i(\Phi^* F(\nabla_i F)\Phi) &= (\nabla_i\Phi^*)F(\nabla_i F)\Phi + \Phi^*(\nabla_i F)^2\Phi + \\ & \Phi^* F(\nabla_i^2 F)\Phi + \Phi^* F(\nabla_i F)(\nabla_i\Phi) \end{aligned}$$

then

$$\begin{aligned} < T > &= -\frac{\hbar^2}{2m}\frac{1}{\mathcal{N}}\sum_{i=1}^{A}\int d\mathbf{x}_1...d\mathbf{x}_A[\Phi^* F^2\nabla_i^2\Phi \\ &+ (\nabla_i\Phi^*)F(\nabla_i F)\Phi + \Phi^*(\nabla_i F)^2\Phi + \Phi^* F(\nabla_i F)(\nabla_i\Phi) \\ &- \nabla_i(\Phi^* F(\nabla_i F)\Phi) - 2(\nabla_i\Phi^*)F(\nabla_i F)\Phi - 2\Phi^*(\nabla_i F)^2\Phi] \\ &= -\frac{\hbar^2}{2m}\frac{1}{\mathcal{N}}\sum_{i=1}^{A}\int d\mathbf{x}_1, d\mathbf{x}_2, ..., d\mathbf{x}_A[\Phi^* F^2\nabla_i^2\Phi \\ &- (\nabla_i\Phi^*)F(\nabla_i F)\Phi - \Phi^*(\nabla_i F)^2\Phi + \Phi^* F(\nabla_i F)(\nabla_i\Phi) \end{aligned}$$

$$- \quad \nabla_i(\Phi^* F(\nabla_i F)\Phi)] \tag{16}$$

We see that:

$$\begin{aligned}
\int d\mathbf{x}_1...d\mathbf{x}_A \nabla_i(\Phi^* F(\nabla_i F)\Phi) &= 0 \\
(\textit{divergence theorem and periodic condition}) & \\
F\nabla_i F &= \frac{1}{2}\nabla_i F^2 \\
\int d\mathbf{x}_1, d\mathbf{x}_2, ..., d\mathbf{x}_A[-(\nabla_i\Phi^*)F(\nabla_i F)\Phi + \Phi^* F(\nabla_i F)(\nabla_i \Phi)] &= \\
\int d\mathbf{x}_1, d\mathbf{x}_2, ..., d\mathbf{x}_A \frac{1}{2}[-(\nabla_i\Phi^*)\Phi + \Phi^*(\nabla_i\Phi)]\nabla_i F^2 &= 0
\end{aligned}$$

then

$$< T >= -\frac{\hbar^2}{2m}\frac{1}{\mathcal{N}}\sum_{i=1}^{A}\int d\mathbf{x}_1, d\mathbf{x}_2, ..., d\mathbf{x}_A[\Phi^* F^2 \nabla_i^2 \Phi - \Phi^*(\nabla_i F)^2\Phi] \tag{17}$$

The equation (14) and (17) are called Pandharipande-Bethe and Clark-Westhaus energy respectively. Now we calculate the Jackson-Feenberg expression of the energy. We consider the Jackson-Feenberg identity [Jac61]:

$$\int d\mathbf{r}_1, ..., d\mathbf{r}_A \Psi^* \nabla^2 \Psi = \frac{1}{2}\int d\mathbf{r}_1, ..., d\mathbf{r}_A[\Psi^*\nabla^2\Psi + (\nabla^2\Psi^*)\Psi - 2(\nabla\Psi^*)(\nabla\Psi)] \tag{18}$$

$$\begin{aligned}
\Psi^*\nabla^2\Psi &= \Phi^* F \nabla^2(\Phi F) = \Phi^* F \nabla\nabla(F\Phi) \\
&= \Phi^* F(\nabla^2 F)\Phi + \Phi^* F\nabla F\nabla\Phi + \Phi^* F\nabla F\nabla\Phi + \Phi^* F^2\nabla^2\Phi \\
(\nabla^2\Psi^*)\Psi &= \nabla^2(F\Phi^*)F\Phi \\
&= \Phi^* F(\nabla^2 F)\Phi + \nabla\Phi^* F(\nabla F)\Phi + \nabla\Phi^* F(\nabla F)\Phi + (\nabla^2\Phi^*)F^2\Phi \\
-2(\nabla\Psi^*)(\nabla\Psi) &= -2[\nabla(F\Phi^*)][\nabla(F\Phi)] \\
&= -2[\phi^*(\nabla F)^2\Phi + \Phi^* F\nabla F\nabla\Phi + \nabla\Phi^* F(\nabla F)\Phi + \nabla\Phi^* F^2\nabla\Phi]
\end{aligned}$$

The we can write the right side of eq.(18) in this form:

$$\begin{aligned}
\int d\mathbf{r}_1, ..., d\mathbf{r}_A[\frac{1}{4}\Phi^* F(\nabla^2 F)\Phi + \frac{1}{2}\Phi^* F(\nabla F)\nabla\Phi + \frac{1}{4}\Phi^* F^2\nabla^2\Phi \\
+\frac{1}{4}\Phi^* F(\nabla^2 F)\Phi + \frac{1}{2}\nabla\Phi^* F(\nabla F)\Phi + \frac{1}{4}(\nabla^2\Phi^*)F^2\Phi \\
-\frac{1}{2}\Phi^*(\nabla F)^2\Phi - \frac{1}{2}\Phi^* F(\nabla F)\nabla\Phi - \frac{1}{2}\nabla\Phi^* F(\nabla F)\Phi - \frac{1}{2}\nabla\Phi^* F^2\nabla\Phi]
\end{aligned}$$

Simplifying we get:

$$
\begin{aligned}
< T > &= \int d\mathbf{r}_1, ..., d\mathbf{r}_A [\frac{1}{2}\Phi^* F(\nabla^2 f)\Phi + \frac{1}{4}\Phi^* F^2 \nabla^2 \Phi \\
&+ \frac{1}{4}(\nabla^2\Phi^*)F^2\Phi - \frac{1}{2}\Phi^*(\nabla F)^2\Phi - \frac{1}{2}\nabla\Phi^* F^2 \nabla\Phi]
\end{aligned}
$$

and by using the identity:

$$
\nabla\Phi^*\nabla\Phi = \frac{1}{2}[\nabla^2(\Phi^*\Phi) - \Phi^*\nabla^2\Phi - (\nabla^2\Phi^*)\Phi]
$$

we get:

$$
\begin{aligned}
< T > &= \int d\mathbf{r}_1, ..., d\mathbf{r}_A [-\frac{1}{4}F^2\nabla^2(\Phi^*\Phi) + \frac{1}{2}[\Phi^*\nabla^2\Phi + (\nabla^2\Phi^*)\Phi]F^2 \\
&+ \frac{1}{2}\Phi[F\nabla^2 F - (\nabla F)^2]\Phi] \\
&= \int d\mathbf{r}_1, ..., d\mathbf{r}_A [-\frac{1}{4}F^2\nabla^2(\Phi^*\Phi) + \Phi^*\nabla^2\Phi \\
&+ \frac{1}{2}\Phi[F\nabla^2 F - (\nabla F)^2]\Phi] \qquad (19)
\end{aligned}
$$

The above equation is the kinetic energy in the Jackson-Feenberg form.

A.5 The uncorrelated one-body densities

In this appendix we write the explicit general expressions for the uncorrelated one-body densities involved in the calculation of the kinetic energy and for systems not necessary saturated in the isospin. For the single particle wave functions we use the expression:

$$
\phi^{\alpha}_{nljm}(x_i) = R^{\alpha}_{nlj}(r_i) \sum_{\mu,s} < l\mu\frac{1}{2}s|jm > Y_{l\mu}(\Omega_i)\chi_s(i)\chi_\alpha(i) \qquad (20)
$$

where R is the radial function, Y is the sherical harmonic and χ_s and χ_α are the spin and isospin functions, respectively.
The one-body density ρ^{α}_{T1} is given by:

$$
\begin{aligned}
\rho^{\alpha}_{T1}(\boldsymbol{r}_1) &= \sum_{nljm} \phi^{\alpha *}_{nljm}(\boldsymbol{r}_1)\nabla^2_1\phi^{\alpha}_{nljm}(\boldsymbol{r}_1) - \sum_{\alpha} \nabla_1\phi^{\alpha *}_{nljm}(\boldsymbol{r}_1)\cdot\nabla_1\phi^{\alpha}_{nljm}(\boldsymbol{r}_1) \\
&= \frac{1}{4\pi}\sum_{nlj}(2j+1)\Big[R^{\alpha}_{nlj}(r_1)\Big(D^{\alpha}_{nlj}(r_1) - \frac{l(l+1)}{r_1^2}R^{\alpha}_{nlj}(r_1)\Big)
\end{aligned}
$$

$$-[R^{\alpha'}_{nlj}(r_1)]^2\Bigg] \tag{21}$$

where we have defined:

$$D^{\alpha}_{nlj}(r_1) = \nabla^2_1 R^{\alpha}_{nlj}(r_1) = R^{\alpha''}_{nlj}(r_1) + \frac{2}{r_1} R^{\alpha'}_{nlj}(r_1) - \frac{l(l+1)}{r_1^2} R^{\alpha}_{nlj}(r_1). \tag{22}$$

For the one-body density matrices ρ_{T2} and ρ_{T2A} we find:

$$\begin{aligned}
\rho^{\alpha\beta}_{T2}(\boldsymbol{r}_1,\boldsymbol{r}_2) &= \rho^{\alpha}_0(\boldsymbol{r}_1,\boldsymbol{r}_2)\nabla^2_1\rho^{\beta}_0(\boldsymbol{r}_1,\boldsymbol{r}_2) - \nabla_1\rho^{\alpha}_0(\boldsymbol{r}_1,\boldsymbol{r}_2)\cdot\nabla_1\rho^{\beta}_0(\boldsymbol{r}_1,\boldsymbol{r}_2) \\
&= \frac{1}{4(4\pi)^2}\sum_{nljn'l'j'}(2j+1)(2j'+1)R^{\alpha}_{nlj}(r_2)R^{\beta}_{n'l'j'}(r_2) \\
&\quad\times\Bigg\{\Big[R^{\alpha}_{nlj}(r_1)D^{\beta}_{n'l'j'}(r_1) - R^{\alpha\prime}_{nlj}(r_1)R^{\beta\prime}_{n'l'j'}(r_1)\Big]P_l(\cos\theta)P_{l'}(\cos\theta) \\
&\quad-\frac{\sin^2\theta}{r_1^2}R^{\alpha}_{nlj}(r_1)R^{\beta}_{n'l'j'}(r_1)P'_l(\cos\theta)P'_{l'}(\cos\theta)\Bigg\} \qquad (23) \\
\rho^{\alpha\beta}_{T2A}(\boldsymbol{r}_1,\boldsymbol{r}_2) &= \frac{1}{(4\pi)^2}\sum_{nljn'l'j'}(-1)^{j+j'-l-l'-1}R^{\alpha}_{nlj}(r_2)R^{\beta}_{n'l'j'}(r_2) \\
&\quad\times\Bigg\{\Big[R^{\alpha}_{nlj}(r_1)D^{\beta}_{n'l'j'}(r_1) - R^{\alpha\prime}_{nlj}(r_1)R^{\beta\prime}_{n'l'j'}(r_1)\Big]Q_l(\cos\theta)Q_{l'}(\cos\theta) \\
&\quad-\frac{\sin^2(\theta)}{r_1^2}R^{\alpha}_{nlj}(r_1)R^{\beta}_{n'l'j'}(r_1)Q'_l(\cos\theta)Q'_{l'}(\cos\theta)\Bigg\} \qquad (24)
\end{aligned}$$

where P_l are Legendre polynomials, θ is the angle between the vectors $\boldsymbol{r}_1$ and $\boldsymbol{r}_2$ and we have defined

$$\begin{aligned}
Q_l(\cos\theta) &= \sin\theta P'_l(\cos\theta) \\
Q'_l(\cos\theta) &= \frac{1}{\sin\theta}\Big(\cos\theta)P'_l(\cos\theta) - l(l+)P_l(\cos\theta)\Big).
\end{aligned}$$

For the ρ_{T3} densities we have

$$\begin{aligned}
\rho^{\alpha}_{T3}(\boldsymbol{r}_1,\boldsymbol{r}_2) = 2\nabla^2_1\rho^{\alpha}_{0,P}(\boldsymbol{r}_1,\boldsymbol{r}_2) &= \frac{1}{4\pi}\sum_{nlj}(2j+1)R^{\alpha}_{nlj}(r_2)D^{\alpha}_{nlj}(r_1)P_l(\cos\theta) \qquad (25) \\
\rho^{\alpha}_{T3,A}(\boldsymbol{r}_1,\boldsymbol{r}_2) = 2\nabla^2_1\rho^{\alpha}_{0,A}(\boldsymbol{r}_1,\boldsymbol{r}_2) &= \frac{1}{2\pi}\sum_{nlj}(-1)^{j-l-\frac{1}{2}}R^{\alpha}_{nlj}(r_2)D^{\alpha}_{nlj}(r_1)Q_l(\cos\theta). \qquad (26)
\end{aligned}$$

The last density that appears in the calculation of the center of mass energy can be written as:

$$\rho^{\alpha}_{T4}(\vec{r}_1,\vec{r}_2) = \rho^{\alpha}_{T6}(\vec{r}_1,\vec{r}_2) - \rho^{\alpha}_{0,P}(\vec{r}_1,\vec{r}_2)\rho^{\alpha}_{T5,P}(\vec{r}_1,\vec{r}_2) - \rho^{\alpha}_{0,A}(\vec{r}_1,\vec{r}_2)\rho^{\alpha}_{T5,A}(\vec{r}_1,\vec{r}_2) \quad (27)$$

where we have defined:

$$\begin{aligned}
\rho^{\alpha}_{T6}(\vec{r}_1,\vec{r}_2) &= 2\Big(\nabla_1\rho^{\alpha}_{0,P}(\vec{r}_1,\vec{r}_2)\cdot\nabla_2\rho^{\alpha}_{0,P}(\vec{r}_1,\vec{r}_2) + \qquad (28)\\
&\quad \nabla_1\rho^{\alpha}_{0,A}(\vec{r}_1,\vec{r}_2)\cdot\nabla_2\rho^{\alpha}_{0,A}(\vec{r}_1,\vec{r}_2)\Big)\\
\rho^{\alpha}_{T5,X}(\vec{r}_1,\vec{r}_2) &= 2\nabla_1\cdot\nabla_2\rho^{\alpha}_{0,X}(\vec{r}_1,\vec{r}_2) \qquad (29)
\end{aligned}$$

where $X = P, A$ and the explicit expressions of the defined quantities are:

$$\begin{aligned}
\rho^{\alpha}_{T5,P}(\vec{r}_1,\vec{r}_2) &= \frac{1}{4\pi}\sum_{nlj}(2j+1)\Bigg[R^{\alpha\prime}_{nlj}(r_1)R^{\alpha\prime}_{nlj}(r_2)\cos\theta P_l(\cos\theta) + \qquad (30)\\
&\quad \left(R^{\alpha}_{nlj}(r_2)\frac{R^{\alpha}_{nlj}(r_1)}{r_1} + R^{\alpha}_{nlj}(r_1)\frac{R^{\alpha}_{nlj}(r_2)}{r_2}\right)\sin^2\theta P_l'(\cos\theta) + \\
&\quad \frac{R^{\alpha}_{nlj}(r_1)R^{\alpha}_{nlj}(r_2)}{r_1 r_2}\Big(\sin^2\theta P_l'(\cos\theta) + l(l+1)\cos\theta P_l(\cos\theta)\Big)\Bigg]\\
\rho^{\alpha}_{T5,A}(\vec{r}_1,\vec{r}_2) &= \frac{1}{2\pi}\sum_{nlj}(-1)^{j-l-1/2}\Bigg[R^{\alpha\prime}_{nlj}(r_1)R^{\alpha\prime}_{nlj}(r_2)\cos\theta Q_l(\cos\theta) + \qquad (31)\\
&\quad \left(R^{\alpha}_{nlj}(r_2)\frac{R^{\alpha}_{nlj}(r_1)}{r_1} + R^{\alpha}_{nlj}(r_1)\frac{R^{\alpha}_{nlj}(r_2)}{r_2}\right)\sin^2\theta Q_l'(\cos\theta) + \\
&\quad \frac{R^{\alpha}_{nlj}(r_1)R^{\alpha}_{nlj}(r_2)}{r_1 r_2}\Bigg\{\sin^2\theta Q_l'(\cos\theta) + \\
&\quad \Big(l(l+1) - \frac{1}{\sin^2\theta}\Big)\cos\theta Q_l(\cos\theta)\Bigg\}\Bigg]\\
\rho^{\alpha}_{T6}(\vec{r}_1,\vec{r}_2) &= \frac{1}{2(4\pi)^2}\sum_{\substack{nlj\\ n'l'j'}}(2j+1)(2j'+1)R^{\alpha}_{nlj}(r_2)R^{\alpha}_{n'l'j'}(r_1) \qquad (32)\\
&\quad \Bigg\{\cos\theta\Bigg[R^{\alpha\prime}_{nlj}(r_2)R^{\alpha\prime}_{n'l'j'}(r_1)P_l(\cos\theta)P_{l'}(\cos\theta) - \\
&\quad \sin^2\theta\frac{R^{\alpha}_{nlj}(r_2)R^{\alpha}_{n'l'j'}(r_1)}{r_1 r_2}P_l'(\cos\theta)P_{l'}'(\cos\theta)\Bigg] + \\
&\quad \sin^2\theta\Bigg[\frac{R^{\alpha}_{nlj}(r_2)}{r_2}R^{\alpha\prime}_{n'l'j'}(r_1)P_l'(\cos\theta)P_{l'}(\cos\theta) + \\
&\quad R^{\alpha\prime}_{nlj}(r_2)\frac{R^{\alpha}_{n'l'j'}(r_1)}{r_1}P_l(\cos\theta)P_{l'}'(\cos\theta)\Bigg]\Bigg\}
\end{aligned}$$

$$\frac{2}{(4\pi)^2} \sum_{\substack{nlj \\ n'l'j'}} (-1)^{j+j'-l-l'-1} R^{\alpha}_{nlj}(r_2) R^{\alpha}_{n'l'j'}(r_1)$$
$$\Bigg\{ \cos\theta \Bigg[R^{\alpha\prime}_{nlj}(r_2) R^{\alpha\prime}_{n'l'j'}(r_1) Q_l(\cos\theta) Q_{l'}(\cos\theta) -$$
$$\sin^2\theta \frac{R^{\alpha}_{nlj}(r_2) R^{\alpha}_{n'l'j'}(r_1)}{r_1 r_2} Q'_l(\cos\theta) Q'_{l'}(\cos\theta) \Bigg] +$$
$$\sin^2\theta \Bigg[\frac{R^{\alpha}_{nlj}(r_2)}{r_2} R^{\alpha\prime}_{n'l'j'}(r_1) Q'_l(\cos\theta) Q_{l'}(\cos\theta) +$$
$$R^{\alpha\prime}_{nlj}(r_2) \frac{R^{\alpha}_{n'l'j'}(r_1)}{r_1} Q_l(\cos\theta) Q'_{l'}(\cos\theta) \Bigg] \Bigg\}$$

A.6 The two-body distribution functions

The goal is the calculation of the integral

$$\rho^{\alpha\beta}_{2,q}(r_{12}) = \frac{1}{A} \int d\boldsymbol{R}_{12} \rho^{\alpha\beta}_{2,q}(\boldsymbol{r}_1, \boldsymbol{r}_2) \tag{33}$$

where $r_{12} = |\boldsymbol{r}_1 - \boldsymbol{r}_2|$ and $\boldsymbol{R}_{12} = (\boldsymbol{r}_1 + \boldsymbol{r}_2)/2$. The equalities

$$\int d\boldsymbol{r}_1 d\boldsymbol{r}_2 \rho^{\alpha\beta}_{2,q}(\boldsymbol{r}_1, \boldsymbol{r}_2) = \int d\boldsymbol{r}_{12} d\boldsymbol{R}_{12} \rho(\boldsymbol{r}_1, \boldsymbol{r}_2) = \int d\boldsymbol{r}_1 d\boldsymbol{r}_{12} \rho^{\alpha\beta}_{2,q}(\boldsymbol{r}_1, \boldsymbol{r}_2) \tag{34}$$

hold since they have the same Jacobian. Moreover we have explicitly

$$\rho^{\alpha\beta}_{2,q}(\boldsymbol{r}_1, \boldsymbol{r}_2) \equiv \rho^{\alpha\beta}_{2,q}(r_1, r_2, \boldsymbol{r}_1 \cdot \boldsymbol{r}_2) = \rho^{\alpha\beta}_{2,q}(r_1, r_2, \cos\theta_{12}) \tag{35}$$

Then we have

$$\rho^{\alpha\beta}_{2,q}(r_0) = \int d\boldsymbol{r}_1 d\boldsymbol{r}_2 \rho^{\alpha\beta}_{2,q}(r_1, r_2, \cos\theta_{12}) \frac{\delta(r_{12} - r_0)}{4\pi r_{12}^2} \tag{36}$$
$$= \int r_1^2 dr d\Omega_1 \int r_2^2 dr_2 d\Omega_2 \rho^{\alpha\beta}_{2,q}(r_1, r_2, \cos\theta_{12}) \frac{\delta(r_{12} - r_0)}{4\pi r_{12}^2} \tag{37}$$

If we choose $r_1 \parallel z$ we have

$$\rho^{\alpha\beta}_{2,q}(r_0) = 2\pi \int_0^R r_1^2 dr_1 \int_0^R r_2^2 dr_2 \int d\Omega_{12} \rho^{\alpha\beta}_{2,q}(r_1, r_2, \cos\theta_{12}) \frac{\delta(r_{12} - r_0)}{4\pi r_{12}^2} \tag{38}$$

Now we know that

$$r_{12}^2 = r_1^2 + r_2^2 - 2 r_1 r_2 \cos\theta_{12} \tag{39}$$

then we can express $\rho_{2,q}^{\alpha\beta}(r_1, r_2, \cos\theta_{12})$ as a function of r_1, r_2 and r_{12}. The above integral reads

$$\begin{aligned}
\rho_{2,q}^{\alpha\beta}(r_0) &= 2\pi \int_0^R r_1^2 dr_1 \int_0^R r_2^2 dr_2 \int_0^{2\pi} d\phi \int_{-1}^1 d(-\cos\theta) \rho_{2,q}^{\alpha\beta}(r_1, r_2, r_{12}) \frac{\delta(r_{12} - r_0)}{4\pi r_{12}^2} \\
&= 2\pi \int_0^R r_1 dr_1 \int_0^R r_2 dr_2 \int_{|r_1 - r_2|}^{r_1 + r_2} \frac{1}{r_{12}} dr_{12} \rho_{2,q}^{\alpha\beta}(r_1, r_2, r_{12}) \delta(r_{12} - r_0) \qquad (40)
\end{aligned}$$

In the above expression the fraction $\frac{1}{r_{12}}$ can create several numerical problems, then we used a different form of integration by expliciting the function ρ with respect the r_1, r_{12} and $\boldsymbol{r}_1 \cdot \boldsymbol{r}_{12}$ coordinates. In this way the integral reads

$$\begin{aligned}
\rho_{2,q}^{\alpha\beta}(r_0) &= 8\pi^2 \int_0^R r_1^2 dr_1 \int_0^R r_{12}^2 dr_{12} \int_{-1}^1 d(-\boldsymbol{r}_1 \cdot \boldsymbol{r}_{12}) \rho_{2,q}^{\alpha\beta}(r_1, r_{12}, \boldsymbol{r}_1 \cdot \boldsymbol{r}_{12}) \frac{\delta(r_{12} - r_0)}{4\pi r_{12}^2} \\
&= 2\pi \int_0^R r_1^2 dr_1 \int_0^R dr_{12} \int_{-1}^1 d(-\boldsymbol{r}_1 \cdot \boldsymbol{r}_{12}) \rho_{2,q}^{\alpha\beta}(r_1, r_{12}, \boldsymbol{r}_1 \cdot \boldsymbol{r}_{12}) \delta(r_{12} - r_0) \\
&= 2\pi \int_0^R r_1^2 dr_1 \int_{-1}^1 d(-\boldsymbol{r}_1 \cdot \boldsymbol{r}_{12}) \rho_{2,q}^{\alpha\beta}(r_1, r_0, \boldsymbol{r}_1 \cdot \boldsymbol{r}_{12}). \qquad (41)
\end{aligned}$$

A.7 Acronyms

CBF:	Correlated Basis Function
FHNC:	Fermi HyperNetted Chain
FHNC/SOC:	Fermi Hypernetted Chain/Single Operator Chain
FP:	Friedman-Pandharipande interaction
HNC:	HyperNetted Chain
IP:	Interacting Particles
IPM:	Independent Particle Model
MBCF:	Many-Body Correlation Function
OBD:	One-Body Density
OBDF:	One-Body Distribution Function
RFHNC:	Renormalized Fermi HyperNetted Chain
SOC:	Single Operator Chain
SOR:	Single Operator Ring
TBCF:	Two Body Correlation Function
TBDF:	Two Body Distribution Function

Bibliography

[Akm97] A. Akmal, V.R. Pandharipande, Phys. Rev. **C56** (1997) 2261.

[Ang01] M. Anguiano, G. Co', Jour.. Phys. **G27** (2001) 2109.

[Ari96] F. Arias de Saavedra, G. Co', A. Fabrocini, S. Fantoni, Nucl. Phys. **A605** (1996) 359.

[Ari97] F. Arias de Saavedra, G. Co', M. M. Renis, Phys. Rev. **C55** (1997) 673.

[Aud93] G. Audi, A. H. Wapstra, Nucl. Phys. **A565** (1993) 1.

[Bal05] M. Baldo, C. Maieron, Ann. Rev., **C72** (2005) 043005.

[Bet71] H.A. Bethe, Ann. Rev. Nucl. Sci., **21** (1971) 93.

[Bru54] K.A. Brueckner, C.A. Levinson, H.M. Mahmond, Phys. Rev., **95** (1971) 217.

[Car83] J. Carlson and V.R. Pandharipande, Nucl. Phys. **A401** (1983) 59.

[Cla79] J.W. Clark, Nucl. Phys. **A328**, (1979) 587.

[Co92] G. Co', A. Fabrocini, S. Fantoni, I.E. Lagaris, Nucl. Phys. **A549** (1992) 439.

[Co94] G. Co', A. Fabrocini, S. Fantoni, Nucl. Phys. **A568** (1994) 73.

[Day67] B.D. Day, Rev. Mod. Phys. **39** (1967) 719.

[Def98] A. De Florio, Sviluppo di una teoria a molti corpi per la descrizione di stati eccitati in base correlata, Thesis (1998).

[Dej87] C. W. Jager, C. De Vries, At Data Nucl. Data Tables **36** (1987) 495.

[Dic82] W.H. Dickoff, A. Faessler, A. Muther, Nucl. Phys. **A389** (1982) 492.

[Fab98] A. Fabrocini, F. Arias de Saavedra, G.Co', P. Folgarait, Phys. Rev. **C57** (1998) 1668.

[Fab00] A. Fabrocini, F. Arias de Saavedra, G.Co', Phys. Rev. **C61** (2000) 44302.

[Fan74] S. Fantoni, S. Rosati, Nuovo Cimento, **A20** (1974) 179.

[Fan79] S. Fantoni, S. Rosati, Nucl. Phys. **A328** (1979) 478.

[Fri80] B. Friedman, V.R. Pandharipande, Nucl. Phys., **A361** (1980) 502.

[Gau71] M. Gaudin, J. Gillespie, G. Ripka, Nucl. Phys., **A176** (1971) 273.

[Jac61] H.W. Jackson, E. Feenberg Ann. Phys.(N.Y.), **15** (1961) 266.

[Jas55] R. Jastrow, Phys. Rev., **98** (1955) 1479.

[Jen76] J.P. Jenkeene, A. Lejeune, C. Mahaux, Phys. Rep., **25** (1976) 83.

[Kam01] H. Kamada et al., Phys. Rev. **C64** (2001) 044001.

[Lag80] I.E. Lagaris, V.R. Pandharipande, Nucl. Phys., **A334** (1980) 217.

[Lag81] I.E. Lagaris, V.R. Pandharipande, Nucl. Phys., **A359** (1981) 349.

[Lag81A] I.E. Lagaris, V.R. Pandharipande, Nucl. Phys., **A369**(1981) 331.

[Lag81B] I.E. Lagaris, V.R. Pandharipande, Nucl. Phys., **A369** (1981) 470.

[Mac87] R. Machleidt, K. Holinde and C. Elster, Phys. Rep. **149** (1987).

[Mac96] R. Machleidt, F. Sammaruca, Y. Song, Phys. Rev. **C53** (1996) RI483.

[May40] J.E. Mayer, M.G. Mayer, Statistical Mechanics (Wiley, New York and London 1940).

[Mut00] H. Muther, A. Polls, Prog. Part. Nucl. Phys., **45** (1979) 243.

[Nef03] T. Neff, H. Feldmeier, Nucl. Phys., **A713** (2003) 311.

[Pan79] V. R. Pandharipande, R.Wiringa, Rev. Mod. Phys., **51** (1979) 821.

[Pan95] V. R. Pandharipande, J. Carlson, S.C. Pieper R.B. Wiringa, R. Schiavilla, Phys. Rev. **C48** (1995) 789.

[Pie01] S.C. Pieper, V.R. Pandharipande, R.B. Wiringa, J. Carlson, Phys. Rev. **C64** (2001) 014001.

[Pie05] S.C. Pieper, Nucl. Phys. **A751** (2005) 516.

[Pud97] B.S. Pudliner, V. R. Pandharipande, J. Carlson, S.C. Pieper, R.B. Wiringa, R. Schiavilla, Phys. Rev. **C56** (1997) 1720

[Sch86] R. Schiavilla, V.R. Pandharipande, R.B. Wiringa, Nucl. Phys. **A449** (1986) 219.

[Sch91] K.W. Schmidt, H. Muther, R. Machleidt, Nucl. Phys. **A530** (1986) 14.

[Son98] H.Q. Song, M. Baldo, G. Giansiracusa, U. Lombardo, Phys. Rev. Lett. (1998) 1584.

[Sto93] V.G.J. Stocks, R.A.M. Klomp, M.C.M. Rentmeester, J.J. De Swant, Phys. Rev. **C48** (1993) 792.

[Sto94] V.G.J. Stocks, R.A.M. Klomp, C,P.F. Terheggen, J.J. De Swart, Phys. Rev. **C49** (1987) 2950.

[Wir95] R.B. Wiringa, V.G.J. Stocks, R. Schiavilla, Phys. Rev. **C51** (1995) 38.

[Wir80] R.B. Wiringa, Nucl. Phys. **A338** (1980) 57.

Acknowledgements

I would like to express special appreciation to Giampaolo Co' and Fernando Arias de Saavedra for their very important support and collaboration during the realization of this work.
Thanks are due also to Adelchi Fabrocini for informative discussion and other communications.